ZooKeys 1129: 1–19 (2022)
doi: 10.3897/zookeys.1129.90986
https://zookeys.pensoft.net

RESEARCH ARTICLE

A peer-reviewed open-access journal
ZooKeys
Launched to accelerate biodiversity research

Gnathia pipinde sp. nov. (Crustacea, Isopoda, Gnathiidae), a temporary parasite of the pufferfish, *Amblyrhynchotes honckenii*, from temperate southern Africa

Nico J. Smit[1], Kerry A. Hadfield[1]

1 *Water Research Group, Unit for Environmental Sciences and Management, North-West University, Private Bag X6001, Potchefstroom, 2520, South Africa*

Corresponding author: Kerry A. Hadfield (kerry.malherbe@nwu.ac.za)

Academic editor: P. T. Aneesh | Received 28 July 2022 | Accepted 24 August 2022 | Published 10 November 2022

https://zoobank.org/3A329C3F-78A3-4DE1-8B5E-96F576D74CBD

Citation: Smit NJ, Hadfield KA (2022) *Gnathia pipinde* sp. nov. (Crustacea, Isopoda, Gnathiidae), a temporary parasite of the pufferfish, *Amblyrhynchotes honckenii*, from temperate southern Africa. ZooKeys 1129: 1–19. https://doi.org/10.3897/zookeys.1129.90986

Abstract

A new species, *Gnathia pipinde* **sp. nov.**, is described from specimens taken from pufferfish, *Amblyrhynchotes honckenii*, at Chintsa and De Hoop Nature Reserve on the southern Indian Ocean coast of South Africa. *Gnathia pipinde* **sp. nov.** is characterised by the straight frontal margin, presence of conical superior frontolateral processes, a strong and bifid mediofrontal process, pronounced and pointed supraocular lobes, mandible strongly curved with a dentate blade, and the claviform penes produced more than a third the length of the pereon. A summary and key to the males of all known species of the Gnathiidae from the Temperate Southern African marine realm is provided.

Keywords

Chintsa, De Hoop Nature Reserve, Indian Ocean, marine fish parasite, taxonomy

Introduction

The Western Indian Ocean is a region of known high but underexplored marine invertebrate diversity. The Temperate Southern African (TSA) marine realm (a realm identified by Spalding et al. 2007) is well known for its high biodiversity and endemism of marine fauna, especially fish (Griffiths et al. 2010). However, there is a large gap in our knowledge of the diversity of small invertebrates, including parasites, from all the potential host species already documented (Smit and Hadfield 2015). This is specifically true for gnathiid isopods that are temporary ectoparasites of both teleost and elasmobranch fishes (Hadfield et al. 2008), and only eight species in three genera have previously been reported or described from the TSA (Table 1).

These small crustaceans (<15 mm, most species <6 mm) have three larval stages that feed on the blood and lymph of their hosts, before dropping to the ocean floor where they moult into the subsequent larval stage or into adult males or females (Smit et al. 2019). In general, gnathiid larvae are not considered host specific, although too little is known about specific larval species to be conclusive on this point. Due to the highly characteristic structures seen in male gnathiids, the taxonomic classification has been, and still is, based predominantly on the morphology of the adults (Smit and Davies 2004).

Gnathiid isopods have traditionally been described from the free-living adult males collected from dredge sampling, elutriation and sorting of coral rubble, from sponge collections, and other standard techniques used to collect small marine crustaceans. However, since the early 2000s, new gnathiid species have been described by moulting final (P3) larval stages into adults, either collected by light (Farquharson et al. 2012) and baited traps (Shodipo et al. 2021) or collected directly from the host (Ferreira et al. 2010). This latter method also provides the opportunity to obtain morphological and ecological information on the larval stage as well as host information that is generally lacking for most species of gnathiids. Following this trend, this study reports on gnathiid larvae collected from the evileye blaasop (pufferfish), *Amblyrhynchotes honckenii* (Bloch, 1795), from the south coast of South Africa, and moulted through to adult males. The male gnathiids did not conform to any of the currently known species from this or any other region in the world and are here described as new to science. In addition, a key to the currently known species from this region is provided.

Methods

Nine *Amblyrhynchotes honckenii* were collected from the De Hoop Nature Reserve (4 specimens) and the small coastal town of Chintsa (5 specimens) on South Africa's south coast during October 1999 and October 2020, respectively. Fish from De Hoop Nature Reserve (34°28'44"S, 20°30'38"E) were captured by luring them into deep pools during evening low tide and then catching them with hand nets (see Smit and Davies 2001). At Chintsa (32°50'01"S, 28°06'58"E), pufferfish were collected using

Table 1. Summary of the location, depth, size and references of 9 gnathiid species from the Temperate Southern African (TSA) realm, including the 8 previously known species and the new species, *Gnathia pipinde* sp. nov.

Species	Location	Size (mm)	Depth (m)	Substratum / Host	References
Afrignathia multicavea Hadfield & Smit, 2008	South Africa (Eastern and Western Cape)	1.5–2.0	26–73		Hadfield and Smit (2008)
Caecognathia cryptopais (Barnard, 1925)	South Africa (Eastern and Western Cape)	2.0–3.9	160		Barnard (1925); Smit et al. (2000)
Gnathia africana Barnard, 1914	South Africa (Eastern and Western Cape)	0–5.1		Tubes of serpulid worms; sponges; *Caffrogobius caffer* (Günther, 1874); *Chorisochismus dentex* (Pallas 1769); *Clinus cottoides* Valenciennes, 1836; *Clinus superciliosus* (Linnaeus, 1758)	Barnard (1914); Smit and Davies (1999); Smit et al. (1999)
Gnathia disjuncta Barnard, 1920	South Africa (Western Cape)	3.5	73		Barnard (1920)
Gnathia nkulu Smit & Van As, 2000	South Africa (Eastern Cape)	3.3–4.9	80–200		Smit and Van As (2000)
	Madagascar (Nosy-Be)	4	1.5		Kensley et al. (2009)
Gnathia pantherina Smit & Basson, 2002	South Africa (Eastern and Western Cape)	3.7–6.8	intertidal	*Haploblepharus edwardsii* (Schinz, 1822); *Poroderma pantherinum* (Müller & Henle, 1838); *Torpedo fuscomaculata* Peters, 1855	Smit and Basson (2002)
Gnathia pilosus Hadfield, Smit & Avenant-Oldewage, 2008	South Africa (Kwazulu-Natal)	1.6–2.0	intertidal	*Abudefduf sordidus* (Forsskål, 1775); *Acanthurus triostegus* (Linnaeus, 1758); *Antennablennius bifilum* (Günther, 1861); *Diplodus capensis* (Smith, 1844); *Epinephelus marginatus* (Lowe, 1834); *Halichoeres nebulosus* (Valenciennes, 1839); *Istiblennius dussumieri* (Valenciennes, 1836); *Istiblennius edentulus* (Forster & Schneider, 1801); *Omobranchus banditus* Smith, 1959; *Plectroglyphidodon leucozonus* (Bleeker, 1859); *Psammogobius knysnaensis* Smith, 1935; *Pterois miles* (Bennett, 1828); *Rhabdosargus sarba* (Forsskål, 1775); *Scartella emarginata* (Günther, 1861); *Terapon jarbua* (Forsskål, 1775); *Thalassoma purpureum* (Forsskål, 1775)	Hadfield et al. (2008, 2009)
Gnathia pipinde sp. nov.	South Africa (Eastern and Western Cape)	4.6–5.1	Intertidal-shallow; subtidal	*Amblyrhynchotes honckenii* (Bloch, 1795)	Current study
Gnathia spongicola Barnard, 1920	South Africa (Western Cape)	5	238–347	hexactinellid sponges	Barnard (1920)

rod and line during early morning low tide. Host nomenclature follows FishBase (Froese and Pauly 2022).

Following capture, live pufferfish were screened for external parasites and fish with gnathiid larvae present were kept alive in fresh, aerated seawater until the gnathiids completed feeding and detached from the host. All the larvae were attached to the dorsal and lateral areas of the body just posterior to the fish's head. Fish were kept alive until the fully fed larvae detached 6–8 h following capture. In order to rear the larvae into the next stage, they were kept alive in fresh seawater. Free swimming gnathiids were collected by pipettes and transferred into small 50 ml bottles with fresh seawater until moulting into adults (see Grutter et al. 2020). Three of the larvae moulted 9 d post-feeding. A subsample of larvae and adults were subsequently fixed in 75% ethanol and transferred to the laboratory for further analysis.

From the collected samples, a single third stage larva and male were cleaned and prepared for scanning electron microscopy (SEM). The fixed specimens were hydrated from 70% ethanol to fresh water. The organisms were then washed and cleaned by brushing them with a soft sable hairbrush to remove salt crystals and debris. Clean specimens were dehydrated through a series of ethanol concentrations and critical-point dried using standard techniques. Dried specimens were mounted on inverted conical stubs with a rapid-drying varnish (Japan Gold Size, Winsor and Newton) normally used in gilding. Specimens were sputter coated with gold and studied with the aid of a JEOL WINSEM JSM 6400 scanning electron microscope. Optimum results were obtained when SEM work was done at 10 kV with a working distance of 39 mm and the stage tilted at 70° to 90°. For light microscopy, temporary slides of lignin pink stained specimens were prepared as whole mounts or dissected appendages. These were examined with a Leitz Laborlux D compound and a Wild M5 dissection microscope and drawings were made from projections using drawing attachments on these microscopes.

The species descriptions of both male and larva were prepared in DELTA (DEscriptive Language for TAxonomy) using a modified Gnathiidae character set (as used in Hadfield et al. 2019) for the male and a newly generated character set for the larva. Terminology follows Monod (1926), Cohen and Poore (1994), and Svavarsson and Bruce (2012, 2019) for the male and Smit and Basson (2002) and Hadfield et al. (2008) for the larva. Isopod classification follows that of Brandt and Poore (2003), and setal terminology is based on Watling (1989) and Svavarsson and Bruce (2019). The habitus total length was measured mid-dorsally, from the frontal margin (excluding the mandibles) to the midpoint of the pleotelson. Appendages (mouthparts, pereopods, pleopods) were dissected from the same side of the isopod.

Research permits for fish collection were provided by the Department of Agriculture, Forestry and Fisheries (DAFF) (RES2019/103 and RES2020/29), and ethical clearance was through the North-West University AnimCare animal ethics committee (NWU-00440-16-A5 and NWU-0051-19-A5). Type material is deposited in the National Museum, Bloemfontein (NMB), South Africa.

Taxonomy

Suborder Cymothoida Wägele, 1989
Superfamily Cymothooidea Leach, 1814
Family Gnathiidae Leach, 1814

***Gnathia* Leach, 1814**

Type species. *Gnathia termitoides* Leach, 1814, by monotypy (Cohen and Poore 1994).

Remarks. A restricted synonymy and diagnosis of *Gnathia* was provided in Hadfield et al. (2019).

***Gnathia pipinde* sp. nov.**
https://zoobank.org/1D3309F5-2048-4E33-A8A4-308C7B523852
Figs 1–6

Material examined. ***Holotype***. South Africa • 1 ♂ (4.6 mm TL, dissected); De Hoop Nature Reserve (34°28'44"S, 20°30'38"E); October 1999; leg. N.J. Smit; from *Amblyrhynchotes honckenii* (NMB P 899). ***Paratypes***. South Africa • 1 ♂ used for SEM (5.1 mm TL), 11 praniza larvae (P3) (3.8–4.6 mm TL), 1 P3 larva for SEM (4.2 mm TL); same info as holotype (NMB P 900) • 2 praniza larvae (P3) (3.8, 4.3 mm TL); Chintsa (32°50'01"S, 28°06'58"E); October 2020; leg. K.A. Hadfield; from *Amblyrhynchotes honckenii* (NMB P 901).

Description of male adult. (Figs 1–4). *Body* 2.8 times as long as greatest width, widest at pereonite 5; dorsal surfaces punctate, sparsely setose. *Cephalosome* quadrate, 0.8 as long as wide, lateral margins subparallel, posterior margin concave; dorsal surface with sensory pits and sparse granules; dorsal sulcus narrow, deep, short; paraocular ornamentation weakly developed, posteromedian tubercle present. *Frontolateral processes* present. *Frontal margin* straight, median point with process. *External scissura* present, narrow, shallow. *Mediofrontal process* present, strong, bifid, without fine setae. *Superior frontolateral process* present, single, strong, conical, with 6 pairs of long simple setae. *Inferior frontolateral process* absent. *Supraocular lobe* pronounced, pointed; accessory supraocular lobe not pronounced. *Eyes* present, elongate, 0.4 as long as cephalosome length, contiguous with head surface, ommatidia arranged in rows.

Pereon lateral margins subparallel, with few setose setae; anteriorly smooth. *Pereonite 1* partially fused dorsally with cephalosome; dorsolateral margins partly obscured by cephalosome. *Pereonite 2* wider than pereonite 1. *Pereonite 4* with prominent anterior constriction separating it from pereonite 3, median groove present. *Areae laterales* present on pereonite 5. *Pereonite 6* with weak lobi laterales; lobuii absent or weak, conical. *Pleon* epimera dorsally visible on all pleonites. *Pleonite* lateral margins with 2 pairs of simple setae, long setose setae randomly distributed on posterior margins.

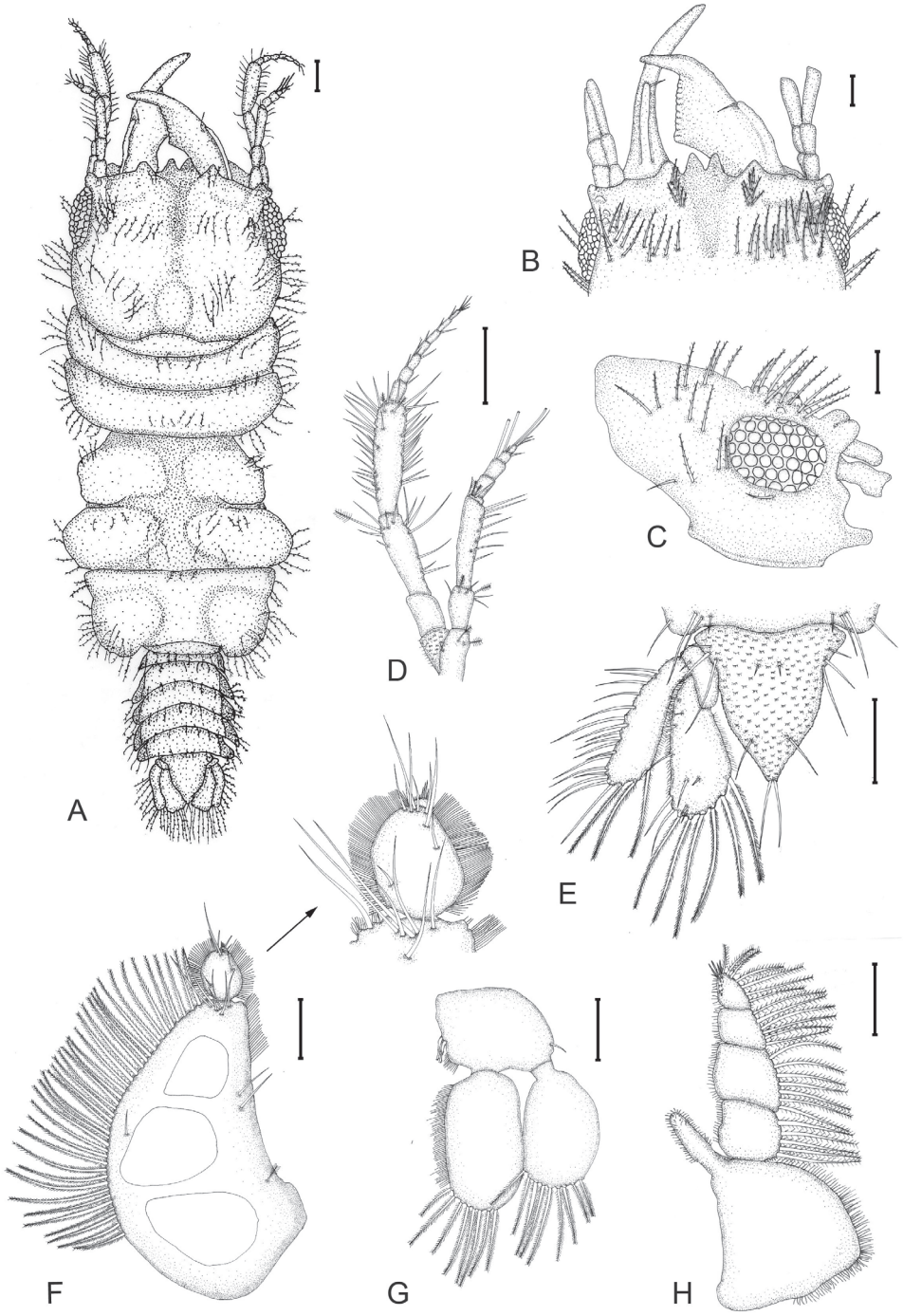

Figure 1. *Gnathia pipinde* sp. nov. (NMB P 899), male holotype (4.6 mm TL) **A** habitus dorsal view **B** dorsal view of frontal border and mandibles **C** lateral view of cephalosome **D** antenna and antennula **E** pleotelson and uropod **F** pylopod **G** pleopod 2 **H** maxilliped. Scale bars: 200 μm.

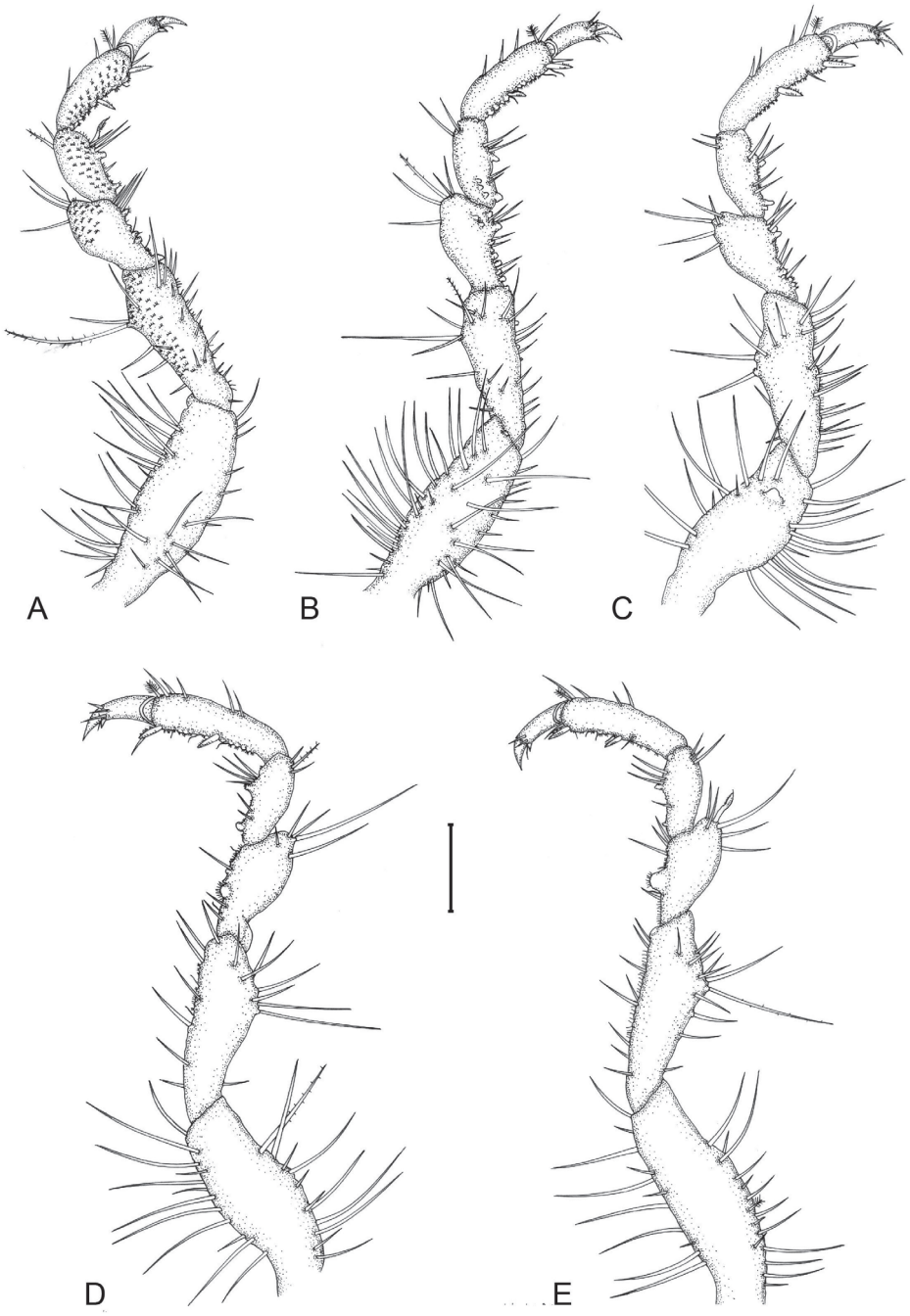

Figure 2. *Gnathia pipinde* sp. nov. (NMB P 899), male holotype (4.6 mm TL) **A–E** pereopods 2–6, respectively. Scale bar: 200 μm.

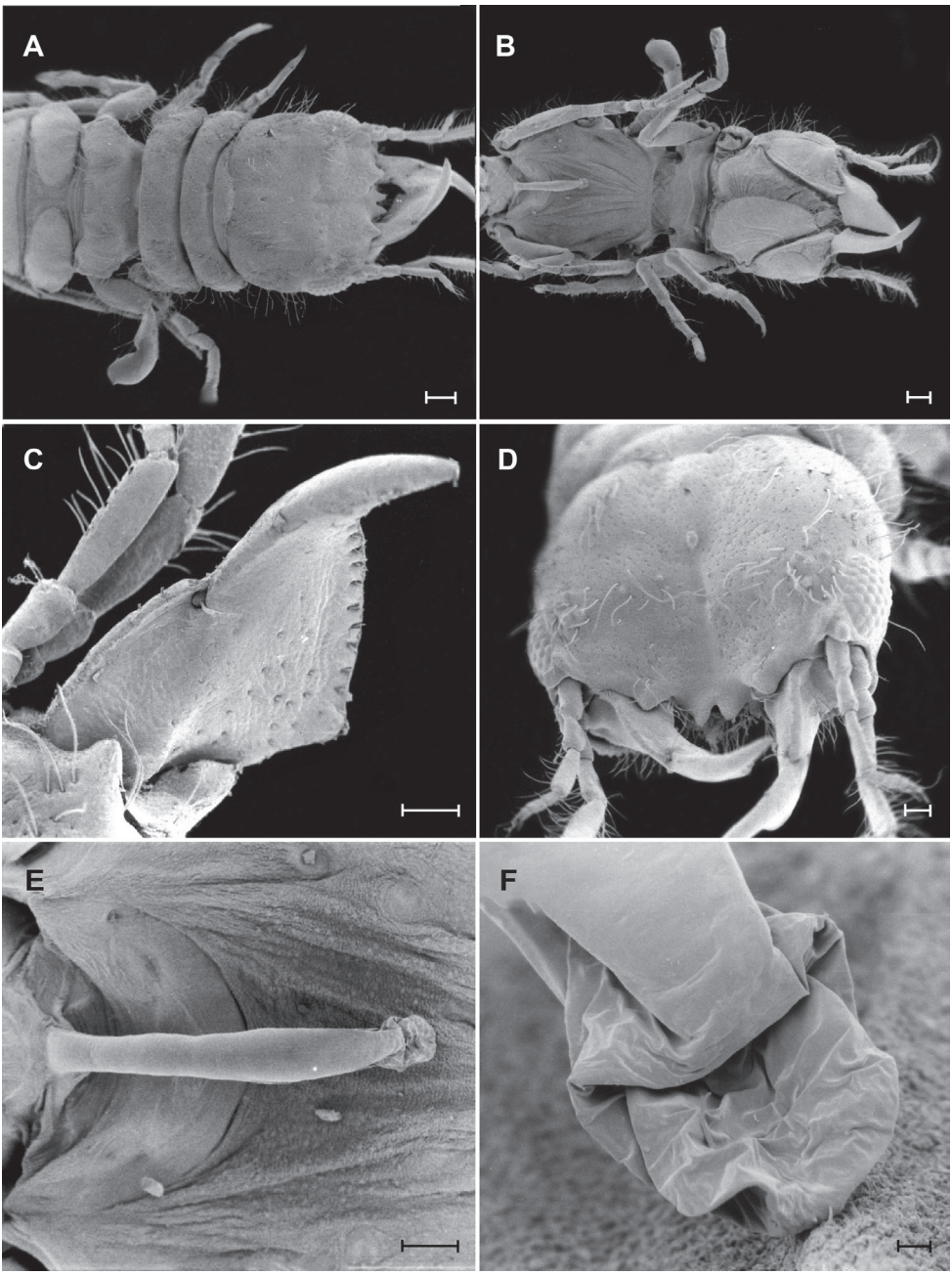

Figure 3. *Gnathia pipinde* sp. nov. (NMB P 900), male scanning electron microscope images. **A** Dorsal view of cephalosome and pereon **B** ventral view of cephalosome and pereon **C** dorsal view of mandible **D** anterodorsal view of cephalosome **E** ventral view of penes **F** ventral view of anterior end of penes. Scale bars: 250 μm (**A**, **B**); 100 μm (**C**–**E**); 10 μm (**F**).

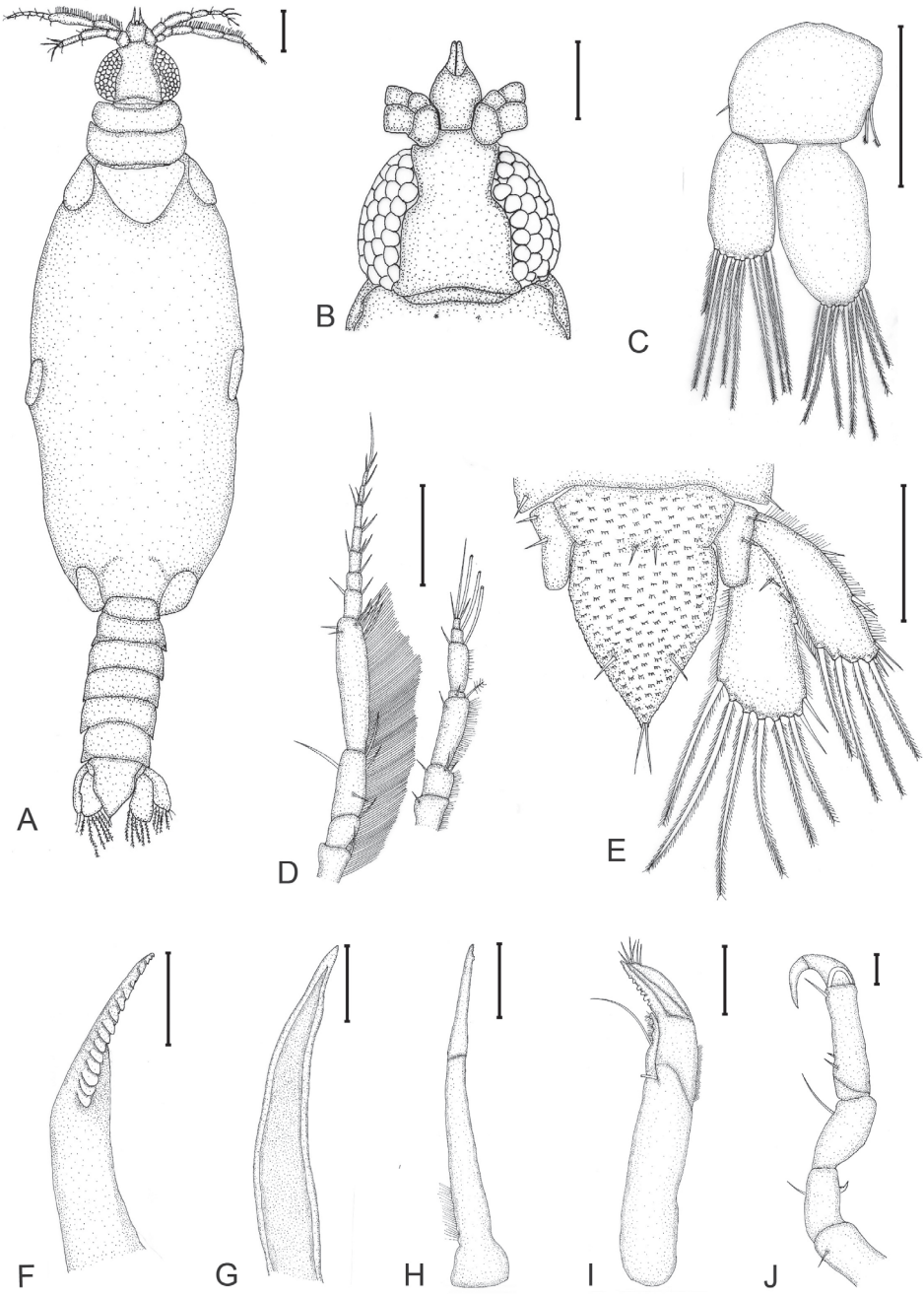

Figure 4. *Gnathia pipinde* sp. nov. (NMB P 901), praniza larva (4.1 mm TL) **A** habitus dorsal view **B** dorsal cephalosome **C** pleopod 1 **D** antenna and antennula **E** pleotelson and uropod **F** mandible **G** paragnath **H** maxillula **I** maxilliped **J** gnathopod. Scale bars: 200 µm (**A–E**); 50 µm (**F–J**).

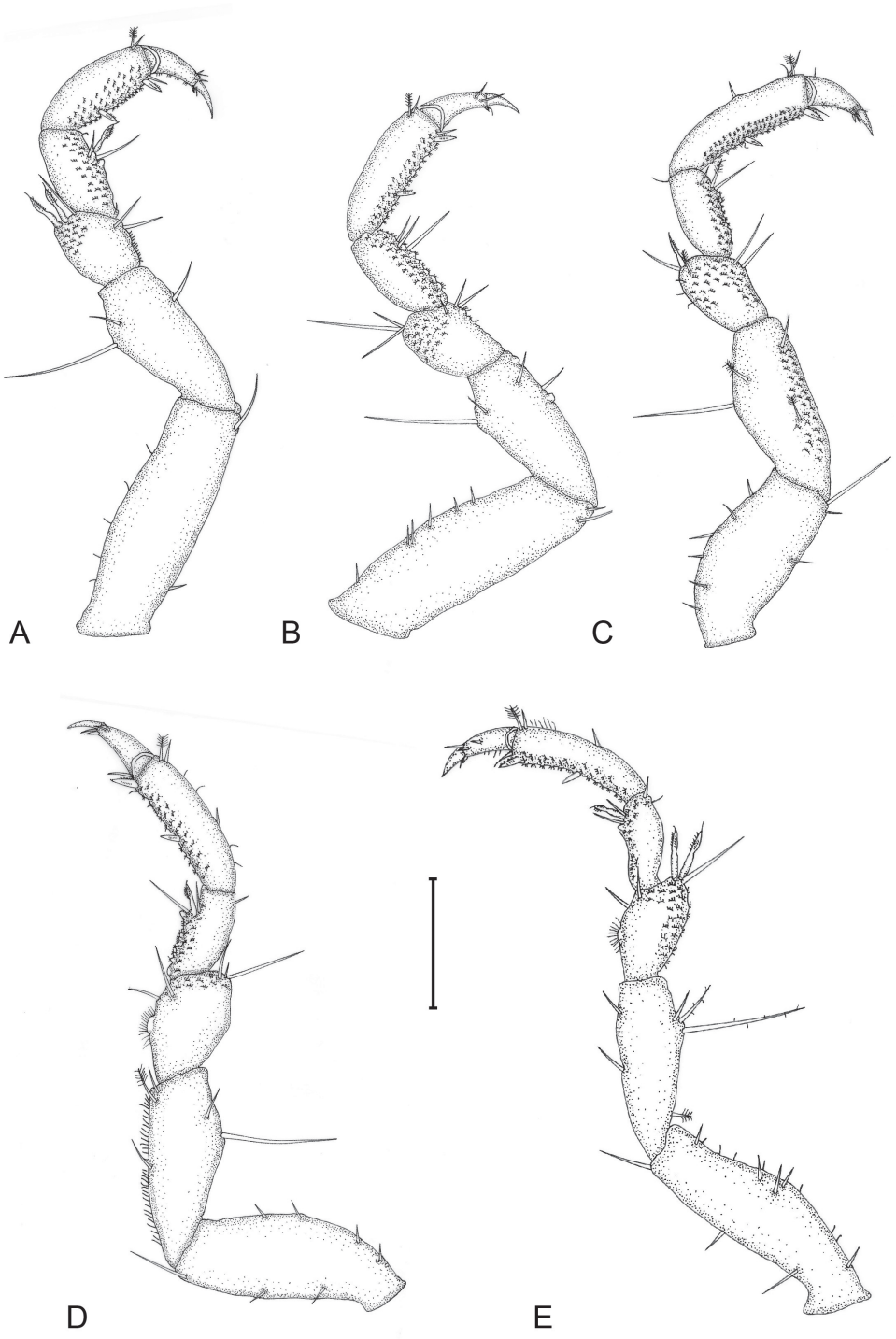

Figure 5. *Gnathia pipinde* sp. nov. (NMB P 901), praniza larva (4.1 mm TL) **A–E** pereopods 2–6, respectively. Scale bar: 200 μm.

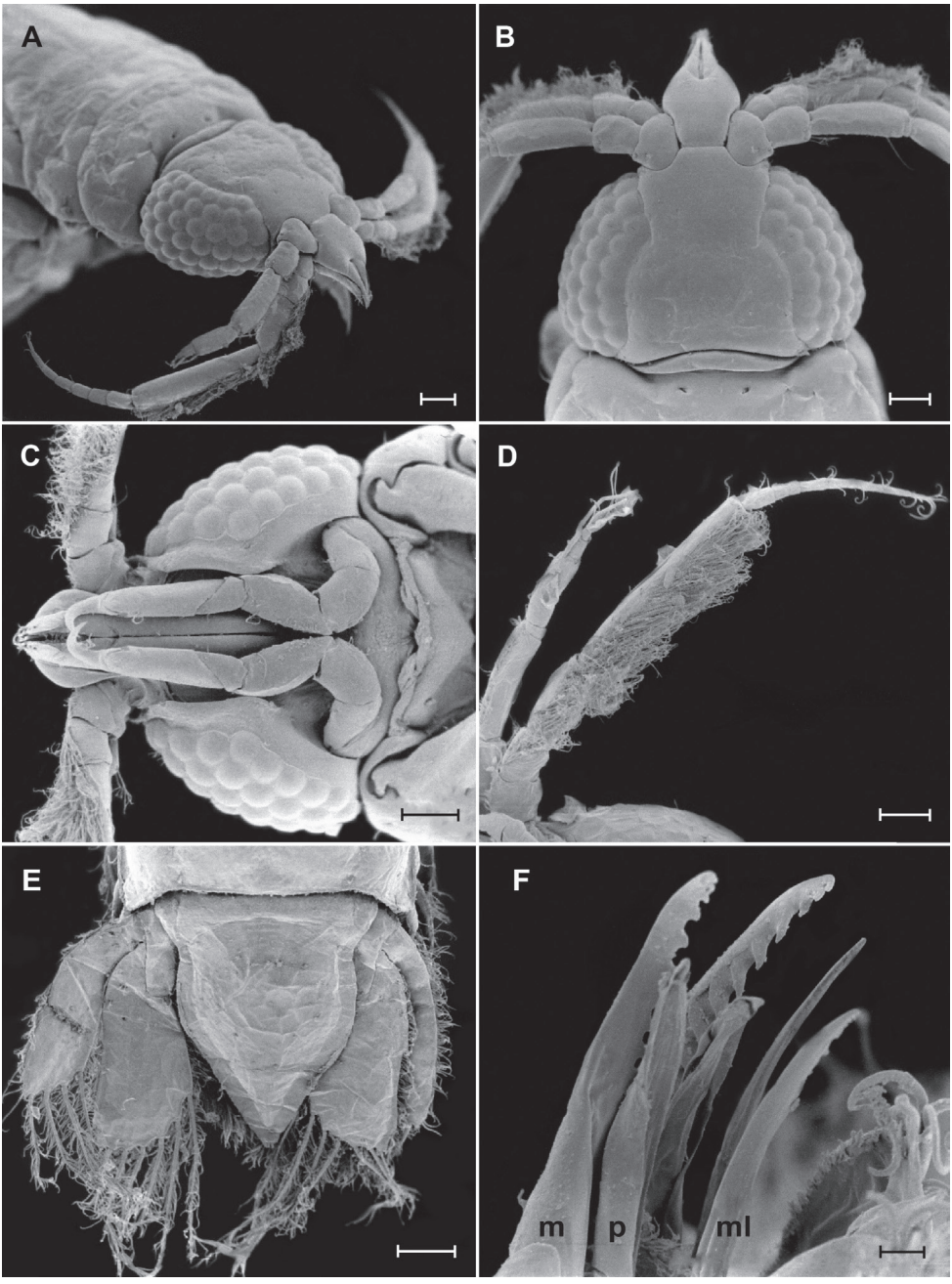

Figure 6. *Gnathia pipinde* sp. nov. (NMB P 901), praniza larva scanning electron microscope images **A** anterolateral view of labrum, cephalosome, and antennae **B** dorsal view of cephalosome **C** ventral view of cephalosome **D** ventral view of antenna and antennula **E** dorsal view of the pleotelson and uropods **F** lateral view of mandible (m), paragnath (p), and maxillula (ml). Scale bars: 100 μm (**A–E**); 10 μm (**F**).

Pleotelson as long as anterior width, covered in pectinate scales; lateral margins finely serrate, anterolateral margins concave, with 3 submarginal setae; posterolateral margin weakly convex, with 2 submarginal setae; mid-dorsal surface with 2 submedian setae, apex with 2 setae.

Antennula shorter than antenna; peduncle article 1 with 2 penicillate setae; article 2 0.8 times as long as article 1, with 2 penicillate setae; article 3 2.1 times as long as article 2, 3.8 times as long as wide. Antennula flagellum 0.8 times as long as article 3, with 5 articles; article 1 with 2 plumose setae; article 3 with 1 aesthetasc seta; article 4 with 1 aesthetasc seta, and 2 simple setae; article 5 terminating with 1 aesthetasc seta, and 3 simple setae. *Antenna* peduncle article 1 covered in pectinate scales and marginal setae; article 3 2.9 times as long as wide, twice as long as article 2, with 1 penicillate seta, and 12–14 simple setae and 1 penicillate seta; article 4 1.3 times as long as article 3, 3.7 times as long as wide, with 2 penicillate setae, and with 40–50 simple setae; flagellum as long as article 4, with 7 articles, terminating with 4 simple setae.

Mandible 0.6 as long as width of cephalosome, rectangular, strongly curved, distally; apex cylindrical, 22% total length, distally raised in lateral view; mandibular seta present. *Carina* present, smooth. *Incisor* knob-like. *Blade* present, dentate, straight, dentate along 100% of margin, with tufts of setae along distal margin. Basal neck short; sensory pits with short simple hair-like setae distributed randomly on dorsal surface of blade. Pseudoblade, internal lobe and dorsal lobe absent; erisma present; lamina dentata absent.

Maxilliped 5-articled, mesial border with short simple hair-like setae; article 1 lateral margin with continuous marginal short setae, endite extending to distal margin of article 2, without coupling setae; article 2 lateral margin with 5 plumose setae; article 3 lateral margin with 7 plumose setae; article 4 lateral margin with 6 plumose setae; article 5 with 7 plumose setae and 5 simple setae.

Pylopod article 1 with three distinct areolae, 1.6 as long as wide, without distolateral lobe; posterior and lateral margins forming rounded curve; lateral margin with 38 large plumose setae; mesial margin with scale-setae on distal part only, 2 simple setae and 1 penicillate seta; distal margin with 6 simple setae; article 2 1.3 as long as wide; with 8 simple setae; article 3 minute, with 4 simple setae.

Pereopods 2–6 with long simple setae and randomly covered in pectinate scales (only illustrated on pereopod 2); inferior margins with weak tubercles. *Pereopod 2* with tubercles on merus and carpus; basis 2.9 times as long as greatest width, superior margin with 19 setae, inferior margin with 12 setae; ischium 0.7 times as long as basis, 2.5 as long as wide, superior margin with 6 simple setae and 1 long setose seta, inferior margin with 17 setae; merus 0.5 as long as ischium, 1.5 as long as wide, superior margin with bulbous protrusion and 4 setae, inferior margin with tubercles and 7 setae; carpus 0.5 as long as ischium, 1.8 as long as wide, superior margin with 2 setae (1 setose), inferior margin with tubercles and 5 setae (1 serrate seta); propodus 0.7 times as long as ischium, 2.5 times as long as wide, superior margin with 3 simple setae and 1 penicillate seta, inferior margin with 2 simple setae and 2 robust setae; dactylus 0.7 as long as propodus, terminates in sharp posterior pointing unguis. *Pereopods 3 and*

4 similar to pereopod 2. *Pereopod 5* similar to pereopod 6. *Pereopod 6* with tubercles on merus and carpus; basis 3 times as long as greatest width, superior margin with 14 setae, and 1 penicillate seta, inferior margin with 11 setae; ischium 0.9 as long as basis, 3.2 as long as greatest width, superior margin with 12 setae, inferior margin with 8 setae; merus 0.5 as long as ischium, 1.8 times as long as wide, superior margin with 6 setae, inferior margin with 4 setae, without dense patch of scale-setae; carpus 0.5 as long as ischium, 2.2 times as long as wide, superior margin with 3 setae, inferior margin with 4 setae; propodus 0.6 as long as ischium, 3.8 times as long as wide, superior margin with 5 setae, inferior margin with 5 setae, and 2 robust setae; dactylus 0.6 as long as propodus.

Penes produced, more than a third length of pereon; penial process 6.5 times as long as basal width, anterior end ending in sac-like extension dorsal to opening.

Pleopod 2 exopod 1.7 as long as wide, distally broadly rounded, with 9 plumose setae; endopod 1.8 as long as wide, distally broadly rounded, with 8 plumose setae; appendix masculina absent; peduncle 0.8 times as wide as long, mesial margin with 2 coupling setae, lateral margin with 1 simple seta.

Uropod rami extending beyond pleotelson, apices narrowly rounded. *Peduncle* with 1 dorsal seta. *Uropod endopod* 2.4 as long as greatest width, dorsally with 4 setae; lateral margin straight, lateral margin with 6 simple setae; proximomesial margin weakly convex, with 6 long plumose setae. *Uropod exopod* not extending to end of endopod, 3.3 times as long as greatest width; lateral margin weakly sinuate, with 17 simple setae; proximomesial margin straight, distally convex, with 3 long plumose setae.

Description of praniza 3 larva. (Figs 4–6). *Body* 3.5 times as long as greatest width; dorsal surfaces sparsely punctate, sparsely setose. *Cephalosome* 0.7 times as long as wide; posterior margin slightly concave; lateral margins convex; dorsal surface with few sensory pits and no setae; anterior margin straight with lateral concave excavations to accommodate first articles of antennae. *Labrum* prominent, 0.4 times as long as cephalosome, semicircular with apical process, anterior margin concave. *Eyes* well developed, oval-shaped; almost as long as cephalosome; one eye 0.3 as wide as cephalosome, bulbous, standing out from head surface; ommatidia arranged in rows; eye colour black.

Pereon elongate, 2.3 times as long as wide, smooth, with no setae or sensory pits. *Pereonite 1* partially fused dorsally with cephalosome; dorsally visible; dorsolateral margins partly obscured by cephalosome. *Pereonite 2 and 3* similar in size and shape. *Pereonite 4* triangular, 2.1 times as wide as long, posterior margin stretching over pereonite 5, lateral shields at leg attachment. *Pereonite 5* consists of elastic membrane fully expanded in praniza stage with blood meal, lateral shields at leg attachment. *Pereonite 6* rectangular, posterior margin slightly concave, lateral shields at leg attachment. *Pereonite 7* dorsally visible; posterior margin rounded, overlapping pleonite 1. *Pleon* with all 5 pleonites dorsally visible; pleon and pleotelson 0.4 times as long as pereon. *Pleonite 5* almost twice the length of the other articles. *Pleotelson* 1.3 times as long as anterior width, covered in pectinate scales; lateral margins finely serrate; anterolateral margins concave, without submarginal setae; posterolateral margin weakly convex, with 2 submarginal setae; mid-dorsal surface with 2 submedian setae, apex with 2 setae.

Antennula shorter than antenna; peduncle with short hair-like setae on anterior borders of all three articles; article 2 with 3 setae, as long as article 1; article 3 with 2 setae (1 penicillate), 2.3 times as long as article 2, 2.9 times as long as wide. Antennula flagellum 1.1 times as long as article 3, with 4 articles; article 1 with 2–3 setae; article 2 with 1 aesthetasc seta and 1 simple seta, 0.6 times as long as flagellum; article 3 with 1 aesthetasc seta; article 4 terminating with 1 aesthetasc seta and 3 simple setae. *Antenna* with rows of long simple setae on anterior margins of all 4 peduncle articles; peduncle article 3 2.3 times as long as wide, 2 times as long as article 2, with 4 simple setae; article 4 twice as long as article 3, 4.2 times as long as wide, with 6 simple setae; flagellum 1.1 times as long as article 4, with 7 articles, terminating with 3 or 4 simple setae.

Mandible stout, distal margin styliform with 16 teeth on mesial margin (3 smaller at tip of mandible), conical and posteriorly directed, increasing in size from anterior to posterior.

Paragnaths elongate, gutter-like, terminates in sharp point, no teeth.

Maxillula long, slender, 6–8 small teeth on distal inner margin, lateral border with marginal setae proximally.

Maxilliped cylindrical with elongated base, endite extending to distal margin of palp article 2, with 1 long simple seta and coupling seta. *Maxilliped palp* 3-articled; article 1 with 6 teeth mesially, lateral margin with setae; article 3 with 5–7 simple setae.

Gnathopod smaller than pereopods, with 7 articles, carpus reduced, few simple setae on articles 1–5, 1 robust seta on article 2.

Pereopods 2–6 with long simple setae, pectinate scales covering inner margins of propodus and carpus, and outer margins of merus. *Pereopod 2* with tubercles on carpus; basis 2.6 times as long as greatest width, superior margin with 5 setae, inferior margin with 2 setae; ischium 0.7 times as long as basis, twice as long as wide, superior margin with 2 setae, inferior margin with 1 seta; merus 0.5 as long as ischium, 1.3 as long as wide, superior margin with bulbous protrusion, with 3 setae (2 serrate) and pectinate scales, inferior margin with 2 setae; carpus 0.5 as long as ischium, 1.6 as long as wide, superior margin with no setae, inferior margin with 4 setae (1 serrate) and pectinate scales; propodus 0.7 times as long as ischium, 2.3 times as long as wide, superior margin with 2 setae (1 penicillate), inferior margin with 1 simple seta, 2 robust setae and pectinate scales; dactylus 0.9 as long as propodus, with 5 setae, terminates in sharp posterior pointing unguis. *Pereopods 3 and 4* similar to pereopod 2 (differ in setation). *Pereopod 5* similar to pereopod 6. *Pereopod 6* with tubercles on carpus; basis 3.3 times as long as greatest width, superior margin with 12 setae, inferior margin with 3 setae; ischium 0.7 as long as basis, 2.5 as long as greatest width, superior margin with 4 setae (1 penicillate, 2 setose), inferior margin with 2 setae; merus 0.6 as long as ischium, 1.4 times as long as wide, superior margin with bulbous protrusion and 3 setae (2 serrate), inferior margin with 2 setae, with dense patches of pectinate scales; carpus 0.6 as long as ischium, 2.2 times as long as wide, superior margin with 2 setae, inferior margin with 3 setae (1 serrate) and pectinate scales; propodus 0.8 as long as ischium, 3.6 times as long as wide, superior margin with 9 setae, inferior margin with 1 seta, 2 robust setae, and pectinate scales; dactylus 0.6 as long as propodus, with 4 setae, terminates in sharp posterior pointing unguis.

Pleopod 1 exopod 1.9 as long as wide, distally broadly rounded, with 8 plumose setae; endopod 1.8 as long as wide, distally narrowly rounded, with 7 plumose setae; peduncle 0.8 times as wide as long, mesial margin with 2 coupling setae, lateral margin with 1 simple seta.

Uropod rami extending to pleotelson apex, apices narrowly rounded, fringes with short simple setae. *Peduncle* with 2 dorsal setae. *Uropod endopod* 1.9 as long as greatest width, dorsally with 3 setae; lateral margin straight, lateral margin with 3 simple setae; proximomesial margin weakly convex, with 6 long plumose setae. *Uropod exopod* not extending to end of endopod, 3 times as long as greatest width; lateral margin weakly convex, with 5 simple setae; proximomesial margin straight, distally concave, with 4 long plumose setae.

Etymology. The Xhosa word "pipinde" was chosen, because "pipi" means penis and the post "nde" means long in the language of this southern African tribe and thus referring to the most distinct characteristic of this species. Pronounced as pie-pie-n-dê. The species epithet is a noun in apposition.

Distribution. South coast of South Africa (Western and Eastern Cape Provinces).

Hosts. *Amblyrhynchotes honckenii* (Bloch, 1785).

Remarks. *Gnathia pipinde* sp. nov. can be identified by the straight frontal margin; presence of conical superior frontolateral processes; a strong and bifid mediofrontal process; pronounced and pointed supraocular lobes; mandible strongly curved with a dentate blade; and the claviform penes produced more than a third the length of the pereon.

When compared to the other known South African gnathiid species, the shape and size of the frontal processes of *G. pipinde* are very similar to those of *G. africana* Barnard 1914 (see Smit et al. 1999) and *G. nkulu* Smit & Van As, 2002 (see Smit and Van As 2002). This species can, however, easily be distinguished from the other South African congeners by the shape and size of its elongated penes, narrowing at the distal end with a sac-like extension.

There are currently 134 species of *Gnathia* known to science (Boyko et al. 2008 onwards). To the authors' knowledge there are nine other *Gnathia* species with elongate penes that differ from each other in shape in size, namely: *Gnathia camuripenis* Tanaka, 2004; *Gnathia cooki* Müller, 1989; *Gnathia dentata* (G.O. Sars, 1872); *Gnathia falcipenis* Holdich & Harrison, 1980; *Gnathia fallax* Monod, 1926; *Gnathia inopinata* Monod, 1926; *Gnathia limicola* Ota & Tanaka; 2007; *Gnathia phallonajopsis* Monod, 1925; and *Gnathia somalia* Kensley, Schotte & Poore, 2009. Of these, only three resemble that of *G. pipinde* sp. nov. These are *G. falcipenis* from the Great Barrier Reef, Australia; *G. cooki* from Morea, Society Islands in the tropical Pacific; and *G. camuripenis* from southern Japan and the Philippines (Shodipo et al. 2021). According to Holdich and Harrison (1980), the mediofrontal process of *G. falcipenis* is conical and, thus, distinctly different from the bifid mediofrontal process of *G. pipinde* sp. nov. The superior frontolateral processes and shape of the pleotelson of *G. cooki* described by Müller (1989) are very similar to those of *G. pipinde* sp. nov. However, in the South African species there are six long simple setae on each superior frontolateral process and the inferior frontolateral processes are absent, whereas in the species from the Pacific there are only three long simple setae and the inferior frontolateral processes are present. In addition, *G. pipinde* sp. nov.

differs in the number of antenna flagellum articles (seven instead of six), and the number of plumose setae on the distal four articles of the maxillipeds (in the order of 5-7-6-7 instead of 5-6-5-7 as in *G. cooki*). The males of *G. camuripenis* can easily be distinguished from *G. pipinde* sp. nov. in its rounded mediofrontal process without a ventral notch and large bifid internal lobe present on the mandibles (Tanaka 2004).

The larvae of *G. pipinde* sp. nov. can be distinguished from the described larvae of the South African species, *G. africana* and *G. pantherina* Smit & Basson, 2002, by the presence of 16 teeth on the mandible (*G. africana* with nine or 10 and *G. pantherina* with eight). The shape of the pleotelson of *G. pipinde* (posterior two-thirds convex) also differs from that of *G. africana* (lateral margins straight) and *G. pantherina* (anterior half of lateral margins slightly concave).

This species is host-specific to *Amblyrhynchotes honckenii* and only occurs on the temperate south coast of South Africa (with low intensity and rare infections), despite the wide distribution of the host fish (temperate south coast to subtropical east coast of South Africa). The specific locality preference is also observed with another parasitic isopod on this host fish, *Cinusa tetrodontis* Schioedte & Meinert, 1884. Hadfield et al. (2010) reported this species from *A. honckenii*, also only from the temperate south coast of South Africa. This specific area seems to be a parasite diversity hotspot within the TSA realm and could still yield other unknown parasites with further research. Information on the nine known gnathiid species from the TSA is summarised in Table 1, along with a key to these species.

Key to species of the family Gnathiidae known from the Temperate Southern African (TSA) realm

This key is based on the morphological characters of the adult male:

1 Cephalosome wider than pereon; frontal border concave ..... ***Gnathia spongicola* Barnard, 1920**
– Cephalosome not wider than pereon; frontal border produced..... **2**
2 Frontal border rounded, strongly produced, without any frontal processes..... ***Caecognathia cryptopais* (Barnard, 1925)**
– Frontal border slightly produced, with frontal processes..... **3**
3 Pylopod single-articled; two rows of teeth on mandible blade ..... ***Afrignathia multicavea* Hadfield & Smit, 2008**
– Pylopod 2- or 3-articled; absent or single row of teeth on blade **4**
4 Mediofrontal processes bifid..... **5**
– Mediofrontal processes absent or not bifid **6**
5 Penes produced, more than a third length of pereon.... ***Gnathia pipinde* sp. nov.**
– Penes not produced, two contiguous papillae as long as wide ..... ***Gnathia africana* Barnard, 1914**
6 Mandibles short and stout (<0.5 length of cephalosome) ..... ***Gnathia pilosus* Hadfield, Smit & Avenant-Oldewage, 2008**
– Mandibles long (>0.5 length of cephalosome)..... **7**

7 Pereonite 5 completely separated into two lateral halves (pereonite 6 in contact with pereonite 4).....***Gnathia disjuncta* Barnard, 1920**
– Pereonite 5 not separated (pereonite 6 not in contact with pereonite 4) **8**
8 Pereonite 5 areae laterales absent, narrower than pereonite 6; pleopod 2 with appendix masculina > 0.5 length of rami .....***Gnathia nkulu* Smit & Van As, 2000**
– Pereonite 5 areae laterales present, as wide or wider than pereonite 6; pleopod 2 with appendix masculina < 0.5 length length of rami.....
.....***Gnathia pantherina* Smit & Basson, 2002**

Acknowledgements

This work was in part supported by the National Research Foundation (NRF) of South Africa (NRF Project Grant No. 20403; KA Hadfield, PI). Opinions, findings, conclusions, and recommendations expressed in this publication are that of the authors, and the NRF accepts no liability in this regard. This is contribution number 699 for the NWU Water Research Group.

References

Barnard KH (1914) Contributions to the crustacean fauna of South Africa. 1. Additions to the marine Isopoda. Annals of the South African Museum 10: 197–230. https://doi.org/10.5962/bhl.part.9314

Barnard KH (1920) Contributions to the crustacean fauna of South Africa. No. 6. Further additions to the list of marine Isopoda. Annals of the South African Museum 17: 319–438. https://doi.org/10.5962/bhl.part.22318 [pls XV–XVII.]

Barnard KH (1925) Contributions to the crustacean fauna of South Africa. No. 9. Further additions to the list of Isopoda. Annals of the South African Museum 20: 381–412.

Boyko CB, Bruce NL, Hadfield KA, Merrin KL, Ota Y, Poore GCB, Taiti S (Eds) (2008 onwards) World Marine, Freshwater and Terrestrial Isopod Crustaceans database. *Gnathia* Leach, 1814. World Register of Marine Species. https://www.marinespecies.org/aphia.php?p=taxdetails&id=118437 [Accessed on 2022-08-22.]

Brandt A, Poore GCB (2003) Higher classification of the flabelliferan and related Isopoda based on a reappraisal of relationships. Invertebrate Systematics 17(6): 893–923. https://doi.org/10.1071/IS02032

Cohen BF, Poore GCB (1994) Phylogeny and biogeography of the Gnathiidae (Crustacea: Isopoda) with descriptions of new genera and species, most from south-eastern Australia. Memoirs of the Museum of Victoria 54(2): 271–397. https://doi.org/10.24199/j.mmv.1994.54.13

Farquharson C, Smit NJ, Grutter AS, Davies AJ (2012) *Gnathia masca* sp. nov. (Crustacea, Isopoda, Gnathiidae) from Lizard Island, Great Barrier Reef, Australia. Zootaxa 3233: 22–36. https://doi.org/10.11646/zootaxa.3233.1.2

Ferreira ML, Smit NJ, Davies AJ (2010) *Gnathia grutterae* sp. nov. (Crustacea, Isopoda, Gnathiidae) parasitising representatives of the Balistidae, Labridae and Tetraodontidae

from Lizard Island, Great Barrier Reef, Australia. Zootaxa 2718(1): 39–50. https://doi.org/10.11646/zootaxa.2718.1.3

Froese R, Pauly D (Eds) (2022) FishBase. World Wide Web electronic publication, version (06/2022). http://www.fishbase.org

Griffiths CL, Robinson TB, Lange L, Mead A (2010) Marine biodiversity in South Africa: An evaluation of current states of knowledge. PLoS ONE 5(8): e12008. https://doi.org/10.1371/journal.pone.0012008

Grutter AS, Feeney WE, Hutson KS, McClure EC, Narvaez P, Smit NJ, Sun D, Sikkel PC (2020) Practical methods for culturing parasitic gnathiid isopods. International Journal for Parasitology 50(10–11): 825–837. https://doi.org/10.1016/j.ijpara.2020.03.014

Hadfield KA, Smit NJ (2008) Description of a new gnathiid, *Afrignathia multicavea* gen. et sp. nov. (Crustacea: Isopoda: Gnathiidae), from South Africa. African Zoology 43(1): 81–89. https://doi.org/10.1080/15627020.2008.11407410

Hadfield KA, Smit NJ, Avenant-Oldewage A (2008) *Gnathia pilosus* sp. nov. (Crustacea, Isopoda, Gnathiidae) from the East Coast of South Africa. Zootaxa 1894(1): 23–41. https://doi.org/10.11646/zootaxa.1894.1.2

Hadfield KA, Smit NJ, Avenant-Oldewage A (2009) Life cycle of the temporary fish parasite, *Gnathia pilosus* (Crustacea: Isopoda: Gnathiidae) from the east coast of South Africa. Journal of the Marine Biological Association of the United Kingdom 89(7): 1331–1339. https://doi.org/10.1017/S0025315409000587

Hadfield KA, Bruce NL, Smit NJ (2010) Redescription of the monotypic genus *Cinusa* Schioedte and Meinert, 1884 (Isopoda, Cymothoidae), a buccal-cavity isopod from South Africa. Zootaxa 2437(1): 51–68. https://doi.org/10.11646/zootaxa.2437.1.3

Hadfield KA, Schizas NK, Chatterjee T, Smit NJ (2019) *Gnathia bermudensis* (Crustacea, Isopoda, Gnathiidae), a new species from the mesophotic reefs of Bermuda, with a key to *Gnathia* from the Greater Caribbean biogeographic region. ZooKeys 891: 1–16. https://doi.org/10.3897/zookeys.891.39564

Holdich DM, Harrison K (1980) The crustacean isopod genus *Gnathia* Leach from Queensland waters with descriptions of nine new species. Marine and Freshwater Research 31(2): 215–240. https://doi.org/10.1071/MF9800215

Kensley B, Schotte M, Poore GCB (2009) Gnathiid isopods (Crustacea: Isopoda: Gnathiidae), mostly new, from the Indian Ocean. Proceedings of the Biological Society of Washington 122(1): 32–51. https://doi.org/10.2988/07-16.1

Monod T (1926) Les Gnathiidæ. Essai monographique (morphologie, biologie, systématique). Mémoires de la Société des Sciences Naturelles du Maroc 13: 1–668.

Müller HG (1989) Two new species of *Gnathia* each from coral reefs at Moorea, Society Islands, with redescription of *Gnathia margaritarum* Monod, 1926 from Panama Pacific (Isopoda: Cymothoidea: Gnathiidae). Bulletin Zoölogisch Museum Universiteit van Amsterdam 12: 65–80.

Shodipo MO, Sikkel PC, Smit NJ, Hadfield KA (2021) First record and molecular characterisation of two *Gnathia* species (Crustacea, Isopoda, Gnathiidae) from Philippine coral reefs, including a summary of all Central-Indo Pacific *Gnathia* species. International Journal for Parasitology. Parasites and Wildlife 14: 355–367. https://doi.org/10.1016/j.ijppaw.2021.03.004

Smit NJ, Basson L (2002) *Gnathia pantherina* sp. nov. (Crustacea: Isopoda: Gnathiidae), a temporary ectoparasites of some elasmobranch species from southern Africa. Folia Parasitologica 49(2): 137–151. https://doi.org/10.14411/fp.2002.025

Smit NJ, Davies AJ (1999) New host records for *Haemogregarina bigemina* from the coast of southern Africa. Journal of the Marine Biological Association of the United Kingdom 79(5): 933–935. https://doi.org/10.1017/S0025315499001101

Smit NJ, Davies AJ (2001) An encapsulated haemogregarine from the evileye pufferfish in South Africa. Journal of the Marine Biological Association of the United Kingdom 81(5): 751–754. https://doi.org/10.1017/S0025315401004556

Smit NJ, Davies AJ (2004) The curious life-style of the parasitic stages of gnathiid isopods. Advances in Parasitology 58: 289–391. https://doi.org/10.1016/S0065-308X(04)58005-3

Smit NJ, Hadfield KA (2015) Marine fish parasitology in South Africa: History of discovery and future direction. African Zoology 50(2): 79–92. https://doi.org/10.1080/15627020.2015.1043644

Smit NJ, Van As JG (2000) A new species, *Gnathia nkulu* sp. nov. (Crustacea: Isopoda: Gnathiidae) from southern Africa. Folia Parasitologica 47(3): 235–240. https://doi.org/10.14411/fp.2000.042

Smit NJ, Van As JG, Basson L (1999) A redescription of the adult male and praniza of *Gnathia africana* Barnard, 1914 (Crustacea, Isopoda, Gnathiidae) from southern Africa. Folia Parasitologica 46: 229–240.

Smit NJ, Basson L, Van As JG (2000) A redescription of the adult male of *Caecognathia cryptopais* (Barnard, 1925) (Crustacea: Isopoda: Gnathiidae) from southern Africa. Folia Parasitologica 47(1): 61–66. https://doi.org/10.14411/fp.2000.012

Smit NJ, Bruce NL, Hadfield KA (2019) Parasitic Crustacea: State of Knowledge and Future Trends. Springer Nature Switzerland, Cham, 481 pp. https://doi.org/10.1007/978-3-030-17385-2

Spalding MD, Fox HE, Allen GR, Davidson N, Ferdaña ZA, Finlayson M, Halpern BS, Jorge MA, Lombana A, Lourie SA, Martin KD, McManus E, Molnar J, Recchia CA, Robertson J (2007) Marine ecoregions of the world: A bioregionalization of coastal and shelf areas. Bioscience 57(7): 573–583. https://doi.org/10.1641/B570707

Svavarsson J, Bruce NL (2012) New and little-known gnathiid isopod crustaceans (Cymothoida) from the northern Great Barrier Reef and the Coral Sea. Zootaxa 3380(1): 1–33. https://doi.org/10.11646/zootaxa.3380.1.1

Svavarsson J, Bruce NL (2019) New gnathiid isopod crustaceans (Cymothoida) from Heron Island and Wistari Reef, southern Great Barrier Reef. Zootaxa 4609(1): 31–67. https://doi.org/10.11646/zootaxa.4609.1.2

Tanaka K (2004) A new species of *Gnathia* (Isopoda: Cymothoida: Gnathiidae) from Ishigaki Island, the Ryukyus, southwestern Japan. Crustacean Research 33(0): 51–60. https://doi.org/10.18353/crustacea.33.0_51

Watling L (1989) A classification system for crustacean setae based on the homology concept. In: Felgenhauer BE, Watling L, Thistle AB (Eds). Functional Morphology of Feeding and Grooming in Crustacea. Crustacean Issues, 6. A.A. Balkema, Rotterdam: 15–26. https://doi.org/10.1201/9781003079354-2

ZooKeys 1129: 21–35 (2022)
doi: 10.3897/zookeys.1129.82981
https://zookeys.pensoft.net

RESEARCH ARTICLE

A peer-reviewed open-access journal
ZooKeys
Launched to accelerate biodiversity research

A comparison of gene organisations and phylogenetic relationships of all 22 squamate species listed in South Korea using complete mitochondrial DNA

Daesik Park[1], Il-Hun Kim[2], Il-Kook Park[1], Alejandro Grajal-Puche[3], Jaejin Park[1]

1 *Kangwon National University, Chuncheon, Republic of Korea* **2** *National Marine Biodiversity Institute of Korea, Seochun, Republic of Korea* **3** *Northern Arizona University, Flagstaff, Arizona, USA*

Corresponding author: Jaejin Park (zhqnfth1217@naver.com)

Academic editor: Johannes Penner | Received 2 March 2022 | Accepted 16 September 2022 | Published 10 November 2022

https://zoobank.org/E56CE31A-C614-46D7-9A88-9B4A26C11340

Citation: Park D, Kim I-H, Park I-K, Grajal-Puche A, Park J (2022) A comparison of gene organisations and phylogenetic relationships of all 22 squamate species listed in South Korea using complete mitochondrial DNA. ZooKeys 1129: 21–35. https://doi.org/10.3897/zookeys.1129.82981

Abstract

Studies using complete mitochondrial genome data have the potential to increase our understanding on gene organisations and evolutionary species relationships. In this study, we compared complete mitochondrial genomes between all 22 squamate species listed in South Korea. In addition, we constructed Maximum Parsimony (MP), Maximum Likelihood (ML) and Bayesian Inference (BI) phylogenetic trees using 13 mitochondrial protein-coding genes. The mitochondrial genes for all six species in the suborder Sauria followed the same organisation as the sequenced Testudines (turtle) outgroup. In contrast, 16 snake species in the suborder Serpentes contained some gene organisational variations. For example, all snake species contained a second control region (*CR2*), while three species in the family Viperidae had a translocated *tRNA-Pro* gene region. In addition, the snake species, *Elaphe schrenckii*, carried a *tRNA-Pro* pseudogene. We were also able to identify a translocation of a *tRNA-Asn* gene within the five tRNA (*WANCY* gene region) gene clusters for two true sea snake species in the subfamily Hydrophiinae. Our BI phylogenetic tree was also well fitted against currently known Korean squamate phylogenetic trees, where each family and genus unit forms monophyletic clades and the suborder Sauria is paraphyletic to the suborder Serpentes. Our results may form the basis for future northeast Asian squamate phylogenetic studies.

Keywords

Full mitochondrial genome, Korea, phylogeny, rearrangement, Squamata, *tRNA-Pro*, *WANCY*

Introduction

Elucidating comparative gene organisations and phylogenetic relationships between species is essential for improving our understanding of their evolutionary histories and may allow for the successful conservation of endangered taxa (Vane-Wright et al. 1991; Crozier 1992; Boore et al. 1995; Mouquet et al. 2012). Knowledge of genetic organisational variations often give further insights into the evolutionary history of species and could be helpful in developing conservation management plans (Swenson 2019). Additionally, gene organisation data provide reliable phylogenetic information within the evolutionary branches (Boore 1999). Furthermore, defining a phylogenetic species, using mitochondrial and nuclear genes, is often vital to designate if a species is endangered at a national level (An et al. 2010).

The mitochondrial genome is an important model system used to understand genome structure, molecular evolution and phylogenetic relationships amongst vertebrates (Moritz and Brown 1986; Pääbo et al. 1991; Inoue et al. 2003; Krishnan et al. 2004; Jiang et al. 2007; Qian et al. 2018). Specific mitochondrial genes, such as the 12S ribosomal RNA (*12S rRNA*), 16S ribosomal RNA (*16S rRNA*), NADH dehydrogenase subunit 4 (*ND4*), cytochrome c oxidase subunit I (*COI*) and cytochrome b (*Cytb*) have been often used to compare phylogenetic relationships between vertebrates (Malhotra and Thorpe 2004; Rivera et al. 2018; Sidharthan et al. 2021). Although phylogenetic studies using mitochondrial sequences have both advantages and disadvantages (Rubinoff and Holland 2005), using the complete mitochondrial genome may provide higher phylogenetic resolution between species (Inoue et al. 2003; Nardi et al. 2003; Qian et al. 2018). In addition, a comparison of gene organisations, using complete mitochondrial genomes, could give a more precise understanding of the evolutionary histories between species (Boore 1999). To date, a total of 6,781 complete vertebrate mitochondrial genome sequences have been deposited in GenBank (National Center for Biotechnology Information; NCBI), of which 303 are squamates. These 303 sequenced mitochondrial genomes account for approximately 3.8% of the total 7,953 known squamate species (http://www.reptile-database.org/).

Squamates are the most speciose order amongst reptiles, have high ecological and morphological diversity and are found nearly worldwide, with the exception of Antarctica (Greene 1997; Pianka et al. 2003; Vitt and Caldwell 2013). Squamates are divided into two suborders, Sauria and Serpentes. In South Korea, there are six saurian species (five lizards and one gecko species) across four genera and 16 snake species across 10 genera. Together, these squamate species account for 71.0% of all South Korean reptiles (two orders, 11 families, 22 genera and 31 species). In South Korea, there have been several phylogenetic studies mapping reptilian phylogenetic associations. Lee (2010) morphologically demarcated several lizard species, while Lee (2011) combined two *Elaphe schrenckii* subspecies by comparing specific mitochondrial genes and microsatellite alleles. *Rhabdophis tigrinus*, listed in both South Korea and Japan, was recently reclassified as *R. lateralis*, based on mitochondrial genes (Takeuchi et al. 2014). More recently, Kim (2018) applied morphological data in addition to complete

mitochondrial genome sequences to classify sea snake species found in Korean waters. Only one large-scale reptilian phylogenetic study has phylogenetically distinguished between Korean serpent species, based on both morphological and isozyme data (Paik 1982). Thus far, there have been no phylogenetic reconstructions using gene organisations amongst Korean squamates using complete mitochondrial genomes.

Recent phylogenetic molecular advances have made it more possible to compare complete mitochondrial genome relationships between species (Lee et al. 2021; Zhang et al. 2021; Vanerelli et al. 2022). These molecular advances make it a prime occasion to update our understanding of the phylogenetic relationships amongst squamates, specifically in South Korea. In this study, we compared mitochondrial gene organisations and constructed three types of phylogenetic trees amongst all 22 squamate species listed in South Korea, using complete mitochondrial sequence data. These results have the potential to impact future squamate phylogenetic studies in northeast Asia.

Materials and methods

Complete mitochondrial DNA (mtDNA) sequences, for all 22 squamate species listed in South Korea, were downloaded from GenBank (NCBI). We tried to obtain mtDNA sequence data from individuals, captured within South Korea. When it was not possible, we used mtDNA data from specimens collected in China, Japan or Russia (Table 1) that were within the distribution range of the same species listed in South Korea (Takeuchi et al. 2014; Lee et al. 2022). The downloaded, foreign-originated sequences from GenBank showed high similarity with the preliminary BLAST analysis using partial 16S ribosomal RNA (*16S rRNA*), cytochrome oxidase subunit I (*COI*) or cytochrome b (*Cytb*) sequences of South Korean specimens (Jeong et al. 2013). For *Hydrophis cyanocinctus* and *H. melanocephalus*, we used the data from individuals caught at locations nearest to South Korea, as there were no data available from South Korean specimens. After confirming complete mitochondrial genes for each species, we arranged and compared the mitochondrial genes between species, based on transfer RNA (tRNA) positions and ribosomal RNA (rRNA) and protein-coding gene (PCG) positions, which were determined using tRNAscan-SE 2.0 (Chan and Lowe 2019) and MITOS Webserver (Bernt et al. 2013), respectively. We excluded *H. cyanocinctus* from the analysis due to the uncertainty of the nucleotide sequence in non-protein-coding regions, such as rRNA, tRNA, O_L and CR within a cluster of five tRNA genes (*WANCY* gene region).

To construct the phylogenetic tree of all 22 squamate species listed in South Korea, we used 13 mitochondrial PCGs (Fenn et al. 2008; Douglas and Gower 2010; He et al. 2010). The sequence of each PCG was extracted and aligned using MUSCLE, with a maximum of 20 iterations (Edgar 2004). Aligned sequence genes were concatenated into one sequence using Geneious v.9.1.8 (Kearse et al. 2012). We used two sea turtle species, *Caretta caretta* and *Chelonia mydas*, as outgroups for our constructed phylogenetic tree. We used PAUP 4.0a168 (Swofford 2001) to create the Maximum Parsimony (MP) phylogenetic tree. To increase the reliability of the MP phylogenetic tree, we performed

Table 1. All 22 analysed squamate species listed in South Korea and their sampling locations analysed in this study. Original sample location, GenBank accession number and mt-genome base pair length are provided.

Suborder	Family	Species	Location	GenBank No.	Length (bp)
Sauria	Gekkonidae	*Gekko japonicus*	S. Korea	KR996131	16,544
	Scincidae	*Scincella vandenburghi*	S. Korea	KU646826	17,103
		Scincella huanrenensis	S. Korea	KU507306	17,212
	Lacertidae	*Takydromus amurensis*	China	KU641018	17,333
		Takydromus wolteri	China	JX181764	18,236
		Eremias argus	S. Korea	JQ086345	18,521
Serpentes	Colubridae	*Elaphe dione*	Russia	MH460961	17,172
		Elaphe schrenckii	China	KP888955	17,165
		Oocatochus rufodorsatus	China	KC990020	17,159
		Rhabdophis lateralis	China	KU641019	17,415
		Hebius vibakari	China	KP684155	17,259
		Lycodon rufozonatus	China	KJ179950	17,188
		Orientocoluber spinalis	S. Korea	MT304473	17,196
		Sibynophis chinensis	S. Korea	KF360246	17,163
	Viperidae	*Gloydius ussuriensis*	China	KP262412	17,208
		Gloydius brevicaudus	China	EU913477	17,227
		Gloydius saxatilis	S. Korea	MW143075	17,223
	Elapidae	*Hydrophis cyanocinctus*	China	MK953550	17,750
		Hydrophis melanocephalus	Japan	MK775532	17,182
		Hydrophis platurus	S. Korea	MK775530	18,101
		Laticauda laticaudata	S. Korea	KY496323	17,209
		Laticauda semifasciata	S. Korea	KY496325	17,170
Cryptodira	Cheloniidae	*Chelonia mydas*	Cyprus	JX454990	16,495
		Caretta caretta	USA	JX454983	16,454

1,000 bootstrap iterations. For estimating the MP tree, we applied a heuristic search using tree bisection and reconnection (TBR) and branch swapping approaches. We used RAxML v.7.2.8 (Stamatakis 2006) to create the Maximum Likelihood (ML) phylogenetic tree. To select the best nucleotide model for the ML analysis, we used jModelTest 2.1.10 (Darriba et al. 2012) and selected the GTR GAMMA I model through AIC calculations. The rapid bootstrapping value was calculated while selecting the best-scoring tree from 100 ML trees. To construct the Bayesian Inference (BI) phylogenetic tree, we used MrBayes v.3.2.6 (Huelsenbeck and Ronquist 2001). For the BI phylogenetic tree, each substitution model and rate variation was set to GTR and gamma, respectively. For the Markov Chain Monte Carlo (MCMC) analysis of the BI tree, the chain length was set to 1,000,000, while the subsampling frequency was set to 100. The MCMC heated chain was also set to 4, the heated chain temperature was set to 0.2 and the burn-in cut-off was at 50,000.

Results

All six species within the suborder Sauria matched the mitochondrial organisation of the sea turtle outgroup (Fig. 1). In contrast, all 16 snake species in the suborder Serpentes had a second control region (*CR2*) between the NADH dehydrogenase subunit 1 (*ND1*) and the NADH dehydrogenase subunit 2 (*ND2*). These 16 snake species also

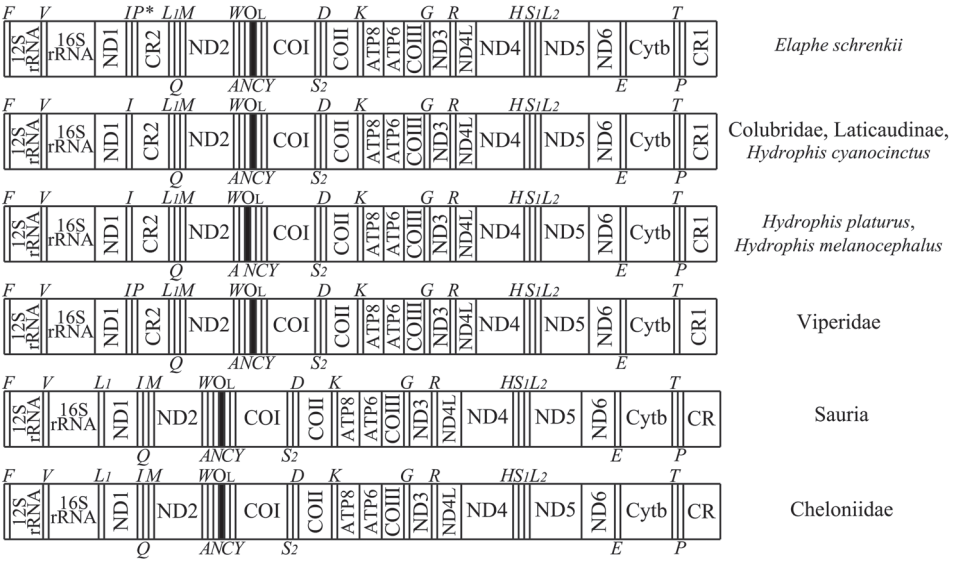

Figure 1. Comparison of the mitochondrial gene organisation for all 22 squamate species listed in South Korea. Two sea turtle species (*Caretta caretta* and *Chelonia mydas*), served as outgroups. *L1*, *L2*, *S1*, *S2*. *P** represent the following genes: *tRNA-Leu* (UUR), *tRNA-Leu* (CUN), *tRNA-Ser* (AGY), *tRNA-Ser* (UCN) and a pseudo *tRNA-Pro* gene, respectively. tRNA genes are abbreviated by the corresponding one-letter amino acid codes, such as *F*, *V*, *I*, *M* etc.

had translocated *tRNA-Leu* (UUA) genes between *tRNA-Ile* and *tRNA-Gln*. In addition, three species in the family Viperidae had a translocated *tRNA-Pro* gene. The *tRNA-Pro* gene was originally between *tRNA-Thr* and *CR1* genes, but was translocated in between the *tRNA-Ile* and *CR2* genes. Moreover, the three viperid species lacked any *tRNA-Pro* pseudogenes observed in the other serpent species. In *H. platurus* and *H. melanocephalus*, the *tRNA-Asn* gene, originally located between *tRNA-Ala* and the light strand replication origin (O_L) in other snakes, had also been translocated between the O_L region and the *tRNA-Cys* gene within the WANCY cluster region. Finally, a pseudo-*tRNA-Pro* gene was discovered between the *tRNA-Ile* and *CR2* genes in *Elaphe schrenckii*.

The aligned sequence data for the 13 mitochondrial protein-coding genes were concatenated to 11,581 bp. The suborders Sauria and Serpentes each formed monophyletic clades in both MP and ML phylogenetic trees (Fig. 2). In contrast, all six species within the suborder Sauria were paraphyletic to the suborder Serpentes in the BI tree (Fig. 3). Branching patterns were the same between Viperidae and Elapidae families amongst our three constructed phylogenetic trees. Specifically, two species in the family Viperidae, *Gloydius ussuriensis* and *G. brevicaudus*, were more closely related, while *G. saxatilis* formed a sister clade. Within the genus *Hydrophis*, *H. cyanocinctus* and *H. melanocephalus* clustered more closely together than *H. platurus*. For the family Colubridae, species in the BI tree were paraphyletic, which differed from our constructed ML and MP trees. In the BI tree, *Gekko japonicus* was basal to all other saurian species.

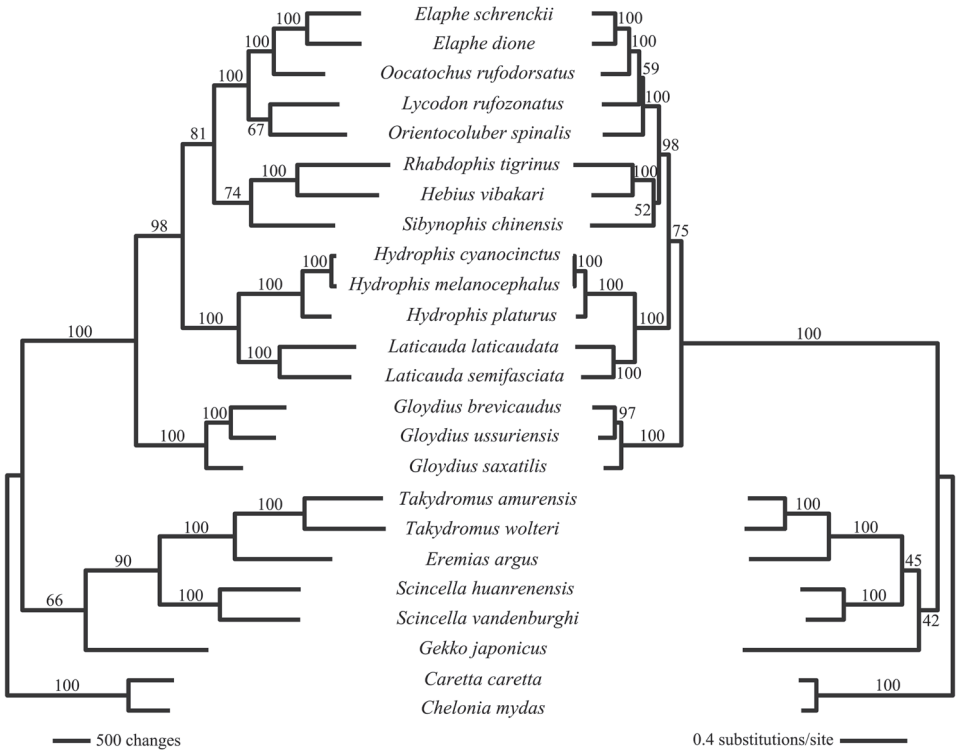

Figure 2. Maximum Parsimony (MP) tree (left) and Maximum Likelihood (ML) tree (right) for all 22 squamates listed in South Korea. Both MP and ML trees are based on 13 mitochondrial protein-coding genes. *Caretta caretta* and *Chelonia mydas* are outgroup species. Bootstrap values are denoted on each tree branch.

Discussion

We compared gene organisations and elucidated phylogenetic relationships, using complete mitochondrial genomes, for all 22 squamate species listed in South Korea. Using this complete mtDNA approach, we were able to uncover unique evolutionary insights amongst South Korean squamates.

Relative to the six saurian species, we discovered that all 16 snake species in the suborder Serpentes had an additional control region (*CR2*) and a translocated *tRNA-Leu* (UUR) gene. These genetic characteristics have been documented in many other snake species, except for the infraorder Scolecophidia (Douglas et al. 2006; Jiang et al. 2007). The *CR2* was located between *ND1* and *ND2* genes and may be an example of a non-independent replication event (Dover 1982; Kumazawa et al. 1998; Dong and Kumazawa 2005). The presence of two control regions may increase the rate of mitochondrial gene replication (Jiang et al. 2007). Duplication of the *CR* is not novel amongst vertebrates and has been identified in fishes (Lee et al. 2001; Inoue et al. 2003), frogs (Sano et al. 2005; Huang et al. 2019), lizards (Kumazawa and Endo 2004; Amer and Kumazawa

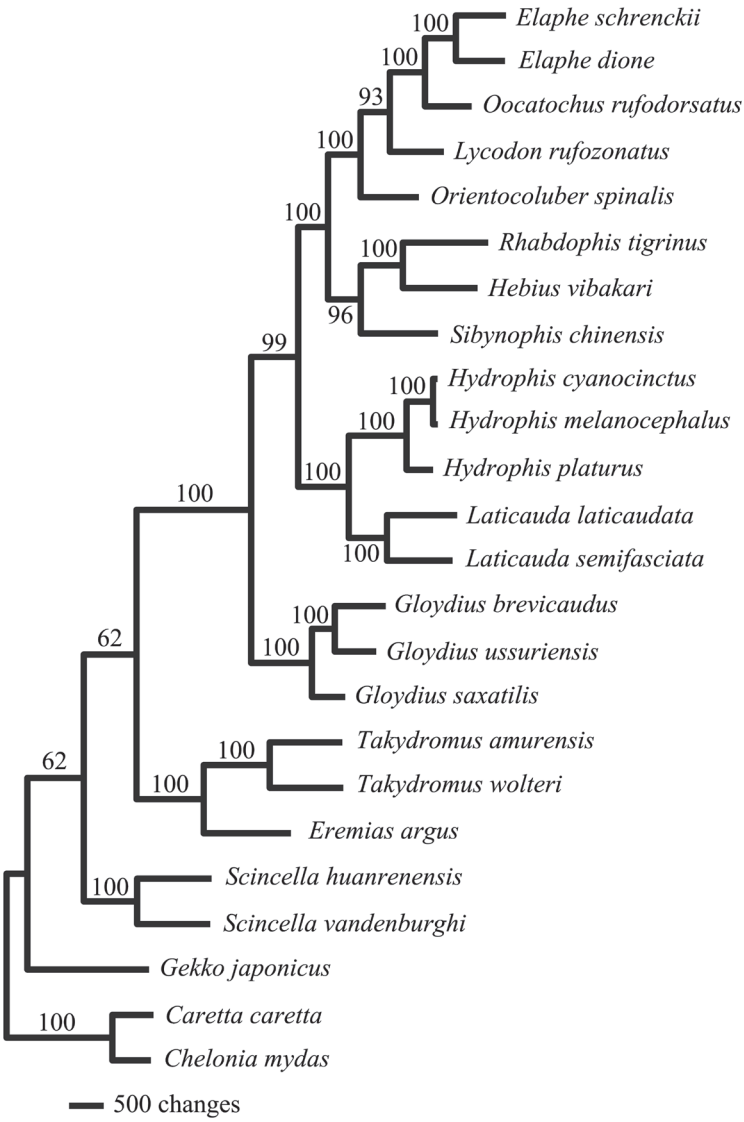

Figure 3. The constructed Bayesian Inference (BI) tree for all 22 squamate species listed in South Korea, based on 13 mitochondrial protein-coding genes. Two cheloniid species (*Caretta caretta* and *Chelonia mydas*) were used as outgroups. Bayesian posterior probabilities are denoted on each tree branch.

2005) and birds (Eberhard et al. 2001; Sammler et al. 2011). The translocation of *tRNA-Leu* (UUR) gene, identified in this study, is considered an ancestral trait of the infraorder Alethinophidia (Dong and Kumazawa 2005). In vertebrates, the *tRNA-Leu* gene has been shown to alter the transcribed ratios between the rRNA and protein-coding gene as terminators for heavy-stranded transcripts (Fernández-Silva et al. 2003). The presence

of the *CR2* and the translocation of the *tRNA-Leu* gene might also prevent a thermodynamic depression of transcriptional enzymes in snakes (Jiang et al. 2007).

All three *Gloydius* species, listed in South Korea, had translocated *tRNA-Pro* gene regions, which is consistent with other previously reported Viperidae species, such as *Agkistrodon piscivorus* (Jiang et al. 2007), *Causus defilippi* (Castoe et al. 2009), *Bothrops pubescens* (GenBank No. MG182598) and *Vipera berus* (Gao et al. 2018). In contrast, we did not detect any half-sized *tRNA-Pro* pseudogenes from the three analysed *Gloydius* species, although the half-sized pseudogenes have been previously reported in a closely-related species, *G. strauchi* (GenBank No. MF523224). The half-sized tRNA-Pro pseudogene, adjacent to the 5' end of *CR1*, has also been reported in *Ovophis okinavensis* (Kumazawa et al. 1996) and in several other crotaline species, such as *Protobothrops kaulbacki* (Kang et al. 2017), *Trimeresurus albolabris* (Song et al. 2015) and *T. sichuanensis* (Zhu et al. 2016). The half-sized *tRNA-Pro* pseudogene is considered a shared ancestral trait amongst crotaline species and may have been lost and subsequently recovered independently between species (Wüster et al. 2008).

In *H. platurus* and *H. melanocephalus*, the *tRNA-Asn* gene was translocated between the O_L and *tRNA-Cys* genes. The *tRNA-Asn* gene is usually located between *tRNA-Ala* and O_L in the WANCY region in other snakes and vertebrates (Boore 2000; Qian et al. 2018; Fig. 4). To our knowledge, this is the first finding of a *tRNA-Asn* translocation in the infraorder Alethinophidia. Mitochondrial genetic rearrangements are often found near control or WANCY regions in serpents (Qian et al. 2018). Tandem duplication random loss (TDRL) models often explain that some gene rearrangements may occur due to random paralog deletions (Moritz et al. 1987; Boore 2000; Xiaokaiti et al. 2022). These random paralog deletions may explain our results, as paralog deletions have caused gene rearrangements in other vertebrates including lizards, marsupials, birds and fishes (Moritz and Brown 1986, 1987; Moritz et al. 1987; Pääbo et al. 1991; Boore 2000; Inoue et al. 2003). We were also able to identify a novel gene rearrangement in sea snakes found off the coasts of South Korea. To our knowledge, this gene rearrangement has not been detected in other elapid species, including cobras (Yan et al. 2008; Castoe et al. 2009; Singchat et al. 2019) and sea kraits (Kim et al. 2018).

The existence of the intergenic spacers, which are non-coding regions between genes, is evidence of certain genetic deletions (San Mauro et al. 2006; Xiaokaiti et al. 2022). The gene rearrangement observed in the true sea snake species may be the result of a duplication of the *WANCY* genes and subsequent deletions of certain parts of other genes (Fig. 4A). We were also able to corroborate the occurrence of similar gene rearrangements in two other foreign sea snake species, *Emydocephalus ijimae* and *H. curtus*, for which complete mt-genome were available (GenBank MK775531, MT712129; Yi et al. 2019; Zhang and Yan 2020) (Fig. 4B, C). This WANCY gene rearrangement was not present in the four sequenced terrestrial cobra species (*Bungarus fasciatus*, *Micrurus fulvius*, *Naja naja* and *Sinomicrurus macclellandi*; GenBank No. EU579523, GU045453, DQ343648, MT547176; Yan et al. 2008; Castoe et al. 2009; Yao et al. 2020). Uploading and comparing additional mt-genome data for closely-related Australian terrestrial cobras and sea snakes may

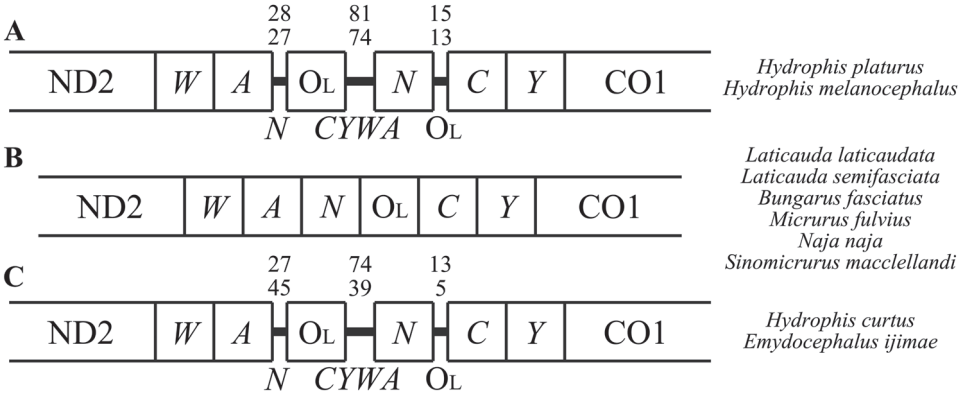

Figure 4. Intergenic spacers located in the cluster of five tRNA genes (*WANCY* gene region) of two sea snake species (*Hydrophis platurus* and *H. melanocephalus*) found off South Korean coastal waters **A** intergenic spacers located in the *WANCY* gene region of two sea krait species (*Laticauda laticaudata* and *L. semifasciata*), four terrestrial cobras (*Bungarus fasciatus*, *Micrurus fulvius*, *Naja naja* and *Sinomicrurus macclellandi*) **B** and two true sea snake species downloaded from GenBank (*H. curtus* and *Emydocephalus ijimae*) **C** intergenic spacer lengths amongst Hydrophiinae species are above the intergenic spacer in the same order as the species are listed. The hypothesised tRNA genes lost due to random deletions are written below the intergenic spacers. The tRNA genes are abbreviated by the corresponding one-letter amino acid codes, such as *W*, *A*, *N* etc.

give further insights into elapid speciation and possibly adaptation from terrestrial to oceanic ecosystems.

Our constructed BI phylogenetic tree was well fitted amongst known Korean squamate phylogenies. In our BI tree, the suborder Sauria was paraphyletic to the superfamily Lacertoidea and was sister to the suborder Serpentes. In addition, the family Gekkonidae formed an independent branch at the most basal position, which is consistent with previous studies (Townsend et al. 2004; Vidal and Hedges 2005; Hugall et al. 2007; Wiens et al. 2012; Pyron et al. 2013; Reeder et al. 2015). Our constructed BI tree also corroborated a recent phylogenetic investigation which used both morphological characters and specific mitochondrial and nuclear genes of 200 squamate species (Reeder et al. 2015). Due to the parallels between our constructed BI tree and the aforementioned study, we hypothesise that South Korean squamates most likely speciated in this manner.

In this study, we used complete mitochondrial sequenced genomes to determine mitochondrial gene organisations and phylogenetic relationships amongst all 22 squamate species listed in South Korea. The analysed species appear to have several unique mitochondrial rearrangements, including family and order-specific gene duplications and translocations. Overall, our constructed BI phylogenetic tree was well fitted amongst Korean squamates and is consistent with other phylogenetic studies which utilised specific mt-gene sequences. These results may form the basis of future phylogenetic investigations, clarifying northeast Asian squamate speciation.

Acknowledgements

This research was supported by the Basic Science Research Program through the National Research Foundation of Korea (NRF) funded by the Ministry of Education (No. 2020R1I1A3051885) and National Marine Biodiversity Institute of Korea (2022M00300).

References

Amer SAM, Kumazawa Y (2005) Mitochondrial genome of *Pogona vitticepes* (Reptilia; Agamidae): Control region duplication and the origin of Australasian agamids. Gene 346: 249–256. https://doi.org/10.1016/j.gene.2004.11.014

An JH, Park DS, Lee JH, Kim KS, Lee H, Min MS (2010) No genetic differentiation of *Elaphe schrenckii* subspecies in Korea based on 9 microsatellite loci. Animal Systematics, Evolution and Diversity 26(1): 15–19. https://doi.org/10.5635/KJSZ.2010.26.1.015

Bernt M, Donath A, Jühling F, Externbrink F, Florentz C, Fritzsch G, Pütz J, Middendorf M, Stadler PF (2013) MITOS: Improved de novo metazoan mitochondrial genome annotation. Molecular Phylogenetics and Evolution 69(2): 313–319. https://doi.org/10.1016/j.ympev.2012.08.023

Boore JL (1999) Animal mitochondrial genomes. Nucleic acids research 27(8): 1767–1780. https://doi.org/10.1093/nar/27.8.1767

Boore JL (2000) The duplication/random loss model for gene rearrangement exemplified by mitochondrial genomes of deuterostome animals. In: Sankoff D, Nadezu JH (Eds) Comparative genomics. Springer Press, Dordrecht, 133–147. https://doi.org/10.1007/978-94-011-4309-7_13

Boore JL, Collins TM, Stanton D, Daehler LL, Brown WM (1995) Deducing the pattern of arthropod phylogeny from mitochondrial DNA rearrangements. Nature 376(6536): 163–165. https://doi.org/10.1038/376163a0

Castoe TA, Gu W, De Koning APJ, Daza JM, Jiang ZJ, Parkinson CL, Pollock DD (2009) Dynamic nucleotide mutation gradients and control region usage in squamate reptile mitochondrial genomes. Cytogenetic and Genome Research 127(2–4): 112–127. https://doi.org/10.1159/000295342

Chan PP, Lowe TM (2019) tRNAscan-SE: Searching for tRNA genes in genomic sequences. In: Kollmar M (Eds) Gene Prediction, Springer Press, New York, 1–14. https://doi.org/10.1007/978-1-4939-9173-0_1

Crozier RH (1992) Genetic diversity and the agony of choice. Biological Conservation 61(1): 11–15. https://doi.org/10.1016/0006-3207(92)91202-4

Darriba D, Taboada GL, Doallo R, Posada D (2012) jModelTest 2: More models, new heuristics and parallel computing. Nature Methods 9(8): 772. https://doi.org/10.1038/nmeth.2109

Dong S, Kumazawa Y (2005) Complete mitochondrial DNA sequences of six snakes: Phylogenetic relationships and molecular evolution of genomic features. Journal of Molecular Evolution 61(1): 12–22. https://doi.org/10.1007/s00239-004-0190-9

Douglas DA, Gower DJ (2010) Snake mitochondrial genomes: Phylogenetic relationships and implications of extended taxon sampling for interpretations of mitogenomic evolution. BMC Genomics 11(1): 1–16. https://doi.org/10.1186/1471-2164-11-14

Douglas DA, Janke A, Arnason U (2006) A mitogenomic study on the phylogenetic position of snakes. Zoologica Scripta 35(6): 545–558. https://doi.org/10.1111/j.1463-6409.2006.00257.x

Dover G (1982) Molecular drive: A cohesive mode of species evolution. Nature 299(5879): 111–117. https://doi.org/10.1038/299111a0

Eberhard JR, Wright TF, Bermingham E (2001) Duplication and concerted evolution of the mitochondrial control region in the parrot genus *Amazona*. Molecular Biology and Evolution 18(7): 1330–1342. https://doi.org/10.1093/oxfordjournals.molbev.a003917

Edgar RC (2004) MUSCLE: Multiple sequence alignment with high accuracy and high throughput. Nucleic Acids Research 32(5): 1792–1797. https://doi.org/10.1093/nar/gkh340

Fenn JD, Song H, Cameron SL, Whiting MF (2008) A preliminary mitochondrial genome phylogeny of Orthoptera (Insecta) and approaches to maximizing phylogenetic signal found within mitochondrial genome data. Molecular Phylogenetics and Evolution 49(1): 59–68. https://doi.org/10.1016/j.ympev.2008.07.004

Fernández-Silva P, Enriquez JA, Montoya J (2003) Replication and transcription of mammalian mitochondrial DNA. Experimental Physiology 88(1): 41–56. https://doi.org/10.1113/eph8802514

Gao D, Liu C, Hao S (2018) Characterization of the complete mitochondrial genome of the European adder (*Vipera berus*) using Illumina sequencing technology. Conservation Genetics Resources 10(4): 793–796. https://doi.org/10.1007/s12686-017-0932-9

Greene HW (1997) Snakes: The evolution of mystery in nature. University of California Press, Berkeley, 477 pp. https://doi.org/10.1525/9780520935433

He M, Feng J, Zhao E (2010) The complete mitochondrial genome of the Sichuan hot-spring keelback (*Thermophis zhaoermii*; Serpentes: Colubridae) and a mitogenomic phylogeny of the snakes. Mitochondrial DNA 21(1): 8–18. https://doi.org/10.3109/19401730903505867

Huang A, Li H, Luo H, Ni Q, Yao Y, Xu H, Zeng B, Li Y, Wei Z, Zhang M (2019) The complete mitochondrial genome of the tree frog, *Polypedates braueri* (Anura, Rhacophoridae). Mitochondrial DNA Part B 4(1): 1739–1740. https://doi.org/10.1080/23802359.2019.1607594

Huelsenbeck JP, Ronquist F (2001) MRBAYES: Bayesian inference of phylogenetic trees. Bioinformatics 17(8): 754–755. https://doi.org/10.1093/bioinformatics/17.8.754

Hugall AF, Foster R, Lee MS (2007) Calibration choice, rate smoothing, and the pattern of tetrapod diversification according to the long nuclear gene RAG-1. Systematic Biology 56(4): 543–563. https://doi.org/10.1080/10635150701477825

Inoue JG, Miya M, Tsukamoto K, Nishida M (2003) Evolution of the deep-sea gulper eel mitochondrial genomes: Large-scale gene rearrangements originated within the eels. Molecular Biology and Evolution 20(11): 1917–1924. https://doi.org/10.1093/molbev/msg206

Jeong TJ, Jun J, Han S, Kim HT, Oh K, Kwak M (2013) DNA barcode reference data for the Korean herpetofauna and their applications. Molecular Ecology Resources 13(6): 1019–1032. https://doi.org/10.1111/1755-0998.12055

Jiang ZJ, Castoe TA, Austin CC, Burbrink FT, Herron MD, McGuire JA, Parkinson CL, Pollock DD (2007) Comparative mitochondrial genomics of snakes: Extraordinary substitution rate dynamics and functionality of the duplicate control region. BMC Evolutionary Biology 7(1): 1–14. https://doi.org/10.1186/1471-2148-7-123

Kang X, Zhang Y, Qian L, Sun P, Wang C, Fang K, Pan T, Zhang B, Rao D, Wang H (2017) The complete mitochondrial genome of *Protobothrops kaulbacki* (Squamata: Viperidae). Mitochondrial DNA Part B 2(1): 201–202. https://doi.org/10.1080/23802359.2017.1307703

Kearse M, Moir R, Wilson A, Stones-Havas S, Cheung M, Sturrock S, Buxton S, Cooper A, Markowitz S, Duran C, Thierer T, Ashton B, Meintjes P, Drummond A (2012) Geneious basic: An integrated and extendable desktop software platform for the organization and analysis of sequence data. Bioinformatics 28(12): 1647–1649. https://doi.org/10.1093/bioinformatics/bts199

Kim IH (2018) Taxonomy and molecular phylogeny of sea snakes (Hydrophinae and Laticaudinae) in Korea. PhD Thesis, Kangwon National University, Chuncheon, South Korea.

Kim IH, Park J, Suk HY, Bae HG, Min MS, Tsai TS, Park D (2018) Phylogenetic relationships of three representative sea krait species (Genus *Laticauda*; Elapidae; Serpentes) based on 13 mitochondrial genes. Mitochondrial DNA Part A 29(5): 772–777. https://doi.org/10.1080/24701394.2017.1357710

Krishnan NM, Raina SZ, Pollock DD (2004) Analysis of among-site variation in substitution patterns. Biological Procedures Online 6(1): 180–188. https://doi.org/10.1251/bpo88

Kumazawa Y, Endo H (2004) Mitochondrial genome of the Komodo dragon: Efficient sequencing method with reptile-oriented primers and novel gene rearrangements. DNA Research 11(2): 115–125. https://doi.org/10.1093/dnares/11.2.115

Kumazawa Y, Ota H, Nishida M, Ozawa T (1996) Gene rearrangements in snake mitochondrial genomes: Highly concerted evolution of control-region-like sequences duplicated and inserted into a tRNA gene cluster. Molecular Biology and Evolution 13(9): 1242–1254. https://doi.org/10.1093/oxfordjournals.molbev.a025690

Kumazawa Y, Ota H, Nishida M, Ozawa T (1998) The complete nucleotide sequence of a snake (*Dinodon semicarinatus*) mitochondrial genome with two identical control regions. Genetics 150(1): 313–329. https://doi.org/10.1093/genetics/150.1.313

Lee SC (2010) Systematic and ecological studies of the Suborder Sauria (Reptilia, Squamata) in Korea. PhD Thesis, University of Incheon, Incheon, South Korea.

Lee JH (2011) Taxonomic status, habitat use and suitability modeling of the Amur ratsnake (*Elaphe schrenckii*). PhD Thesis, Kangwon National University, Chuncheon, South Korea.

Lee JS, Miya M, Lee YS, Kim CG, Park EH, Aoki Y, Nishida M (2001) The complete DNA sequence of the mitochondrial genome of the self-fertilizing fish *Rivulus marmoratus* (Cyprinodontiformes, Rivulidae) and the first description of duplication of a control region in fish. Gene 280(1–2): 1–7. https://doi.org/10.1016/S0378-1119(01)00765-X

Lee YS, Do MS, Jeon HS, Lee SC, Jung JH, Suh JH, An J (2021) Complete mitochondrial genome of *Gloydius saxatilis* (Viperidae: Crotalinae) from Korea. Mitochondrial DNA Part B 6(2): 645–647. https://doi.org/10.1080/23802359.2021.1878957

Lee YS, Do MS, Kim W, Jeon HS, Lee SC, Jung JH, An J (2022) Phylogenetic relationships between three Korean pit viper *Gloydius* (Serpentes: Crotalinae) species using mitochondrial DNA genes. Genes & Genomics 44(5): 517–526. https://doi.org/10.1007/s13258-022-01222-3

Malhotra A, Thorpe RS (2004) A phylogeny of four mitochondrial gene regions suggests a revised taxonomy for Asian pitvipers (*Trimeresurus* and *Ovophis*). Molecular Phylogenetics and Evolution 32(1): 83–100. https://doi.org/10.1016/j.ympev.2004.02.008

Moritz C, Brown WM (1986) Tandem duplication of D-loop and ribosomal RNA sequences in lizard mitochondrial DNA. Science 233(4771): 1425–1427. https://doi.org/10.1126/science.3018925

Moritz C, Brown WM (1987) Tandem duplications in animal mitochondrial DNAs: Variation in incidence and gene content among lizards. Proceedings of the National Academy of Sciences of the United States of America 84(20): 7183–7187. https://doi.org/10.1073/pnas.84.20.7183

Moritz C, Dowling TE, Brown WM (1987) Evolution of animal mitochondrial DNA: Relevance for population biology and systematics. Annual Review of Ecology and Systematics 18(1): 269–292. https://doi.org/10.1146/annurev.es.18.110187.001413

Mouquet N, Devictor V, Meynard CN, Munoz F, Bersier L, Chave J, Couteron P, Dalecky A, Fontaine C, Gravel D, Hardy OJ, Jabot F, Lavergne S, Leibold M, Mouillot D, Münkemüller T, Pavoine S, Prinzing A, Rodrigues ASL, Rohr RP, Thébault E, Thuiller W (2012) Ecophylogenetics: Advances and perspectives. Biological Reviews of the Cambridge Philosophical Society 87(4): 769–785. https://doi.org/10.1111/j.1469-185X.2012.00224.x

Nardi F, Spinsanti G, Boore JL, Carapelli A, Dallai R, Frati F (2003) Hexapod origins: Monophyletic or paraphyletic? Science 299(5614): 1887–1889. https://doi.org/10.1126/science.1078607

Pääbo S, Thomas WK, Whitfield KM, Kumazawa Y, Wilson AC (1991) Rearrangements of mitochondrial transfer RNA genes in marsupials. Journal of Molecular Evolution 33(5): 426–430. https://doi.org/10.1007/BF02103134

Paik NK (1982) Systematic studies on the Suborder Serpentes (Reptilia) in Korea. PhD Thesis, Sungkyunkwan University, Seoul, South Korea.

Pianka ER, Pianka ER, Vitt LJ (2003) Lizards: Windows to the evolution of diversity University of California Press, Berkeley, 246 pp. https://doi.org/10.1525/california/9780520234017.001.0001

Pyron RA, Burbrink FT, Wiens JJ (2013) A phylogeny and revised classification of Squamata, including 4161 species of lizards and snakes. BMC Evolutionary Biology 13(1): 1–54. https://doi.org/10.1186/1471-2148-13-93

Qian L, Wang H, Yan J, Pan T, Jiang S, Rao D, Zhang B (2018) Multiple independent structural dynamic events in the evolution of snake mitochondrial genomes. BMC Genomics 19(1): 1–11. https://doi.org/10.1186/s12864-018-4717-7

Reeder TW, Townsend TM, Mulcahy DG, Noonan BP, Wood Jr PL, Sites Jr JW, Wiens JJ (2015) Integrated analyses resolve conflicts over squamate reptile phylogeny and reveal unexpected placements for fossil taxa. PLoS ONE 10(3): e0118199. https://doi.org/10.1371/journal.pone.0118199

Rivera PC, González-Ittig RE, Robainas Barcia A, Trimarchi LI, Levis S, Calderón GE, Gardenal CN (2018) Molecular phylogenetics and environmental niche modeling reveal a cryptic species in the *Oligoryzomys flavescens* complex (Rodentia, Cricetidae). Journal of Mammalogy 99(2): 363–376. https://doi.org/10.1093/jmammal/gyx186

Rubinoff D, Holland BS (2005) Between two extremes: Mitochondrial DNA is neither the panacea nor the nemesis of phylogenetic and taxonomic inference. Systematic Biology 54(6): 952–961. https://doi.org/10.1080/10635150500234674

Sammler S, Bleidorn C, Tiedemann R (2011) Full mitochondrial genome sequences of two endemic *Philippine hornbill* species (Aves: Bucerotidae) provide evidence for pervasive mitochondrial DNA recombination. BMC Genomics 12(1): 1–10. https://doi.org/10.1186/1471-2164-12-35

San Mauro D, Gower DJ, Zardoya R, Wilkinson M (2006) A hotspot of gene order rearrangement by tandem duplication and random loss in the vertebrate mitochondrial genome. Molecular Biology and Evolution 23(1): 227–234. https://doi.org/10.1093/molbev/msj025

Sano N, Kurabayashi A, Fujii T, Yonekawa H, Sumida M (2005) Complete nucleotide sequence of the mitochondrial genome of Schlegel's tree frog *Rhacophorus schlegelii* (family Rhacophoridae): Duplicated control regions and gene rearrangements. Genes & Genetic Systems 80(3): 213–224. https://doi.org/10.1266/ggs.80.213

Sidharthan A, Raghavan R, Anoop V, Keskar A, Dahanukar N (2021) Phylogenetic position and relationships of mountain loaches (Teleostei: Balitoridae) of the Western Ghats as revealed by CO1 sequences. Zootaxa 4926(1): 79–92. https://doi.org/10.11646/zootaxa.4926.1.5

Singchat W, Areesirisuk P, Sillapaprayoon S, Muangmai N, Baicharoen S, Suntrarachun S, Chanhome L, Peyachoknagul S, Srikulnath K (2019) Complete mitochondrial genome of Siamese cobra (*Naja kaouthia*) determined using next-generation sequencing. Mitochondrial DNA Part B 4(1): 577–578. https://doi.org/10.1080/23802359.2018.1558123

Song T, Zhang C, Zhang L, Huang X, Hu C, Xue C, Zhang B (2015) Complete mitochondrial genome of *Trimeresurus albolabris* (Squamata: Viperidae: Crotalinae). Mitochondrial DNA 26(2): 291–292. https://doi.org/10.3109/19401736.2013.825780

Stamatakis A (2006) RAxML-VI-HPC: Maximum likelihood-based phylogenetic analyses with thousands of taxa and mixed models. Bioinformatics 22(21): 2688–2690. https://doi.org/10.1093/bioinformatics/btl446

Swenson NG (2019) Phylogenetic ecology: A history, critique, and remodeling. University of Chicago Press, Chicago, 240 pp. https://doi.org/10.7208/chicago/9780226671642.001.0001

Swofford DL (2001) PAUP*. Phylogenetic analysis using parsimony (*and Other Methods). 4.0b10 edn. Sinauer Associates, Inc., Sunderland.

Takeuchi H, Zhu GX, Ding L, Tang Y, Ota H, Mori A, Oh HS, Hikida T (2014) Taxonomic validity and phylogeography of the East Eurasian natricine snake, *Rhabdophis lateralis* (Berthold, 1859)(Serpentes: Colubridae), as inferred from mitochondrial DNA sequence data. Current Herpetology 33(2): 148–153. https://doi.org/10.5358/hsj.33.148

Townsend TM, Larson A, Louis E, Macey JR (2004) Molecular phylogenetics of Squamata: The position of snakes, amphisbaenians, and dibamids, and the root of the squamate tree. Systematic Biology 53(5): 735–757. https://doi.org/10.1080/10635150490522340

Vane-Wright RI, Humphries CJ, Williams PH (1991) What to protect? Systematics and the agony of choice. Biological Conservation 55(3): 235–254. https://doi.org/10.1016/0006-3207(91)90030-D

Vanerelli AA, Miller AH, Comsa LC, Geneva AJ, Reynolds RG (2022) Mitochondrial genome of the critically Endangered silver boa (*Chilabothrus argentum*; Squamata: Boidae). Mitochondrial DNA Part B 7(6): 1180–1182. https://doi.org/10.1080/23802359.2022.2089067

Vidal N, Hedges SB (2005) The phylogeny of squamate reptiles (lizards, snakes, and amphisbaenians) inferred from nine nuclear protein-coding genes. Comptes Rendus Biologies 328(10–11): 1000–1008. https://doi.org/10.1016/j.crvi.2005.10.001

Vitt LJ, Caldwell JP (2013) Herpetology: An introductory biology of amphibians and reptiles. Academic Press, Cambridge, 35–82. https://doi.org/10.1016/B978-0-12-386919-7.00002-2

Wiens JJ, Hutter CR, Mulcahy DG, Noonan BP, Townsend TM, Sites Jr JW, Reeder TW (2012) Resolving the phylogeny of lizards and snakes (Squamata) with extensive sampling of genes and species. Biology Letters 8(6): 1043–1046. https://doi.org/10.1098/rsbl.2012.0703

Wüster W, Peppin L, Pook CE, Walker DE (2008) A nesting of vipers: phylogeny and historical biogeography of the Viperidae (Squamata: Serpentes). Molecular Phylogenetics and Evolution 49(2): 445–459. https://doi.org/10.1016/j.ympev.2008.08.019

Xiaokaiti X, Hashiguchi Y, Ota H, Kumazawa Y (2002) Evolution of the noncoding features of sea snake mitochondrial genomes within Elapidae. Genes 13(8): e1470. https://doi.org/10.3390/genes13081470

Yan J, Li H, Zhou K (2008) Evolution of the mitochondrial genome in snakes: Gene rearrangements and phylogenetic relationships. BMC Genomics 9(1): 1–7. https://doi.org/10.1186/1471-2164-9-569

Yao LZ, Gong YA, Tang XS (2020) Complete mitochondrial genome of the MacClelland's Coral Snake *Sinomicrurus macclellandi* (Reinhardt, 1844) (Serpentes: Elapidae). Mitochondrial DNA Part B 5(3): 2582–2584. https://doi.org/10.1080/23802359.2020.1781571

Yi CH, Park J, Sasai T, Kim HS, Kim JG, Kim MS, Cho IY, Kim IH (2019) Complete mitochondrial genome of the Ijima's Sea Snake (*Emydocephalus ijimae*) (Squamata, Elapidae). Mitochondrial DNA Part B 4(2): 2658–2659. https://doi.org/10.1080/23802359.2019.1641438

Zhang J, Yan C (2020) The mitochondrial genome of the *Hydrophis curtus* (Squamata: Elapidae). Mitochondrial DNA Part B 5(3): 3096–3097. https://doi.org/10.1080/23802359.2020.1800430

Zhang H, Liu Q, Lu C, Deng J, Huang X (2021) The first complete mitochondrial genome of Lachninae species and comparative genomics provide new insights into the evolution of gene rearrangement and the repeat region. Insects 12(1): 55. https://doi.org/10.3390/insects12010055

Zhu F, Liu Q, Zhong G, Xiao R, Fang M, Guo P (2016) Complete mitochondrial genome of *Sinovipera sichuanensis* (Reptilia: Squamata: Viperidae). Mitochondrial DNA Part A 27(5): 3666–3667. https://doi.org/10.3109/19401736.2015.1079846

ZooKeys 1129: 37–44 (2022)
doi: 10.3897/zookeys.1129.95245
https://zookeys.pensoft.net

SHORT COMMUNICATION

A peer-reviewed open-access journal
ZooKeys
Launched to accelerate biodiversity research

An unusual species of *Pseudophanias* Raffray from West Tianmu Mountain, China (Coleoptera, Staphylinidae, Pselaphinae)

Zi-Wei Yin[1], Tie-Xiong Zhao[2]

1 *Laboratory of Systematic Entomology, College of Life Sciences, Shanghai Normal University, Shanghai 200234, China* **2** *44 East Genta Road, Zhuji, Shaoxing, Zhejiang 311800, China*

Corresponding author: Zi-Wei Yin (pselaphinae@gmail.com)

Academic editor: Adam Brunke | Received 23 September 2022 | Accepted 25 October 2022 | Published 10 November 2022

https://zoobank.org/B19E8A19-D8A0-4CA3-8620-D8532B447D17

Citation: Yin Z-W, Zhao T-X (2022) An unusual species of *Pseudophanias* Raffray from West Tianmu Mountain, China (Coleoptera, Staphylinidae, Pselaphinae). ZooKeys 1129: 37–44. https://doi.org/10.3897/zookeys.1129.95245

Abstract

The genus *Pseudophanias* Raffray includes 19 species distributed in the Oriental Region. Here, the first species from continental China, *P. tianmuensis* Yin & Zhao **sp. nov.**, is described and illustrated from West Tianmu Mountain. This species can be readily separated from all congeners by the coarse vestiture, along with its male features. A previous key to *Pseudophanias* species of East and South Asia is modified to accommodate the new species.

Keywords

East China, new species, *Pseudophanias*, taxonomy, Zhejiang

Introduction

With greatly reduced maxillary palpi and often a C-shaped aedeagus, the genus *Pseudophanias* Raffray is an easily recognizable group among the Oriental genera of the ant-loving beetle tribe Tmesiphorini (Staphylinidae: Pselaphinae). After removing two species from former *Chandleriella* Hlaváč (now a junior synonym of *Pseudophanias*; Hlaváč 2000; Yin 2019), the genus currently comprises 19 species distributed in the

Oriental Region (Inoue et al. 2020; Inoue and Nomura 2020, 2021). Members are usually taken from the forest leaf-litter layer, in decomposing wood, and sometimes also with ants or termites. One species from Nepal was collected in a cave and possesses an exceptionally elongate body and appendages that are typical for a cavernicolous beetle (Yin et al. 2015).

In 2006 an unidentified pselaphine collected by our friend Xiao-Bin Song from a decomposing log on West Tianmu Mountain was made available for study. At first look, the beetle hardly recalled a *Pseudophanias* because of its unusual coarsely punctate body surface, subquadrate elytra, and cylindrical antennal clubs which are unknown among all previously described members of the genus. In the following 12 years, two more specimens were collected in the same area; one was sifted from leaf litter, and the other was, again, found in dead wood with termites. This species is confirmed to belong to *Pseudophanias* and is formally described here.

Materials and methods

The type material of the new species is deposited in the Insect Collection of Shanghai Normal University (**SNUC**), Shanghai, China. The label data of the material are quoted verbatim.

Dissected parts were mounted in Euparal on plastic slides pinned with the specimen. The habitus image of the beetle was photographed using a Canon 5D Mark III camera with Canon MP-E 65 mm f/2.8 1–5× macro lens, with a Canon MT-24EX Macro Twin Lite Flash as the light source. Images of the morphological details were produced using a Canon G9 camera mounted to an Olympus CX31 microscope under reflected or transmitted light. Zerene Stacker (v. 1.04) was used for image stacking. All images were modified and grouped into plates using Adobe Photoshop CC 2020.

Measurements were taken as follows: total body length was measured from the anterior margin of the clypeus to the apex of the abdomen; head length was measured from the anterior margin of the clypeus to the head base, excluding the occipital constriction; head width was measured across the eyes; the length of the pronotum was measured along the midline, the width of the pronotum equals pronotum's maximum width; the length of the elytra was measured along the suture; the width of the elytra was measured as the maximum width across both elytra; the length of the abdomen is the length of the dorsally exposed part of the abdomen along its midline, the width is abdomen's maximum width. Since one male paratype is completely disarticulated, only the holotype and the female paratype were measured. Abdominal tergites and sternites are numbered following Chandler (2001), in Arabic (starting from the first visible segment) and Roman (reflecting true morphological position) numerals, e.g., tergite 1 (IV), or sternite 1 (III). Paired appendages in the description of the new species are treated as singular.

Taxonomy

***Pseudophanias tianmuensis* Yin & Zhao, sp. nov.**
https://zoobank.org/4476E74C-644F-4667-8AF5-45C75D21638A
Figs 1–3
Chinese common name: 天目隐须蚁甲

Type material. (3 exx.). ***Holotype*: China:** ♂, 'China: Zhejiang, Linan District, West Tianmu Mountain, 1100 m, 23.viii.2014, *Cryptomeria* leaf, sift, Tie-Xiong Zhao leg., 浙江省临安市西天目山(此路不通)' (in SNUC). ***Paratypes*: China:** 1 ♂ [completely disarticulated specimen], China: Zhejiang, Linan District, West Tianmu Mountain, 1150 m, 2.vii.2006, decomposing log, sift, Xiao-Bin Song leg., 浙江省临安市西天目山(停车场); 1 ♀, 'China: Zhejiang, Linan District, West Tianmu Mountain, 1180 m, 18.viii.2019, decomposing log, sift, Zi-Wei Yin leg., 浙江省临安市西天目山(消防道)' (both in SNUC).

Diagnosis. Body length 2.8–2.9 mm; dorsal vestiture coarsely punctate and densely setose. Head subrounded at base, with small vertexal and frontal foveae; antennomeres moniliform. Elytra with discal and lateral longitudinal ridges, areas between ridges impressed. Tergite 1 (IV) longer than 2 (V) at middle but clearly shorter than 2 and 3 (VI) combined. **Male:** antennal clubs formed by apical four enlarged, cylindrical antennomeres. Aedeagus symmetric dorso-ventrally; median lobe C-shaped laterally; parameres thin and elongate, each with two long apical and one preapical seta.

Description. Male. Body (Fig. 1A) length 2.91 mm; color red-brown, tarsi and mouthparts lighter. Dorsal vestiture coarsely punctate and covered with short, dense setae.

Head (Fig. 2A) subrounded at base, longer than wide, length 0.63 mm, width 0.49 mm; vertex weakly convex, with two small, asetose vertexal foveae (dorsal tentorial pits); antennal tubercles indistinct; frons with single small fovea, protruding anteriorly to form rostrum; clypeus sharply descending, its surface coarse, anterior margin rounded and slightly carinate; lacking ocular-mandibular carina. Venter with two small, well-separated gular foveae (posterior tentorial pits), lacking median carina/sulcus. Maxillary palpus (Fig. 2B) small in size, palpomere 1 minute, 2 pedunculate basally and broadened apically, 3 roundly trapezoidal, 4 broadly at approximately basal 1/3 and gradually narrowing apically. Compound eyes moderately prominent, reniform in lateral view, each composed of approximately 55 ommatidia. Antenna elongate, length 1.75 mm, distinct club (Fig. 2C) formed by greatly enlarged antennomeres 8–11 and approximately as long as antennomeres 1–7 combined (0.88 mm *vs* 0.87 mm); antennomere 1 large, subcylindrical, 2–7 moniliform, of similar shape, 8, 9 and 10 each much larger than 7, subquadrate, 11 longest, slightly narrower than 10 and as long as 9 and 10 combined.

Pronotum (Fig. 2A) approximately as long as wide, length 0.66 mm, width 0.63 mm, widest anterior middle; sides from widest point greatly convergent anteriorly

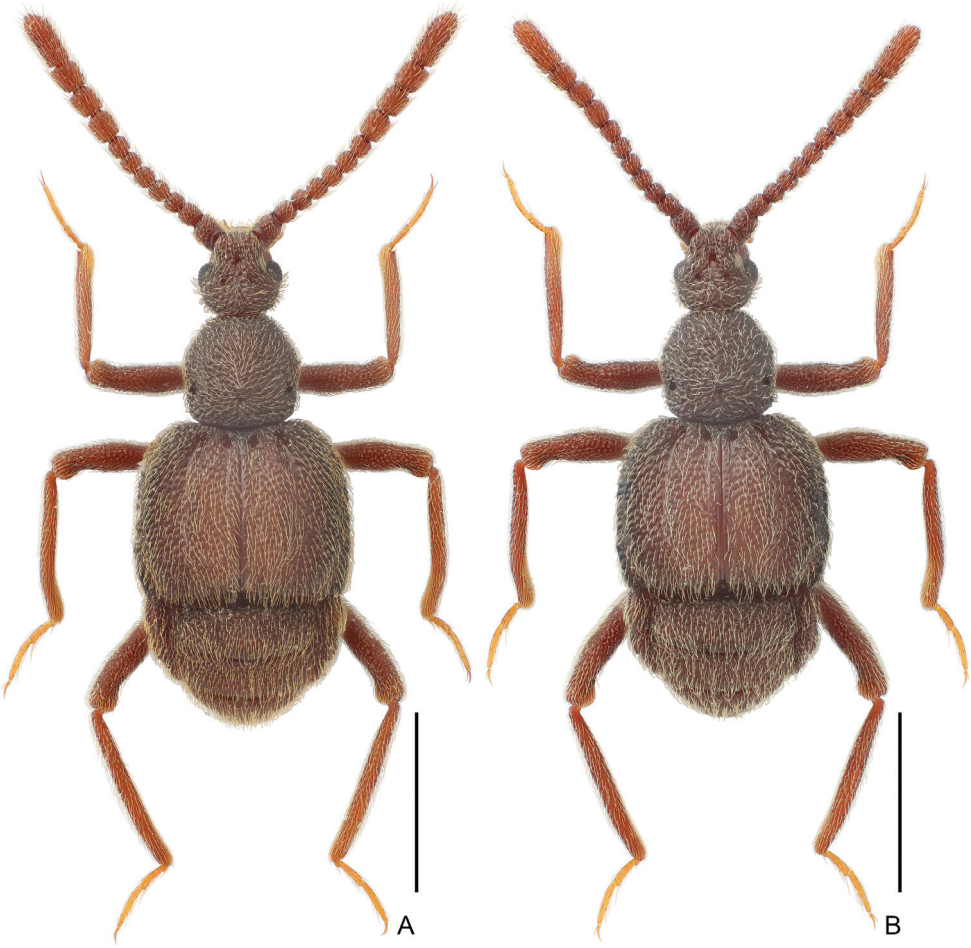

Figure 1. Habitus of *Pseudophanias tianmuensis* sp. nov. **A** male **B** female. Scale bars: 1.0 mm.

and subparallel posteriorly; disc distinctly convex to form hump at middle, lacking carina or sulcus; with small asetose median and lateral antebasal foveae; lacking basolateral foveae. Prosternum with anterior part much shorter than coxal part at middle, with small, asetose lateral procoxal foveae; hypomeron lacking ridge that demarcating it from pronotum; margin of coxal cavity non-carinate.

Elytra much wider than long, length 0.96 mm, width 1.24 mm, truncate at bases; each elytron (Fig. 2D) with two moderately large, asetose basal foveae; with one discal and one lateral ridge, discal stria formed by broad impressed area between ridges; humeral region lacking subhumeral fovea nor marginal stria; epipleural area broad; posterolateral margin with broad notch. Metathoracic wings fully developed.

Mesoventrite (Fig. 2E) with rough surface, with pair of thick admesal carinae, lateral area fully demarcated from metaventrite, openings of median mesoventral

Figure 2. Morphology of *Pseudophanias tianmuensis* sp. nov., male **A** head and pronotum **B** maxillary palpus **C** antennal club **D** elytron **E** meso- and metaventrite **F** Mesotarsal claws. Scale bars: 0.5 mm (**A, D, E**); 0.1 mm (**B, F**); 0.3 mm (**C**).

foveae widely separated, foveae greatly extended internally, lateral mesoventral foveae unforked, extended internally and overlapped with median foveae; intercoxal process short. Metaventrite (Fig. 2E) coarsely punctate, greatly prominent medially and with

Figure 3. Morphology and habitat of *Pseudophanias tianmuensis* sp. nov. **A–C** aedeagus **A** dorsal **B** lateral **C** ventral **D** paramere, lateral **E** general environment of the collecting site **F** decomposing tree branches inhabited by the beetle. Scale bars: 0.2 mm (**A–C**); 0.1 mm (**D**).

small crest; with large, asetose lateral mesocoxal foveae; posterior margin roundly emarginate at middle.

Legs elongate; femora coarsely punctate; each tarsus (Fig. 2F) with one major and one reduced pretarsal claw.

Abdomen widest at lateral margins of tergite 1 (IV), length 0.86 mm, width 1.15 mm. Tergite 1 (IV) slightly less than twice as long as 2 (V), with broad, deep basal sulcus and two basolateral foveae at lateral ends of sulcus, 2 and 3 (VI) successively shorter, lacking basal sulcus nor fovea, 4 (VII), much longer than 3, narrowed posteriorly, with one pair of basolateral foveae; tergites 1–3 each with pair of quadrangular

and 4 with pair of triangular paratergites, 5 (VIII) broadly rounded, with one pair of small basolateral foveae, posterior margin roundly emarginate at middle. Sternite 2 (IV) longest, with densely setose basal sulcus and pair of basolateral foveae at lateral ends of sulcus, 3 (V) and 4 (VI) each short at middle, combined approximately as long as 5 (VII), 3–5 lacking sulcus nor fovea at base, 6 (VIII) transverse, posterior margin slightly protruding at middle, 7 (IX) composed of pair of membranous lamellae.

Aedeagus (Fig. 3A–C) 0.51 mm long, dorso-ventrally symmetric; median lobe C-shaped in lateral view and broadened in apical half in dorso-ventral view, with large basal capsule and oval foramen; parameres (Fig. 3D) each thin, elongate and curved ventrally in lateral view, with two apical and one preapical macroseta and four short setae near base.

Female. Similar to male in external morphology (Fig. 1B). Antenna slightly shorter, club less enlarged (0.77 mm for antennomeres 1–7 vs. 0.82 mm for antennomeres 8–11); each compound eye composed of approximately 43 ommatidia; elytra slightly shorter; metathoracic wings also well developed; metaventrite lacking crest at middle. Measurements (as for male): body length 2.84 mm; length/width of head 0.62/0.49 mm, pronotum 0.63/0.65 mm, elytra 0.91/1.22 mm; abdomen 0.83/1.13 mm; length of antenna 1.59 mm.

Comparative notes. This species is unique among all known members of the genus in the coarsely punctate body surface, and a rather different type of the male antennal modifications.

Bionomics. The male holotype was collected by sifting *Cryptomeria* (Cupressaceae) leaves, while the other two individuals were found inside decomposing wood with termites. Although indicated by a set of morphological traits such as the compact body segments and moniliform antennomeres, it is still inconclusive as to whether the beetle has an obligate association with social insects, pending further observations in the field or at the laboratory.

Distribution. East China: Zhejiang.

Etymology. The specific epithet refers to West Tianmu Mountain, the type locality of this species.

Remarks. To accommodate the new species, the key to East and South Asian species of *Pseudophanias* by Inoue et al. (2020) is modified as follow:

0 Whole body surface roughly punctate and with dense, short setae; antennal club formed by enlarged, subcylindrical antennomeres 8–11; elytra roundly quadrate, broadly truncate at bases.....
...***Pseudophanias tianmuensis*** **Yin & Zhao, sp. nov. (East China: Zhejiang)**

– Body surface usually finely punctate (head with coarse punctation in *P. excavatus* Inoue, Nomura & Yin) and with moderately long pubescence; antennal club formed by antennomere 11 alone, or by variously modified antennomeres 5–11, 8–11, or 9–11; elytra roundly triangular, and more strongly constricted at bases..... **1**

Acknowledgements

We thank Xiao-Bing Song (宋晓彬) for providing the first male specimen and associated collecting data 16 years ago. Donald S. Chandler (University of New Hampshire, Durham, USA) and Shûhei Nomura (National Museum of Nature and Science, Tsukuba, Japan) read the draft manuscript and provided helpful comments. This study was supported by the National Natural Science Foundation of China (no. 31872965) granted to ZWY.

References

Chandler DS (2001) Biology, morphology, and systematics of the ant-like litter beetles of Australia (Coleoptera: Staphylinidae: Pselaphinae). Memoirs on Entomology International 15: [i–x,] 1–560.

Hlaváč P (2000) *Chandleriella*, new genus of Tmesiphorini from Borneo (Coleoptera: Staphylinidae: Pselaphinae). Entomological Problems 31(1): 91–93.

Inoue S, Nomura S (2020) A new species of the genus *Pseudophanias* Raffray, 1890 from Thailand (Coleoptera: Staphylinidae: Pselaphinae). Japanese Journal of Systematic Entomology 26(2): 336–339.

Inoue S, Nomura S (2021) Two new species of *Pseudophanias* Raffray from Myanmar (Coleoptera: Staphylinidae: Pselaphinae). Zootaxa 4996(3): 591–599. https://doi.org/10.11646/zootaxa.4996.3.11

Inoue S, Nomura S, Yin Z-W (2020) Three new species of *Pseudophanias* Raffray from Japan and Taiwan Island, and synonymy of *Chandleriella* Hlaváč with *Pseudophanias* (Coleoptera, Staphylinidae, Pselaphinae). ZooKeys 987: 135–156. https://doi.org/10.3897/zookeys.987.53648

Yin Z-W (2019) First record of the genus *Chandleriella* Hlaváč (Coleoptera: Staphylinidae: Pselaphinae) from China, with description of a second species. Zootaxa 4571(3): 432–438. https://doi.org/10.11646/zootaxa.4571.3.11

Yin Z-W, Coulon G, Bekchiev R (2015) A new species of *Pseudophanias* Raffray from a cave in central Nepal (Coleoptera: Staphylinidae: Pselaphinae). Zootaxa 4048(3): 446–450. https://doi.org/10.11646/zootaxa.4048.3.10

ZooKeys 1129: 45–54 (2022)
doi: 10.3897/zookeys.1129.91398
https://zookeys.pensoft.net

SHORT COMMUNICATION

A peer-reviewed open-access journal
ZooKeys
Launched to accelerate biodiversity research

New arthropod-Podostemaceae associations in Central and South America

Jacob Bethin[1], Rayda K. Krell[2], C. Thomas Philbrick[2]

1 *University of Florida, Entomology and Nematology Department, 1881 Natural Area Dr., Gainesville, FL 32608, USA* **2** *Western Connecticut State University, Department of Biology, 181 White St., Danbury, CT 06810, USA*

Corresponding author: Jacob Bethin (bethinj@ufl.edu)

Academic editor: Pavel Stoev | Received 8 August 2022 | Accepted 26 September 2022 | Published 11 November 2022

https://zoobank.org/4B225043-C157-4DC1-B4F4-3477AC1A0067

Citation: Bethin J, Krell RK, Philbrick CT (2022) New arthropod-Podostemaceae associations in Central and South America. ZooKeys 1129: 45–54. https://doi.org/10.3897/zookeys.1129.91398

Abstract

Podostemaceae are a unique family of aquatic angiosperms found in river rapids and waterfalls throughout southern Asia, Africa, and the Americas. Podostemaceae are understudied, and consequently, the arthropods associated with these plants are not well known. We sought to expand knowledge of arthropod-Podostemaceae associations to better understand the impact of these plants on aquatic ecosystems and biodiversity. We examined samples of Podostemaceae collected between 1998 and 2007 from Brazil, Costa Rica, Suriname, and Venezuela for arthropods even though these samples were not collected with the intent to investigate arthropod-Podostemaceae associations. We examined 15 samples of Podostemaceae, including 10 species never evaluated for arthropod associations, and found over 9000 arthropods representing 12 different orders. The most abundant orders were Diptera (77.88%), Trichoptera (12.90%), Coleoptera (3.35%), and Lepidoptera (2.42%). We found several arthropods not previously reported from Podostemaceae, including Collembola and Acari, documented several instances of insects boring into plant tissues, and provide the first report of an insect-induced gall on *Ceratolacis pedunculatum* C.T. Philbrick, Novelo & Irgang.

Keywords

Aquatic arthropods, freshwater biodiversity, lotic invertebrates, plant-insect interactions, river ecosystems

Introduction

Many aquatic arthropods have close associations with aquatic plants (Hutchens et al. 2004). One unusual family of aquatic plants with infrequently studied arthropod associations is Podostemaceae (Fig. 1). Podostemaceae (Malpighiales) comprise 50 genera and 300 species (Philbrick and Novelo 2004; Xi et al. 2012). They have distinctive morphological traits and resemble seaweeds and bryophytes (Cook and Rutishauser 2007). Their geographic distribution includes southern Asia, Africa, and the Americas, with 60% of all species found in the Americas and only one species, *Podostemum ceratophyllum* Michx., found in North America (Philbrick and Crow 1983; Philbrick and Novelo 2004). These plants are also primarily found in river rapids and waterfalls attached to rocks (Philbrick and Novelo 2004; de Sá-Haiad et al. 2010).

Podostemaceae provide habitat and food for a diverse assemblage of aquatic arthropods (Tavares et al. 1998). Podostemaceae grow abundantly and form large beds that provide arthropods with protected habitat in areas with rich oxygen flow (Tavares et al. 1998). The large Podostemaceae beds and associated surface area of plant tissue can provide habitat to which arthropods can attach and feed. The plants simultaneously protect arthropods from predators and rapid water flow (Hutchens et al. 2004; Argentina et al. 2010). Arthropods commonly associated with Podostemaceae in South America include Diptera, Ephemeroptera, and Lepidoptera (Tavares et al. 1998). Similar associations have been found in North America, with a notable lack of Lepidoptera (Grubaugh and Wallace 1995). Arthropods utilize the entire plant, and chironomid larvae have been found inside the stem, inducing galls on *Marathrum utile* Tul. and *Noveloa coulteriana* (Tul.) C.T. Philbrick (Jäger-Zürn et al. 2013).

Investigating the community of arthropods that are associated with Podostemaceae is important for understanding lotic arthropod biodiversity and ecosystem conservation. Freshwater systems are extremely fragile and are easily impacted by external factors (Su et al. 2021). Some examples of human behavior that can impact these systems include dam building, introducing invasive species, and modifying the land (Su et al. 2021). The potential impact of Podostemaceae loss on aquatic biodiversity was documented in a study that experimentally removed Podostemaceae from an ecosystem (Hutchens et al. 2004). When Podostemaceae were removed, there was a 90% decrease in biomass and an 88% decrease of invertebrate species abundance (Hutchens et al. 2004). A decrease of total invertebrate biomass and species abundance can be detrimental to other species in the ecosystem because of their diverse interactions as detritivores, predators, and prey. A decrease in Podostemaceae biomass was demonstrated to decrease local fish populations because the large populations of arthropods were no longer readily available to eat for the insectivorous fish (Argentina et al. 2010).

Tavares et al. (1998) investigated insects on nine species of Podostemaceae in the genera *Apinagia*, *Mourera*, and *Rhyncholacis* in eastern Amazonia, Brazil. Their work is currently the most extensive study of arthropod-Podostemaceae associations in South America. They identified 26 families of arthropods in nine orders. Most of the

arthropods identified were Diptera, making up 67% of insects found on Podostemaceae, followed by Lepidoptera (14%) and Ephemeroptera (12%) (Tavares et al. 1998). Tavares et al. (1998) were the first to document the extent of arthropod biodiversity associated with Podostemaceae in South America and they reiterated these associations in subsequent publications (Collart et al. 1998; Tavares et al. 2006).

Another study suggesting arthropod associations with Podostemaceae was in Suriname as part of an effort to expand taxonomic knowledge of aquatic arthropods in the country (Pereira and Berrenstein 2006). Although the study did not focus on arthropods on Podostemaceae, Podostemaceae were present in most sampling locations suggesting a possible baseline for understanding specific associations. The survey investigated arthropod populations in the Central Suriname Nature Reserve and found 31 families in nine different orders. Diptera were most abundant (60%), followed by Ephemeroptera (31%), and Lepidoptera (1%) (Pereira and Berrenstein 2006).

More recently, an investigation of larval Lepidoptera collected from Podostemaceae in Central and South America found several new species (Bethin et al. 2021). This study noted several species with new morphologies ranging from new respiratory structures to morphological traits with unknown purposes, such as a membranous sac and a small tail. These newly reported insect morphological traits demonstrated the potential to discover new insect diversity associated with Podostemaceae.

The urgency to understand global biodiversity has become heightened with recent reports of a 68% decline in wildlife populations between 1970 and 2016 (Almond et al. 2020). Rivers are at an especially high risk of ecosystem change with global increases in dam construction (Dethier et al. 2022). Our study sought to further document lotic arthropod biodiversity by exploring associations with Podostemaceae in Central and South America from 12 Podostemaceae species, 10 of which had never been evaluated for arthropod diversity. We chose samples collected from northern Costa Rica to southern Brazil, expanding the geographic range of known arthropod associations with Podostemaceae in Central and South America.

Figure 1. Carrao River, Orinoco River Basin, Venezuela with Podostemaceae beds.

Materials and methods

Podostemaceae were collected during the dry seasons in Brazil, Costa Rica, Suriname, and Venezuela for systematic botanical study (Fig. 2, Table 1). Because the original goal of the expeditions was to better understand Podostemaceae diversity, arthropod collections were incidental, and a specific collecting protocol for arthropods was not followed. Data on the locations, other than coordinates, were also not collected because they were not required for the original intent of the collections. Plant samples were collected by separating the plant from the substrate and vigorously shaking the specimen in the water to remove arthropods and debris. Individual plant specimens were then placed in separate plastic bags with 70% ethanol. The ethanol was periodically changed and emptied throughout the days of collection before being transported for study at Western Connecticut State University in the United States. The samples were transferred to plastic containers with 70% ethanol for long-term storage.

We initially evaluated approximately 200 plant samples for presence of arthropods and created a catalog of approximately 100 samples with relatively higher arthropod abundance. Subsequently, we chose 15 samples to evaluate based on the presence of unique arthropods, broad geographic representation, and plant species that had not been previously investigated. The 15 Podostemaceae samples consisted of eight genera and 12 species and were collected between 1998 and 2007 from Suriname, Brazil, Costa Rica, and Venezuela (Table 1). We also assigned each sample of the same species a superscript identifier (ex: *A. richardiana*[1]) to easily distinguish between the two samples.

To evaluate each sample, we removed each stem and leaf from the collection container and rinsed it with 70% ethanol to separate the arthropods from the plant into a Petri dish where they were manually sorted and counted. We inspected each portion of the plant with a dissecting microscope at a maximum of 40× magnification to remove

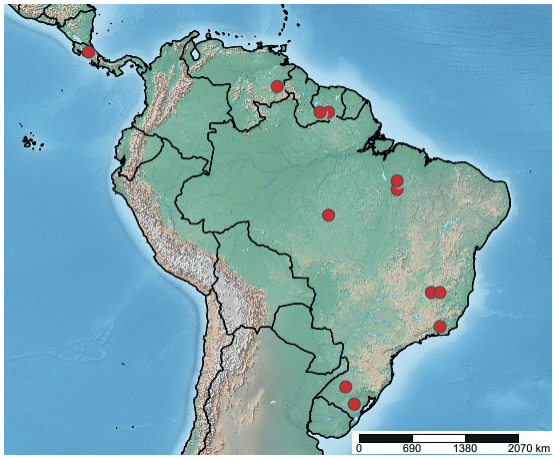

Figure 2. Map of sampling locations, appearing as red dots, across Central and South America (SimpleMappr). Some samples of different species were collected in the same river at the same approximate coordinates and appear as the same dot.

Table 1. Voucher specimens of Podostemaceae listing taxon, country, state/district, river, primary collector, collection number, month, year and acronym (http://sweetgum.nybg.org/science/ih/) of the herbarium where the voucher is located. Super scripts are used to differentiate between replicate species/samples.

Taxon	Country	State/District	River	Primary Collector	Collection Number	Month	Year	Acronym
***Apinagia digitata*[1]**	Suriname	Sipaliwini	Zuid River	Philbrick	6159	Oct.	2007	MICH
***Apinagia digitata*[2]**	Suriname	Sipaliwini	Zuid River	Philbrick	6171	Oct.	2007	MICH
***Apinagia richardiana*[1]**	Suriname	Sipaliwini	Lucie River	Philbrick	6184	Oct.	2007	MICH
***Apinagia richardiana*[2]**	Suriname	Sipaliwini	Lucie River	Philbrick	6155	Oct.	2007	MICH
Apinagia riedelii	Brazil	Tocantins	Rio Lontra	Philbrick	5992	Jul.	2006	MICH
Ceratolacis pedunculatum	Brazil	Minas Gerais	Rio Bicudo	Philbrick	5761	Jul.	2002	MICH
Diamantina lombardii	Brazil	Minas Gerais	Rio do Peixe	Philbrick	5783	Aug.	2002	MICH
***Lophogyne* s.1. sp.**	Brazil	Para	Rio Sao Benedito	Bove	1864	Sep.	2007	MICH
Marathrum foeniculaceum	Costa Rica	Alajuela	Rio Quequer	Philbrick	5901	Mar.	2006	MICH
Mourera elegans	Brazil	Para	Rio Araguaia	Philbrick	5976	Jul.	2006	MICH
Podostemum muelleri	Brazil	Rio Grande do Sul	Arroio do Lajeado	Philbrick	5024	Jan.	1998	MICH
Podostemum rutifolium	Brazil	Rio Grande do Sul	Tributary of Rio Jaguari	Philbrick	5032	Jan.	1998	MICH
Podostemum weddellianum	Brazil	Rio de Janeiro	Rio da Cidade	Philbrick	5000	Jan.	1998	MICH
***Rhyncholacis* sp.[1]**	Venezuela	Bolivar	Rio Carrao	Philbrick	6058	Jan.	2007	MICH
***Rhyncholacis* sp.[2]**	Venezuela	Bolivar	Rio Carrao	Philbrick	6052	Jan.	2007	MICH

any remaining arthropods manually. We identified each arthropod to order and placed them in individual vials, or vials with 10–100 arthropods of the same order or family, containing 70% ethanol. After cataloging all arthropods from the samples, we calculated the proportion of each taxon in each sample. We also calculated the Shannon-Wiener diversity index for arthropods collected from each plant species as a relative indicator of arthropod diversity by plant species.

Results

In total we counted 9197 arthropods and identified 12 orders (Table 2). Overall, Diptera were the most abundant, comprising 77.88% of all arthropods collected. Trichoptera (12.90%), Coleoptera (3.35%), Lepidoptera (2.42%), and Ephemeroptera (1.71%) were the next most abundant. The other nine orders comprised the remaining 3.45% of collected arthropods (Table 2).

Diptera were found in all 15 (100%) samples, Ephemeroptera found in 14 (93.3%), and Lepidoptera and Trichoptera were found in 13 (86.7%) samples (Table 3). *Apinagia riedelii* (Bong.) Tul. was among the most diverse samples with specimens from all 10 orders of aquatic arthropods, plus Hymenoptera (Table 3). *Mourera elegans* Baill was among the least diverse plant samples evaluated with only three arthropod orders present. However, over 1000 arthropods, mostly Diptera and Trichoptera (Table 3), were found in *Mourera elegans* making it the sample with the third highest number of arthropods in this study. The least common arthropods, found on *A. riedelii*, were Collembola (one specimen) and Megaloptera (two specimens).

Table 2. Proportion of arthropods found in all samples by insect order with total number of arthropod individuals counted.

Arthropod order	Total
Acari	0.21%
Coleoptera	3.35%
Collembola	0.01%
Diptera	77.88%
Ephemeroptera	1.71%
Hemiptera	0.41%
Hymenoptera	0.03%
Lepidoptera	2.42%
Megaloptera	0.02%
Odonata	0.04%
Plecoptera	0.5%
Trichoptera	12.90%
Unknown	0.51%
Number of arthropods	**9197**

Table 3. Proportion and total number of arthropod specimens for each order, and the Shannon-Weiner diversity index score of each sample of Podostemaceae.

	A. digitata[1]	*A. digitata*[2]	*A. richardiana*[1]	*A. richardiana*[2]	*A. riedelii*	*C. pedunculatum*	*D. lombardii*	*Lophogyne* s.l. sp.	*Ma. foeniculaceum*	*Mo. elegans*	*P. muelleri*	*P. rutifolium*	*P. weddellianum*	*Rhyncholacis* sp.[1]	*Rhyncholacis* sp.[2]
Acari	0.001	0.0006	0.034	-	-	0.006	0.010	-	-	-	0.015	-	0.003	0.100	0.038
Coleoptera	0.009	0.0006	-	-	0.076	0.111	0.207	-	0.082	-	0.403	0.514	0.040	-	0.038
Collembola	-	-	-	-	0.001	-	-	-	-	-	-	-	-	-	-
Diptera	0.928	0.9628	0.759	0.714	0.604	0.718	0.617	0.405	0.056	0.502	0.388	0.135	0.850	0.500	0.423
Ephemeroptera	0.028	0.0036	0.095	0.029	0.012	0.108	0.024	0.143	0.007	-	0.015	0.027	0.037	0.050	0.038
Hemiptera	-	0.0003	-	0.057	0.015	-	0.007	-	0.041	-	-	-	-	-	-
Hymenoptera	-	-	-	-	0.001	-	0.005	-	-	-	-	-	-	-	-
Lepidoptera	0.017	0.0281	0.017	0.029	0.037	0.024	-	0.190	0.020	0.005	0.015	0.243	-	0.200	0.462
Megaloptera	-	-	-	-	0.002	-	-	-	-	-	-	-	-	-	-
Odonata	-	-	0.009	-	0.001	0.003	-	-	-	-	-	-	0.003	-	-
Plecoptera	-	0.0032	-	0.029	0.034	-	0.002	0.024	0.002	-	-	-	-	-	-
Trichoptera	0.015	0.0008	0.052	0.057	0.200	0.021	0.105	0.238	0.790	0.493	0.134	0.081	0.059	-	-
Unknown	0.002	-	0.034	0.086	0.017	0.009	0.024	-	0.002	-	0.030	-	0.008	0.150	-
Total arthropods	**1721**	**3632**	**116**	**35**	**894**	**333**	**420**	**42**	**461**	**1039**	**67**	**37**	**354**	**20**	**26**
Diversity index	0.37	0.19	0.92	1.08	1.28	0.98	1.15	1.39	0.82	0.72	1.29	1.26	0.63	1.33	1.09

We also documented a few instances of arthropods directly using the plants. We found Diptera inside the tissue of *A. digitata* P. Royen, *A. richardiana* (Tul.) P. Royen, and *C. pedunculatum* C.T. Philbrick, Novelo & Irgang and Lepidoptera using the plant by creating a pupal case out of leaves.

The Shannon-Wiener index varied from a low index of 0.19 from *A. digitata*[2] to a high index of 1.39 from *Lophogyne* s.l. sp. (Table 3). The next two samples with the highest indices were *Rhyncholacis* sp.[1] at 1.33 and *Podostemum muelleri* Warm at 1.29 (Table 3).

Discussion

Our study expands the understanding of arthropods associated with Podostemaceae both geographically and taxonomically. All arthropods we identified represent an association with Podostemaceae, however, because the sampling method attempted to remove arthropods from the samples, it is likely there are additional associations. We found similar orders with similar proportional abundance as previous South American studies and added reports of arthropods on Podostemaceae species that were previously never reported (Tavares et al. 1998; Pereira and Berrenstein 2006). We increased the total Podostemaceae species evaluated for arthropods in South America from nine to 20 species. We also report the first evaluation of arthropods on *Ceratolacis* sp., *Lophogyne* sp. and *Podostemum* spp., other than *P. ceratophyllum* in North America. The arthropods found on *C. pedunculatum* and *Diamantina lombardii* Novelo, C.T. Philbrick & Irgang were part of the collections that aided in the type description of these plant species and offer a small glimpse into the potential ecological importance of these relatively new plant species. *Ceratolacis* is a ditypic genus, while *Diamantina* is monotypic, endemic to Minas Gerais, Brazil (Philbrick and Novelo 2004), highlighting the importance of understanding these unique plants.

Of the 9197 arthropods found in the samples, Diptera were dominant, comprising 77.88% of all arthropods (Table 2). However, on *P. rutifolium* and *P. muelleri*, Coleoptera were dominant (Table 3). It is not surprising that Diptera were abundant because they commonly comprise most arthropods in aquatic arthropod samples (Tavares et al. 1998; Zequi et al. 2019). We found relatively high abundance of Trichoptera and Lepidoptera, with a higher proportion of Trichoptera than previously reported on Podostemaceae (Tavares et al. 1998).

We also report the first specimen of Collembola (Entomobryomorpha) from Podostemaceae. Although it was only a single specimen, it had not been described by both Tavares et al. (1998) or Pereira and Berrenstein (2006). We also documented several mites (Acari) and it is possible the mites were parasitizing the arthropods or Podostemaceae. This likely association is especially interesting because they had not been previously noted or documented on Podostemaceae. We also documented Ephydridae on species of *Apinagia*, *Ceratolacis*, *Marathrum*, *Podostemum* and *Rhyncholacis* where it had only previously been documented on *Rhyncholacis* sp. (Tavares et al. 1998). We also found Helicopsychidae in the sample of *C. pedunculatum* where it had only been previously reported on *Apinagia guyanenesis* (Pulle) P. Royen (Tavares et al. 1998).

We documented several arthropods directly using the plants. We found 438 Simuliidae (Diptera) pupae attached to most of the plants except *A. richardiana*, *D. lombardii*, *Lophogyne* s.1. sp., *Rhyncholacis* sp.[1]. We also documented Chironomidae (Diptera) boring into the plant tissue of *A. richardiana*[2], *A. digitata*[2], and *C. pedunculatum*. We are also the first to document a chironomid-induced gall on *C. pedunculatum*. We found Lepidoptera pupae that had created a casing using the leaves of the plants (Bethin et al. 2021). These documented instances of direct use by insects are likely a conservative representation of the interactions because many of the insects were removed during the collection process and in storage.

The samples with the highest diversity were *Lophogyne* s.1. sp., *Rhyncholacis* sp.[1], *P. muelleri*, and *A. riedelii* with Shannon-Wiener values between 1.39 and 1.28 (Table 3). *Lophogyne* s.1. sp. and *Rhyncholacis* sp.[1] had the highest diversity index values, which reflects the relatively even abundance of the orders found, even though overall abundance was low. The sample of *A. riedelii* was the most diverse, with the most orders found in a single sample, which is reflected in the higher index value. The two lowest indices, 0.19 and 0.37, were from *A. digitata*, which also contained the most arthropods with approximately 5400 arthropods combined. However, both samples were mostly Diptera, over 92%, resulting in a lower diversity index value.

Identifying arthropod-Podostemaceae associations was not the original intent of these plant collections. The incidental arthropod collections reported in this study are likely a snapshot into arthropod-Podostemaceae interactions. While the associations we identified do not represent a complete understanding because arthropods were removed during collection, they still present associations that have not been previously identified from these plant species in these locations. Simply because we examined arthropods from plants that few others have researched, we documented two new arthropod orders associated with Podostemaceae and added 10 Podostemaceae species to the total evaluated for arthropod associations.

With this expanded knowledge of these freshwater communities, conservation and restoration efforts can reference our data as baseline evidence for the contribution of Podostemaceae to river biodiversity throughout Central and South America. It is evident that Podostemaceae create unique habitats ideal for arthropod diversity. As deforestation and dam construction continue in Central and South America, the likely impact on rivers could contribute to loss of biodiversity before it is even documented. It is clear that more research is needed to fully understand the extent of arthropod diversity found in Podostemaceae beds and the ecological importance of these communities.

Acknowledgements

We thank Dr Mitch Wagener and Dr Alma Solis for assistance with identification and Dr Neeta Connally for sharing her lab equipment. We also thank James Wood for reviewing this manuscript. This study was supported from National Science Foundation grants DEB-0444589 & DEB-1754199 to C. T. Philbrick.

References

Almond REA, Grooten M, Peterson T (2020) Living Planet Report 2020- Bending the curve of biodiversity loss. World Wildlife Fund 2020. https://pure.iiasa.ac.at/id/eprint/16870/1/ENGLISH-FULL.pdf

Argentina JE, Freeman MC, Freeman BJ (2010) The response of stream fish to local and reach-scale variation in the occurrence of a benthic aquatic macrophyte. Freshwater Biology 55(3): 643–653. https://doi.org/10.1111/j.1365-2427.2009.02301.x

Bethin J, Solis MA, Krell RK (2021) The undiscovered frontier of aquatic moth caterpillars on river weeds. News of the Lepidopterists' Society 63: 143–146. https://images.peabody.yale.edu/lepsoc/nls/2020s/2021/2021_v63_n3.pdf

Collart OO, Enriconi A, Tavares AS (1998) Seasonal Dynamics of the insect community associated with the aquatic macrophyte *Rhyncholacis hydrocichorium* (Podostemaceae) in amazonian waterfalls (Pitinga river, Brazil). Archiv für Hydrobiologie 26: 183–1088. https://doi.org/10.1080/03680770.1995.11900888

Cook CDK, Rutishauser R (2007) Podostemaceae. In: Flowering Plants. Eudicots. Springer, Berlin, Heidelberg, Germany, 304–344. https://doi.org/10.1007/978-3-642-39417-1

de Sá-Haiad B, Torres CA, de Abreu VHR, Gonçalves MR, Mendonça CBF, de Santiago-Fernandes LDR, Bove CP, Gonçalves-Esteves V (2010) Floral structure and palynology of *Podostemum weddellianum* (Podostemaceae: Malpighiales). Plant Systematics and Evolution 290(1–4): 141–149. https://doi.org/10.1007/s00606-010-0356-4

Dethier EN, Renshaw CE, Magilligan FJ (2022) Rapid changes to global river suspended sediment flux by humans. Science 376(6600): 1447–1452. https://doi.org/10.1126/science.abn7980

Grubaugh JW, Wallace JB (1995) Functional structure and production of the bentic community in a Piedmont River: 1956–1957 and 1991–1992. Limnology and Oceanography 40(3): 490–501. https://doi.org/10.4319/lo.1995.40.3.0490

Hutchens Jr JJ, Wallace JJ, Romaniszyn ED (2004) Role of *Podostemum ceratophyllum* Michx. In structuring benthic macroinvertebrate assemblages in a southern Appalachian River. Journal of the North American Benthological Society 23(4): 713–727. https://doi.org/10.1899/0887-3593(2004)023<0713:ROPCMI>2.0.CO;2

Jäger-Zürn I, Spies M, Philbrick CT, Bove CP, Mora-Olivo A (2013) Plant galls (cecidia) in the neotropical water plant family Podostemaceae induced by larvae of Chironomidae. Spixiana 36: 97–112.

Pereira G, Berrenstein HJ (2006) A survey of the aquatic arthropods of the Coppename River, Central Suriname Nature Reserve. A rapid biological assessment of the aquatic ecosystems of the Coppename River basin, Suriname. Conservation International, Washington DC. Rapid Assessment Program Bulletin of Biological Assessment 39: 56–66.

Philbrick CT, Crow GE (1983) Distribution of *Podostemum ceratophyllum* Michx. (Podostemaceae). Rhodora 85: 325–341. https://www.jstor.org/stable/23311203?seq=1&cid=pdf-reference#references_tab_contents

Philbrick CT, Novelo RA (2004) Monograph of *Podostemum* (Podostemaceae). Systematic Botany Monographs 70: 1–106. https://doi.org/10.2307/25027922

Su G, Logez M, Xu J, Villeger S, Brosse S (2021) Human impacts on global freshwater fish biodiversity. Science 371(6531): 835–838. https://doi.org/10.1126/science.abd3369

Tavares AS, Enriconi A, Collart OO (1998) Insect communities associated with aquatic macrophytes Podostemaceae in Amazonian waterfalls. Internationale Vereinigung für theoretische und angewandte Limnologie. Verhandlungen 26: 2158–2161. https://doi.org/10.1080/03680770.1995.11901126

Tavares AS, Odinetz O, Enricone A (2006) The Podostemaceae family in Amazonian rivers and insect community associated. INSULA Revista de Botanica 35: 19–50.

Xi Z, Ruhfel BR, Schaefer H, Amorim AM, Sugumaran M, Wurdack KJ, Endress PK, Matthews ML, Stevens PF, Mathews S, Davis CC (2012) Phylogenomics and a posteriori data partitioning resolve the Cretaceous angiosperm radiation Malpighiales. Proceedings of the National Academy of Sciences of the United States of America 109(43): 17519–17524. https://doi.org/10.1073/pnas.1205818109

Zequi JAC, Espinpza AA, de Almeida Paccola J, Lopes J (2019) Aquatic insect communities in small stream in the south of Brazil. Environmental Monitoring and Assessment 191(7): 1–9. https://doi.org/10.1007/s10661-019-7536-7

ZooKeys 1129: 55–72 (2022)
doi: 10.3897/zookeys.1129.91543
https://zookeys.pensoft.net

RESEARCH ARTICLE

A peer-reviewed open-access journal
ZooKeys
Launched to accelerate biodiversity research

Genome-wide survey reveals the phylogenomic relationships of *Chirolophis japonicus* Herzenstein, 1890 (Stichaeidae, Perciformes)

Lu Liu[1], Qi Liu[2], Tianxiang Gao[3,4]

1 *Naval Architecture and Port Engineering College, Shandong Jiaotong University, Weihai, China* **2** *Wuhan Onemore-tech Co., Ltd. Wuhan, Hubei, China* **3** *Fishery College, Zhejiang Ocean University, Zhoushan, Zhejiang, China* **4** *Zhejiang Provincial Key Laboratory of Mariculture and Enhancement, Zhejiang Marine Fisheries Research Institute, Zhoushan, China*

Corresponding author: Tianxiang Gao (gaotianxiang0611@163.com)

Academic editor: Maria Elina Bichuette | Received 11 August 2022 | Accepted 6 October 2022 | Published 11 November 2022

https://zoobank.org/B99966E1-EF69-46FD-8CDF-D6D1417102C1

Citation: Liu L, Liu Q, Gao T (2022) Genome-wide survey reveals the phylogenomic relationships of *Chirolophis japonicus* Herzenstein, 1890 (Stichaeidae, Perciformes). ZooKeys 1129: 55–72. https://doi.org/10.3897/zookeys.1129.91543

Abstract

Fish are the largest vertebrate group, consisting of more than 30 000 species with important ecological and economical value, while less than 3% of fish genomes have been published. Herein, a fish, *Chirolophis japonicus*, was sequenced using the next-generation sequencing. Approximately 595.7 megabase pair of the *C. japonicus* genome was assembled (49 901 contigs with 42.61% GC contents), leading to a prediction of 46 729 protein-coding gene models. A total of 554 136 simple sequence repeats was identified in the whole genome of *C. japonicus*, and dinucleotide microsatellite motifs were the most abundant, accounting for 59.49%. Phylogenomic analysis of 16 genomes based on the 694 single-copy genes suggests that *C. japonicus* is closely related with *Anarrhichthys ocellatus*, *Cebidichthys violaceus*, and *Pholis gunnellus*. The results provide more thorough genetic information of *C. japonicus* and a theoretical basis and reference for further genome-wide analysis.

Keywords

Chirolophinae, draft genome, genome assembly, genome evolution, next-generation sequencing, Stichaeidae, Zoarcales

Introduction

Chirolophis Swainson, 1839 belongs to the family Stichaeidae of the order Perciformes, which is widely distributed between cold and temperate areas in the Pacific Ocean and along the coasts of Europe in the Atlantic Ocean (Jing et al. 2005; Balanov et al. 2020). *Chirolophis* contains nine species (https://www.fishbase.se/search.php) which are important commercial bony fishes, especially in China (Chen et al. 2017). Among these species, *Chirolophis japonicus* (Herzenstein, 1890), also known as *Azuma emmnion* (Jordan & Snyder, 1902), lives in rocky shallow coastal waters of the Pacific Ocean, including the Yellow Sea, the Bohai Sea, the northern Sea of Japan, and the Okhotsk Sea to the Bering Sea (Shiogaki 1983; Jing et al. 2005; Balanov et al. 2020). They display strong cryptic habits and are almost impossible to be observed by SCUBA diving observations. Studies on this species are relatively rare, mainly including mitochondrial genome data (Yang et al. 2016), the origin of the cortical protrusion of head (Sato 1977), and reproductive biology research (Chen 2017).

Genome-based phylogenetic studies have provided new opportunities for exploring the phylogeny of fishes. With the development of molecular biology and sequencing technology, more and more species are being sequenced and genomes published, ranging from model fishes to many commercial species. There are nearly 9900 species published genomes in the Eukaryota on the NCBI database (https://www.ncbi.nlm.nih.gov/genome/), accessed on 7 July 2022. Genome survey sequencing (GSS) was considered useful for providing basic genome information. Besides productively identifying genome-wide simple sequence repeats (SSRs) effectively, it can predict putative gene functions efficiently and target the potential exon-intron boundaries. A series of research advances has been made in the study of phylogenomic relationships of organisms, such as plants (Ran et al. 2018; Li et al. 2019b), animals (Koepfli et al. 2015; Heras et al. 2020), and fungi (Spatafora et al. 2016; Liu et al. 2022), which have provided insight into evolutionary history.

In the order Perciformes, the genomes of only three species, *Anarrhichthys ocellatus* (Ayres, 1855), *Cebidichthys violaceus* (Girard, 1854), and *Pholis gunnellus* (Linnaeus, 1758), have been published so far (Li et al. 2019a; Heras et al. 2020; Potter and Consortium 2022). Meanwhile, the complete mitogenomes of two species, *Chirolophis ascanii* and *Chirolophis japonicus* (or *Azuma emmnion*), provided robust phylogenetic relationships (Yang et al. 2016; Chen et al. 2017; Margaryan et al. 2021). Completed genome sequences of *C. japonicus* would improve our understanding of phylogeny, even though the genomic information of *C. japonicus* remains unknown.

In this present study, we perform a genomic survey for *C. japonicus* using next-generation sequencing technology for the first time, investigate its genomic feature and reconstruct the phylogenomic relationships with single-copy orthologs genes of *C. japonicus*. The draft genome assembly of *C. japonicus* can help us find more useful information for taxonomic studies, adaptive evolutionary mechanisms, and phylogenetic studies, as well as understand the genomic evolution of *Chirolophis*, and provide a molecular basis of *C. japonicus*.

Materials and methods

Material collection

In this study, a male specimen of *C. japonicus* with body length 186 mm and body weight 225 g was collected from coastal waters of Qingdao (35°40'N, 119°30'E), China in July 2021 (Fig. 1). Firstly, we identified it by morphological characteristics and DNA barcoding (mitochondrial DNA COI gene), then the examined sample was quickly preserved in –80 °C ultra-low temperature freezer. All subsequent animal experiments took place at Fisheries Ecology and Biodiversity Laboratory (**FEBL**) of Zhejiang Ocean University, Zhoushan, China. Experiments were conducted under the guidelines and approval of the Ethics Committee for Animal Experimentation of Zhejiang Ocean University (ZJOU-ECAE20211876). Secondly, a piece of fresh muscle tissue was clipped from the base of dorsal fin and preserved in absolute 95% ethanol.

Genomic DNA extraction and next-generation sequencing

The total cell DNA was extracted using the phenol-chloroform method (Sambrook et al. 1982), following the protocol in a previous study (Yang et al. 2021), and then carried out with DNA/Protein Analyzer and 1% agarose gel electrophoresis. High-quality DNA was randomly interrupted using ultrasonic crusher, and the obtained short reads (300–350 bp) were sequenced with Illumina NovaSeq 6000 with a paired-end library following the manufacturer's instructions (OneMore-Tech, Wuhan, China) in January 2022.

Sequence quality control, genome assembly, and K-mer analysis

Quality control was performed on the raw data from the Illumina sequencing platform using the FastQC v. 0.11.9 (Andrews 2010) and Trimmomatic v. 0.39 (Bolger et al. 2014) based on four criteria: 1) removal of the A-tail and adaptors, 2) deletion of the low-quality reads where N contents are more than 10%, 3) filtration of the reads whose base quality is less than 10, and 4) discard of duplicated reads. The genome size, heterozygosity, and repeat content of *C. japonicus* was estimated based on a K-mer method (Liu et al. 2013). De novo assembly of the *C. japonicus* genome was conducted using MaSuRCA v. 3.3.3 (Zimin et al. 2013) based on clean data.

Figure 1. *Chirolophis japonicus* (Herzenstein, 1890), 186 mm, from Qingdao.

The quality of the assembled genome was evaluated by Quast v. 5.0.2 and BUSCO v. 5.3.2 (Simão et al. 2015). The mitochondrial DNA analyses followed the method of previous studies (Yang et al. 2016, 2021; Nie et al. 2021). In brief, the software NOVOPlasty v. 4.2.1 (Dierckxsens et al. 2017) and GetOrganelle v. 1.7.6.1 (Jin et al. 2020) were used to assemble the mitogenome with clean data. The mitogenome of *C. japonicus* was annotated using MFannot tool (http://megasun.bch.umontreal.ca/cgi-bin/mfannot/mfannotInterface.pl) and GeSeq (Tillich et al. 2017), then manually annotated and drawn with OGDraw v. 1.3.1 (Lohse et al. 2013; Greiner et al. 2019). The clean data and complete assembled mitochondrial genome were uploaded to GenBank.

Gene prediction and functional annotation

The gene predictors Augustus v. 3.3.3 (Stanke and Waack 2003), SNAP (Johnson et al. 2008), and GeneMark-ES v. 4.69 (Lomsadze et al. 2005) were trained on the gene models, and all the gene models were integrated using EvidenceModeler v. 1.1.1 (Haas et al. 2008). The amino acid sequences from *C. japonicus* were annotated by GO (Ashburner et al. 2000), Eggnog (Huerta-Cepas et al. 2019), CAZymes (Cantarel et al. 2009), InterPro (Hunter et al. 2009), KEGG (Kanehisa et al. 2006), KOG https://www.creative-proteomics.com/services/kog-annotation-analysis-service.html, and Pfam (El-Gebali et al. 2019), using Diamond v. 2.0.2 with the e-value less than 1×10^{-5} (Buchfink et al. 2015).

Microsatellite identification and non-coding RNA annotation

In this study, MIcroSAtellite identification tool (MISA) v. 2.1 was used to identify simple sequence repeats (SSR) in the draft genome of *C. japonicus* (Thiel et al. 2003). The tRNA and rRNA were predicted by tRNAscan-SE v. 3.0 (Lowe and Eddy 1997) and RNAmmer v. 1.2 (Lagesen et al. 2007), respectively.

Phylogenomic analysis of *C. japonicus*

A total of 15 genomes of other bony fish were downloaded from the NCBI database (Table 1). The amino acid sequences of single-copy orthologs genes among the 16 species were found using OrthoFinder v. 2.5.4 (Emms and Kelly 2019), and these sequences were aligned by using MAFFT v. 7 (Katoh and Standley 2013). In order to reconstruct the phylogenomic relationship of *C. japonicus*, a maximum likelihood (ML) tree was analyzed/constructed using RaxML v. 8.2.12 based on the amino acid sequences of single-copy orthologs genes (Stamatakis 2014). The best model was PROTGAMMAILGF with 100 bootstrap replicates. Finally, the phylogram was viewed using FigTree v. 1.4.4 (http://tree.bio.ed.ac.uk/software/figtree/).

Table 1. Information on genomes used in this study.

Species	Biosample	Bioproject	References
Anarrhichthys ocellatus	SAMN10245424	PRJNA496475	
Archocentrus centrarchus	SAMN09948522	PRJNA489129	Koepfli et al. 2015
Cebidichthys violaceus	SAMN06857690	PRJNA384078	Heras et al. 2020
Chirolophis japonicus			**This study**
Cyclopterus lumpus	SAMN12629502	PRJNA625538	
Gasterosteus aculeatus	SAMN15223905	PRJNA707557	Berner et al. 2019; Nath et al. 2021
Gymnodraco acuticeps	SAMEA104242997	PRJEB37639	
Liparis tanakae	SAMN10970109	PRJNA523297	
Micropterus salmoides	SAMN15299117	PRJNA687018	Broughton and Reneau 2006; Sun et al. 2021
Myoxocephalus scorpius	SAMEA4028818	PRJEB12469	
Pholis gunnellus	SAMEA7522838	PRJEB45449	
Pseudoliparis sp.	SAMN10662039	PRJNA512070	Mu et al. 2021
Seriola lalandi	SAMN04902367	PRJNA319656	Purcell et al. 2018
Taurulus bubalis	SAMEA7522994	PRJEB45317	
Toxotes jaculatrix	SAMN18445299	PRJNA723051	
Ophiodon elongatus	SAMN13559843	PRJNA595583	Longo et al. 2020

Data availability statement

Raw sequencing data for genome have been deposited at the Sequence Read Archive SRR21530970. These data can be quickly accessed by checking the project ID PRJNA879413 at NCBI Project.

Results

Sequencing data statistics and K-mer analysis

In this study, a total of 65.4 Gb clean reads was obtained by next-generation sequencing from an Illumina NovaSeq 6000 platform. The Q20 value, Q30 value, and GC content were 98.17%, 94.83%, and 43.14%, respectively. The K-mer analysis with a depth of 71 shows that genome size of *C. japonicus* was 596 Mb with 0.50% heterozygosity rate and 30.30% repeat sequences (Table 2, Suppl. material 1), resulting in *C. japonicus* being a diploid.

Genomic and mitochondrial features

The genome sequences of *C. japonicus* were sequenced from a male with an Illumina NovaSeq 6000 platform, spanning 595.7 Mb with GC contents of 42.61% that were assembled using the software MaSuRCA (Table 3; Zimin et al. 2013). A total of 49

Table 2. The genome characteristics of *Chirolophis japonicus* based on the K-mer method.

Species	K-mer number	K-mer depth	Genome size (Mb)	Heterozygous ratio (%)	Repeat sequences (%)
C. japonicus	4.353×10^{10}	71	596	0.50	30.30

Table 3. Gene prediction and annotation of *Chirolophis japonicus*.

Category	Database	Number of reads	Percent (%)
Protein-coding gene model		46 729	
Annotated	InterPro	37 169	79.54
	Eggnog	37 742	80.98
	GO	9353	20.02
	KEGG_KO	17 747	37.98
	Pfam	26 530	56.77
	KOG	35 440	75.84
	CAZymes	765	1.64
Assembly BUSCO coverage			88.9

901 contigs was generated with the largest contigs of 365 029 bp. The final contigs N50 and L50 were 29 108 bp and 5388 bp long, respectively (Table 3). A total of 69 rRNA was identified, including 66 8S rRNA, two 18S rRNA, and single 28S rRNA. In addition, 846 tRNA were annotated using the tRNAscan-SE.

The complete mitogenome of *C. japonicus* is 16,522 bp long with a GC content of 45.97%. It consists of two ribosomal RNA genes (rnl and rns), 20 tRNA genes, and 13 protein-coding genes (PCGs) without an intron (Fig. 2).

Chirolophis japonicus genome annotation

A total of 46 729 protein-coding genes was predicted by a combination of different software, including Augustus v. 3.3.3 (Stanke and Waack 2003), SNAP (Johnson et al. 2008) and GeneMark-ES v4.69 (Lomsadze et al. 2005). Among these, 79.54%, 80.98%, 20.02%, 39.98%, 56.77%, 75.84%, and 1.64% genes were annotated in the InterPro, Eggnog, GO, KEGG_KO, Pfam, KOG, and CAZymes databases, respectively.

Distribution and features of SSR

A total of 554 136 of SSR was identified in the complete genome of *C. japonicus*, including 166 077 of mononucleotide microsatellite motifs (29.97%), 329 685 of dinucleotide microsatellite motifs (59.49%), 37 615 of trinucleotide microsatellite motifs (6.79%), 17 896 of tetranucleotide microsatellite motifs (3.23%), 1568 of pentanucleotide microsatellite motifs (0.28%), and 1322 of hexanucleotide microsatellite motifs (0.24%;) (Fig. 2). A/T, AC, GAG, AGAC, CTCTC, and CCCTAA were the highest repeats in mono-, di-, tri-, tetra-, penta-, and hexanucleotide microsatellite motifs, respectively (Fig. 3).

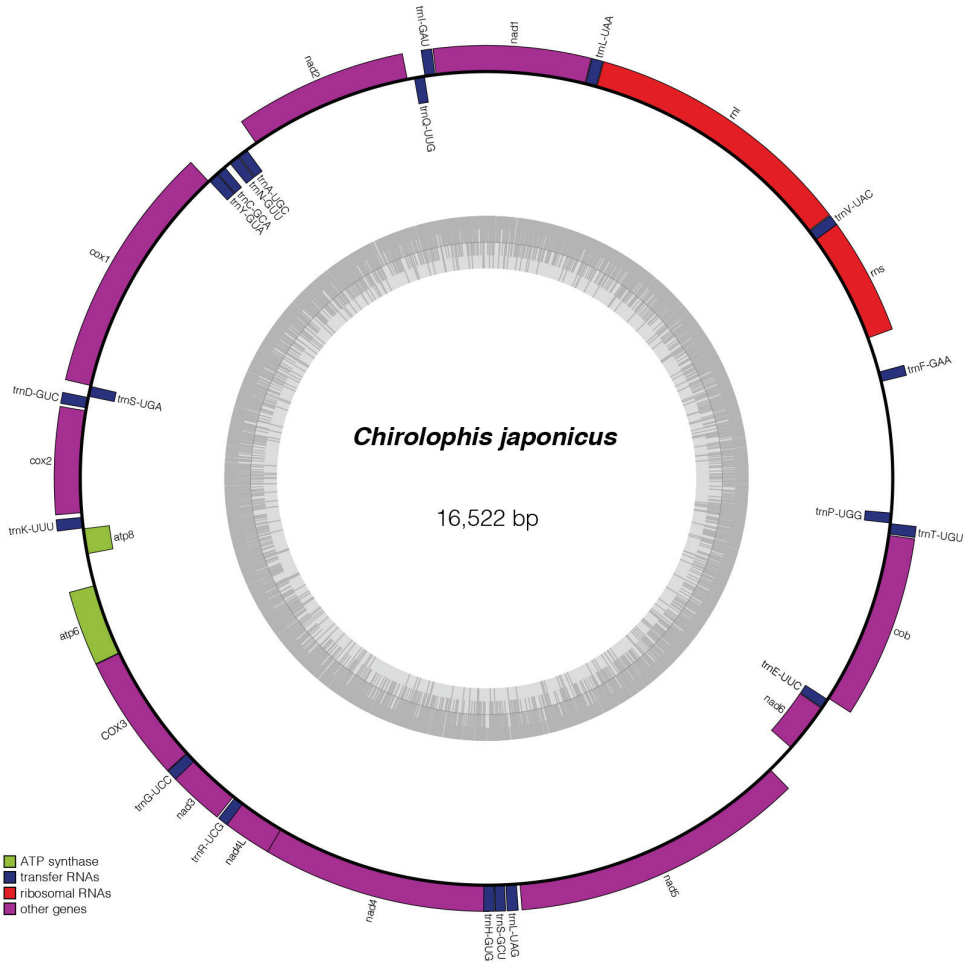

Figure 2. The complete mitogenome structure of *Chirolophis japonicus*.

Phylogenomic relationships of *Chirolophis japonicus*

In the present study, the phylogenomic relationship of a total of 16 bony fish (Table 1, Fig. 4) was reconstructed. A total of 694 single copy genes (Suppl. material 2) was identified from 16 male fish genomes using OrthoFinder (Emms and Kelly 2019), which consisted of 361 031 characters from amino acid sequences. The phylogenomic tree suggested that *Chirolophis japonicus* is closely related with *Anarrhichthys ocellatus*, *Cebidichthys violaceus*, and *Pholis gunnellus*, and provided robust phylogenetic relationships within the order Zoarcales, with full support. Although *Chirolophis japonicus* and *Cebidichthys violaceus* belong to the family Stichaeidae, they did not form a clade based on the amino acid sequences of 694 single-copy genes. In addition, *Ophiodon elongatus*, *Cyclopterus lumpus*, *Liparis tanakae*, *Pseudoliparis* sp., *Taurulus bubalis*, and *Myoxocephalus scorpius* clustered into a clade; other species, including *Gymnodraco acuticeps*, *Archocentrus*

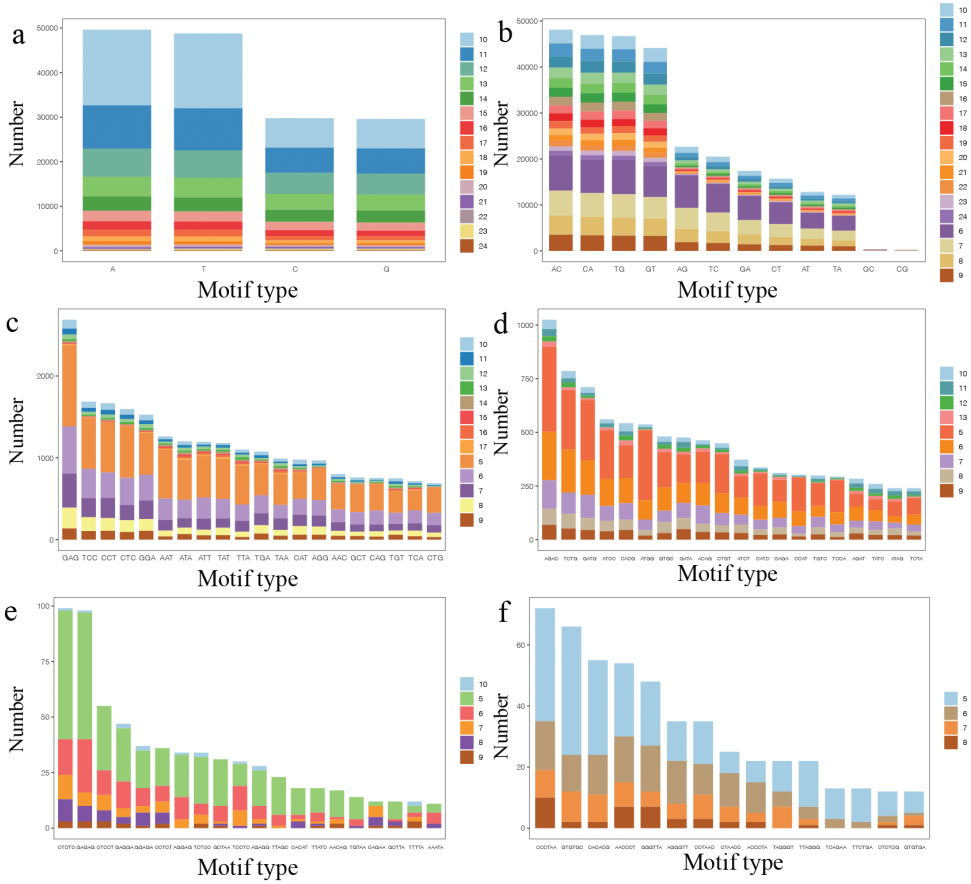

Figure 3. The distributions and frequencies of microsatellite motifs of *Chirolophis japonicus* **a** mononucleotide microsatellite motifs **b** dinucleotide microsatellite motifs **c** trinucleotide microsatellite motifs **d** tetranucleotide microsatellite motifs **e** pentanucleotide microsatellite motifs **f** hexanucleotide microsatellite motifs.

centrarchus, *Seriola lalandi*, *Toxotes jaculatrix*, *Micropterus salmoides* and *Gasterosteus aculeatus*, formed a separate clade. In addition, the phylogenomic analysis based on the amnio acid of 13 protein-coding genes of mitogenome show that *Chirolophis japonicus* is closely related with the *Chirolophis ascanii* (Fig. 5).

Discussion

Currently, there are more than 30 000 species of fishes, including bony, jawless, and cartilaginous fishes, living on the earth, some with great ecological and economic value. In 2002, the first fish genome, *Fugu rubripes* (also known as "torafugu") was published, which provided a framework for future studies of fish genomes (Aparicio

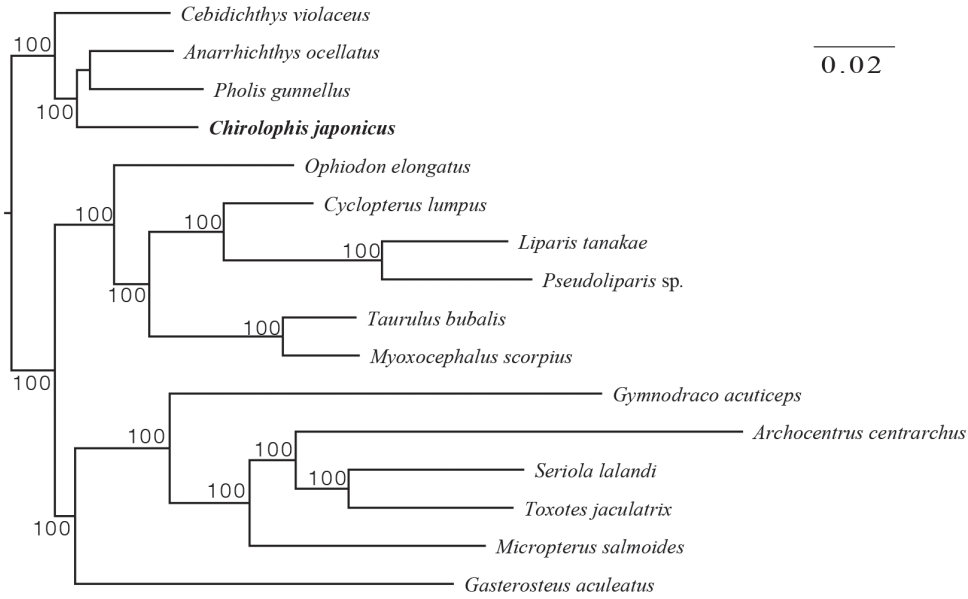

Figure 4. A maximum likelihood (ML) phylogenomic tree of *Chirolophis japonicus* based on amino acid sequences of 694 single-copy genes. *Chirolophis japonicus* is in bold. Maximum likelihood bootstrap values (90%) of each clade are indicated along branches. A scale bar in the upper right indicates substitutions per site.

et al. 2002). With the rapid development of the whole genome sequencing (WGS) technology, a large number of fish genomes have since been sequenced, such as fish as model organisms *Oryzias latipes* and *Danio rerio*, and economically important fishes such as *Cyprinus carpio* and *Ctenopharyngodon idella* (Kasahara et al. 2007; Howe et al. 2013; Xu et al. 2014; Wu et al. 2022). In addition, the Chinese "Aquatic 10-100-1000 Ge- nomics Program" and the "Fish 10K Project" have facilitated the understanding of fish genomes (Liu et al. 2017; Fan et al. 2020). Until now, a total of 819 fish genomes has been released in the NCBI database (https://www.ncbi.nlm.nih.gov/genome/, assessed on 7 July 2022), which is less than3% of the known 30 000 species.

In the present study, a new fish genome, *Chirolophis japonicus*, was sequenced. The genomes size was estimated to be 596 Mb based on the K-mer analysis, and the genome spanned 595.7 Mb, assembled using the MaSuRCA (Table 3; Zimin et al. 2013), which followed the predicted genome size of the K-mer method. Among the published teleost genomes, the size ranges from 322.5 Mb (*Fugu rubripes*) to 40 Gb (*Protopterus annectens*) (Aparicio et al. 2002; Wang et al. 2021), with an average length less than 1 Gb (Fan et al. 2020). Meanwhile, the genome of three species in Zoarcales, including *Anarrhichthys ocellatus* (612.19 Mb), three genomes of *Cebidichthys violaceus* (575.66 Mb, 593.00 Mb, 606.18 Mb), and two genomes of *Pholis gunnellus* (588.7 Mb, 590.3 Mb), are slightly larger than that of *C. japonicus* (https://www.ncbi.nlm.nih.gov/genome/, assessed on 7 July 2022). In addition, the heterozygous ratio of

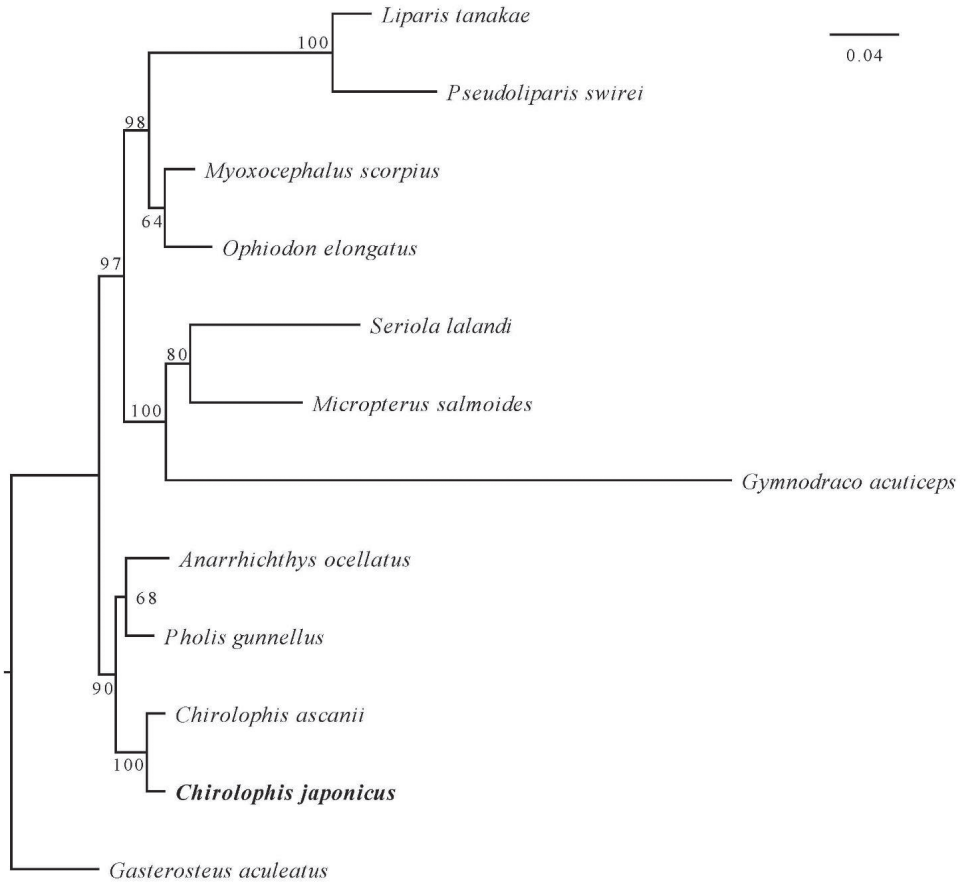

Figure 5. The maximum likelihood (ML) phylogenomic tree of fungi based on amino acid of 13 protein-coding genes (PCGs): ATP6, ATP8, COX1, COX2, COX3, CYTB, ND1, ND2, ND3, ND4, ND4L, ND5 and ND6. Support values for ML analysis greater than 60% is given on relative clade. A scale bar in the upper left indicates substitutions per site.

C. japonicus was 0.50%, probably mid-level compared to other teleost genomes (Aird et al. 2011; Li et al.2019c; Xu et al. 2020; Yang et al. 2021).

At present, phylogenomic analysis has become an important method for studying the evolutionary relationships of an organism, such as plants (Ran et al. 2018; Li et al. 2019b), animals (Koepfli et al. 2015; Heras et al. 2020), and fungi (Spatafora et al. 2016; Liu et al. 2022). Although the phylogenetic relationships of the genus *Chirolophis* have been published based on the mitogenomes (Yang et al. 2016; Chen et al. 2017; Margaryan et al. 2021), we provided a phylogenomic relationship according to the 694 single-copy genes (Fig. 3, Suppl. material 2) among *C. japonicus* and 15 other species. The results of the phylogenomic tree shows that *C. japonicus* is closely related with three species in the order Zoarcales, while *C. japonicus* and *Cebidichthys violaceus*, belonging to the family Stichaeidae,

are without a clade (Fig. 2). Thus, solving this problem requires more fish genomes to be sequenced.

Microsatellite DNA markers shows many advantages, such as codominant, extensive distribution, abundant polymorphisms, and a convenient analysis, and was considered to be an effective tool in genetic analysis and evolutionary research (Yang et al. 2022). In this study, the highest number and type of repeats is dinucleotide repeats, which was consistent with data for *Ophichthus evermanni* (Yang et al. 2022), *Padon nehereus* (Yang et al. 2021), *Cociella crocodilus* (Zhao et al. 2021), *Acanthogobius ommaturus* (Chen et al. 2020), *Sillago sihama* (Qiu et al. 2020), and other species. SSR polymorphic loci are mainly distributed among mononucleotide and dinucleotide repeats. Based on this, the search of polymorphic SSR markers from low repetitive motifs will greatly help in subsequent population genetics research of *C. japonicus*. The complexity of repeated motif usually reflects DNA mutation rate and evolutionary level (Katti et al. 2001). The frequency from mononucleotides to trinucleotides was up to 96.25%, which implies that *C. japonicus* has experienced a long evolutionary history and accumulated more genetic variation.

Finally, the genome assembly of *C. japonicus* can help us understand the genome evolution of *Chirolophis* and teleosts, as well as provide a molecular basis for breeding and cultivation.

Acknowledgements

We sincerely thank the reviewers for their constructive comments. We would like to thank Yuan Zhang and Chenghao Jia for assistance in sample collection and sorting. This work was supported by the Zhejiang Provincial Key Research and Development Program (2021C02047); The Doctoral Research Foundation of Shandong Jiaotong University, Grant/Award Numbers: BS201902051.

References

Aird D, Ross MG, Chen WS, Danielsson M, Fennell T, Russ C, Jaffe DB, Nusbaum C, Gnirke A (2011) Analyzing and minimizing PCR amplification bias in Illumina sequencing libraries. Genome Biology 12(2): 1–14. https://doi.org/10.1186/gb-2011-12-2-r18

Andrews S (2010) FastQC: a quality control tool for high throughput sequence data. http://www.bioinformatics.babraham.ac.uk/projects/fastqc/ [Date last accessed: April 18, 2020]

Aparicio S, Chapman J, Stupka E, Putnam N, Chia JM, Dehal P, Christoffels A, Rash S, Hoon S, Smit A, Gelpke MDS, Roach J, Oh T, Ho IY, Wong M, Detter C, Verhoef F, Predki P, Tay A, Lucas S, Richardson P, Smith SF, Clark MS, Edwards YJK, Doggett N, Zharkikh A, Tavtigian SV, Pruss D, Barnstead M, Evans C, Baden H, Powell J, Glusman G, Rowen L, Hood L, Tan YH, Elgar G, Hawkins T, Venkatesh B, Rokhsar D, Brenner S (2002) Whole-genome shotgun assembly and analysis of the genome of *Fugu rubripes*. Science 297(5585): 1301–1310. https://doi.org/10.1126/science.1072104

Ashburner M, Ball CA, Blake JA, Botstein D, Butler H, Cherry JM, Davis AP, Dolinski K, Dwight SS, Eppig JT, Harris MA, Hill DP, Issel-Tarver L, Kasarskis A, Lewis S, Matese JC, Richardson JE, Ringwald M, Rubin GM, Sherlock G (2000) Gene ontology: Tool for the unification of biology. Nature Genetics 25(1): 25–29. https://doi.org/10.1038/75556

Balanov A, Epur I, Shelekhov V (2020) A Description of *Chirolophis japonicus* and *Ch. saitone* (Stichaeidae) Pelagic Larvae from Peter the Great Bay, Sea of Japan. Journal of Ichthyology 60(3): 364–374. https://doi.org/10.1134/S0032945220030042

Berner D, Roesti M, Bilobram S, Chan SK, Kirk H, Pandoh P, Taylor GA, Zhao Y, Jones SJM, DeFaveri J (2019) De novo sequencing, assembly, and annotation of four three spine stickleback genomes based on microfluidic partitioned DNA libraries. Genes 10(6): 426. https://doi.org/10.3390/genes10060426

Bolger AM, Lohse M, Usadel B (2014) Trimmomatic: A flexible trimmer for Illumina sequence data. Bioinformatics 30(15): 2114–2120. https://doi.org/10.1093/bioinformatics/btu170

Broughton RE, Reneau PC (2006) Spatial covariation of mutation and nonsynonymous substitution rates in vertebrate mitochondrial genomes. Molecular Biology and Evolution 23(8): 1516–1524. https://doi.org/10.1093/molbev/msl013

Buchfink B, Xie C, Huson DH (2015) Fast and sensitive protein alignment using DIAMOND. Nature Methods 12(1): 59–60. https://doi.org/10.1038/nmeth.3176

Cantarel BL, Coutinho PM, Rancurel C, Bernard T, Lombard V, Henrissat B (2009) The Carbohydrate-Active EnZymes database (CAZy): An expert resource for glycogenomics. Nucleic Acids Research 37(Database): 233–238. https://doi.org/10.1093/nar/gkn663

Chen F (2017) Study on the biological characteristics of *Azuma emmnion*. Master thesis, Dalian Ocean University, Dalian, China.

Chen X, Chen Y, Yu M, Sha Z, Shan X (2017) The complete mitochondrial genome of the *Azuma emmnion*. Mitochondrial DNA. Part A, DNA Mapping, Sequencing, and Analysis 28(1): 77–78. https://doi.org/10.3109/19401736.2015.1110806

Chen B, Sun Z, Lou F, Gao T, Song N (2020) Genomic characteristics and profile of microsatellite primers for *Acanthogobius ommaturus* by genome survey sequencing. Bioscience Reports 40(11): 1–8. https://doi.org/10.1042/BSR20201295

Dierckxsens N, Mardulyn P, Smits G (2017) NOVOPlasty: De novo assembly of organelle genomes from whole genome data. Nucleic Acids Research 45: e18. https://doi.org/10.1093/nar/gkw955

El-Gebali S, Mistry J, Bateman A, Eddy SR, Luciani A, Potter SC, Qureshi M, Richardson LJ, Salazar GA, Smart A, Sonnhammer ELL, Hirsh L, Paladin L, Piovesan D, Tosatto SCE, Finn RD (2019) The Pfam protein families database in 2019. Nucleic Acids Research 47(D1): D427–D432. https://doi.org/10.1093/nar/gky995

Emms DM, Kelly S (2019) OrthoFinder: Phylogenetic orthology inference for comparative genomics. Genome Biology 20(1): 238. https://doi.org/10.1186/s13059-019-1832-y

Fan G, Song Y, Yang L, Huang X, Zhang S, Zhang M, Yang X, Chang Y, Zhang H, Li Y, Liu S, Yu L, Chu J, Seim I, Feng C, Near TJ, Wing RA, Wang W, Wang K, Wang J, Xu X, Yang H, Liu X, Chen N, He S (2020) Initial data release and announcement of the 10,000 Fish Genomes Project (Fish10K). GigaScience 9(8): giaa0080. https://doi.org/10.1093/gigascience/giaa080

Greiner S, Lehwark P, Bock R (2019) Organellar Genome DRAW (OGDRAW) version 1.3. 1: Expanded toolkit for the graphical visualization of organellar genomes. Nucleic Acids Research 47(W1): W59–W64. https://doi.org/10.1093/nar/gkz238

Haas BJ, Salzberg SL, Zhu W, Pertea M, Allen JE, Orvis J, White O, Buell CR, Wortman JR (2008) Automated eukaryotic gene structure annotation using evidence modeler and the program to assemble spliced alignments. Genome Biology 9(1): 1–22. https://doi.org/10.1186/gb-2008-9-1-r7

Heras J, Chakraborty M, Emerson JJ, German DP (2020) Genomic and biochemical evidence of dietary adaptation in a marine herbivorous fish. Proceedings. Biological Sciences 287(1921): e20192327. https://doi.org/10.1098/rspb.2019.2327

Howe K, Clark MD, Torroja CF, Torrance J, Berthelot C, Muffato M, Collins JE, Humphray S, McLaren K, Matthews L, McLaren S, Sealy I, Caccamo M, Churcher C, Scott C, Barrett JC, Koch R, Rauch G-J, White S, Chow W, Kilian B, Quintais LT, Guerra-Assunção JA, Zhou Y, Gu Y, Yen J, Vogel J-H, Eyre T, Redmond S, Banerjee R, Chi J, Fu B, Langley E, Maguire SF, Laird GK, Lloyd D, Kenyon E, Donaldson S, Sehra H, Almeida-King J, Loveland J, Trevanion S, Jones M, Quail M, Willey D, Hunt A, Burton J, Sims S, McLay K, Plumb B, Davis J, Clee C, Oliver K, Clark R, Riddle C, Elliott D, Threadgold G, Harden G, Ware D, Begum S, Mortimore B, Kerry G, Heath P, Phillimore B, Tracey A, Corby N, Dunn M, Johnson C, Wood J, Clark S, Pelan S, Griffiths G, Smith M, Glithero R, Howden P, Barker N, Lloyd C, Stevens C, Harley J, Holt K, Panagiotidis G, Lovell J, Beasley H, Henderson C, Gordon D, Auger K, Wright D, Collins J, Raisen C, Dyer L, Leung K, Robertson L, Ambridge K, Leongamornlert D, McGuire S, Gilderthorp R, Griffiths C, Manthravadi D, Nichol S, Barker G, Whitehead S, Kay M, Brown J, Murnane C, Gray E, Humphries M, Sycamore N, Barker D, Saunders D, Wallis J, Babbage A, Hammond S, Mashreghi-Mohammadi M, Barr L, Martin S, Wray P, Ellington A, Matthews N, Ellwood M, Woodmansey R, Clark G, Cooper JD, Tromans A, Grafham D, Skuce C, Pandian R, Andrews R, Harrison E, Kimberley A, Garnett J, Fosker N, Hall R, Garner P, Kelly D, Bird C, Palmer S, Gehring I, Berger A, Dooley CM, Ersan-Ürün Z, Eser C, Geiger H, Geisler M, Karotki L, Kirn A, Konantz J, Konantz M, Oberländer M, Rudolph-Geiger S, Teucke M, Lanz C, Raddatz G, Osoegawa K, Zhu B, Rapp A, Widaa S, Langford C, Yang F, Schuster SC, Carter NP, Harrow J, Ning Z, Herrero J, Searle SMJ, Enright A, Geisler R, Plasterk RHA, Lee C, Westerfield M, de Jong PJ, Zon LI, Postlethwait JH, Nüsslein-Volhard C, Hubbard TJP, Crollius HR, Rogers J, Stemple DL (2013) The zebrafish reference genome sequence and its relationship to the human genome. Nature 496(7446): 498–503. https://doi.org/10.1038/nature12111

Huerta-Cepas J, Szklarczyk D, Heller D, Hernández-Plaza A, Forslund SK, Cook H, Mende DR, Letunic I, Rattei T, Jensen LJ, von Mering C, Bork P (2019) eggNOG 5.0: A hierarchical, functionally and phylogenetically annotated orthology resource based on 5090 organisms and 2502 viruses. Nucleic Acids Research 47(D1): D309–D314. https://doi.org/10.1093/nar/gky1085

Hunter S, Apweiler R, Attwood TK, Bairoch A, Bateman A, Binns D, Bork P, Das U, Daugherty L, Duquenne L, Finn RD, Gough J, Haft D, Hulo N, Kahn D, Kelly E, Laugraud A, Letunic I, Lonsdale D, Lopez R, Madera M, Maslen J, McAnulla C, McDowall J, Mistry J,

Mitchell A, Mulder N, Natale D, Orengo C, Quinn AF, Selengut JD, Sigrist CJA, Thimma M, Thomas PD, Valentin F, Wilson D, Wu CH, Yeats C (2009) InterPro: The integrative protein signature database. Nucleic Acids Research 37(Database): D211–D215. https://doi.org/10.1093/nar/gkn785

Jin JJ, Yu WB, Yang JB, Song Y, DePamphilis CW, Yi TS, Li DZ (2020) GetOrganelle: A fast and versatile toolkit for accurate de novo assembly of organelle genomes. Genome Biology 21(1): 1–31. https://doi.org/10.1186/s13059-020-02154-5

Jing L, Mingcheng T, Feng Y (2005) Taxonomic reexamination of the genus *Chirolophis* in China waters. Chinese Journal of Oceanology and Limnology 23(2): 199–203. https://doi.org/10.1007/BF02894239

Johnson AD, Handsaker RE, Pulit SL, Nizzari MM, O'Donnell CJ, De Bakker PI (2008) SNAP: A web-based tool for identification and annotation of proxy SNPs using HapMap. Bioinformatics 24(24): 2938–2939. https://doi.org/10.1093/bioinformatics/btn564

Kanehisa M, Goto S, Hattori M, Aoki-Kinoshita KF, Itoh M, Kawashima S, Katayama T, Araki M, Hirakawa M (2006) From genomics to chemical genomics: New developments in KEGG. Nucleic Acids Research 34(90001): D354–D357. https://doi.org/10.1093/nar/gkj102

Kasahara M, Naruse K, Sasaki S, Nakatani Y, Qu W, Ahsan B, Yamada T, Nagayasu Y, Kasai Y, Jindo T (2007) The medaka draft genome and insights into vertebrate genome evolution. Nature 447(7145): 714–719. https://doi.org/10.1038/nature05846

Katoh K, Standley DM (2013) MAFFT Multiple Sequence Alignment Software Version 7: Improvements in Performance and Usability. Molecular Biology and Evolution 30(4): 772–780. https://doi.org/10.1093/molbev/mst010

Katti MV, Ranjekar PK, Gupta VS (2001) Differential distribution of simple sequence repeats in eukaryotic genome sequences. Molecular Biology and Evolution 18(7): 1161–1167. https://doi.org/10.1093/oxfordjournals.molbev.a003903

Koepfli KP, Paten B, O'Brien SJ (2015) The Genome 10K Project: A way forward. Annual Review of Animal Biosciences 3(1): 57–111. https://doi.org/10.1146/annurev-animal-090414-014900

Lagesen K, Hallin P, Rødland EA, Stærfeldt HH, Rognes T, Ussery DW (2007) RNAmmer: Consistent and rapid annotation of ribosomal RNA genes. Nucleic Acids Research 35(9): 3100–3108. https://doi.org/10.1093/nar/gkm160

Li F, Chen X, Lu G, Qu J, Bian L, Chang Q, Ge J, Liu C, Zhang S, Chen S (2019a) Sequence and phylogenetic analysis of the mitochondrial genome for the Wolf-eel, *Anarrhichthys ocellatus* (Anarhichadidae: Perciformes). Mitochondrial DNA. Part B, Resources 4(2): 2884–2885. https://doi.org/10.1080/23802359.2019.1660260

Li H, Yi T, Gao L, Ma P, Zhang T, Yang J, Gitzendanner M, Fritsch P, Cai J, Luo Y, Wang H, van der Bank M, Zhang S-D, Wang Q-F, Wang J, Zhang Z-R, Fu C-N, Yang J, Hollingsworth PM, Chase MW, Soltis DE, Soltis PS, Li D-Z (2019b) Origin of angiosperms and the puzzle of the Jurassic gap. Nature Plants 5(5): 461–470. https://doi.org/10.1038/s41477-019-0421-0

Li Z, Tian C, Huang Y, Lin X, Wang Y, Jiang D, Zhu C, Chen H, Li G (2019c) A first insight into a draft genome of silver sillago (*Sillago sihama*) via genome survey sequencing. Animals (Basel) 9(10): 756. https://doi.org/10.3390/ani9100756

Liu B, Shi Y, Yuan J, Hu X, Zhang H, Li N, Li Z, Chen Y, Mu D, Fan W (2013) Estimation of genomic characteristics by analyzing k-mer frequency in de novo genome projects. ArXiv Preprint ArXiv:1308: 2012. https://doi.org/10.48550/arXiv.1308.2012

Liu Y, Xu P, Xu J, Huang Y, Liu Y, Fang H, Hu Y, You X, Bian C, Sun M, Gu R, Cui L, Zhang X, Xu P, Shi Q (2017) China is initiating the Aquatic 10-100-1,000 Genomics Program. Science China. Life Sciences 60(3): 329–332. https://doi.org/10.1007/s11427-016-0273-9

Liu F, Ma Z, Hou L, Diao Y, Wu W, Damm U, Song S, Cai L (2022) Updating species diversity of Colletotrichum, with a phylogenomic overview. Studies in Mycology, 1–86. https://doi.org/10.3114/sim.2022.101.01

Lohse M, Drechsel O, Kahlau S, Bock R (2013) Organellar Genome DRAW – A suite of tools for generating physical maps of plastid and mitochondrial genomes and visualizing expression data sets. Nucleic Acids Research 41(W1): W575–W581. https://doi.org/10.1093/nar/gkt289

Lomsadze A, Ter-Hovhannisyan V, Chernoff YO, Borodovsky M (2005) Gene identification in novel eukaryotic genomes by self-training algorithm. Nucleic Acids Research 33(20): 6494–6506. https://doi.org/10.1093/nar/gki937

Longo GC, Lam L, Basnett B, Samhouri J, Hamilton S, Andrews K, Williams G, Goetz G, McClure M, Nichols KM (2020) Strong population differentiation in lingcod (*Ophiodon elongatus*) is driven by a small portion of the genome. Evolutionary Applications 13(10): 2536–2554. https://doi.org/10.1111/eva.13037

Lowe TM, Eddy SR (1997) tRNAscan-SE: A program for improved detection of transfer RNA genes in genomic sequence. Nucleic Acids Research 25(5): 955–964. https://doi.org/10.1093/nar/25.5.955

Margaryan A, Noer CL, Richter SR, Restrup ME, Bülow-Hansen JL, Leerhøi F, Langkjær EMR, Gopalakrishnan S, Carøe C, Gilbert MTP, Bohmann K (2021) Mitochondrial genomes of Danish vertebrate species generated for the national DNA reference database DNAmark. Environmental DNA 3(2): 472–480. https://doi.org/10.1002/edn3.138

Mu Y, Bian C, Liu R, Wang Y, Shao G, Li J, Qiu Y, He T, Li W, Ao J, Shi Q, Chen X (2021) Whole genome sequencing of a snailfish from the Yap Trench (~7,000 m) clarifies the molecular mechanisms underlying adaptation to the deep sea. PLOS Genetics 17(5): e1009530. https://doi.org/10.1371/journal.pgen.1009530

Nath S, Shaw DE, White MA (2021) Improved contiguity of the three-spine stickleback genome using long-read sequencing. G3 (Bethesda) 11: jkab007. https://doi.org/10.1093/g3journal/jkab007

Nie Y, Zhao H, Wang Z, Zhou Z, Liu X, Huang B (2021) The gene rearrangement loss transfer and deep intronic variation in mitochondrial genomes of *Conidiobolus*. Frontiers in Microbiology 12: 765733–765733. https://doi.org/10.3389/fmicb.2021.765733

Potter S, Consortium DTOL (2022) The genome sequence of the rock gunnel *Pholis gunnellus* (Linnaeus 1758). Wellcome Open Research 7: 58. https://doi.org/10.12688/wellcomeopenres.17699.1

Purcell CM, Seetharam AS, Snodgrass O, Ortega-García S, Hyde JR, Severin AJ (2018) Insights into teleost sex determination from the *Seriola dorsalis* genome assembly. BMC Genomics 19(1): 31. https://doi.org/10.1186/s12864-017-4403-1

Qiu BX, Fang SB, Ikhwanuddin M, Wong LL, Ma HY (2020) Genome survey and development of polymorphic microsatellite loci for *Sillago sihama* based on Illumina sequencing technology. Molecular Biology Reports 47(4): 3011–3017. https://doi.org/10.1007/s11033-020-05348-z

Ran JH, Shen TT, Wu H, Gong X, Wang X (2018) Phylogeny and evolutionary history of Pinaceae updated by transcriptomic analysis. Molecular Phylogenetics and Evolution 129: 106–116. https://doi.org/10.1016/j.ympev.2018.08.011

Sambrook J, Fritsch EF, Maniatis T (1982) Molecular Cloning: A Laboratory Manual; Cold Spring Harbor Laboratory Press: New York NY, USA.

Sato M (1977) Histological observations on the cutaneous processes on the head of *Azuma emmnion* and *Hemitripterus villosus*. Japanese Journal of Ichthyology 24: 12–16. https://doi.org/10.11369/jji1950.24.12

Shiogaki M (1983) On the life history of the stichaeid fish *Chirolophis japonicus*. Japanese Journal of Ichthyology 29: 446–455. https://doi.org/10.11369/jji1950.29.446

Simão FA, Waterhouse RM, Ioannidis P, Kriventseva EV, Zdobnov EM (2015) BUSCO: assessing genome assembly and annotation completeness with single-copy orthologs. Bioinformatics 31: 3210–3212. https://doi.org/10.1093/bioinformatics/btv351

Simão FA, Waterhouse RM, Ioannidis P, Kriventseva EV, Zdobnov EM (2015) BUSCO: Assessing genome assembly and annotation completeness with single-copy orthologs. Bioinformatics 31(19): 3210–3212. https://doi.org/10.1093/bioinformatics/btv351

Spatafora JW, Chang Y, Benny GL, Lazarus K, Smith ME, Berbee ML, Bonito G, Corradi N, Grigoriev I, Gryganskyi A, James TY, O'Donnell K, Roberson RW, Taylor TN, Uehling J, Vilgalys R, White MM, Stajich JE (2016) A phylum-level phylogenetic classification of zygomycete fungi based on genome-scale data. Mycologia 108(5): 1028–1046. https://doi.org/10.3852/16-042

Stamatakis A (2014) RAxML version 8: A tool for phylogenetic analysis and post-analysis of large phylogenies. Bioinformatics 30(9): 1312–1313. https://doi.org/10.1093/bioinformatics/btu033

Stanke M, Waack S (2003) Gene prediction with a hidden Markov model and a new intron submodel. Bioinformatics 19: ii215–ii225. https://doi.org/10.1093/bioinformatics/btg1080

Sun C, Li J, Dong J, Niu Y, Hu J, Lian J, Li W, Li J, Tian Y, Shi Q, Ye X (2021) Chromosome-level genome assembly for the largemouth bass *Micropterus salmoides* provides insights into adaptation to fresh and brackish water. Molecular Ecology Resources 21(1): 301–315. https://doi.org/10.1111/1755-0998.13256

Thiel T, Michalek W, Varshney R, Graner A (2003) Exploiting EST databases for the development and characterization of gene-derived SSR-markers in barley (*Hordeum vulgare* L). Theoretical and Applied Genetics 106(3): 411–422. https://doi.org/10.1007/s00122-002-1031-0

Tillich M, Lehwark P, Pellizzer T, Ulbricht-Jones ES, Fischer A, Bock R, Greiner S (2017) GeSeq-versatile and accurate annotation of organelle genomes. Nucleic Acids Research 45(W1): W6–W11. https://doi.org/10.1093/nar/gkx391

Wang K, Wang J, Zhu C, Yang L, Ren Y, Ruan J, Fan G, Hu J, Xu W, Bi X (2021) African lungfish genome sheds light on the vertebrate water-to-land transition. Cell 184(5): 1362–1376[e1318]. https://doi.org/10.1016/j.cell.2021.01.047

Wu CS, Ma ZY, Zheng GD, Zou SM, Zhang XJ, Zhang YA (2022) Chromosome-level genome assembly of grass carp (*Ctenopharyngodon idella*) provides insights into its genome evolution. BMC Genomics 23(1): 271. https://doi.org/10.1186/s12864-022-08503-x

Xu P, Zhang X, Wang X, Li J, Liu G, Kuang Y, Xu J, Zheng X, Ren L, Wang G, Zhang Y, Huo L, Zhao Z, Cao D, Lu C, Li C, Zhou Y, Liu Z, Fan Z, Shan G, Li X, Wu S, Song L, Hou G, Jiang Y, Jeney Z, Yu D, Wang L, Shao C, Song L, Sun J, Ji P, Wang J, Li Q, Xu L, Sun F, Feng J, Wang C, Wang S, Wang B, Li Y, Zhu Y, Xue W, Zhao L, Wang J, Gu Y, Lv W, Wu K, Xiao J, Wu J, Zhang Z, Yu J, Sun X (2014) Genome sequence and genetic diversity of the common carp *Cyprinus carpio*. Nature Genetics 46(11): 1212–1219. https://doi.org/10.1038/ng.3098

Xu S, Song N, Xiao S, Gao T (2020) Whole genome survey analysis and microsatellite motif identification of *Sebastiscus marmoratus*. Bioscience Reports 40(2): BSR20192252. https://doi.org/10.1042/BSR20192252

Yang H, Bao X, Wang B, Liu W (2016) The complete mitochondrial genome of *Chirolophis japonicus* (Perciformes: Stichaeidae). Mitochondrial DNA. Part A, DNA Mapping, Sequencing, and Analysis 27(6): 4419–4420. https://doi.org/10.3109/19401736.2015.1089552

Yang T, Huang X, Ning Z, Gao T (2021) Genome-Wide Survey Reveals the microsatellite characteristics and phylogenetic relationships of *Harpadon nehereu*. Current Issues in Molecular Biology 43(3): 1282–1292. https://doi.org/10.3390/cimb43030091

Yang T, Ning Z, Liu Y, Zhang S, Gao T (2022) Genome-wide survey and genetic characteristics of *Ophichthus evermanni* based on Illumina sequencing platform. Bioscience Reports 42(5): BSR20220460. https://doi.org/10.1042/BSR20220460

Zhao R, Lu Z, Cai S, Gao T, Xu S (2021) Whole genome survey and genetic markers development of crocodile flathead *Cociella crocodilus*. Animal Genetics 52(6): 891–895. https://doi.org/10.1111/age.13136

Zimin AV, Marçais G, Puiu D, Roberts M, Salzberg SL, Yorke JA (2013) The MaSuRCA genome assembler. Bioinformatics 29(21): 2669–2677. https://doi.org/10.1093/bioinformatics/btt476

Supplementary material 1

K-mer analyses (K = 71) of *Chirolophis japonicus*, X-axis and Y-axis represent the K-mer depth and frequency for the corresponding depth

Authors: Lu Liu, Qi Liu, Tianxiang Gao

Data type: image

Link: https://doi.org/10.3897/zookeys.1129.91543.suppl1

Supplementary material 2

Maximum likelihood phylogenomic tree of *Chirolophis japonicus*

Authors: Lu Liu, Qi Liu, Tianxiang Gao

Data type: phylogenomic tree

Explanation note: Maximum likelihood phylogenomic tree of *Chirolophis japonicus* based on amino acids of 694 single-copy genes.

Link: https://doi.org/10.3897/zookeys.1129.91543.suppl2

ZooKeys 1129: 73–83 (2022)
doi: 10.3897/zookeys.1129.90577
https://zookeys.pensoft.net

RESEARCH ARTICLE

A peer-reviewed open-access journal
ZooKeys
Launched to accelerate biodiversity research

First record of *Tamarixia dahlsteni* Zuparko (Hymenoptera, Eulophidae), a parasitoid of *Trioza eugeniae* Froggatt (Hemiptera, Triozidae) and current status of the *Tamarixia* species in Mexico

Kenzy I. Peña-Carrillo[1], Antonio Rodríguez-Rivas[2], Sara G. Díaz-Ramos[2], Mayra A. Gómez-Govea[3], Patricia Zambrano-Robledo[4], Iram P. Rodríguez-Sánchez[3], María de Lourdes Ramírez-Ahuja[3]

1 *INIFAP, Campo Experimental General Terán, km 31 carretera Montemorelos-China, 67400, General Terán, N.L. Mexico* **2** *Universidad de Guadalajara, Centro Universitario de Ciencias Exacta e Ingenierías, Departamento de Madera Celulosa y Papel, Km 15.5, Autopista Guadalajara-Nogales, 45020 Jalisco, Mexico* **3** *Universidad Autónoma de Nuevo León, Facultad de Ciencias Biológicas, Laboratorio de Fisiología Molecular y Estructural. Av. Universidad s/n Cd. Universitaria, San Nicolás de los Garza, NL 66455, Mexico* **4** *Universidad Autónoma de Nuevo León, FIME-Centro de Investigación e Innovación en ingeniería Aeronáutica (CIIIA), Av. Universidad s/n, Ciudad Universitaria, San Nicolás de los Garza 66455, Mexico*

Corresponding author: María de Lourdes Ramírez-Ahuja (lulu.ahuja@hotmail.com)

Academic editor: Norman Johnson | Received 19 July 2022 | Accepted 24 October 2022 | Published 11 November 2022

https://zoobank.org/A145F05D-E8C7-458E-A4D7-15066FDA7770

Citation: Peña-Carrillo KI, Rodríguez-Rivas A, Díaz-Ramos SG, Gómez-Govea MA, Zambrano-Robledo P, Rodríguez-Sanchez IP, Ramírez-Ahuja ML (2022) First record of *Tamarixia dahlsteni* Zuparko (Hymenoptera, Eulophidae), a parasitoid of *Trioza eugeniae* Froggatt (Hemiptera, Triozidae) and current status of the *Tamarixia* species in Mexico. ZooKeys 1129: 73–83. https://doi.org/10.3897/zookeys.1129.90577

Abstract

Parasitic wasps of the genus *Tamarixia* represent important biological control agents of members of the true bug group, Psylloidea, and are host specific; therefore, they can be used to control insect pests. In this study we report, for the first time, the presence of the parasitoid *Tamarixia dahlsteni* in Mexico and its mitochondrial barcode region of the cytochrome oxidase I gene (COI). We also review the species diversity of the genus *Tamarixia* in Mexico.

Keywords

Biological control, COI, eugenia psyllid, parasitic wasps

Introduction

Biological control agents represent a sustainable pest management option that help to maintain pest populations under accepted levels (Wang et al. 2019; Al-Ani et al. 2020). Parasitic wasps from the family Eulophidae represent a very important group of biological control agents as they have a wide range of insect hosts with different degrees of specialization. The genus *Tamarixia* Mercet represents one example of parasitoids with a high degree of host specificity (Urbaneja-Bernat et al. 2019). Most species act as ectoparasitoids, but in some cases endoparasitism has been reported (Noyes 2022). Species of the genus *Tamarixia* parasitize free-living and gall-forming species of true bugs, Psylloidea. It was proposed that they reached this host restriction through a specialization on their host (LaSalle 1994), although the species has also been reported parasitizing aphids (Zuparko et al. 2011). According to the Universal Chalcidoidea database, the genus *Tamarixia* comprises 54 species to date, which are distributed worldwide (Noyes 2022).

In Mexico, five species (both native and exotic) of *Tamarixia* are found: *Tamarixia aguacatensis* Yefremova (Yefremova et al. 2014), *Tamarixia leucaenae* Boucek (McClay 1990), *Tamarixia radiata* (Waterston) (González-Hernández et al. 2009), *Tamarixia schina* Zuparko (Zuparko et al. 2011), and *Tamarixia triozae* (Burks) (Lomelí-Flores and Bueno 2002). Some of these species have already been part of integrated pest management strategies with remarkable results. For instance, *T. triozae*, the parasitoid of the potato psyllid *Bactericera cockerelli*, was introduced to New Zealand for the biological control of the psyllids that vector the bacterium *Candidatus* Liberibacter *solanacearum* (CLso) (Workman and Whiteman 2009). This bacterium has been linked to different diseases in plants of the nightshade family Solanaceae (Munyaneza et al. 2007). In Mexico, *T. triozae* was found naturally in tomato crops and, according to parasitism evaluation, the percentage of parasitism reached by *T. triozae* on *B. cockerelli* has been up to eighty percent when insecticides are not used to control the psyllid populations (Lomelí-Flores and Bueno 2002). *Tamarixia triozae* is commercially available in Mexico through Koppert Mexico, and several studies have been carried out on its biological cycle (Rojas et al. 2015), its release into the environment either individually or in combination with other natural enemies for the control of *B. cockerelli* (Cerón-González et al. 2014; Ramírez-Ahuja et al. 2017). Other examples of *Tamarixia* species used for biological control are *T. schina*, which was introduced in California for the control of *Calophya schini* Tuthill (Psyllidae: Calophyidae), *T. dahlsteni* Zuparko, which was introduced for the control of *Trioza eugeniae* Froggatt (Hemiptera: Triozidae) (Zuparko et al. 2011) and *T. radiata*. The latter is native to Pakistan (Chen and Stansly 2014), but has been introduced into countries such as Taiwan, the United States and France (Guadeloupe), to control populations of the psyllid *Diaphorina citri* Kuwayama (Hemiptera: Liviidae), a vector of the bacterium *Candidatus* Liberibacter *asiaticus* (Chien et al. 1989; Michaud 2002; De León and Sétamou 2010). In Texas, a reduction of more than ninety percent of *D. citri* populations has been observed in regions where *T. radiata* was released (Flores and Ciomperlik 2017). In Mexico, the parasitoid was reported as an accidentally introduced species (De León and Sétamou 2010).

Currently, DNA barcodes are important tools for species identification with potential for bio-surveillance programs in agriculture (Ashfaq and Hebert 2016). DNA barcodes have been useful to identify important arthropod pests even at immature stages (Ashfaq and Hebert 2016). The common barcoding method used for animal identification is based on the sequencing of a part of the mitochondrial gene cytochrome oxidase subunit I (COI). COI has been used to create universal and public databases of sequences, such as the Barcode of Life Data System (BOLD), which includes agriculturally important insect sequences (Hebert et al. 2003). In this regard, here we report the occurrence of *T. dahlsteni* in Mexico for the first time, and the first mitochondrial cytochrome oxidase subunit one (COI) sequences for this species. We also discuss the potential of additional species of *Tamarixia* in Mexico.

Materials and methods

Biological samples

We obtained parasitoids emerged from nymphs of *Trioza eugeniae* feeding on *Syzygium paniculatum*, collected in an urban area from Zapopan, Jalisco, Mexico [Colonia Las Palomas, Tesistán (20.7890, -103.4831) and Club Deportivo UdeG (20.7793, -103.6075)]. The nymphs were taken to the laboratory (HR 70%, T 25 ± 2 °C) and were placed into Petri dishes until the parasitoids emerged. The parasitoids were placed in 96% ethanol for morphological and molecular determination.

Morphological determination

According to Zuparko et al. (2011), the psyllid *Trioza eugeniae* is parasitized by *Tamarixia dahlsteni*; therefore, we employed Zuparko's morphological description to identify the newly emerged parasitoids. Voucher specimens of the recovered parasitoids were deposited in the Beneficial Insects Collection of the Universidad Autónoma de Nuevo León (CIBE–UANL). All individuals followed the same diagnosis and, given the low number of specimens recovered, only one female was photographed with a scanning electronic microscope (JEOL JSM–6510LV) in order to illustrate its diagnostic characteristics.

Barcoding determination

Genomic DNA was non-destructively isolated according to the protocol described by Giantsis et al. (2016). We extracted three individual specimens that corresponded to *T. dahlsteni*, two specimens of *T. triozae* and two of *T. schina*. Polymerase chain reaction (PCR) was carried out to amplify the DNA barcode region of the cytochrome oxidase subunit I (COI) using the LCO1490 (5'-GGTCAACAAATCATAAAGATATTGG-3') and HCO2198 (5'-TAAACTTCAGGGTGACCAAAAAATCA-3') primers (Folmer et al. 1994). PCRs were performed in a 20 µl reaction volume: 2 µl

of DNA, 2 µl of 10× Qiagen PCR buffer containing 15 mM MgCl2, 0.9 µl of each primer (10 um), 0.6 µl of dNTPs (25 mM each), 0.2 µl of (5 U/µl) Taq DNA Polymerase (Qiagen, Hilden, Germany), and 13.4 µl of H_2O. PCR conditions were as follows: 94 °C for 3 min, followed by 40 cycles of 94 °C for 30 s, 52 °C for 1 min, 72 °C for 1 min with a final extension at 72 °C for 10 min. All PCR products were electrophoresed through an agarose gel (1%) and sequenced in both directions in an Applied Biosystems model 3500 automated sequencer in Lanbama–Ipicyt (San Luis Potosí, Mexico).

Phylogenetic analysis

We employed the resulting COI sequences to reconstruct the phylogenetic relations of the emerged parasitoids. For this objective, we included COI sequences of all available species of the genus *Tamarixia*, which were downloaded from the BOLD Systems database and GenBank. All sequences were aligned in Mesquite ver. 3.70 (Maddison and Maddison 2021) with the program MUSCLE ver. 3 (Edgar 2004). Later, the alignment was used for the phylogenetic analysis inferred with the Maximum Likelihood method in the online server IQ-tree ver. 1.6.12 (Trifinopoulos et al. 2016), and the model GTR+F+I+G4 which was inferred with the function Model Finder (Kalyaanamoorthy et al. 2017). Branch support was obtained with the ultrafast bootstrap approximation (Hoang et al. 2018) with 10 000 replicates. Sequences generated in this study were deposited in GenBank.

Results

Morphological and barcoding determination

From the collected material for this study, seven females and seven males of the genus *Tamarixia* emerged. They agreed with the diagnosis of *T. dahlsteni*: the entire ventral surface of the gaster was yellow, and in the dorsal part the yellow color extending to, or slightly beyond, the apex of the second tergite (Fig. 1). The specimens had a paraspicular carina posteriorly bifurcated and located medial to the propodeal spiracle (Figs 2, 3). Regarding the barcoding determination, the sequences generated in this study represent the first barcoding evidence for the species *T. dahlsteni* (GenBank accession ON491415, ON491416, ON491417) and *T. schina* (GenBank accession ON548243, ON684328).

Phylogenetic analysis

Our sequence alignment contained 893 bp, and included sequences of the species *Tamarixia drukyulensis* Yefremova and Yegorenkova, *Tamarixia dryi* Waterston, *Tamarixia*

pronomus Walker, *Tamarixia pubescens* Nees, *T. radiata*, *T. triozae* and *Tamarixia upis* Walker, obtained from public databases and those of *T. dahlsteni* and *T. schina* generated in this study. In the phylogenetic reconstruction, sequences of each species were clustered in individual subclades with high support (ultrabootstrap values >95) (Fig. 4). Therefore, the barcoding region appears to be useful for the molecular identification of the *Tamarixia* species included in this study. Our analysis did not resolve interspecific relations due to the low bootstrap support for interior branches. On the other hand, the presence of highly supported (ultrabootstrap values >95) intraspecific subclades within *T. drukyulensis* and *T. dryi* suggests intraspecific genetic structure.

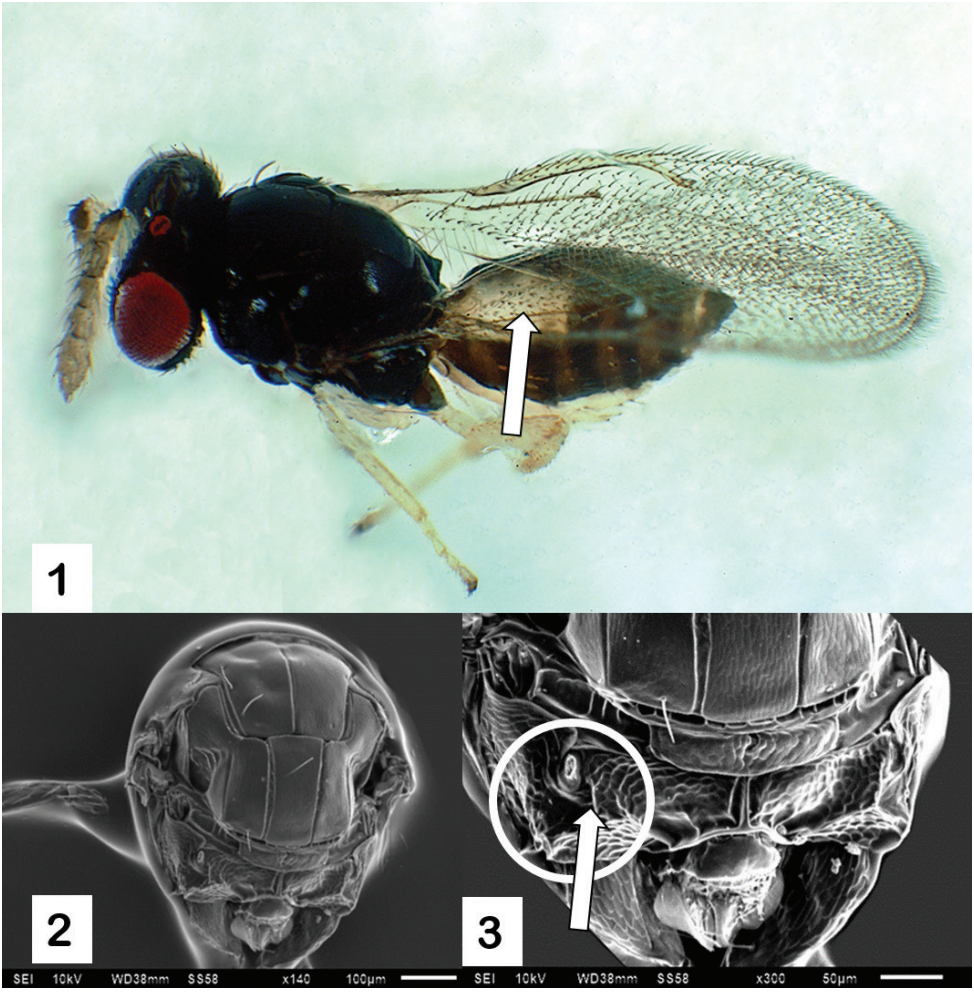

Figures 1–3. *Tamarixia dahlsteni* **1** gaster (dorsal view), arrow pointing the yellow color extending to the apex of the second tergite **2** mesosoma (dorsal view) **3** arrow pointing paraspicular carina. Scale bars: 100 µm (**2**); 50 µm (**3**).

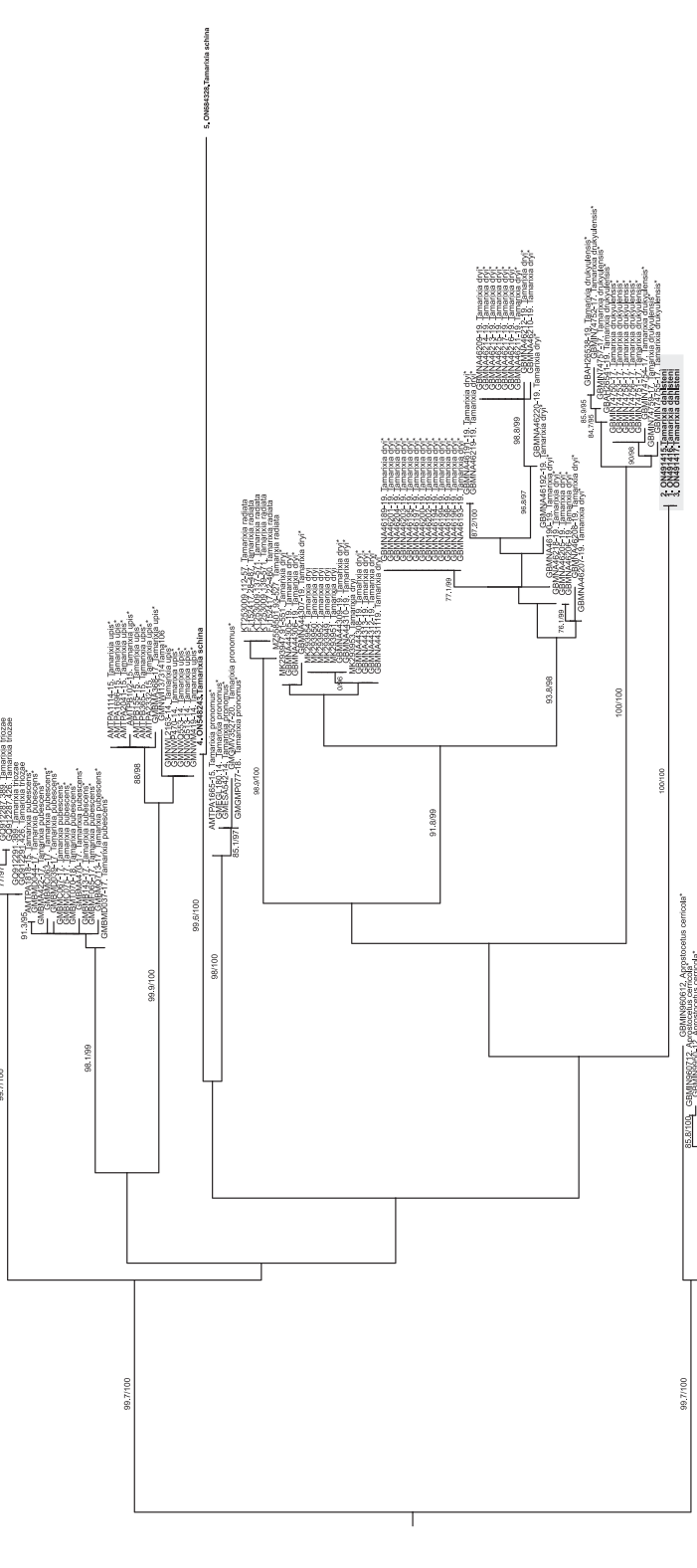

Figure 4. Phylogenetic tree showing the genetic relations between species of the genus *Tamarixia*. *Aprostocetus cerricola* was included as an outgroup and *Tamarixia dahlsteni* is highlighted in gray color. Bootstrap branch support ≥ 95% is shown above branches; samples in bold represent sequences generated in this study, while samples with an asterisk (*) were downloaded from the BOLD Systems database. The rest of the samples were downloaded from GenBank. BOLD Systems specimen records and GenBank accession numbers are shown before the species name.

Discussion

According to the literature, seven of the 54 existing species of *Tamarixia* are reported from the Nearctic and Neotropical regions (Noyes 2022). Mexico spans both regions and, following this study, the number of *Tamarixia* species was updated to six. In addition, our phylogenetic analysis suggested the COI barcoding region to be a useful molecular marker for the distinction of *Tamarixia* species. The phylogeny obtained suggested intraspecific genetic structure for some of the species, which unveils the necessity of robust and wider phylogenetic analysis at the genus level.

The host for *T. dahlsteni* is the eugenia psyllid *Trioza eugeniae*. Both species were found in Australia associated with the ornamental tree *Syzygium paniculatum*, and in 1988 the psyllid was found for the first time in California, USA. The damage caused by the psyllid on *S. paniculatum* trees prompted a search for its natural enemies in Australia. As a result, the wasp *T. dahlsteni* was identified as the primary parasitoid of *T. eugeniae* and was later imported to the USA to control eugenia psyllid populations (Dahlsten et al. 1993). A similar case is the one of *Tamarixia schina*. The wasp was reported as a natural enemy of the exotic psyllid *Calophya rubra* (Blanchard) which feeds on *Schinus molle* trees (Álvarez-Zagoya and Cibrián-Tovar 1999). According to Zuparko et al. (2011), new undescribed *Tamarixia* species were found in both California and Florida, USA, parasitizing psyllid species which have potential distribution in Mexico.

In biological research, names of species are essential to ensure comparable results when working with model organisms (Pante et al. 2015), and in agriculture they are also required for biosecurity and quarantine concerns (Lyal et al. 2008). Notwithstanding, in some cases species identification is not an easy task and deep taxonomic studies are needed. For instance, in 2019 the misidentification of the eugenia psyllid *T. eugeniae* was uncovered by Taylor and Martoni (2020), who indicated that the true name of the species should be *Trioza adventicia* Tuthill. Taylor and Martoni mentioned that the two exotic species resemble each other, and only a detailed study based on a series of morphological characters and DNA barcoding supported the separation and validity of both species.

As already mentioned, psyllids are main hosts for the *Tamarixia* species and because of their possible broad dietary tolerance some species might migrate and disperse to new geographic regions (Percy et al. 2012). This might also promote the introduction and dispersion of exotic or new species of parasitoids in countries like Mexico. For example, *T. schina* apparently migrated to Mexico from California (Yefremova et al. 2014). According to the study by Percy et al. (2012), in the same region (California, USA), different species of psyllids attacked by some unidentified *Tamarixia* species exist, hosted by plants with potential distribution in Mexico. Moreover, in this country more than 114 species of psyllids (Méndez-Tobar 2015) exist, which may also represent possible hosts for exotic *Tamarixia* species. Therefore, the diversity of this genus might be currently underestimated in Mexico.

In agriculture, species identification protocols based on DNA represent powerful tools for the success of early detection programs, or monitoring of species (Lyal et al.

2008; Boykin et al. 2012; Poland and Rassati 2019). However, for some groups of insects, the lack of reference barcodes, errors in databases, scarcity of voucher specimens and presence of cryptic species represent strong limitations. As an example, recently a new *Tamarixia* species (*T. aguacatensis*) was described based on morphological characters, but because their sampling seems to be seasonally restricted (Yefremova et al. 2014), the generation of barcodes for further studies on their biology and phylogeny represents a challenge.

Conclusion

Besides reporting the presence of *Tamarixia dahlsteni* in Mexico, we also provided barcodes that may be employed as a reference for further monitoring programs or studies about this economically important group of wasps. Moreover, our phylogenetic analysis suggests the need for a deeper and wider taxonomic revision of the genus.

Acknowledgements

The authors are grateful to Dave Burns and Laurie Jo Elliot for providing English editing of the manuscript.

References

Al-Ani LKT, Aguilar Marcelino L, Fiorotti J, Sharma V, Sarker MS, Furtado EL, Wijayawardene NN, Herrera-Estrella A (2020) Biological control agents and their importance for plant health. In: Singh JS, Vimal SR (Eds) Microbial Services in Restoration Ecology, Elsevier, Netherlands, 13–36. https://doi.org/10.1016/B978-0-12-819978-7.00002-6

Álvarez-Zagoya R, Cibrián-Tovar D (1999) Biología del psílido del pirú *Calophya rubra* (Blanchard) (Homoptera: Psyllidae). Revista Chapingo de Ciencias Forestales y del Ambiente 5: 51–57. https://revistas.chapingo.mx/forestales/?section=articles&subsec=issues&numero=211

Ashfaq M, Hebert PD (2016) DNA barcodes for bio-surveillance: Regulated and economically important arthropod plant pests. Genome 59(11): 933–945. https://doi.org/10.1139/gen-2016-0024

Boykin LM, Armstrong KF, Kubatko L, De Barro P (2012) Species delimitation and global biosecurity. Evolutionary Bioinformatics Online 8: 1–37. https://doi.org/10.4137/EBO.S8532

Cerón-González C, Lomelí-Flores JR, Rodríguez-Leyva E, Torres-Ruíz A (2014) Fertility and feeding of *Tamarixia triozae* (Hymenoptera: Eulophidae) on potato psyllid *Bactericera cockerelli*. Revista Mexicana de Ciencias Agrícolas 5: 893–899. https://doi.org/10.29312/remexca.v5i5.912

Chen X, Stansly PA (2014) Biology of *Tamarixia radiata* (Hymenoptera: Eulophidae), Parasitoid of the Citrus Greening Disease Vector *Diaphorina citri* (Hemiptera: Psylloidea): A Mini Review. The Florida Entomologist 97(4): 1404–1413. https://doi.org/10.1653/024.097.0415

Chien CC, Chiu SC, Ku SC (1989) Biological control of *Diaphorina citri* in Taiwan. Fruits 44: 401–407. https://www.cabi.org/ISC/abstract/19921175104

Dahlsten DL, Kent DM, Rowney DL, Cooper WA, Young TE, Tassan RL (1993) Parasitoid shows potential for biocontrol of eugenia psyllid. California Agriculture 49(4): 36–40. https://doi.org/10.3733/ca.v049n04p36

De León JH, Sétamou M (2010) Molecular Evidence suggests that populations of the Asian Citrus Psyllid parasitoid *Tamarixia radiata* (Hymenoptera: Eulophidae) from Texas, Florida, and Mexico represent a single species. Annals of the Entomological Society of America 103(1): 100–110. https://doi.org/10.1603/008.103.0113

Edgar RC (2004) MUSCLE: A multiple sequence alignment method with reduced time and space complexity. BMC Bioinformatics 5(1): 113. https://doi.org/10.1186/1471-2105-5-113

Flores D, Ciomperlik M (2017) Biological control using the ectoparasitoid, *Tamarixia radiata*, against the Asian citrus psyllid, *Diaphorina citri*, in the Lower Rio Grande Valley of Texas. Southwestern Entomologist 42(1): 49–59. https://doi.org/10.3958/059.042.0105

Folmer O, Black M, Hoeh W, Lutz R, Vrijenhoek R (1994) DNA primers for amplification of mitochondrial cytochrome c oxidase subunit I from diverse metazoan invertebrates. Molecular Marine Biology and Biotechnology 3: 294–299. https://pubmed.ncbi.nlm.nih.gov/7881515/

Giantsis IA, Chaskopoulou A, Bon MC (2016) Mild-Vectolysis: Nondestructive DNA extraction method for vouchering sand flies and mosquitoes. Journal of Medical Entomology 53(3): 692–695. https://doi.org/10.1093/jme/tjv236

González-Hernández A, Arredondo-Bernal HC, Robles-González M, Martínez-Carrillo JL, Pérez J, López-Arroyo JI (2009) Determinación de especies de parasitoides del psílido asiático de los cítricos *Diaphorina citri* (Hemiptera: Psyllidae) en México. Entomología Mexicana 8: 373–377.

Hebert PDN, Ratnasingham S, de Waard JR (2003) Barcoding of animal life: Cytochrome c oxidase subunit 1 divergence among closely related species. Proceedings. Biological Sciences 270: S96–S99. https://doi.org/10.1098/rsbl.2003.0025

Hoang DT, Chernomor O, von Haeseler A, Minh BQ, Vinh LS (2018) UFBoot2: Improving the ultrafast bootstrap approximation. Molecular Biology and Evolution 35(2): 518–522. https://doi.org/10.1093/molbev/msx281

Kalyaanamoorthy S, Minh B, Wong TKF, von Haeseler A, Jermiin LS (2017) ModelFinder: Fast model selection for accurate phylogenetic estimates. Nature Methods 14(6): 587–589. https://doi.org/10.1038/nmeth.4285

LaSalle J (1994) North American genera of Tetrastichinae (Hymenoptera: Eulophidae). Journal of Natural History 28(1): 109–236. https://doi.org/10.1080/00222939400770091

Lomelí-Flores JR, Bueno R (2002) Nuevo registro de *Tamarixia triozae* (Burks) parasitoide del psílido del tomate *Paratrioza cockerelli* (Sulc) (Homoptera: Psyllidae) en México. Folia Entomologica Mexicana 41: 375–376.

Lyal C, Kirk P, Smith D, Smith R (2008) The value of taxonomy to biodiversity and agriculture. Biodiversity (Nepean) 9(1–2): 8–13. https://doi.org/10.1080/14888386.2008.9712873

Maddison WP, Maddison DR (2021) Mesquite: a modular system for evolutionary analysis. Version 3.70. http://www.mesquiteproject.org

McClay AS (1990) Distribution of *Leucaena psyllid* and its natural enemies in México: Implications for biological control. In: Napompeth B, MacDicken KG (Eds) *Leucaena psyllid*: problems and management. Proceedings of an international workshop held in Bogor (Indonesia), January 16–21 1989. Winrock International Institute for Agricultural Development, Bangkok, 139–143.

Méndez-Tobar P (2015) Psílidos (Hemiptera: Psylloidea) de la región central del estado de Michoacán, México. Tesis de maestría, Colegio de Posgraduados, Texcoco, México, 1–95. http://colposdigital.colpos.mx:8080/xmlui/handle/10521/2910

Michaud JP (2002) Biological control of Asian citrus psyllid, *Diaphorina citri* (Hemiptera: Psyllidae) in Florida: a preliminary report. Entomological News 113: 216–222. https://www.cabi.org/ISC/abstract/20023136574

Munyaneza JE, Crosslin JM, Upton JE (2007) Association of *Bactericera cockerelli* (Homoptera: Psyllidae) with 'Zebra chip', a new potato disease in Southwestern United States and Mexico. Journal of Economic Entomology 100(3): 656–663. https://doi.org/10.1093/jee/100.3.656

Noyes JS (2022) Universal Chalcidoidea database. World wide web electronic publication. http://www.nhm.ac.uk/chalcidoids

Pante E, Schoelinck C, Puillandre N (2015) From integrative taxonomy to species description: One step beyond. Systematic Biology 64(1): 152–160. https://doi.org/10.1093/sysbio/syu083

Percy DM, Rung A, Hoddle MS (2012) An annotated checklist of the psyllids of *California* (Hemiptera: Psylloidea). Zootaxa 3193(1): 1–27. https://doi.org/10.11646/zootaxa.3193.1.1

Poland TM, Rassati D (2019) Improved biosecurity surveillance of non-native forest insects: A review of current methods. Journal of Pest Science 92(1): 37–49. https://doi.org/10.1007/s10340-018-1004-y

Ramírez-Ahuja ML, Rodríguez-Leyva E, Lomelí-Flores JR, Torres-Ruíz A, Guzmán-Franco AW (2017) Evaluating combined use of a parasitoid and a zoophytophagous bug for biological control of the potato psyllid, *Bactericera cockerelli*. Biological Control 106: 9–15. https://doi.org/10.1016/j.biocontrol.2016.12.003

Rojas P, Rodríguez-Leyva E, Lomelí-Flores JR, Liu TX (2015) Biology and life history of *Tamarixia triozae*, a parasitoid of the potato psyllid *Bactericera cockerelli*. BioControl 60(1): 27–35. https://doi.org/10.1007/s10526-014-9625-4

Taylor GS, Martoni F (2020) Case of mistaken identity: resolving the taxonomy between *Trioza eugeniae* Froggatt and *T. adventicia* Tuthill (Psylloidea: Triozidae). Bulletin of Entomological Research 110(3): 340–351. https://doi.org/10.1017/S0007485319000695

Trifinopoulos J, Nguyen LT, von Haeseler A, Minh BQ (2016) W-IQ-TREE: A fast online phylogenetic tool for maximum likelihood analysis. Nucleic Acids Research 44(W1): W232–W235. https://doi.org/10.1093/nar/gkw256

Urbaneja-Bernat P, Pérez-Rodríguez J, Krüger K, Catalán J, Rizza R, Hernández-Suárez E, Tena A (2019) Host range testing of *Tamarixia dryi* (Hymenoptera: Eulophidae) sourced from South Africa for classical biological control of *Trioza erytreae* (Hemiptera: Psyllidae) in Europe. Biological Control 135: 110–116. https://doi.org/10.1016/j.biocontrol.2019.04.018

Wang Z, Liu Y, Shi M, Huang J, Chen X (2019) Parasitoid wasps as effective biological control agents. Journal of Integrative Agriculture 18: 705–715. https://doi.org/10.1016/S2095-3119(18)62078-7

Workman PJ, Whiteman SA (2009) Importing *Tamarixia triozae* into containment in New Zealand. New Zealand Plant Protection 62: 412–412. https://doi.org/10.30843/nzpp.2009.62.4864

Yefremova Z, González-Santarosa G, Lomeli-Flores JR, Bautista-Martínez N (2014) A new species of *Tamarixia* Mercet (Hymenoptera, Eulophidae), parasitoid of *Trioza aguacate* Hollis and Martin (Hemiptera, Triozidae) in Mexico. ZooKeys 368: 23–35. https://doi.org/10.3897/zookeys.368.6468

Zuparko LR, De Queiroz DL, LaSalle J (2011) Two new species of *Tamarixia* (Hymenoptera: Eulophidae) from Chile and Australia, established as biological control agents of invasive psyllids (Hemiptera: Calophyidae, Triozidae) in California. Zootaxa 2921(1): 13–27. https://doi.org/10.11646/zootaxa.2921.1.2

ZooKeys 1129: 85–107 (2022)
doi: 10.3897/zookeys.1129.87706
https://zookeys.pensoft.net

RESEARCH ARTICLE

A peer-reviewed open-access journal
ZooKeys
Launched to accelerate biodiversity research

The intraspecific variation of morphology and coloration of field crickets: a taxonomic revision of Chinese *Gymnogryllus* Saussure, 1877 and *Phonarellus* Gorochov, 1983 (Orthoptera, Gryllidae, Gryllini)

Ning Wang[1], Huateng Huang[1], Li-Bin Ma[1]

1 *College of Life Sciences, Shaanxi Normal University, Xi'an, China, 710119*

Corresponding authors: Huateng Huang (huanghuateng@snnu.edu.cn), Li-Bin Ma (libinma@snnu.edu.cn)

Academic editor: Zhu-Qing He | Received 13 June 2022 | Accepted 1 September 2022 | Published 15 November 2022

https://zoobank.org/CF6FB3C5-FD72-4040-913B-371386CA9B9A

Citation: Wang N, Huang H, Ma L-B (2022) The intraspecific variation of morphology and coloration of field crickets: a taxonomic revision of Chinese *Gymnogryllus* Saussure, 1877 and *Phonarellus* Gorochov, 1983 (Orthoptera, Gryllidae, Gryllini). ZooKeys 1129: 85–107. https://doi.org/10.3897/zookeys.1129.87706

Abstract

After extensive sampling of specimens from species found in China, we examined the intraspecific morphological variation of several characters used for species delimitation in two closely related cricket genera, *Gymnogryllus* Saussure, 1877 and *Phonarellus* Gorochov, 1983. We found that the characters (male genitalia in *Gymnogryllus odonopetalus* Xie & Zheng, 2003 and *Phonarellus ritsemae* (Saussure, 1877), and coloration of the hind leg in *Phonarellus minor* (Chopard, 1959)) exhibit considerable amounts of variation within species, and are thus not reliable characters for species differentiation. Therefore, we revised the taxonomy of these two genera. Five synonyms are proposed: *G. yunnanensis* (= *G. odonopetalus*) **syn. nov.**, *G. striatus* (= *G. odonopetalus*) **syn. nov.**, *G. longus* (= *G. odonopetalus*) **syn. nov.**, *G. tumidulus* (= *G. odonopetalus*) **syn. nov.**, and *P. flavipes* (= *P. minor*) **syn. nov.** All species mentioned above are described and illustrated. Keys and a distribution map are provided.

Keywords

Cricket, genitalia, Grylloidea, morphological diversity, new synonym, taxonomy

Introduction

Gymnogryllus Saussure, 1877 and *Phonarellus* Gorochov, 1983 have species in China that are difficult to distinguish based on morphology, and we found that some of the "different" species co-occur at the same collection site and at the same time. Many of these species were proposed based on a limited number of specimens (e.g., Xia et al. 1991; Ma and Zhang 2011). That meant some of the characteristics for species delimitation in the previous taxonomic literature might reflect diversity within species rather than differences between species. The validity of these species needed re-examination.

Gymnogryllus was established by Saussure in 1877 with *Gryllus elegans* Guérin-Méneville, 1834 as the type species. It is distinguished from other genera of the tribe Gryllini by the face (distinctly longer than wide), oblique veins (slightly curved), and the ovipositor (short and armed with a small hook in the anterior of the lower valvae). Species of this genus have a similar appearance, and the male genitalia features are the primary characteristics for species identification. Currently, 45 species are reported worldwide, from India to Australia, and most of them are found in tropical Southeast Asia (Indian subcontinent, western Himalayas, Burma, Vietnam, and Malaysia) (Cigliano et al. 2022). In China, there are eight *Gymnogryllus* species. *Gymnogryllus contractus* Liu et al., 1995 and *Gymnogryllus odonopetalus* Xie & Zheng, 2003 were described in the 20th century. In 2011, an additional six Chinese species were reported (*Gymnogryllus dolichodens* Ma & Zhang, 2011, *Gymnogryllus longus* Ma & Zhang, 2011, *Gymnogryllus tumidulus* Ma & Zhang, 2011, *Gymnogryllus extrarius* Ma & Zhang, 2011, *Gymnogryllus yunnanensis* Ma & Zhang, 2011, and *Gymnogryllus striatus* Ma & Zhang, 2011). These six Chinese species are distributed in the same province and are similar in body size and forewing morphology, for example, inclined rectangular mirror and internal dividing vein with three branches. The only characteristic for identifying these species is the posterior angle of the epiphallus. Here, we examined whether this diagnostic feature is stable by using multiple specimens per species to assess the amount of intraspecific variation.

Gorochov established the genus *Phonarellus* for species originally belonging to *Gymnogryllus* and designated *Gymnogryllus minor* Chopard, 1959 as the type species (Gorochov, 1983). Compared to *Gymnogryllus*, species of *Phonarellus* are smaller, the cercus base is of light color, and the apical area of the genitalia is obviously different between both genera. We recognize the genus by its contrasting coloration of antennae (proximal segments colored light and most of the hind portion colored dark, sometimes completely white), ocelli almost arranged in a line, shiny and smooth pronotum, and somewhat leathery elytra (Fig. 1). The genus contains 16 species and they are distributed from Africa to the Indo-Malayan region (Afghanistan, Bangladesh, Burkina Faso, China, Gabon, India, Japan, Kenya, Mali, Sierre Leone, and Vietnam) (Cigliano et al. 2022). Four *Phonarellus* species are recorded from China (*Phonarellus ritsemae* (Saussure, 1877), *Phonarellus minor* (Chopard, 1959), *Phonarellus flavipes* Xia, Liu & Yin, 1991, and *Phonarellus zebripe* He, 2022). Two species, *P. minor* and *P. flavipes*, occur in Yunnan and Guangdong and are of very similar appearance. The only difference between *P. minor* and *P. flavipes* is that the posterior femora of *P. flavipes* have no black area and the markedly separated first and second

Figure 1. Living photos of some *Phonarellus* and *Gymnogryllus* species **A, B** male of *P. minor* (with varing proportion of black areas on hind legs) **C** female of *P. minor* **D** male of *P. ritsemae* **E** male of *G. odonopetalus* **F** female of *G. odonopetalus* (Photos **A–D** were provided by Zhang, Tao, and **E, F** were photographed by He, Zhixin).

oblique veins at the base (Xia et al. 1991). However, the proportion of the black area varies even within *P. minor*. Thus, classification based only on this feature is questionable.

To address the problems with species of Chinese *Gymnogryllus* and *Phonarellus*, we collected more than 100 specimens (35 specimens of *Gymnogryllus* and 130 specimens of *Phonarellus*) and examined their morphological characteristics. Based on our results, we consider that four species in *Gymnogryllus* are junior synonyms of *G. odonopetalus*, and *P. flavipes* is a junior synonym of *P. minor*. The diagnostic characteristics previously proposed for species identification are unreliable because of extensive variation. New checklists of Chinese *Gymnogryllus* and *Phonarellus* species, with keys to species and distribution maps (Fig. 2), are provided.

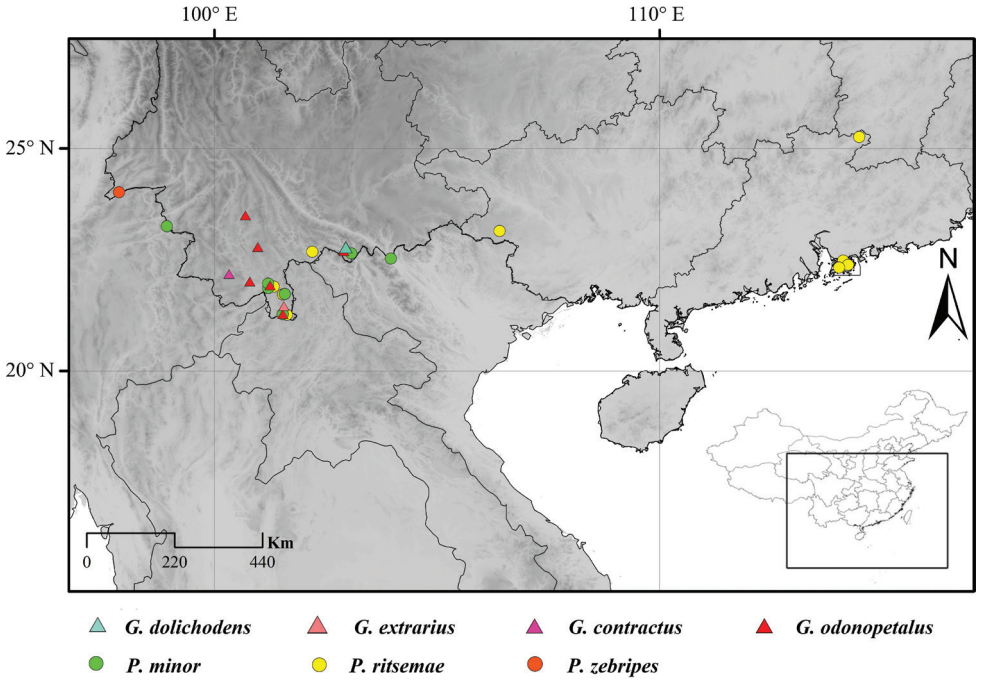

Figure 2. Distributions of *Phonarellus* and *Gymnogryllus* in China (Note: the locality of *P. zebripes* cited from Liu and He (2022), and the remaining location information is based on the data of examined materials).

Materials and methods

Specimens and photographs

Most specimens were attracted to a high-pressure mercury lamp (500W) in the field. The specimens were preserved in analytical-grade ethanol during fieldwork and then pinned and dry-preserved in laboratory. After softening, dissecting needles were used to pull out the male genitalia from the gonopore. The dissected genitalia complexes were prepared by placing them into a concentrated solution of alkaline protease (0.2 g/ml, AOBOX, China) with a water bath temperature of 40–50 °C for 48 hours. Identification of involved species is mainly based on male morphology. Whole bodies were photographed with a VHX-6000 digital microscope (Keyence, Osaka, Japan). Figures of genitalia and body details were produced using a ToupCam Digital camera and bundled software (ToupTek, Hangzhou, China).

Measurements and abbreviations

All specimens were measured using ToupCam Digital camera (E3ISPM05000KPA) and bundled software (ToupTek, Hangzhou, China). All the measurements are in millimeters (mm). Nomenclature of male genitalia follows Gorochov (1996) and Ma and Zhang (2011) and measurement abbreviations are as below: **BL** body length (from head

to tip of abdomen); **HW** head width; **EW** eye width; **PL** pronotum length; **PW** pronotum width (max. width of pronotum); **FWL** forewing length; **HWL** hind wing length (length of uncovered part); **DVL** length of dialogue vein; **ML** mirror length (from fore to hind margin); **CL** cercus length; **FTL** fore tibiae length; **TTL** length of tibial tympanum; **MTL** middle tibiae length; **HLL** hind femur length; **HTL** hind tibiae length.

Proportion of colored area on posterior femora of *Phonarellus minor*

We used 42 *P. minor* specimens with at least one intact hind leg. Photos of these posterior femora were taken with a VHX-6000 digital microscope (Keyence, Osaka, Japan) and processed in ImageJ. We used the Threshold function in ImageJ ver.1.53k (Schneider et al. 2012) software to obtain the size of the posterior femora and the size of the black area on each photographed hind leg. The proportion of black area (the ratio between the size of the black area and the total area) is calculated, and the distribution is drawn in Microsoft Excel (Microsoft Office 2016).

Distance between the base of the first and second oblique veins of *P. minor*

We used a ToupCam Digital camera (E3ISPM05000KPA) and bundled software (ToupTek, Hangzhou, China) to measure the distances between the first and second oblique veins at the base of 42 specimens. The distributions were graphed in Microsoft Excel (Microsoft Office 2016).

Acronyms used for the institutions where those examined materials are deposited:

SNNU Museum of Flora and Fauna of Shaanxi Normal University, Xi'an, China;
NWAFU Entomological Museum of Northwest A&F University, Yangling, China;
SEM (IEAS) Shanghai Entomological Museum, CAS, Shanghai, China.

Taxonomy

Checklist of Chinese *Gymnogryllus* and *Phonarellus* species

Genus *Gymnogryllus* Saussure, 1877
***Gymnogryllus contractus* Liu, Yin & Liu, 1995**
Chinese name. 狭膜裸蟋
Distribution. Yunnan.
***Gymnogryllus odonopetalus* Xie & Zheng, 2003**
***Gymnogryllus yunnanensis* Ma & Zhang, 2011, syn. nov.**
***Gymnogryllus striatus* Ma & Zhang, 2011, syn. nov.**
***Gymnogryllus longus* Ma & Zhang, 2011, syn. nov.**
***Gymnogryllus tumidulus* Ma & Zhang, 2011, syn. nov.**
Chinese name. 齿瓣裸蟋
Distribution. Yunnan, Guangxi, Guangdong.

***Gymnogryllus dolichodens* Ma & Zhang, 2011**
Chinese name. 长突裸蟋
Distribution. Yunnan.
***Gymnogryllus extrarius* Ma & Zhang, 2011**
Chinese name. 外突裸蟋
Distribution. Yunnan.
Genus *Phonarellus* Gorochov, 1983
***Phonarellus minor* (Chopard, 1959)**
***Phonarellus flavipes* Xia, Liu & Yin, 1991, syn. nov.**
Chinese name. 小音蟋
Distribution. Guangxi, Hainan, Guangdong, Yunnan.
***Phonarellus ritsemae* (Saussure, 1877)**
Chinese name. 利特音蟋
Distribution. Guangxi, Zhejiang, Yunnan, Guangdong, Hong Kong.
***Phonarellus zebripes* He, 2022**
Chinese name. 斑腿音蟋
Distribution. Yunnan.

Species accounts

Orthoptera: Grylloidea; Gryllidae; Gryllinae

Genus *Gymnogryllus* Saussure, 1877

Gymnogryllus Brunner von Wattenwyl 1893: 197; Gorochov 1983: 321; Yin and Liu 1995: 194; Ma and Zhang 2011: 31; Gorochov 2022: 4.
Brachytrypus (*Gymnogryllus*) Saussure, 1877: 291.

Type species. *Gryllus elegans* (= *Gymnogryllus leucostictus*). *Brachytrypus* (*Gymnogryllus*) Saussure, 1877: 291.

Distribution. India, Australia, western Himalayas, Burma, Vietnam, Malaysia, China.

Diagnosis. Body large. Head, pronotum and much of hind femur blackish brown; rest of body of light color. Light brown bands uniformly distributed over posterior peduncle. Forewings not reaching tip of abdomen; hind wings largely surpassing abdomen. Mirror inclined rectangular. The length of the apical field of forewings varies among individuals. Subgenital plate shaped as hook. Genitalia large, in caudal view, epiphallus arch-shaped and the apically armed with a pair of long teeth. The space between the teeth and the shape of them varied among individuals (Fig. 5). Ovipositor very short, almost straight.

Remarks. Eight species of *Gymnogryllus* are reported from China, and six of them have been found in Yunnan. Among them, *G. longus*, *G. tumidulus*, *G. yunnanensis*, and *G. striatus* have been described for differences in the angle of the epiphallic apex

and the length of the apical field of tegmen. However, they are similar to *G. odonopetalus* in appearance and can be collected from the same location at the same time. We compared specimens collected from the same site and concluded that these two features present intraspecific variation and are unreliable for species delimitation. We consider that all four taxa are synonyms of *G. odonopetalus*.

Key to *Gymnogryllus* species in China

1	Mirror narrow	***G. contractus***
–	Mirror much broad	**2**
2	Forewings extended to tip of abdomen	***G. dolichodens***
–	Forewings not extended to tip of abdomen	**3**
3	Epistomal suture curved upward medially, frons with light angular patch	***G. odonopetalus***
–	Epistomal suture straight, frons uniform colored	***G. extrarius***

Gymnogryllus odonopetalus Xie & Zheng, 2003

Figs 1E–F, 3, 4, 5

Gymnogryllus odonopetalus Xie & Zheng, 2003: 496, 498.
Gymnogryllus yunnanensis Ma & Zhang, 2011: 31–40, syn. nov.
Gymnogryllus longus Ma & Zhang, 2011: 31–40, syn. nov.
Gymnogryllus tumidulus Ma & Zhang, 2011: 31–40, syn. nov.
Gymnogryllus striatus Ma & Zhang, 2011: 31–40, syn. nov.

Holotype. Type locality: Menglun, Xishuangbanna, Yunnan, China. Deposited at Museum of Flora and Fauna of Shaanxi Normal University, Xi'an, China (SNNU).

Specimens examined. China: 1 male (holotype), Yunnan, Xishuangbanna, Menglun, Sept. 8, 1999, Xie, Lingde coll. (SNNU); 2 males and 1 female, Yunnan, Honghe, Wengdang, Jun. 11, 2009, Ma, Libin coll. (SNNU); 1 female, Yunnan, Mengla, Shangyong, Longmen, May 13, 2013, Ma, Libin coll. (SNNU); 1 male, Yunnan, Mengla (or Wangtianshu), Oct. 2, 2014, Zhang, Tao coll. (SNNU); 3 males, Yunnan, Jinghong, Jul. 11, 2018, Peng, Zhong coll. (SNNU); 2 males, Yunnan, Pu'er, Jinggu, Aug. 17, 2021, He, Zhixin coll. (SNNU); 7 males, Yunnan, Pu'er, Simaoqu, Aug. 18, 2021, He, Zhixin coll. (SNNU); 15 males, Yunnan, Mengla, Menglun, Aug. 25, 2021, He, Zhixin coll. (SNNU); 3 females, Yunnan, Mengla, Menglun, Aug. 25, 2021, He, Zhixin coll. (SNNU).

Distribution. (Fig. 2). China (Yunnan, Guangxi, Guangdong).

Measurements (mm). Male (*N* = 30): BL 27.73–29.42; HW 6.42–6.84; PL 4.86–5.32; FWL 18.62–21.32; HLL 16.27–17.12; HTL 9.43–10.14; EW 1.56–1.79; PW 7.62–7.98; HWL 6.04–6.84; DVL 4.62–4.96; ML 3.72–3.98; CL 8.15–8.54; FTL 5.42–5.76; MTL 6.29–6.45.

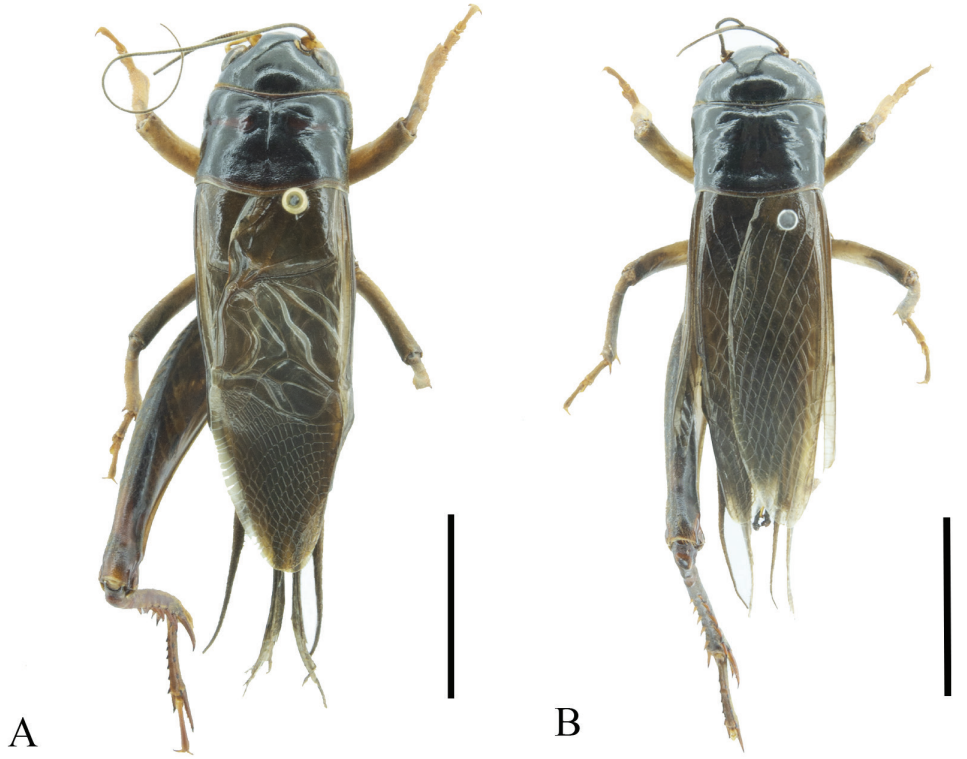

Figure 3. Bodies of *G. odonopetalus* **A** male **B** female. Scale bar: 10 mm.

Description. ***Male*** (Figs 1E, 3A). Head longer than wide, as wide as fore margin of pronotum. Vertex smooth and broad. Occiput slightly inclined. Frontal rostrum as wide as one eye and flattened. Scape of antennae flat, shield-like, and as wide as half of frontal rostrum. With three small ocelli, arranged in a straight line, median ocellus semilunar. Eyes about 1/4 length of head. Epistomal suture straight and close to eyes. Labrum slightly convex and rhombus shaped. Last segment of maxillary palpi slightly narrower than the third. Labial palpi the middle segment longer than the others.

Pronotum disc rectanglur, anterior margin concave, posterior margin sinuated; a longitudinal groove in middle of pronotum, about 2/3 the length of the pronotum. Fore margin of pronotum rough and densely pubescent. Tegmen reaching tip of abdomen; with three oblique veins, outmost nearly vertical and straight, two internal inclined and longer than outmost; and them converging diagonal vein. Diagonal vein curved and anteriorly forked. Chord veins three, the internal two extremely curved, connected at bottom. Between diagonal vein and the most internal chord vein armed with two transverse veins. Mirror large, inclined rectangular. Apical field triangular, about 2/5 the length of tegmina, variable among individuals, armed with rectangular cells.

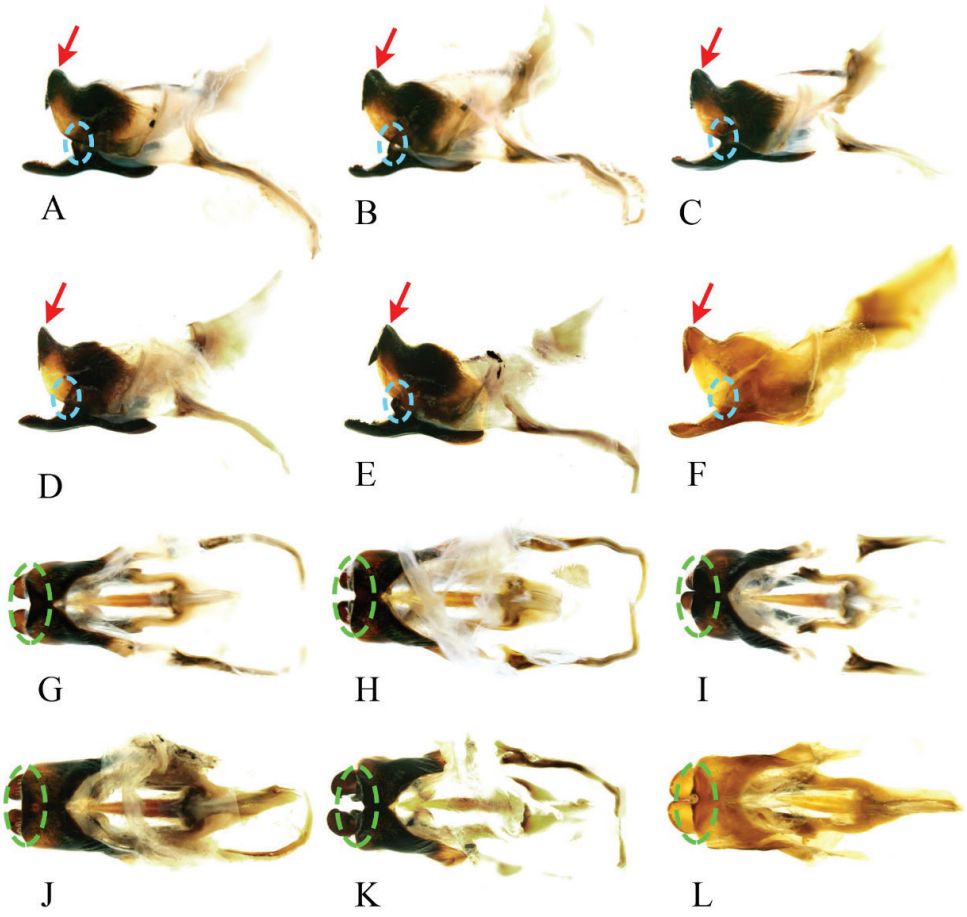

Figure 4. Intraspecific variation of genitalia in *G. odonopetalus* **A–F** genitalia from six individuals in lateral view (Note: the red arrows point to the posterior of epiphallus, highlighting variations among individuals; the blue circles indicate the protuberance of mid-ectoparamere) **G–L** genitalia of the same six individuals in dorsal view (Note: the green circles indicate the median lobe of the epiphallus posterior).

Fore tibiae with inner and outer tympanum, inner tympanum small and ovoid, outer longer-oval. Hind femora brown with light stripes. Distal of hind tibiae with five dorsal spurs on both sides; apical spurs six, the inner apical spurs three (the dorsal one longest, the ventral one shortest and 1/4 length of the longest one, the middle one about 2/3 length of the longest), and the outer apical spurs three (equal length of the dorsal one and the ventral one, about 2/3 length of the middle one). Subgenital plate hook-like. Cercus straight and short; with long hair sparse and short hair dense.

Genitalia (Figs 4, 5). Male genitalia robust, epiphallus arch-shaped in front view; inner side of medial lobe armed with a pair of teeth. Median notch between paired apical teeth and length of teeth varyable between individuals. End of middle lobes of epiphallus bent upward, for less than 90°, varyable between individuals. Notch of

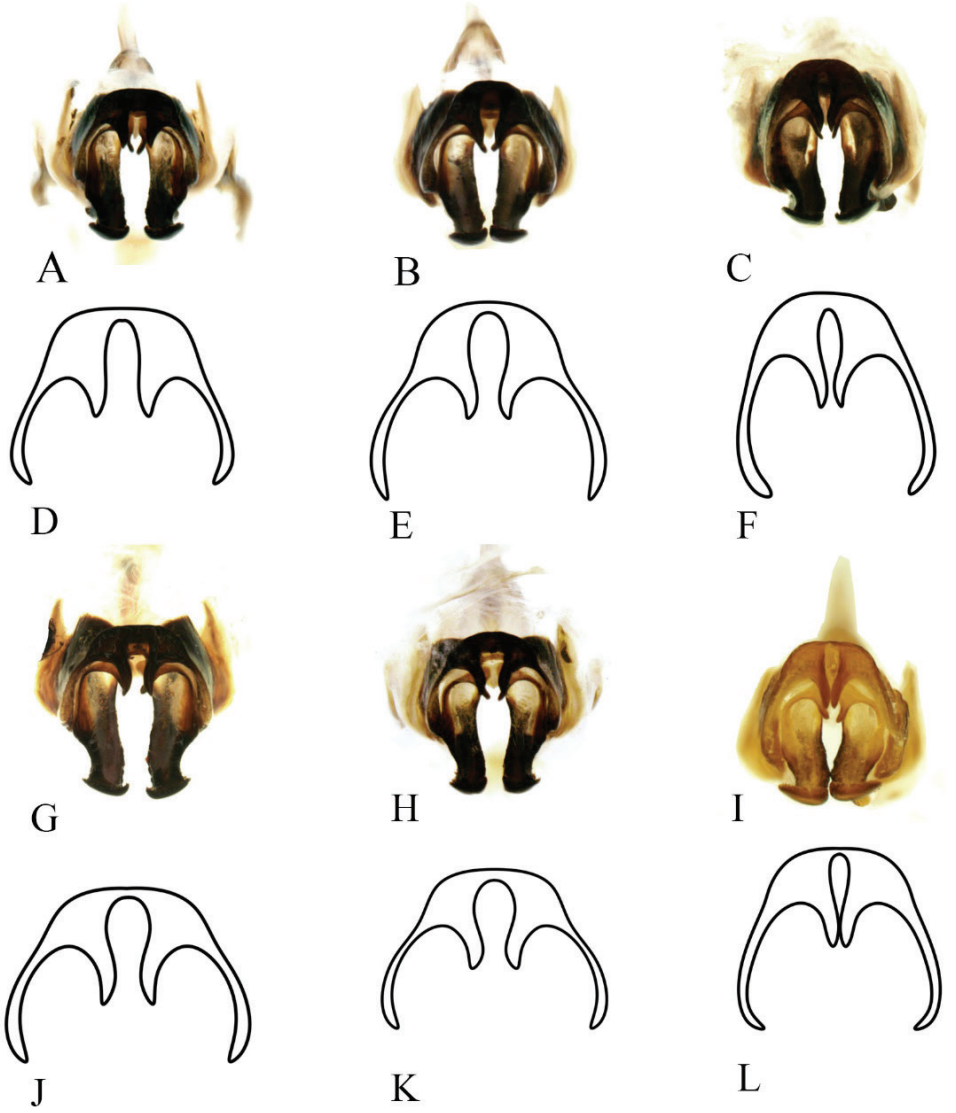

Figure 5. Intraspecific variation of genitalia in *G. odonopetalus* **A–C** and **G–I** photos of genitalia from six individuals in caudal view **D–F** and **J–L** drawings of genitalia from the same six individuals in caudal view.

epiphallus anterior variable, with bottom angular or broad and arc-shaped. Outer edge of end of ectoparamere armed with irregular numbers of teeth.

Coloration (Fig. 3). Head, pronotum and much of the hind femur blackish brown. Occiput uniformly blackish brown. 1/3 part of cheek bottom brown. Frons black, ventral quarter of lateral lobe with a light stripe. Hind femur black.

Female (Figs 1F, 3B). Slightly smaller than male, with tegmina dark brown. Ovipositor as long as pronotum.

Remarks. Ma and Zhang (2011) proposed four species, *G. yunnanensis*, *G. striatus*, *G. longus*, and *G. tumidulus*, based on the angle between the apical epiphallic teeth, the posterior edge of the medial lobe of epiphallus, and the apical field of the forewing. We examined our specimens and determined that these characters present intraspecific variation. In particular, the angle between the apical teeth of epiphallus shows tremendous variation between specimens (Fig. 4A–F). Besides, the epiphalli of these four species are armed with two pairs of teeth inside, which is consistent with the holotype of *G. odonopetalus* deposited in SNNU (in fact, we found that one pair of teeth is formed by the ectoparamere curved at the tip on the type specimen of *G. odonopetalus*). Therefore, we regard *G. yunnanensis*, *G. striatus*, *G. longus*, and *G. tumidulus* as junior synonyms of *G. odonopetalus*.

Hence, the species *G. odonopetalus* has some charecters showing intraspecific variation even within specimens collected from the same place and time. In lateral view, the angle between the apical teeth and the posterior edge of the medial lobe of epiphallus is variable among individuals (red arrows in Fig. 4); the protuberances in the middle of the ectoparamere vary in size (blue circles indicate the protuberance of mid-ectoparamere in Fig. 4). In dorsal view, the end of the epiphallus is variable (shown by green circles in Fig. 4G–L); the anterior notch of epiphallus is morphologically also diverse. In caudal view, shape and space between apical teeth of epiphallus are variable (drawing of epiphallus in Fig. 5D–F, J–L); the length of the apical area of the ectoparamere varies among individuals.

Genus *Phonarellus* Gorochov, 1983

Phonarellus Gorochov, 1983: 323; Yin and Liu 1995: 194; Ma and Zhang 2011: 31.

Type species. *Gymnogryllus minor*.

Distribution. Afghanistan, Bangladesh, Burkina Faso, China, Gabon, India, Japan, Kenya, Mali, Sierre Leone, Vietnam.

Diagnosis. Ocelli positioned in an almost straight line. Antenna ornamented with white ring-like pattern. Scapus conspicuously narrower than the half-width of the rostrum. Apical field shorter than mirror or slightly longer. Both tympana present. Hind tibiae shorter than half the length of hind femur. Epiphallus with large lateral lobes but without median lobe. Cerci usually dark with light proximally. We regard all species as belonging to *Phonarellus*, whose characters are as follows: ovipositor well developed and rather long; ectoparamere short.

Remarks. Four species of this genus have been reported from China (*P. ritsemae*, *P. minor*, *P. flavipes*, and *P. zebripes*). *Phonarellus flavipes* has been described for its yellow hind legs and the interval between the anterior of the first and second oblique veins. But these characters can also be found in *P. minor* living side by side with *P. flavipes*. Studying a large number of specimens of these three taxa from Yunnan and Guangdong, we tested whether the color of hind legs is a valid trait for species delimitation, and provided a description of *P. ritsemae*.

Key to *Phonarellus* species in China

1 Body bicolored, head reddish with most of the remainder dark.....***P. minor***
– Body almost uniformly dark **2**
2 Hind femora uniformly dark .....***P. ritsemae***
– Hind femora black and white ..... ***P. zebripes***

***Phonarellus minor* (Chopard, 1959)**

Figs 1A–C, 6, 7, 8

Gymnogryllus minor Chopard, 1959: 1; Bhowmik 1985: 14.
Gymnogryllus kashmirensis Bhowmik, 1977: 24, misidentification.
Phonarellus (*Phonarellus*) *minor*: Gorochov 1983: 91, 323–328; Kim and Pham 2014: 61; Gu et al. 2018: 11.
Phonarellus minor: Yin and Liu 1995: 138–139; Saeed et al. 2000: 176; Xie 2004: 116
Gymnogryllus (*Phonarellus*) *minor*: Ingrisch and Garai 2001: 759.
Phonarellus flavipes Xia et al., 1991: 123; Yin and Liu 1995: 49, syn. nov.

Holotype information. Type locality: Asia-Tropical, Indian Subcontinent, India, Kerala, Malabar Coast, Mahé. Deposited at Muséum National d'Histoire Naturelle, Paris, France (not examined).

Specimens examined. China: 36 males and 28 females, Yunnan, Mengla, Shangyong, Longmen, 1030 m, May 13, 2013, Ma, Libin coll. (SNNU); 5 females, same location as before, 1030 m, May 18, 2013, Ma, Libin coll. (SNNU); 4 males and 4 females, same location as before, 943 m, May 13, 2013, Ma, Libin coll. (SNNU); 3 males, same location as before, 996 m, May 13, 2013, Ma, Libin coll. (SNNU); 1 male, Yunnan, Jinping, Mengla, Xinmeng, 450 m, May 3, 2013, Ma, Libin coll. (SNNU); 3 males, Yunnan, Mengla, Mengban, Hebianzhai, 855 m, May 23, 2013, Ma, Libin coll. (SNNU); 4 males, Yunnan, Mengla, Menglun, 690 m, May 28, 2013, Ma, Libin coll. (SNNU) ; 6 males, Yunnan, Cangyuan, Banlao, 1134 m, Jun. 5, 2013, Ma, Libin coll. (SNNU); 2 males, Yunnan, Hekou, 100 m, Jun. 7, 1982, Jin, Gentao coll. (SEM); 2 males and 1 female, Yunnan, Xishuangbanna, Menglun, 1000 m, Jun. 3, 2009, Liu, Xianwei coll. (SEM); 3 males and 2 females, Yunnan, Mengla, Yaoqu, Jun. 1, 2009, Ma, Libin coll. (NWAFU). **Vietnam:** 1 female, Tonkin, Jul. 1940, A. De Cooman coll. (SEM).

Distribution. (Fig. 2). China (Yunnan, Guangdong), India, Vietnam.

Measurements. BL 12.86–14.23; HW 3.54–3.75; PL 2.26–2.39; PW 4.12–4.56; FWL 9.13–9.68; HWL 7.45–8.23; MTL 3.24–3.46; CL 4.67–5.31; HTL 4.73–5.21; HLL 8.11–8.42; OL 7.28–7.64.

Diagnosis. Body bicolored; head and legs often yellow or yellowish-brown, remainders always dark brown. Body size small for the genus. Both proximal and anterior notch of epiphallus arc-like and posterior notch almost right angular. Coloration of hind legs variable.

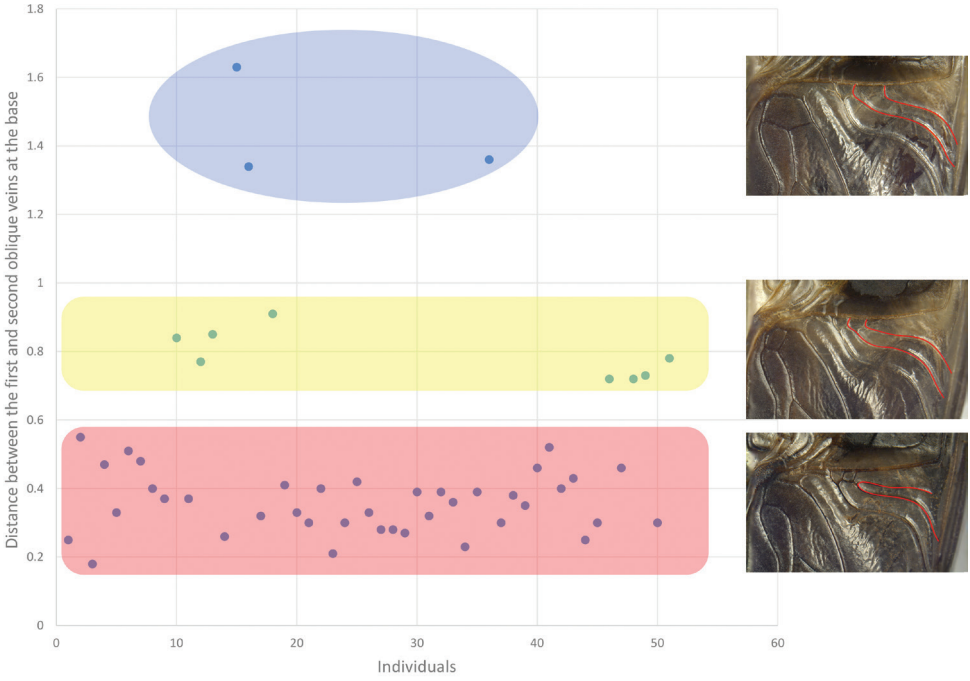

Figure 6. Distance between the first and second oblique vein of *P. minor* (Note: The data in the graph were measured from 42 samples. All the data can be roughly divided into three groups: distance less than 0.6 mm, distance greater than 1.2 mm, and distance between 0.7 mm and 1 mm, among which, individuals with distance less than 0.6 mm are the majority. The figure of the veins on the right, from top to bottom, represents the maximum, median and minimum distances, respectively. Units: mm).

Description. (Figs 1A–C, 8A–D, I). Body sized small for the genus, fusiform. Frons rounded. Median ocellus small, oval; lateral ocelli larger and rounded. Epistomal suture slightly upward convex and sometimes almost straight. Rostrum slightly widened. Scapus about half as wide as rostrum. Labrum rounded and slightly laterally widened, with apical margin arc-like, sometimes straight or with notch. Last segment of maxillary palpi rod-like, nearly as wide as third segment.

Disc of pronotum laterally widened and with hind margin slightly wider than fore margin; anterior margin broadly concave, posterior margin almost straight. Oblique veins three, the outmost one short and two internal of them longer and inclined; the top of them close each other. Diagonal vein straight. Chord veins three, the internal two veins extremely bent, connected at the bottom. Between the diagonal vein and the most internal chord vein armed with a transverse vein. The most internal chord vein linking with mirror by two transverse veins. Mirror small; the basal margin of mirror angle-like, dividing vein angular and the width of mirror nearly equal to the length. Field area short, close to the length of mirror, or slightly longer than mirror. Hind wings long and the uncovered portions longer than the half-length of forewings.

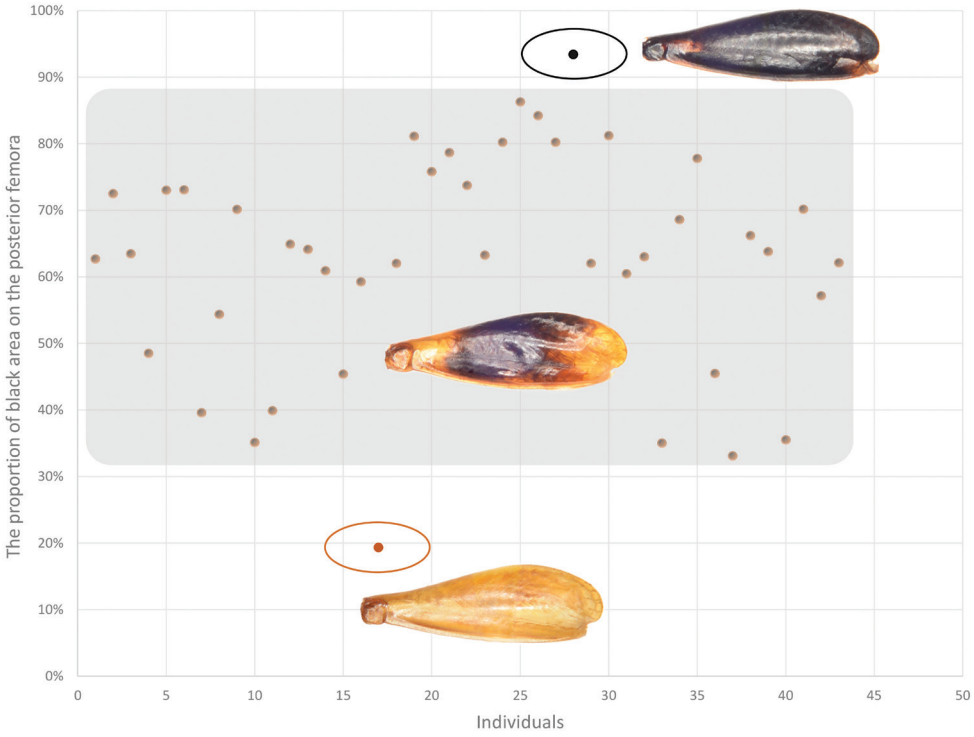

Figure 7. This figure shows that the distribution of the area-to-total area ratio of the black area of *P. minor* (Note: The data in the graph were measured from 42 samples. In the figure, miscellaneous colors, i.e., individuals with black proportions between 30% and 90%, accounted for the majority, while light-colored individuals, i.e., individuals with black proportions no higher than 20%, and black individuals, i.e., individuals with black proportions higher than 90%, were very few and only one in our sampling respectively.).

Fore tibiae with inner tympanum small and ovoid; the outer one large and oblong. Hind tibiae short, half the length of hind femur. Inner dorsal spurs of hind tibiae curved distally and longer than the outer ones. The length and number of dorsal spurs varied, while the basal spurs rather short, they numbered five or six of both the inner and outer; while spurs vary in length, the number of inner and outer spurs always 4:4. Inner apical spurs longer than outer ones. The median one of outer apical spurs longest and the remaining ones almost equal in length, and the bottom one of inner apical spurs shortest and the remaining ones in similar length. Inner dorsal spines of the first hind tarsus numbered 5–7 and outer ones numbered 7–9. Cercus thickness proximally and tapering. Subgenital plate simple and cucullate with acute apex.

Genitalia (Fig. 8E–G). Lateral lobes of epiphallus large. In lateral view apex obtuse and slightly upward curved. Epiphallus without median lobe, hind margin broad arc-like in middle, proximal margin arcuate, similar to outer margin. In caudal view, ectoparamere with three ridges, two horizontal and one vertical; area around ridges dark, and central area whitish.

Female (Fig. 8B, D, J). Ovipositor short, arrow-like. Tegmina dark brown.

Figure 8. *Phonarellus minor* (Chopard, 1959) (**A–J**) **A–D** bodies of *P. minor* (**A, C** males **B, D** females; scale bar: 10mm **A, B** specimens with dark colored hind legs **C, D** specimens with light-colored hind legs) **E–G** genitalia (**E** dorsally viewed **F** laterally viewed **G** ventrally viewed) **H** color variation of hind legs from dark to light **I** variable intervals at the base of oblique veins (Note: The red line point to the first and second oblique veins. The distance between the two veins in the rightmost figure is the smallest (see Fig. 6, i.e., less than 0.6 mm), and the sampled individual has black hind legs (see Fig. 7, i.e., the percentage of black is higher than 90%); the distance between the two veins in the middle figure is the largest (see Fig. 6, i.e., greater than 1.2 mm), and the sampled individual has miscellaneous colored hind legs (see Fig. 7, i.e., 30%–90% black); the distance between the two veins in the rightmost figure is medium (Fig. 6, i.e. 0.7mm-1mm), and the hind legs of the sampled individuals are light colored (Fig. 7, i.e. the percentage of black is less than 20%). Combining the information in Figs 6, 7, it can be inferred that the change in veins distance does not correlate entirely with the variation in the color of the hind legs) **J** ovipositor.

Coloration (Fig. 8A–D, H). Head orange. Fore and median legs and hind tibiae yellowish-brown. Coloration of hind femur variable, either uniformly dark brown, or dark brown in middle and basal, and apical areas yellowish-brown or wholy yellowish-brown. Female's forewings dark brown. Male's forewings dark brown, but harp area and mirror light colored (these parts membranous and lucent). Cercus yellowish-brown with apical area dark brown.

Remarks. The original description of *P. flavipes* does not mention genital characters. Xia et al. (1991) only pointed out that coloration of the hind femur and differences in the distance between the first and second oblique veins at the base could distinguish this species from *P. minor*. We showed that the distance at the base of oblique veins varies among individuals in *P. minor* (Figs 6, 8I). Moreover, the proportion of the black area on the hind femur also has a considerable amount of variation within *P. minor* (Fig. 7). The typical color scheme is 70% black (35% of the individuals), but more than 5% of the individuals have less than 10% or more than 95% of black area. The coloration of the hind femur is a continuous trait, and both extremes exist in *P. minor*. Hence, we consider that *P. flavipes* is a junior synonym of *P. minor*.

Phonarellus ritsemae (Saussure, 1877)

Figs 1D, 9, 10, 11

Liogryllus ritsemae Saussure, 1877: 304; Chopard 1936: 4.
Acheta ritsemae: Shiraki 1930: 200.
Gryllus ritsemae: Hisumatsu 1952: 43.
Tartarogryllus ritsemae: Chopard 1961: 272; Randell 1964: 1582; Leroy 1966: 39; Chopard 1967: 73.
Phonarellus ritsemae: Yin and Liu, 1995: 138–139; Ichikawa et al. 2000: 260; Hollier et al. 2013: 515.

Holotype. Type locality: Japan. Deposited at National Nature Historical Museum, Leiden, Netherlands (not examined).

Specimens examined. China: 1 female, Yunnan, Mengla, Shangyong, Longmen, May 13, 2013, Ma, Libin (SNNU); 1 male, same location as before, May 14, 2013, Ma, Libin (SNNU); 1 male and 2 females, same location as before, May 18, 2013, Ma, Libin (SNNU); 1 male, Yunnan, Lvchun, Banpo, May 9, 2013, Ma, Libin. (SNNU); 1 female, Yunnan, Mengla, Yaoqu, May 25, 2013, Ma, Libin (SNNU); 1 female, Yunnan, Mengla, Menglun, May 28, 2013, Ma, Libin (SNNU); 9 males and 1 female, Guangdong, Shaoguan, Luoshanzhen, May 13, 2015, Zhang, Tao (SNNU); 8 males, Guangdong, Shenzhen, May 17, 2015, Zhang, Tao (SNNU); 1 male, Guangxi, Jingxi, Longbang, May 2, 2019, Ma, Libin and Zhang, Tao (SNNU); 1 male, Hong Kong, Damaoshan, May 9, 2018, Ma, Libin (SNNU); 1 male, Hong Kong, Fei'eshan, May 18, 2018, Ma, Libin and Peng, Zhong (SNNU).

Distribution. China (Yunnan, Guangdong, Guangxi, Hong Kong), Japan..

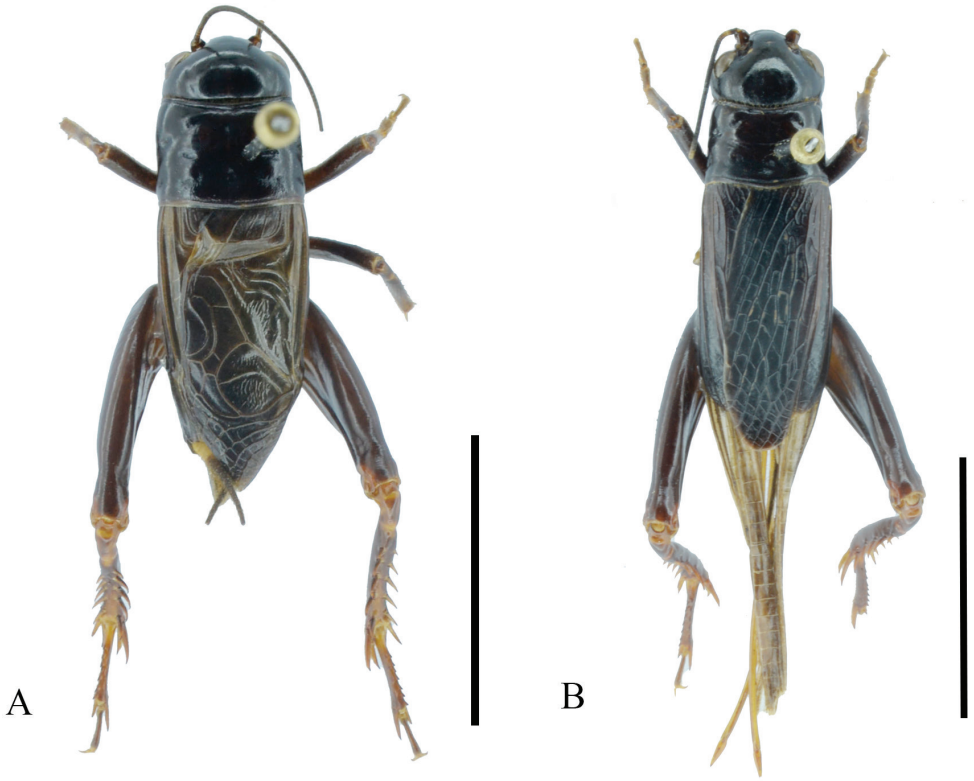

Figure 9. Body of *P. ritsemae* **A** male **B** female. Scale bar: 10 mm.

Measurements (mm). Male (*N* = 22): BL 13.07–15.16; HW 3.76–4.15; PL 2.74–2.81; PW 4.05–4.25; FWL 7.88–10.05; HFL 8.97–9.62; HTL 4.74–5.75; **Female (*N* = 6):** BL 15.65–16.48; HW 3.83–4.06; PL 2.51–2.75; PW 3.85–4.06; FWL 8.86–9.92; HFL 8.83–10.71; HTL 4.95–5.63.

Description. ***Male*** (Figs 1D, 9A). Body medium sized, fusiform. Head smooth, about as wide as pronotum. Occiput narrowed and convex. Vertex smooth and broad. Frontal rostrum rather wide, inverted trapezoid. Median ocellus small and shaped ovoid or semilunar. Lateral ocelli larger and located on both sides of the frontal rostrum. Eyes convex, about 1/4 length of head. Antennal socket triangular. Epistomal suture straight and twice as long as frontal rostrum. Postclypeus narrow. Labrum slightly convex and elliptical. The third of maxillary palpi longest, apical segments enlarge. Each section of labial palpi progressively longer. Disc of pronotum rectangular and middle groove unconspicuous. Forewings almost as long as abdomen. Hind femora about twice as long as tibiae; armed with five dorsal spurs on inner and outer dorsal margins and with three apical spurs on both sides (the ventral one shortest, and half-length of the others, the middle one with equal length of the dorsal), the outer apical spurs three (the middle one about twice longer than the others). Subgenital plate fusiform, at end narrowed and flattened.

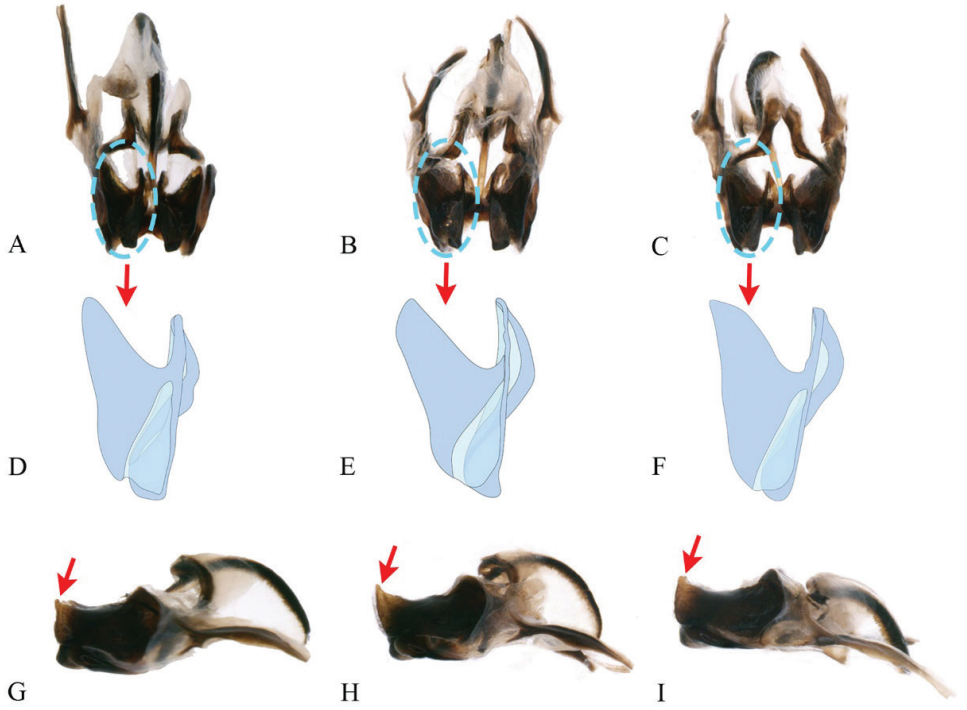

Figure 10. Intraspecific variation of genitalia of *P. ritsemae* **A–C** genitalia of three individuals in ventral view **D–F** drawing of ectoparamere in ventral view **G–I** Genitalia of the same three individuals in lateral view (Note: The blue circles of the **A–C** graph point to the ectoparamere, highlighting variations among individuals; the red arrows in the **G–I** graph point to the teeth of epiphallic posterior).

Genitalia (Figs 10, 11). Dark brown. Epiphallus with lateral lobes large with apex acute and slightly curved upward; without median lobe but in middle sinuate with angular notch. Epiphallic anterior margin angulates with straight lateral edges or with arc-like lateral edges (Fig. 11D–F). The bottom edge of the epiphallic lateral lobes extends horizontally at the posterior and downward at the anterior. Ectoparamere with three ridges (Fig. 10D–F), a pair of horizontal ones and a vertical one; area around ridges dark, and central area whitish lucent.

Female (Fig. 9B). Resembles male but larger. Ovipositor as long as forewings. Hindwings white and of equal length as forewings.

Coloration (Figs 1D, 9). Body dark brown. Head, pronotum black-brown. Femora reddish brown.

Remarks. Yin and Liu (1995) recorded this species from Shanghai, China, but there was no detailed description of this species. We collected a large number of specimens from Yunnan and Guangdong, China and identified them as *P. ritsemae*. We observed a few traits with intraspecies variation: (1) the posterior teeth of the epiphallus are variable among individuals in lateral view (as shown in Fig. 10G–I); (2) the ectoparamere can have different shapes in ventral view (as shown in Fig. 10D–F). (3) the

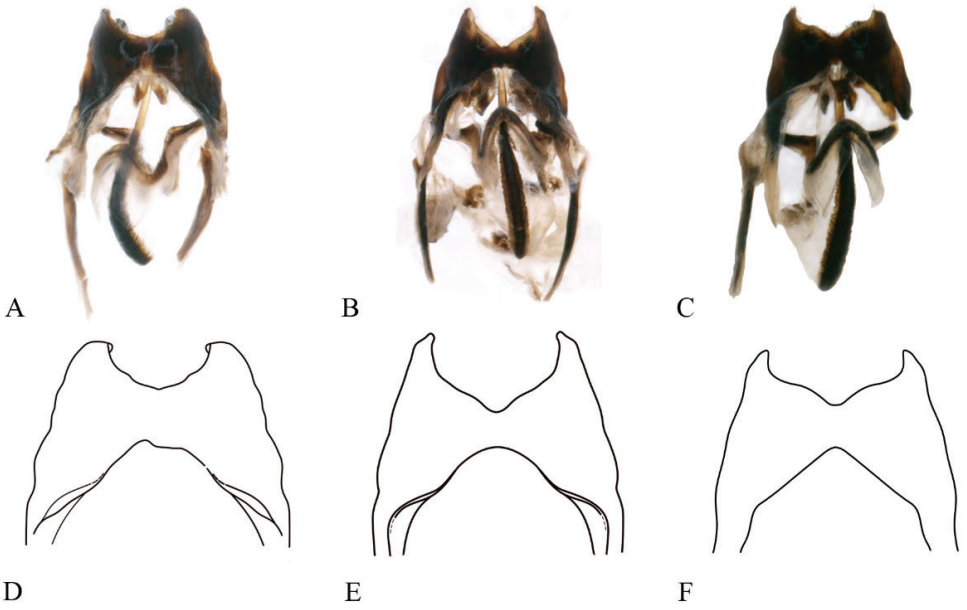

Figure 11. Intraspecific variation of genitalia in *P. ritsemae* **A–C** photos of genitalia of three individuals in dorsal view **D–F** drawing of epiphallus of the same three individuals in dorsal view (Note: the drawing shows the notch variation)

notch at hind margin of the epiphallus can be rather wide or slightly contracted, and the ventral margin can be broad or angular in dorsal view (as shown in Fig. 11D–F); and (4) the epiphallic anterior margin can be angle-like with straight lateral edges or broad and arc-like in dorsal view (as shown in Fig. 11D–F).

Discussion

Species delimitation is the foundation for biodiversity research, and finding robust and reliable characters for species identification is crucial for taxonomy. However, one difficulty faced by morphology-based species delimitation is distinguishing intraspecific variation from interspecific difference. When only a few specimens are accessible, we might mistake variation within species as species difference. Then, species identification might be unstable, leading to confusion in future taxonomic work. Here, we examined a large number of specimens in two cricket genera *Gymnogryllus* and *Phonarellus*. With multiple specimens, we revealed a considerable amount of morphological variation within species.

Notably, both genera possess intraspecific variation in male genitalia, features which are primary characters for species identification in insects (Song 2009) and crucial for cricket taxonomy (Alexander and Otte 1967). The most famous hypothesis to explain the diversity in male genitalia between species is the lock-and-key hypothesis: male genitalia need to structurally match female genitalia of the same species (Du-

four 1844). However, in this case, there should be minimal variation in male genitalia within species (Andrade et al. 2009). Comparing specimens collected at the same time from the same site, we found that the end of the epiphallus of *G. odonopetalus* is flattened or grooved to varying degrees among individuals. The apical epiphallus notch of *P. ritsemae* could expand outward or contract, and the depth of the notch varyable among individuals. These genitalic features are probably involved in holding and fixing the female during mating (Edvardsson and Canal 2006). For example, the ectoparamere is movable, and epiphallic teeth can provide a good grasping function and ensure the stability of the mating process. However, in *G. odonopetalus*, epiphallic teeth could be stubby or slender in shape, and the size of the space between the teeth varies in different individuals. These intraspecific variations we observed contradict the lock-and-key hypothesis. Instead, it is concordant with the hypothesis of sexual selection, which predicts a larger variation within species. More quantitative morphometric analyses are needed to test alternative hypotheses further.

We also observed intraspecific polymorphism with regard to body color in *P. minor*. Body color plays an essential role in adapting to environmental changes, resisting diseases, and avoiding predators (Ahnesjo and Forsman 2006). Varying the proportion of black color on body surface might be related to temperature regulation (Clusella-Trullas et al. 2007) and minimizing the likelihood of being founded by natural enemies (Forsman and Appelquist 1998). In this species, the distribution of the black color proportion on the hind femora is a continuous, bell-shaped distribution. It probably is a quantitative trait under stabilizing selection.

Based on our discovery of intraspecific variation, we considered some diagnostic features previously used as characters for separating species in these two genera invalid. The new species checklist showed five synonymus (*G. yunnanensis*, *G. striatus*, *G. longus*, *G. tumidulus* and *P. minor*), which reduces the number of Chinese species of the genera *Gymnogryllus* and *Phonarellus* to four and three, respectively. Our work highlights the importance of extensive specimen collection and considering intraspecific variation in species identification.

Acknowledgements

We appreciate Dr Peng, Zhong (Shanghai Normal University) for providing specimens. We also thank Zhang, Tao and He, Zhixin for their specimen photos and Ma, Ge for her pictures. This work is supported by the National Natural Science Foundation of China (no. 32070474, 31750002).

References

Ahnesjo J, Forsman A (2006) Differential habitat selection by pygmy grasshopper color morphs: Interactive effects of temperature and predator avoidance. Evolutionary Ecology 20(3): 235–257. https://doi.org/10.1007/s10682-006-6178-8

Alexander RD, Otte D (1967) The evolution of genitalia and mating behavior in crickets (Gryllidae) and other Orthoptera. Miscellaneous Publications Museum of Zoology University of Michigan 133: 1–62.

Andrade CAC, Vieira RD, Ananina G, Klaczko LB (2009) Evolution of the male genitalia: Morphological variation of the aedeagi in a natural population of *Drosophila mediopunctata*. Genetica 135(1): 13–23. https://doi.org/10.1007/s10709-008-9247-9

Bhowmik HK (1977) Studies on Indian crickets (Orthoptera: Insecta) with description of two new species. Records of the Zoological Survey of India, Calcutta 73(1–4): 23–39. https://doi.org/10.26515/rzsi/v73/i1-4/1977/161900

Bhowmik HK (1985) Contribution to the gryllid fauna of the Western Himalayas (Orthoptera: Gryllidae). Records of the Zoological Survey of India, Miscellaneous Publication, Occasional Paper 73: 1–85.

Chopard L (1936) Note sur les gryllides de Chine. Notes d'Entomologie Chinoise. Musée Heude 3(1): 1–14.

Chopard L (1959) Gryllides d'Iran. Stuttgarter Beiträge zur Naturkunde, Serie A (Biologie) 24: 1–5.

Cigliano MM, Braun H, Eades DC, Otte D (2022) Orthoptera Species File. Version 5.0/5.0. [Aug. 15, 2022] http://Orthoptera.SpeciesFile.org

Clusella-Trullas S, van Wyk JH, Spotila JR (2007) Thermal melanism in ectotherms. Journal of Thermal Biology 32(5): 235–245. https://doi.org/10.1016/j.jtherbio.2007.01.013

Dufour L (1844) Anatomie générale des Dipteres. Annales des Sciences Naturelles Zoologie 3(1): 244–264.

Edvardsson M, Canal D (2006) The effects of copulation duration in the bruchid beetle *Callosobruchus maculatus*. Behavioral Ecology 17(3): 430–434. https://doi.org/10.1093/beheco/arj045

Forsman A, Appelquist S (1998) Visual predators impose correlational selection on prey color pattern and behavior. Behavioral Ecology 9(4): 409–413. https://doi.org/10.1093/beheco/9.4.409

Gorochov AV (1983) To the knowledge of the cricket tribe Gryllini (Orthoptera, Gryllidae). Entomologicheskoe Obozrenie 62: 314–330. [in Russian]

Gorochov AV (1996) New and little known crickets from the collection of the Humboldt University and some other collections (Orthoptera: Grylloidea). Part 1. Zoosystematica Rossica 4: 87–92.

Hollier J, Bruckner H, Heads SW (2013) An annotated list of the Orthoptera (Insecta) species described by Henri de Saussure, with an account of the primary type material housed in the Muséum d'histoire naturelle de Genève, Part 5: Grylloidea. Revue Suisse de Zoologie 120: 445–535.

Ichikawa A, Murai T, Honda E (2000) Monograph of Japanese crickets (Orthoptera; Grylloidea). Bulletin of the Hoshizaki Green Foundation 4: 257–332.

Ingrisch S, Garai A (2001) Orthopteroid Insects from Ganesh Himal, Nepal. Esperiana 8: 755–770.

Kim TW, Pham HT (2014) Checklist of Vietnamese Orthoptera (Saltatoria). Zootaxa 3811(1): 53–82. https://doi.org/10.11646/zootaxa.3811.1.3

Liu YJ, He ZQ (2022) A new species of genus *Phonarellus* Gorochov, 1983 from Yunnan, China (Orthoptera: Gryllidae: Gryllinae). Zootaxa 5093(1): 94–100. https://doi.org/10.11646/zootaxa.5093.1.7

Ma LB, Zhang YL (2011) The cricket genus *Gymnogryllus* (Grylloidea: Gryllidae: Gryllinae: Gryllini) from China with description of six new species. Zootaxa 2733(1): 31–40. https://doi.org/10.11646/zootaxa.2733.1.3

Saeed A, Saeed M, Yousof M (2000) New species and records of some crickets (Gryllinae: Gryllidae: Orthoptera) from Pakistan. International Journal of Agriculture and Biology 2(3): 175–182.

Saussure H (1877) Mélanges orthoptérologiques V. fascicule Gryllides. Mémoires de la Société de Physique et d'Histoire Naturelle de Genève 25: 169–504. [161–352]

Schneider CA, Rasband WS, Eliceiri KW (2012) NIH Image to ImageJ: 25 years of image analysis. Nature Methods 9(7): 671–675. https://doi.org/10.1038/nmeth.2089

Shiraki T (1930) Orthoptera of the Japanese Empire. Part I. (Gryllotalpidae and Gryllidae). Insecta Matsumurana 4: 181–252.

Song H (2009) Species-specificity of male genitalia is characterized by shape, size, and complexity. Insect Systematics & Evolution 40(2): 159–170. https://doi.org/10.1163/187631209X424571

Xia KL, Liu XW, Yin HS (1991) Two new species of the Chinese crickets (Orthoptera: Grylloidea). Contributions from the Shanghai Institute of Entomology 10: 121–123.

Xie LD (2004) Orthoptera: Grylloidea: Trigonidiidae, Gryllomorphidae, Mogoplistidae, Oecanthidae and Eneopteridae. In: Yang XK (Ed.) Insects from Mt. Shiwandashan Area of Guangxi. China Forestry Publishing House, Beijing, 116–121.

Xie LD, Zheng ZM (2003) Description of a new species of the genus *Gymnogryllus* from China (Orthoptera, Gryllidae). Acta Zootaxonomica Sinica 28: 496–498.

Yin HS, Liu XW (1995) Synopsis of the Classification of Grylloidea and Gryllotalpoidea from China. Shanghai Scientific and Technological Literature Publishing House Press, Shanghai, 237 pp.

Supplementary material 1

The distance between the first and second oblique veins at the base varies of 42 specimens of the *P. minor*

Authors: Ning Wang, Huateng Huang, Li-Bin Ma

Data type: statistical data

Link: https://doi.org/10.3897/zookeys.1129.87706.suppl1

Supplementary material 2

The area to total area ratio of the black area of the posterior femora of 42 specimens of the *P. minor*

Authors: Ning Wang, Huateng Huang, Li-Bin Ma

Data type: statistical data

Link: https://doi.org/10.3897/zookeys.1129.87706.suppl2

ZooKeys 1129: 109–162 (2022)
doi: 10.3897/zookeys.1129.90535
https://zookeys.pensoft.net

RESEARCH ARTICLE

A peer-reviewed open-access journal
ZooKeys
Launched to accelerate biodiversity research

Integrative taxonomy delimits and diagnoses cryptic arboreal species of the *Cyrtodactylus brevipalmatus* group (Squamata, Gekkonidae) with descriptions of four new species from Thailand

L. Lee Grismer[1,2], Anchalee Aowphol[3], Siriporn Yodthong[4], Natee Ampai[5], Korkhwan Termprayoon[3], Akrachai Aksornneam[3], Attapol Rujirawan[3]

1 *Herpetology Laboratory, Department of Biology, La Sierra University, 4500 Riverwalk Parkway, Riverside, California 92505, USA* **2** *Department of Herpetology, San Diego Natural History Museum, PO Box 121390, San Diego, California, 92112, USA* **3** *Animal Systematics and Ecology Speciality Research Unit, Department of Zoology, Faculty of Science, Kasetsart University, Bangkok 10900, Thailand* **4** *Department of Biology, Faculty of Science, Thaksin University, Pa Phayom, Phattalung 93210, Thailand* **5** *Department of Biology, Faculty of Science, Srinakharinwirot University, Bangkok 10110, Thailand*

Corresponding author: Attapol Rujirawan (fsciapr@ku.ac.th)

Academic editor: Thomas Ziegler | Received 19 July 2022 | Accepted 25 October 2022 | Published 15 November 2022

https://zoobank.org/3D73FEE9-44FD-4DA9-8E2B-C07536739901

Citation: Grismer LL, Aowphol A, Yodthong S, Ampai N, Termprayoon K, Aksornneam A, Rujirawan A (2022) Integrative taxonomy delimits and diagnoses cryptic arboreal species of the *Cyrtodactylus brevipalmatus* group (Squamata, Gekkonidae) with descriptions of four new species from Thailand. ZooKeys 1129: 109–162. https://doi.org/10.3897/zookeys.1129.90535

Abstract

Species delimitation and species diagnosis must remain separate operations to avoid constructing taxonomies comprised of non-monophyletic species based on morphological similarity as opposed to phylogenetic propinquity. This is particularly true for highly specialized species such as the range-restricted upland taxa in the *Cyrtodactylus brevipalmatus* group of Indochina where strong selection pressure for an arboreal lifestyle has contributed to morphologically similar but distantly related species. This in turn, has resulted in a history of erroneous taxonomies that have actually obscured rather than revealed the diversity within this group. A Bayesian phylogeny of the *C. brevipalmatus* group recovered at least 15 putative species-level lineages, at least seven of which are undescribed, and of which four are described herein. A total evidence morphological data set comprised of 16 normalized morphometric, 15 meristic, and seven categorical characters scored across 51 individuals was subjected to a multiple factor analysis (MFA) and an analysis of variance (ANOVA) to diagnose the putative species. These new species descriptions contribute to focusing attention to the unrealized diversity in upland tropical ecosystems, which due to climate change, are some of the most impearled ecosystems on the planet. Thus, it is paramount that taxonomies do not conflate species identities and underrepresent true diversity.

Keywords
geckos, genetics, morphology, Southeast Asia, taxonomy

Introduction

A cornerstone of biodiversity conservation is a phylogenetic-based taxonomy where the names of the component species are consistent with the patterns and processes by which they evolved. Taxonomies constructed from paraphyletic or polyphyletic species misrepresent history, thus obscuring true diversity and potentially countermanding the effectiveness of conservation efforts. Before a newly discovered population can be given a new name, or the name of an existing species be successfully challenged, it should be properly delimited and diagnosed. Delimiting and diagnosing species are independent operations used together to construct taxonomies that reflect, and are consistent with evolutionary history. Unfortunately, these two operations are often conflated when analyses to diagnose species, which are most often rooted in morphological similarity, are equated with analyses to delimit species, which are rooted in phylogenetic propinquity. The unfortunate consequence of this is that taxonomies may be constructed using non-monophyletic species, thus obscuring rather than revealing the group's actual diversity. This is especially true for taxonomies comprised of highly specialized cryptic species where, in the absence of a phylogeny, morphological convergence can be mistaken for common ancestry (see Grismer 2008; Grismer et al. 2020, 2022). Despite methodological improvements over the years that have increased the efficacy of both delimitation and diagnostic procedures, they have had little effect on operational decisions to not conflate them.

Convergent morphology results from the specific resource requirements that necessitate a particular functional morphology (Ricklefs 2012; Dehling et al. 2016; Baulechner et al. 2020). In such cases, phylogenetic analysis becomes paramount to disentangle convergence from common ancestry in order to construct proper phylogenetic taxonomies. This is especially true of clades containing highly specialized species such as the *Cyrtodactylus brevipalmatus* group (sec. Grismer et al. 2021a, b, c). This group currently contains four nominal species that range from northern Vietnam and Laos, southward through Thailand to southern Peninsular Malaysia (Fig. 1). Nearly all members of this adaptive radiation are highly specialized for an arboreal lifestyle and all have a prehensile tail carried in a tightly coiled position, a cryptic color pattern of different shades of brown that closely match the substrate of their microhabitat, and generally slow, deliberate "chameleon-like" movements. Presumably, the selection pressures for such a specialized lifestyle have contributed to morphological convergence within this relatively small group (Grismer et al. 2022). Thus, as demonstrated by Grismer (2008) and Grismer et al. (2021c, 2022), previous morphology-based operations intending to delimit species resulted in reoccurring taxonomies composed of non-monophyletic species (Smith 1935; Welch et al. 1990; Ulber 1993; Manthey and Grossmann 1997; Stuart 1999; Nabhitabhata et al. 2004; Nabhitabhata and Chan-ard 2005; Pauwels and Chan-ard 2006; Ellis and Pauwels 2012) that underrepresented the group's diversity. Grismer et al. (2021c, 2022) were the first to employ phylogenetic analyses to the

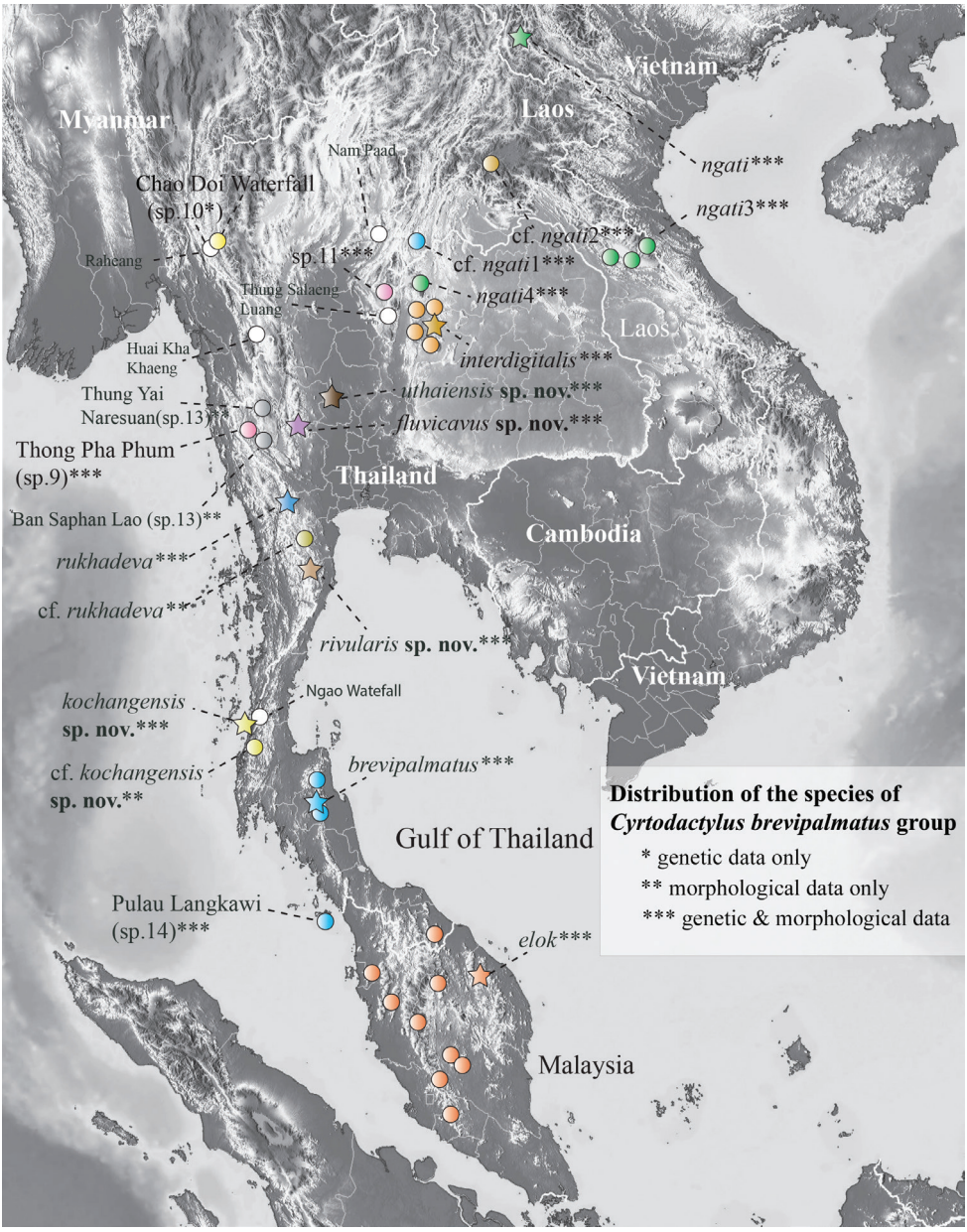

Figure 1. Distribution of nominal species and unnamed populations and specimens of the *Cyrtodactylus brevipalmatus* group. Stars denote type localities. White circles are literature localities from which specimens were not examined and remain unidentified. Locality data for all material examined is in Table 1.

brevipalmatus group to delimit species and statistically based morphological analyses to diagnose those species. As such, by treating these analyses as independent operations and their results as corroborating evidence, a revised taxonomy consistent with the group's evolutionary history was disentangled from a convergence-based taxonomy.

The phylogenetic-based taxonomy of Grismer et al. (2022) is expanded here with significantly increased morphological and genetic sampling from new localities in Thailand at Ko (= island) Chang (ZMKU R 00945) and Khlong Nakha Wildlife Sanctuary (THNHM 01667), Ranong Province; Hua Hin, Prachuap Khiri Khan Province (ZMKU R 00946–47); Si Sawat (ZMKU R 00958–64) and Thong Pha Phum (ZMKU R 00950–57), Kanchanaburi Province; and an isolated population from a small hilly region at Lan Sak, Uthai Thani Province (ZMKU R 00949) in the Chao Phraya River Basin. In this analysis, we discuss the high degree of morphological similarity throughout the phylogeny despite the relatively high degrees of genetic divergence. The analyses also recovered the existence of 4–10 new populations we hypothesize to be distinct species, four of which are described herein.

Materials and methods

Species delimitation

The general lineage concept (GLC: de Queiroz 2007) adopted herein proposes that a species constitutes a population of organisms evolving independently from other such populations owing to a lack of, or limited gene flow. By "independently," it is meant that new mutations arising in one species cannot spread readily into another species (Barraclough et al. 2003; de Queiroz 2007). Under the GLC implemented herein, molecular phylogenies recovered monophyletic mitochondrial lineages of individuals (populations) that were used to develop initial species-level hypotheses, the grouping stage of Hillis (2019). Discrete color pattern data and univariate and multivariate analyses of morphological data were then used to search for characters and morphospatial patterns consistent with the tree-designated species-level hypotheses, the construction of boundaries representing the hypothesis-testing step of Hillis (2019), –thus providing independent diagnoses to complement the molecular analyses. In this way, delimiting (phylogeny) and diagnosing (taxonomy) species are not conflated (Frost and Hillis 1990; Frost and Kluge 1994; Hillis 2019).

Species boundaries were cross-checked using a Bayesian Poisson Tree Process for species delimitation (bPTP; Zhang et al. 2013), thus providing an independent framework to complement the empirically based thresholds of the morphological and molecular analyses. This method delimits species from single-locus gene trees with low population samples (Lin et al. 2018) by detecting genetic clustering beyond the expected levels of a null hypothesis which infers that all individuals of a population form a genetically, interacting nexus. A Markov Chain Monte Carlo (MCMC) was run for 10,000 generations on the bPTP web server at https://species.h-its.org/ptp/ and checked for convergence. Delimitation accuracy was based on the normalized mutual information criterion (NMI) (Vinh et al. 2010). The model relies on the prediction that independent evolution leads to the appearance of distinct genetic clusters, separated by relatively longer internal branches (Barraclough et

al. 2003; Acinas et al. 2004). Such groups therefore diverge into discrete clades of genetic variation. These clades are then diagnosed by statistically defensible morphological analyses.

Genetic data

Methods for DNA extraction, sequencing, and editing followed Grismer et al. (2022) and resulted in a 1,386 base pair segment of the mitochondrial NADH dehydrogenase subunit 2 gene (ND2) and adjacent tRNAs. All material examined is listed in Table 1 along with GenBank accession numbers for the new and published genetic materials.

Morphological data

Morphological data included both meristic and morphometric characters. To reduce the degree of researcher bias, data were taken using the protocol of Le et al. (2021) and Grismer et al. (2022) and where possible, double checked by LLG using high resolution digital photographs and/or the actual specimens. All data were taken on the left side of the body (when possible) and measured to the nearest 0.1 mm using digital calipers under a Nikon SMZ745 stereomicroscope. Morphometric data taken were: snout-vent length **(SVL)**, taken from the tip of the snout to the vent; tail length **(TL)**, taken from the vent to the tip of the tail–original or partially regenerated; tail width **(TW)**, taken at the base of the tail immediately posterior to the postcloacal swelling; humeral length **(HumL)**, taken from the proximal end of the humerus at its insertion point in the glenoid fossa to the distal margin of the elbow while flexed 90°; forearm length **(ForL)**, taken on the ventral surface from the posterior margin of the elbow while flexed 90° to the inflection of the flexed wrist; femur length **(FemL)**, taken from the proximal end of the femur at its insertion point in the acetabulum to the distal margin of the knee while flexed 90°; tibia length **(TibL)**, taken on the ventral surface from the posterior margin of the knee while flexed 90° to the base of the heel; axilla to groin length **(AG)**, taken from the posterior margin of the forelimb at its insertion point on the body to the anterior margin of the hind limb at its insertion point on the body; head length **(HL)**, the distance from the posterior margin of the retroarticular process of the lower jaw to the tip of the snout; head width **(HW)**, measured at the angle of the jaws; head depth **(HD)**, the maximum height of head measured from the occiput to base of the lower jaw posterior to the eyes; eye diameter **(ED)**, the greatest horizontal diameter of the eye-ball; eye to ear distance **(EE)**, measured from the anterior edge of the ear opening to the posterior edge of the bony orbit; eye to snout distance or snout length **(ES)**, measured from anteriormost margin of the bony orbit to the tip of snout; eye to nostril distance **(EN)**, measured from the anterior margin of the bony orbit to the posterior margin of the external nares; interorbital distance **(IO)**, measured between the dorsomedial-most edges of the bony orbits; internarial distance **(IN)**, measured between the external nares across the rostrum; and ear length **(EL)**, greatest oblique length across the auditory meatus.

Table 1. *Cyrtodactylus* specimens examined in this study. Institutional abbreviations follow Sabaj (2020) except that YC = Yodchaiy Chuaynkern from Department of Biology, Faculty of Science, Khon Kaen University, Khon Kaen, Thailand.

Species	Location	Catalog no.	GenBank no.
C. brevipalmatus	Thailand, no data	LSUHC 1899	not in tree
C. brevipalmatus	Thailand, Nakhon Si Thammarat Province, Nopphitam District, Khao Nan National Park, Huay Lak Protected Unit	THNHM 10670	not in tree
C. brevipalmatus	Thailand, Nakhon Si Thammarat Province, Lan Saka District, Khao Luang National Park	THNHM 14112	not in tree
C. brevipalmatus	Thailand, Nakhon Si Thammarat Province, Khao Ram Mt.	AUP-00573	OK626313
C. cf. *brevipalmatus*	Peninsular Malaysia, Kedah State, Pulau Langkawi, Gunung Raya	LSUHC 11788	not in tree
C. cf. *brevipalmatus*	Peninsular Malaysia, Kedah State, Pulau Langkawi, Gunung Raya	LSUHC 15076	not in tree
C. elok	Peninsular Malaysia, Pahang State, Fraser's Hill, the Gap	ZRC 2.6091/ LSUHC 6471	JQ889180
C. elok	Peninsular Malaysia, Negeri Sembilan State	LSUHC 8238	not in tree
C. elok	Peninsular Malaysia, Pahang State, near Cameron Highlands	LSUHC 12180	not in tree
C. elok	Peninsular Malaysia, Pahang State, near Cameron Highlands	LSUHC 12181	not in tree
C. elok	Malaysian pet trade, no data	ZMMU R-16144	not in tree
Cyrtodactylus fluvicavus sp. nov.	Thailand, Kanchanaburi Province, Si Sawat District, Khao Chot Subdistrict, Chaloem Rattanakosin National Park	ZMKU R 00958 paratype	OP620036
Cyrtodactylus fluvicavus sp. nov.	Thailand, Kanchanaburi Province, Si Sawat District, Khao Chot Subdistrict, Chaloem Rattanakosin National Park	ZMKU R 00959 holotype	OP620037
Cyrtodactylus fluvicavus sp. nov.	Thailand, Kanchanaburi Province, Si Sawat District, Khao Chot Subdistrict, Chaloem Rattanakosin National Park	ZMKU R 00960 paratype	OP620038
Cyrtodactylus fluvicavus sp. nov.	Thailand, Kanchanaburi Province, Si Sawat District, Khao Chot Subdistrict, Chaloem Rattanakosin National Park	ZMKU R 00961 paratype	OP620039
Cyrtodactylus fluvicavus sp. nov.	Thailand, Kanchanaburi Province, Si Sawat District, Khao Chot Subdistrict, Chaloem Rattanakosin National Park	ZMKU R 00962 paratype	OP620040
Cyrtodactylus fluvicavus sp. nov.	Thailand, Kanchanaburi Province, Si Sawat District, Khao Chot Subdistrict, Chaloem Rattanakosin National Park	ZMKU R 00963 paratype	OP620041
Cyrtodactylus fluvicavus sp. nov.	Thailand, Kanchanaburi Province, Si Sawat District, Khao Chot Subdistrict, Chaloem Rattanakosin National Park	ZMKU R 00964 paratype	OP620042
C. interdigitalis	Thailand, Phetchabun Province, Nam Nao National Park, Tham Yai Nam Nao	THNHM 20226 paratype	not in tree
C. interdigitalis	Thailand, Phetchabun Province, Nam Nao National Park, Tham Yai Nam Nao	THNHM 20227 paratype	not in tree
C. interdigitalis	Thailand, Phetchabun Province, Nam Nao National Park, Tham Yai Nam Nao	THNHM 20228 paratype	not in tree
C. interdigitalis	Thailand, Phetchabun Province, Nam Nao National Park, Tham Yai Nam Nao	THNHM 20229 paratype	not in tree
C. interdigitalis	Thailand, Phetchabun Province, Nam Nao National Park, Tham Yai Nam Nao	YC000952	ON055281
Cyrtodactylus kochangensis sp. nov.	Thailand, Ranong Province, Mueng Ranong District, Ko Phayam Subdistrict, Ko Chang	ZMKU R 00945 holotype	OP620023
C. cf. *kochangensis* sp. nov.	Thailand, Ranong Province, Khlong Nakha Wildlife Sanctuary	THNHM 01667	not in tree
C. ngati	Vietnam, Dien Bien Province, Dien Bien District, Pa Thom Commune, Pa Xa Lao Village, karst forest near Pa Thom Cave	HNUE-R00111 holotype	ON411220
C. ngati	Vietnam, Dien Bien Province, Dien Bien District, Pa Thom Commune, Pa Xa Lao Village, karst forest near Pa Thom Cave	HNUE-R00112 paratype	not in tree
C. ngati	Vietnam, Dien Bien Province, Dien Bien District, Pa Thom Commune, Pa Xa Lao Village, karst forest near Pa Thom Cave	IEBR 4829 paratype	OK626318
C. ngati	Vietnam, Dien Bien Province, Dien Bien District, Pa Thom Commune, Pa Xa Lao Village, karst forest near Pa Thom Cave	VNUF R.2020.12 paratype	OK626319
*C. ngati*3	Laos, Khammouane Province	VNUF R.2014.50	ON411221
*C. ngati*3	Laos, Khammouane Province, Phou Hin Poun National Biodiversity Conservation Area	FMNH 255454	JQ889181
*C. ngati*3	Laos, Khammouane Province, Phou Hin Poun National Biodiversity Conservation Area	FMNH 270492	OK626315
*C. ngati*3	Laos, Khammouane Province, Phou Hin Poun National Biodiversity Conservation Area	FMNH 270493	not in tree
*C. ngati*4	Thailand, Loei Province, Nam San Noi River, Phu Luang Wildlife Sanctuary	FMNH 265806	JX519471
C. cf. *ngati*1	Laos, Xaignabouli Province, Ban Pha Liep, Houay Liep Stream	NCSM 79472	OK626316
C. cf. *ngati*2	Laos, Vientiane Province	ZMMU R-14917	not in tree

Species	Location	Catalog no.	GenBank no.
C. cf. *ngati2*	Laos, Vientiane Province, tributary of Nam Pha River, Houay Wan Stream	NCSM 80100	OK626317
Cyrtodactylus rivularis sp. nov.	Thailand, Prachuap Khiri Khan Province, Hua Hin District, Huai Sat Yai Subdistrict, Kaeng Krachan National Park, Pa La-U Waterfall	ZMKU R 00946 paratype	OP620024
Cyrtodactylus rivularis sp. nov.	Thailand, Prachuap Khiri Khan Province, Hua Hin District, Huai Sat Yai Subdistrict, Kaeng Krachan National Park, Pa La-U Waterfall	ZMKU R 00947 holotype	OP620025
C. rukhadeva	Thailand, Ratchaburi Province, Suan Phueng District, Khao Laem Mountain	ZMMU R-16851 holotype	OK626320
C. rukhadeva	Thailand, Ratchaburi Province, Suan Phueng District, Hoop Phai Tong	ZMMU R-16852 paratype	not in tree
C. rukhadeva	Thailand, Ratchaburi Province, Suan Phueng District, Suan Phueng Subdistrict	ZMKU R 00948	OP620026
C. cf. *rukhadeva*	Thailand, Phetchaburi Province, Kaeng Krachan National Park	THNHM 01807	not in tree
C. cf. *rukhadeva*	Thailand, Phetchaburi Province, Kaeng Krachan National Park	THNHM 03251	not in tree
C. cf. *rukhadeva*	Thailand, Phetchaburi Province, Kaeng Krachan National Park	THNHM 03252	not in tree
C. cf. *rukhadeva*	Thailand, Phetchaburi Province, Kaeng Krachan National Park	THNHM 03253	not in tree
C. cf. *rukhadeva*	Thailand, Phetchaburi Province, Kaeng Krachan National Park	THNHM 03254	not in tree
C. cf. *rukhadeva*	Thailand, Phetchaburi Province, Kaeng Krachan National Park	THNHM 24622	not in tree
C. cf. *rukhadeva*	Thailand, Phetchaburi Province, Kaeng Krachan National Park	THNHM 24838	not in tree
Cyrtodactylus uthaiensis sp. nov.	Thailand, Uthai Thani Province, Lan Sak District, Thung Na Ngam Subdistrict	ZMKU R 00949 holotype	OP620027
C. sp.9	Thailand, Kanchanaburi Province, Thong Pha Phum District, Thong Pha Phum National Park	AUP-01715	MT468909
C. sp.9	Thailand, Kanchanaburi Province, Thong Pha Phum District, Pilok Subdistrict, Thong Pha Phum National Park	ZMKU R 00950	OP620028
C. sp.9	Thailand, Kanchanaburi Province, Thong Pha Phum District, Pilok Subdistrict, Thong Pha Phum National Park	ZMKU R 00951	OP620029
C. sp.9	Thailand, Kanchanaburi Province, Thong Pha Phum District, Pilok Subdistrict, Thong Pha Phum National Park	ZMKU R 00952	OP620030
C. sp.9	Thailand, Kanchanaburi Province, Thong Pha Phum District, Pilok Subdistrict, Thong Pha Phum National Park	ZMKU R 00953	OP620031
C. sp.9	Thailand, Kanchanaburi Province, Thong Pha Phum District, Pilok Subdistrict, Thong Pha Phum National Park	ZMKU R 00954	OP620032
C. sp.9	Thailand, Kanchanaburi Province, Thong Pha Phum District, Pilok Subdistrict, Thong Pha Phum National Park	ZMKU R 00955	OP620033
C. sp.9	Thailand, Kanchanaburi Province, Thong Pha Phum District, Pilok Subdistrict, Thong Pha Phum National Park	ZMKU R 00956	OP620034
C. sp.9	Thailand, Kanchanaburi Province, Thong Pha Phum District, Pilok Subdistrict, Thong Pha Phum National Park	ZMKU R 00957	OP620035
C. sp.10	Thailand, Tak Province, Tha Song Yang District, Mae Moei National Park, Chao Doi Waterfall	AUP-00680	MT468902
C. sp.11 (*C.* cf. *interdigitalis*)	Thailand, Phitsanulok Province, Phu Hin Rong Kla National Park	ZMMU R-16492	MW792061
C. sp.13	Thailand, Tak Province, Umphang District, Thung Yai Naresuan Wildlife Sanctuary	THNHM 00104	not in tree
C. sp.13	Thailand, Kanchanaburi Province, Thong Pha Phum District, Ban Saphan Lao	THNHM 27821	not in tree
C. sp.14 (*C.* cf. *brevipalmatus*)	Peninsular Malaysia, Kedah State, Pulau Langkawi, Gunung Raya	USMHC 2555	OK626314

Meristic characters evaluated were the number of supralabial scales **(SL)**, counted from the largest scale at the corner of the mouth or posterior to the eye, to the rostral scale; infralabial scales **(IL)**, counted from termination of enlarged scales at the corner of the mouth to the mental scale; number of paravertebral tubercles **(PVT)** between the limb insertions counted in a straight line immediately left of the vertebral column; number of longitudinal rows of body tubercles **(LRT)** counted transversely across the body midway between the limb insertions from one ventrolateral body fold to the other; number of longitudinal rows of ventral scales **(VS)** counted transversely across the abdomen midway between limb insertions from one ventrolateral fold to the other; number of transverse rows of ventral scales **(VSM)** counted along the midline of the body from

the postmentals to just anterior to the cloacal opening, stopping where the scales become granular; number of expanded subdigital lamellae on the fourth toe proximal to the digital inflection **(TL4E)** counted from the base of the first phalanx where it contacts the body of the foot to the largest scale on the digital inflection–the large contiguous scales on the palmar and plantar surfaces were not counted; number of small, generally unmodified subdigital lamellae distal to the digital inflection on the fourth toe **(TL4U)** counted from the digital inflection to the claw including the claw sheath; total number of subdigital lamellae **(TL4T)** beneath the fourth toe (i.e. TL4E + TL4U = TL4T); number of expanded subdigital lamellae on the fourth finger proximal to the digital inflection **(FL4E)** counted the same way as with TL4E; number of small generally unmodified subdigital lamellae distal to the digital inflection on the fourth finger **(FL4U)** counted the same way as with TL4U; total number of subdigital lamellae **(FL4T)** beneath the fourth toe (i.e. FL4E + FL4U = FL4T); total number of enlarged femoral scales **(FS)** from each thigh combined as a single metric; number of enlarged precloacal scales **(PCS)**; number of precloacal pores **(PP)** in males; the number of femoral pores **(FP)** in males from each thigh combined as a single metric; and the number of dark body bands **(BB)** between the dark band on the nape and the hind limb insertions on the body. A post-sacral or sacral band when present, was not counted. Categorical characters evaluated were the presence or absence of tubercles on the flanks **(FKT)**; single enlarged, unmodified, medial subcaudal scales **(SC2)**; enlarged medial subcaudals intermittent, medially furrowed, posteriorly emarginated **(SC3)**; slightly enlarged medial subcaudals **(SC1)**; large or small dorsolateral caudal tubercles **(DCT)** forming a narrow or wide ventrolateral caudal fringe **(VLF1)**; ventrolateral caudal fringe scales generally homogenous or not **(VLF2)**; and the cross-section of the tail round or square **(TLcross)**.

Phylogenetic analyses

An input file implemented in BEAUti (Bayesian Evolutionary Analysis Utility) v. 2.4.6 was run in BEAST (Bayesian Evolutionary Analysis Sampling Trees) v. 2.4.6 (Drummond et al. 2012) on CIPRES (Cyberinfrastructure for Phylogenetic Research; Miller et al. 2010) in order to generate a BEAST phylogeny, employing a lognormal relaxed clock with unlinked site models and linked trees and clock models. bModelTest (Bouckaert and Drummond 2017), implemented in BEAST, was used to numerically integrate over the uncertainty of substitution models while simultaneously estimating the phylogeny using Markov chain Monte Carlo (MCMC). MCMC chains were run using a Yule prior for 40,000,000 generations and logged every 4,000 generations. The BEAST log file was visualized in Tracer v. 1.7.0 (Rambaut et al. 2018) to ensure effective sample sizes (ESS) were clearly above 200 for all parameters. A maximum clade credibility tree using mean heights at the nodes was generated using TreeAnnotator v. 1.8.0 (Rambaut and Drummond 2013) with a burn-in of 1,000 trees (10%). Nodes with Bayesian posterior probabilities (BPP) of 0.95 and above were considered strongly supported (Huelsenbeck et al. 2001; Wilcox et al. 2002). Uncorrected pairwise sequence divergences were calculated in MEGA 11 (Tamura et al. 2021) using the complete deletion option to remove gaps and missing data from the alignment prior to analysis.

Statistical analyses

All statistical analyses were conducted using R Core Team (2018). Morphometric characters used in statistical analyses were SVL, AG, HumL, ForL, FemL, TibL, HL, HW, HD, ED, EE, ES, EN, IO, EL, and IN. Tail metrics were not used due to the high degree of incomplete sampling (i.e., regenerated, broken, or missing). In order to most successfully remove the effects of allometry (sec. Chan and Grismer 2022), size was normalized using the following equation: $X_{adj} = \log(X)-\beta[\log(SVL)-\log(SVL_{mean})]$, where X_{adj} = adjusted value; X = measured value; β = unstandardized regression coefficient for each population; and SVL_{mean} = overall average SVL of all populations (Thorpe 1975, 1983; Turan 1999; Lleonart et al. 2000), accessible in the R package *GroupStruct* (available at https://github.com/chankinonn/GroupStruct). The morphometrics of each species were normalized separately and then concatenated so as not to conflate potential intra- with interspecific variation (Reist 1986; McCoy et al. 2006). The juvenile *Cyrtodactylus ngati* (HNUE-R00112) was removed from the data so as not to skew the normalization results. All data were scaled to their standard deviation to ensure they were analyzed on the basis of correlation and not covariance. Meristic characters analyzed were SL, IL, PVT, LRT, VS, VSM, TL4E, TL4U, TL4T, FL4E, FL4U, FL4T, FS, PCS, and BB. Precloacal and femoral pores were omitted from the multivariate analyses due to their absence in females. Categorical characters analyzed were DCT, VLF1, VLF2, TLcross, SC1, SC2, and SC3.

Small sample sizes ($N = 1$ or 2) for some of the species/populations precluded them from statistical analyses. A Levene's test for the normalized morphometric and meristic characters was conducted to test for equal variances across all groups. Characters with equal variances were analyzed with an analysis of variance (ANOVA) and TukeyHSD *post hoc* test for mean comparisons involving more than three groups. Those with unequal variances were subjected to Welch's *F*-test and Games-Howell *post hoc* test to test for mean comparisons involving more than three groups.

Morphospatial clustering and positioning among the species/populations was analyzed using multiple factor analysis (MFA) on a concatenated data set comprised of 15 meristic characters, 16 normalized morphometric characters, and seven categorical characters (Suppl. material 1). For this test, it was not necessary to remove populations represented by small sample sizes. The MFA was implemented using the *mfa*() command in the R package *FactorMineR* (Husson et al. 2017) and visualized using the *Factoextra* package (Kassambara and Mundt 2017). MFA is a global, unsupervised, multivariate analysis that incorporates qualitative and quantitative data (Pagès 2015) simultaneously, making it possible to analyze different data types in a nearly total evidence environment. In an MFA, each individual is described by a different set of variables (i.e., characters) which are structured into different data groups in a global data frame, in this case quantitative data (i.e., meristics and normalized morphometrics) and categorical data (i.e., scale, tubercle, and caudal morphology). In the first phase of the analysis, separate multivariate analyses are carried out for each set of variables: principal component analyses (PCA) for each quantitative data set and a multiple correspondence analysis (MCA) for the categorical data. The data sets are then normalized separately by dividing all their elements by the square root of their first eigenvalue. For the second phase of the analysis,

these normalized data sets are concatenated into a single matrix for a final global PCA of the normalized data. Standardizing the data in this manner prevents one data type from overleveraging another. In other words, the normalization of the data in the first phase prevents data types with the greatest number of characters or the greatest amount of variation from outweighing other data types in the second phase. This way, the contributions of each data type to the overall variation in the data set are scaled to define the morphospatial distance between individuals as well as calculating each data type's contribution to the overall variation in the analysis (Pagès 2015; Kassambara and Mundt 2017).

A non-parametric permutation multivariate analysis of variance (PERMANOVA) from the *vegan* package 2.5–3 in R (Oksanen et al. 2020) was used to determine if the centroid locations and group clustering of each species/population in the MFA were statistically different from one another (Skalski et al. 2018). The analysis was based on the calculation of a Gower (dis)similarity matrix using 50,000 permutations based on the loadings of the first four dimensions of the MFA. A pairwise *post hoc* test calculates the differences between all combinations of population pairs, generating a *p*-value, a Bonferroni-adjusted *p*-value, and a pseudo-*F* ratio (*F* statistic). A $p < 0.05$ is considered significant and larger *F* statistics indicate more pronounced group separation. A rejection of the null hypothesis (i.e., centroid positions and/or the spread of the data points [i.e. clusters] are no different from random) signifies a statistically significant difference between species/populations.

Phylomorphospace

The BEAST phylogeny was projected onto the first two dimensions of the MFA plot using the *phylomorphospace*() command from the R package phytools (Revell 2012). This allows one to map the history of a group's morphological diversification and infer the magnitude and direction of shape change along branches of the phylogeny (Sidlauskas 2008). Outgroups and species from the phylogenetic analyses not represented in the morphological dataset were excluded. To eliminate a potential bias caused by the highly derived *Cyrtodactylus elok* (see Grismer et al. 2022), it was not included.

Some of the populations examined had only genetic or morphological data. However, only phylogenetically delimited populations bearing morphological differences from other populations were described as new species. In some cases, populations represented by only morphological data but in close geographic proximity to named species from which they could not be separated morphologically, were considered *conferre* (cf.) to the named species pending further investigation.

Results

Phylogenetic analysis

The BEAST analysis recovered 8–10 new species and two major clades within the *brevipalmatus* group: a weakly supported clade (BPP = 0.82) from the southernmost portion of the Thai-Malay Peninsula south of the Isthmus of Kra comprised of

Cyrtodactylus elok, *C. brevipalmatus*, and *C.* sp.14 and a well-supported clade (1.00) comprised of all other species north of the Isthmus of Kra (Figs 1, 2). Within the latter, a well-supported (1.00) more exclusive clade containing the sister species from Hua Hin, Prachuap Khiri Khan (*Cyrtodactylus rivularis* sp. nov. [see below]) and *C. rukhadeva* with the Ko Chang population (*Cyrtodactylus kochangensis* sp. nov. [see below]) being sister to these. All relationships within this clade have strong nodal support (1.00) and its taxa occur only in the northernmost portion of the Thai-Malay Peninsula (Fig. 1). The population from Si Sawat (*Cyrtodactylus fluvicavus* sp. nov. [see below]), *C.* sp.10 from Chao Doi Waterfall, Mae Moei National Park, Tak Province, and *C.* sp.9 from Thong Pha Phum are sequentially related to a strongly supported (1.00) clade containing the remaining species. Within that latter clade, *C. interdigitalis* is the strongly supported (1.00) sister species to *C.* sp.11 from Phu Hin Rong Kla National Park and together they compose the well-supported (0.93) sister lineage to the Uthai Thani population (*Cyrtodactylus uthaiensis* sp. nov. [see below]). The remaining species all form a strongly supported (1.00) sequentially related clades with *C. ngati*.

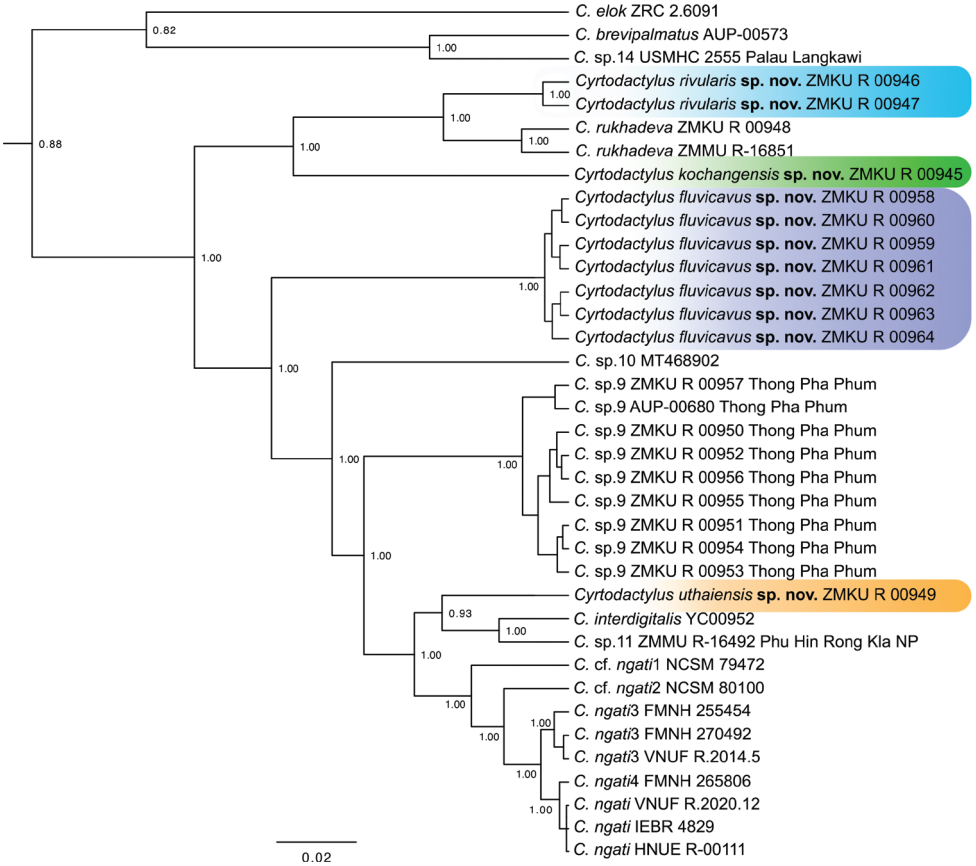

Figure 2. Maximum clade credibility BEAST phylogeny of the *Cyrtodactylus brevipalmatus* group highlighting the new species described herein. Bayesian posterior probabilities (BPP) are listed at the nodes.

Uncorrected pairwise sequence divergences within the *brevipalmatus* group range from 2.84–22.84% (Table 2). Ranges for those of the new species described below are as follows: *Cyrtodactylus rivularis* sp. nov. ranges from 3.61–21.81%, being most similar to *C. rukhadeva* and most distant to *C. elok*; *Cyrtodactylus fluvicavus* sp. nov. ranges from 9.55–20.26%, being most similar to the Thong Pha Phum population (*C.* sp.9) and most distant to *C. elok*; *Cyrtodactylus kochangensis* sp. nov. ranges from 12.00–20.90%, being most similar to *Cyrtodactylus rivularis* sp. nov. and most distant to *C. elok*; and *Cyrtodactylus uthaiensis* sp. nov. ranges from 5.81–21.16%, being most similar to *C.* cf. *ngati*1 and most distant to *C. elok.*

Bayesian Poisson Tree Process (bPTP)

The bPTP species delimitation analysis recovered 16 putative species within the *brevipalmatus* group with varying degrees of support (Table 3). The newly acquired material in this study recovered as distinct species are *Cyrtodactylus fluvicavus* sp. nov., *Cyrtodactylus kochangensis* sp. nov., *Cyrtodactylus rivularis* sp. nov., the holotype of *C. rukhadeva* (ZMMU R-16851), *C. rukhadeva* (ZMKU R 00948), *Cyrtodactylus uthaiensis* sp. nov., *C.* sp.9 from Thong Pha Phum, and *C.* sp.14 from Pulau Langkawi. However, *Cyrtodactylus rivularis* sp. nov. and *C.* sp.9 were not recovered with strong support (NMI 0.575 and 0.565, respectively) despite them being genetically distinct (Table 2) and morphologically diagnosable (Tables 4–6). The analysis also separated the two specimens of *C. rukhadeva* from the same locality which only differ by a genetic distance of 1.55% and are similar in morphology. Sukumaran and Knowles (2017) demonstrated that many species delimitation analyses recover clades not species and that a wider range of empirical data are necessary to interpret these boundaries (Coyne and Orr 1998; Feulner et al. 2007; Fontaneto et al. 2007; Knowles and Carstens 2007; Leach et al. 2009) as was done here (see below).

Statistical analyses

The ANOVA and TukeyHSD *post hoc* analyses of the adjusted morphometric and meristic characters were consistent with the phylogenetic and pairwise distance data in recovering a number of statistically significant differences between the *Cyrtodactylus fluvicavus* sp. nov. and *C. interdigitalis* as well as others (Table 6). *Cyrtodactylus fluvicavus* sp. nov. plotted separately in the MFA, only slightly overlapping with *C. brevipalmatus* (Fig. 3A). *Cyrtodactylus kochangensis* sp. nov., *Cyrtodactylus rivularis* sp. nov. and *Cyrtodactylus uthaiensis* sp. nov. plotted separately from each other and all other populations. A PERMANOVA analysis recovered several instances of various combinations of statistically significant differences among all the populations/species numbering more than two samples in regards to their clustering and centroid placement (Table 7). The contributions of each data type are shown in Fig. 3C.

Table 2. Mean (minimum–maximum) percentages of uncorrected pairwise sequence divergence (*p*-distances) among the putative species of the *Cyrtodactylus brevipalmatus* group based on 1,386 base pairs of mitochondrial NADH dehydrogenase subunit 2 gene (ND2) and adjacent tRNAs. Intraspecific *p*-distance are in bold font. n/a = data not applicable.

	C. brevipalmatus	***C.* cf. *ngati1***	***C.* cf. *ngati2***	***C. elok***	***Cyrtodactylus fluvicavus* sp. nov.**	***C. interdigitalis***	***Cyrtodactylus kochangensis* sp. nov.**	***C. ngati*, *C. ngati3* and *C. ngati4***	***Cyrtodactylus rivularis* sp. nov.**	***C. rukhadeva***	***C.* sp.9 (Thong Pha Phum)**	***C.* sp.10**	***C.* sp.11**	***C.* sp.14**	***Cyrtodactylus uthaiensis* sp. nov.**
C. brevipalmatus *N* = 1	**n/a**														
C. cf. *ngati1* *N* = 1	21.03	**n/a**													
C. cf. *ngati2* *N* = 1	21.68	4.39	**n/a**												
C. elok *N* = 1	20.77	22.58	21.42	**n/a**											
Cyrtodactylus fluvicavus sp. nov. *N* = 7	18.86 (18.84–18.97)	10.64 (10.58–10.84)	11.02 (10.97–11.23)	20.15 (20.13–20.26)	**0.10 (0.00–0.26)**										
C. interdigitalis *N* = 1	20.77	6.97	9.16	22.84	12.02 (12.00–12.13)	**n/a**									
Cyrtodactylus kochangensis sp. nov. *N* = 1	19.35	14.58	14.71	20.90	12.31 (12.26–12.31)	15.23	**n/a**								
C. ngati, *C. ngati3* and *C. ngati4* *N* = 7	20.70 (20.65–20.90)	3.30 (2.84–4.00)	3.71 (3.35–4.26)	21.11 (20.90–21.42)	11.34 (11.10–11.87)	8.13 (7.74–8.65)	14.58 (14.45–14.84)	**0.84 (0.00–1.55)**							
Cyrtodactylus rivularis sp. nov. *N* = 2	20.00 (19.74–20.26)	15.87 (15.61–16.13)	15.03 (14.84–15.23)	21.61 (21.42–21.81)	12.57 (12.26–13.03)	15.48 (15.23–15.74)	12.26 (12.00–12.52)	15.03 (14.71–15.48)	**0.52**						
C. rukhadeva *N* = 2	20.65 (20.13–21.16)	15.42 (14.84–16.00)	15.48 (14.84–16.13)	21.61 (21.16–22.06)	12.25 (11.61–13.03)	16.00 (15.35–16.65)	13.10 (12.52–13.68)	15.23 (14.19–16.23)	4.65 (3.61–5.68)	**1.55**					
C. sp.9 (Thong Pha Phum) *N* = 9	20.34 (20.13–20.65)	7.93 (7.74–8.00)	9.51 (9.42–9.55)	22.02 (21.81–22.32)	9.75 (9.55–9.94)	8.96 (8.77–9.03)	13.22 (13.03–13.29)	8.81 (8.13–9.68)	13.12 (12.77–13.42)	13.25 (12.52–13.94)	**0.22 (0.00–0.52)**				
C. sp.10 *N* = 1	19.87	9.29	10.84	21.94	10.12 (10.06–10.32)	10.19	13.68	10.21 (10.06–10.45)	13.94 (13.68–14.19)	14.32 (13.68–14.97)	8.06 (7.87–8.13)	**n/a**			
C. sp.11 *N* = 1	20.39	7.23	8.90	22.19	11.12 (11.10–11.23)	3.87	14.58	8.28 (8.00–8.65)	15.35 1) (15.10–15.6	15.61 (14.97–16.26)	8.96 (8.77–9.03)	10.45	**n/a**		
C. sp.14 *N* = 1	6.45	20.90	20.65	20.00	18.34 (18.32–18.45)	20.13	19.10	20.52 (20.26–20.65)	19.74 (19.48–20.00)	20.00 (19.48–20.52)	19.60 (19.48–19.87)	18.84	19.61	**n/a**	
Cyrtodactylus uthaiensis sp. nov. *N* = 1	19.74	5.81	8.13	21.16	10.12 (10.06–10.32)	7.1	13.94	6.97 (6.58–7.61)	13.94 (13.68–14.19)	13.94 (13.29–14.58)	7.80 (7.61–7.87)	8.39	6.58	19.48	**n/a**

Table 3. Species delimited by the bPTP analysis.

Species	NMI
C. brevipalmatus	1
C. cf. *ngati*1	1
C. cf. *ngati*2	0.967
C. elok	1
Cyrtodactylus fluvicavus sp. nov.	0.957
C. interdigitalis	0.997
Cyrtodactylus kochangensis sp. nov.	1
C. ngati	0.841
Cyrtodactylus rivularis sp. nov.	0.575
C. rukhadeva ZMKU R 00948	0.947
C. rukhadeva ZMMU R-16851	0.947
Cyrtodactylus uthaiensis sp. nov	1
C. sp.9 (Thong Pha Phum)	0.565
C. sp.10	1
C. sp.11	0.997
C. sp.14	1

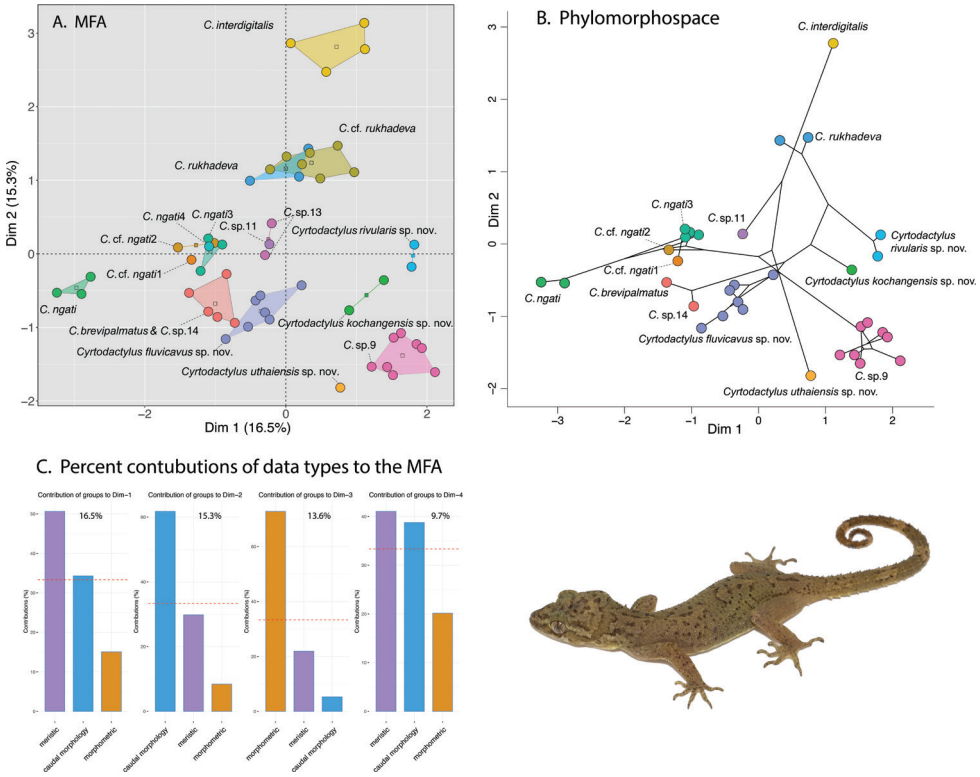

Figure 3. A MFA of the species-level lineages based on the BEAST phylogeny (Fig. 2) **B** phylomorphospace projection of the BEAST phylogeny **C** percent contribution of each data type to Dim 1–4 of the MFA. The percentage score at the top of each graph is the percent contribution of that dimension to the overall variation in the data set.

Morphological and phylogenetic discordance

The phylomorphospace analysis illustrates that the morphological similarities among the species/populations in the MFA are discordant with their phylogenetic placement in the tree (Fig. 3A, B). In other words, species/populations that are similar in morphology are not necessarily each other's closest relatives. For example, *Cyrtodactylus interdigitalis* is morphologically more similar to the distantly related *C. rukhadeva* than it is to *C.* sp.11 or *Cyrtodactylus uthaiensis* sp. nov. to which it is closely related. Similarly, *C.* sp.9 is morphologically similar to the distantly related *Cyrtodactylus kochangensis* sp. nov. than to the closely related clade containing *Cyrtodactylus uthaiensis* sp. nov., *C.interdigitalis*, *C.* sp.11, *C.* cf. *ngati*1, *C.* cf. *ngati*2, *C. ngati*3, *C. ngati*4, and *C. ngati.* Other examples of morphological and phylogenetic discordance can be seen by comparing Fig. 3A, B.

Taxonomy

Given the phylogenetic delimitation of the Si Sawat, Prachuap Khiri Khan, Uthai Thani, and Ko Chang populations (Figs 2, 3), the statistically significant diagnostic placement of the Si Sawat population in morphospace (Fig. 3A; Table 7) and its statistically significant diagnostic morphological differences (Table 6), we describe them below as new species. The phylogenetic delimitation and statistically significant morphological differences among *C.* sp.9 from Thong Pha Phum and *C.* sp.11 from Phu Hin Rong Kla National Park will require descriptions at a future date.

***Cyrtodactylus fluvicavus* sp. nov.**
https://zoobank.org/B65469C6-55A1-401B-9EC3-FAFF151A2973
Figs 4, 5
Suggested Common Name: Tham Than Lot Bent-toed Gecko

Cyrtodactylus sp. Yodthong, Rujirawan, Stuart, Grismer, Aksornneam, Termprayoon, Ampai & Aowphol, 2022: 161.

Holotype. Adult male ZMKU R 00959 from Tham Than Lot Noi-Tham Than Lot Yai Nature Trail, Chaloem Rattanakosin National Park, Khao Chot Subdistrict, Si Sawat District, Kanchanaburi Province, Thailand (14.66930°N, 99.29060°E, 526 m a.s.l.), collected by Korkhwan Termprayoon, Akrachai Aksornneam, Natee Ampai, and Siriporn Yodthong on 20 April 2019.

Paratypes. Adult males ZMKU R 00958 and ZMKU R 00960 and adult females ZMKU R 00961–64 bear the same collection site as the holotype.

Diagnosis. *Cyrtodactylus fluvicavus* sp. nov. can be separated from all other species of the *brevipalmatus* group by the combination of having 11–13 supralabials, 9 or 10

infralabials, 26–30 paravertebral tubercles, 14–18 rows of longitudinally arranged tubercles, 30–39 transverse rows of ventrals, 154–175 longitudinal rows of ventrals, 9–11 expanded subdigital lamellae on the fourth toe, 10–13 unexpanded subdigital lamellae on the fourth toe, 19–22 total subdigital lamellae on the fourth toe; 7–9 expanded subdigital lamellae on the fourth finger, 9–11 unexpanded subdigital lamellae on the fourth finger, 17–19 total subdigital lamellae on the fourth finger; 9–12 total enlarged femoral scales, 8–11 total femoral pores in males; 14 or 15 precloacal pores in males; 14 or 15 enlarged precloacals; enlarged femorals and enlarged precloacals not continuous; proximal femorals less than one-half the size of the distal femorals; small tubercles on forelimbs and flanks; small dorsolateral caudal tubercles and narrow ventrolateral caudal fringe; ventrolateral caudal fringe composed scales of different size; tail circular in cross-section; slightly enlarged unpaired medial subcaudals not posteromedially furrowed; maximum SVL 78.2 mm; three dark transverse body bands (Tables 4–6).

Description of holotype (Fig. 4). Adult male SVL 72.5 mm; head moderate in length (HL/SVL 0.28), width (HW/HL 0.70), depth (HD/HL 0.42), distinct from neck, triangular in dorsal profile; lores concave slightly anteriorly, weakly inflated posteriorly; prefrontal region concave; canthus rostralis rounded; snout elongate (ES/HL 0.42), rounded in dorsal profile; eye large (ED/HL 0.25); ear opening obliquely elongate, small; eye to ear distance greater than diameter of eye; rostral rectangular, divided by a deep furrow, bordered posteriorly by large left and right supranasals and one small azygous internasal, bordered laterally by first supralabials; external nares bordered anteriorly by rostral, dorsally by large supranasal, posteriorly by two smaller postnasals, bordered ventrally by first supralabial; 12R/12L rectangular supralabials, second through seventh supralabials nearly same size as first, then tapering abruptly below eye; 10R/10L infralabials tapering smoothly to just below and slightly past posterior margin of eye; scales of rostrum and lores flat to domed, larger than granular scales on top of head and occiput; scales of occiput intermixed with distinct, small tubercles; superciliaries subrectangular, largest dorsally; mental triangular, bordered laterally by first infralabials and posteriorly by large left and right trapezoidal postmentals contacting medially for 50% of their length posterior to mental; one row of slightly enlarged, elongate sublabials extending posteriorly to sixth(L) and fifth(R) infralabial; gular and throat scales small, granular, grading posteriorly into slightly larger, flatter, smooth, imbricate, pectoral and ventral scales.

Body relatively short (AG/SVL 0.46) with well-defined ventrolateral folds; dorsal scales small, granular interspersed with larger, conical, semi-regularly arranged, weakly keeled tubercles; tubercles extend from occipital region onto base of tail and slightly beyond as paravertebral rows; smaller tubercles extend anteriorly onto nape and occiput, diminishing in size anteriorly; approximately 17 longitudinal rows of tubercles at midbody; approximately 30 paravertebral tubercles; small tubercles on flanks; 34 longitudinal rows of flat, imbricate, ventral scales much larger than dorsal scales; 155 transverse rows of ventral scales; 15 large, pore-bearing, precloacal scales; no deep precloacal groove or depression; and two rows of post-precloacal scales on midline.

Forelimbs moderate in stature, relatively short (ForL/SVL 0.14); granular scales of forearm slightly larger than those on body, interspersed with large tubercles; palmar scales rounded, slightly raised; digits well-developed, relatively short, inflected at

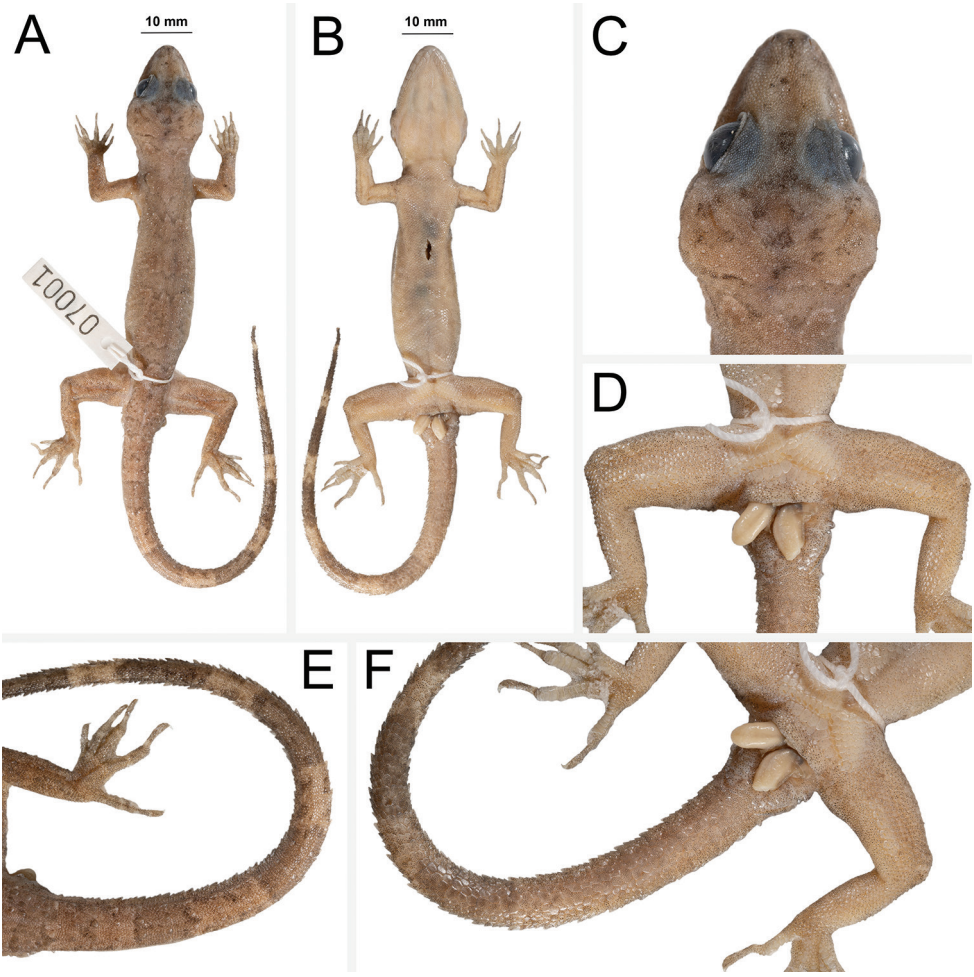

Figure 4. Holotype of *Cyrtodactylus fluvicavus* sp. nov. ZMKU R 00959 (field no. AA 07001) from Thailand, Kanchanaburi Province, Si Sawat District, Khao Chot Subdistrict, Chaloem Rattanakosin National Park **A** dorsal view **B** ventral view **C** dorsal view of head **D** ventral view of femoral and precloacal regions **E** dorsal view of tail **F** ventral view of tail.

basal interphalangeal joints; digits narrower distal to inflections; subdigital lamellae wide, transversely expanded proximal to joint inflections, narrower transverse lamellae distal to joint inflections; claws well-developed, claw base sheathed by a dorsal and ventral scale; 8R/8L expanded and 10R/10L unexpanded lamellae beneath the fourth finger; hind limbs larger and thicker than forelimbs, moderate in length (TibL/SVL 0.16), covered dorsally by granular scales interspersed with moderately sized, conical tubercles dorsally and posteriorly and anteriorly by flat, slightly larger, subimbricate scales; ventral scales of thigh flat, subimbricate, larger than dorsals; subtibial scales flat, imbricate; one row of 5R/6L enlarged pore-bearing femoral scales not continuous with enlarged pore-bearing precloacal scales, terminating distally at knee; proximal femoral

scales smaller than distal femorals, the former forming an abrupt union with much smaller, rounded, ventral scales of posteroventral margin of thigh; plantar scales flat; digits relatively long, well-developed, inflected at basal interphalangeal joints; 9R/9L wide, transversely expanded subdigital lamellae on fourth toe proximal to joint inflection extending onto sole, and 11R/11L unexpanded lamellae beneath the fourth toe; and claws well-developed, claw base sheathed by a dorsal and ventral scale.

Tail original, 97.6 mm long (TL/SVL 1.34), 5.2 mm in width at base, tapering to a point; sub-circular or nearly round in cross-section; dorsal scales flat, square bearing tubercles forming paravertebral rows and small tubercles forming a dorsolateral longitudinal row; slightly larger, posteriorly directed, semi-spinose tubercles forming narrow but distinct ventrolateral caudal fringe; larger scales of ventrolateral fringe occur at regular intervals; medial subcaudals slightly enlarged but not paired, distinctly enlarged single medial subcaudals absent; subcaudals, larger than dorsal caudals; base of tail bearing hemipenial swellings; 3R/2L conical postcloacal tubercles at base of hemipenial swellings; and postcloacal scales flat, imbricate.

Coloration in life (Fig. 5). Ground color of the head, body, limbs, and tail brown; faint, diffuse mottling on the top of the head; thin, dark brown postorbital stripe; ventral portion of lores and suborbital region dark brown; nuchal band faint, bearing two dark-colored posterior projections; paired dark brown paravertebral blotches on nape; three wide faint irregularly shaped body bands edged in dark brown between limb insertions; band interspaces bearing irregularly shaped dark-colored markings; dark-colored speckling on limbs and digits; digits bearing pale-colored bands; eight wide dark-colored caudal bands separated by seven pale-colored bands; first six dark-colored and seven pale-colored caudal bands encircle tail; all ventral surfaces beige, generally immaculate; iris orange-gold in color.

Variation (Fig. 5). Individuals of the type series are very similar in overall coloration and pattern. TL and TW of complete original tails (ZMKU R 00959–00960, ZMKU R 00963–00964) are 79.7–97.6 mm (mean 91.4 ± 8.2 mm; $N = 4$) and 4.0–5.2 mm (mean 4.5 ± 0.5; $N = 4$), respectively. The posterior one-third of the tail of ZMKU R 00958 is regenerated (TL 72.0 mm, TW 4.9 mm); that of ZMKU R 00962 is missing (TL 83.8 mm, TW 4.4 mm); and that of ZMKU R 00961 is broken one-third of the way passed the base and nearly all of the broken section is regenerated (TL 73.6 mm, TW 4.07 mm). Regenerated tail sections lack a color pattern. ZMKU R 00963–64 have seven dark-colored and six pale-colored caudal bands as opposed to eight and seven bands, respectively, in the holotype. ZMKU R 00958, ZMKU R 00960, ZMKU R 00962, ZMKU R 00964 are slight less boldly marked than the holotype. Meristic and morphometric differences are listed in Table 5.

Distribution. *Cyrtodactylus fluvicavus* sp. nov. is currently known from the type locality at Tham Than Lot Noi-Tham Than Lot Yai Nature Trail in Chaloem Rattanakosin National Park, Si Sawat District, Kanchanaburi Province, western Thailand (Fig. 1).

Etymology. The specific epithet *fluvicavus* comes from the Latin *fluvius*, meaning stream, river, or flow and the Latin *cavus*, meaning hollow or hole and refers to a landmark cave in the Chaloem Rattanakosin National Park which has a stream that flows through it.

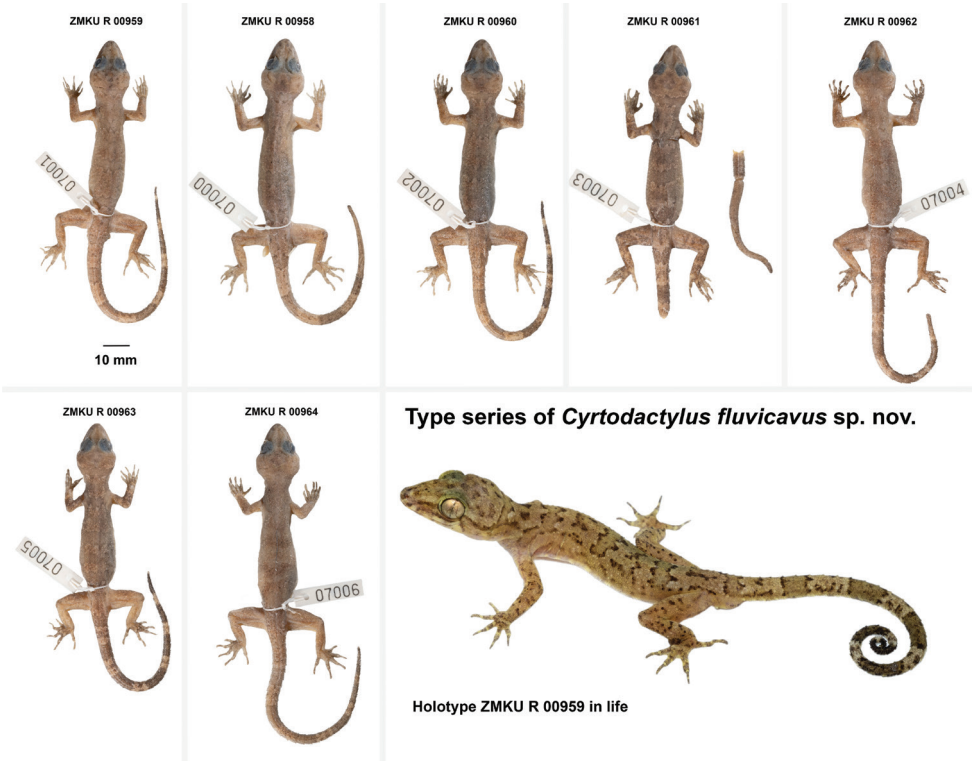

Figure 5. Type series of *Cyrtodactylus fluvicavus* sp. nov. from Thailand, Kanchanaburi Province, Si Sawat District, Khao Chot Subdistrict, Chaloem Rattanakosin National Park.

Comparisons. *Cyrtodactylus fluvicavus* sp. nov. is the sister species to a clade composed of ten lineages in a phylogenetic sequence of *C.* sp.9, *C.* sp.10, *Cyrtodactylus uthaiensis* sp. nov., *C.* sp.11, *C. interdigitalis*, *C.* cf. *ngati*1, *C.* cf. *ngati*2, *C. ngati*3, and the sister lineages *C. ngati*4 and *C. ngati* (Fig. 2). *Cyrtodactylus fluvicavus* sp. nov. differs from those lineages by an uncorrected pairwise sequence divergence of 9.55–12.13% and from all members of the *brevipalmatus* group by 11.61–20.26% (Table 2). It differs categorically from *C. elok* by having as opposed to lacking paravertebral tubercles and femoral pores, and by having 14–18 as opposed to 4–7 longitudinal rows of tubercles. It differs from *C. brevipalmatus*, *C. interdigitalis*, *C. ngati*, *C. ngati*3, *C. rukhadeva*, and *C.* sp.9 in having statistically significant different mean values of the morphometric characters of AG, HumL, ForL, FemL, TibL, HL, HW, HD, EE, ES, EN, EL and IN (Table 6). It differs further from *C. brevipalmatus*, *C. interdigitalis*, *C. ngati*, *C. ngati*3, *C. rukhadeva*, and *C.* sp.9 in having statistically significant different mean values of the meristic characters of SL, PVT, LRT, VS, VSM, TL4E, TL4T, FL4E, FL4U, FL4T, FS, PCS, and BB. Statistically significant and discrete differences between *Cyrtodactylus fluvicavus* sp. nov. and all other species and populations are presented in Tables 4–6.

Natural history. All individuals were found in karst forests bearing mixed deciduous and dry evergreen trees amidst rocky streams and a nearby waterfall (Fig. 6). This area is surrounded by agricultural fields and residential areas. Specimens (N = 7) were collected at night (1900–2100 h) during the dry season (April) on the tree trunks or palm tree leaves (57.1%; N = 4), twigs of shrubs (14.3%; N = 1), karst walls (14.3%; N = 1), and a wooden bridge (14.3%; N = 1) at 526 m elevation with a temperature of 31.9 °C and relative humidity of 56.9%. The holotype (ZMKU R 00959) and two specimens (ZMKU R 00960, ZMKU R 00962) were found on tree trunks ≤ 100 cm above ground level. One specimen (ZMKU R 00964) was found on a palm tree branch approximately 50 cm above the ground. Another specimen (ZMKU R 00963) was found on the twig of a shrub. Another specimen (ZMKU R 00961) was found on a karst wall approximately 3 m above the ground, and another (ZMKU R 00958) on a wooden bridge over a stream. Given these observations, this species appears to be an arboreal habitat generalist. The new species was found to co-occur with two other species of gekkonid lizards, *Cyrtodactylus monilatus* Yodthong, Rujirawan, Stuart, Grismer, Aksornneam, Termprayoon, Ampai & Aowphol, 2022 and *Dixonius siamensis* (Boulenger, 1899).

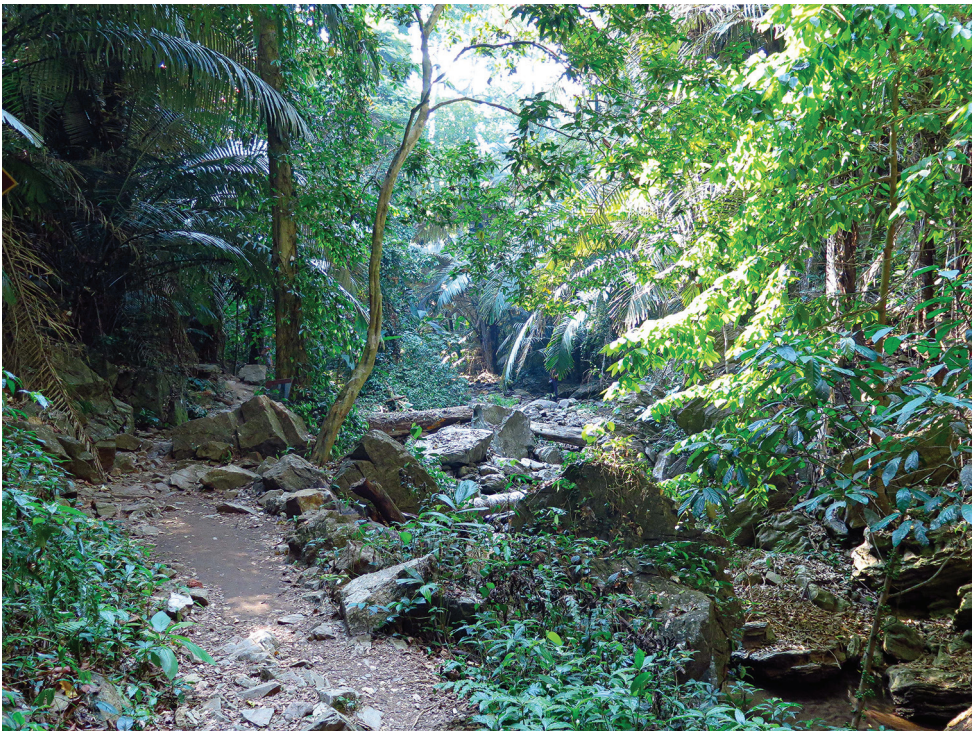

Figure 6. Habitat of *Cyrtodactylus fluvicavus* sp. nov. at Thailand, Kanchanaburi Province, Si Sawat District, Khao Chot Subdistrict, Chaloem Rattanakosin National Park.

Table 4. Summary statistics of the normalized morphometric data for the putative species of the *Cyrtodactylus brevipalmatus* group. SD = ± standard deviation. Character abbreviations are listed in the Materials and methods.

Species	SVL	AG	HumL	ForL	FemL	TibL	HL	HW	HD	ED	EE	ES	EN	IO	EL	IN
C. brevipalmatus (*N* = 5)																
Mean	1.82	1.49	0.96	0.96	1.06	1.02	1.27	1.10	0.87	0.67	0.75	0.86	0.73	0.68	0.07	0.32
SD	0.020	0.027	0.031	0.023	0.024	0.036	0.012	0.006	0.017	0.041	0.025	0.008	0.019	0.043	0.058	0.041
Lower	1.80	1.46	0.92	0.92	1.02	0.97	1.25	1.10	0.86	0.63	0.71	0.85	0.70	0.62	-0.02	0.25
Upper	1.85	1.52	0.99	0.98	1.09	1.07	1.29	1.11	0.89	0.73	0.77	0.87	0.75	0.73	0.13	0.36
C. elok (*N* = 4)																
Mean	1.91	1.59	0.80	1.05	1.14	1.13	1.34	1.20	1.00	0.71	0.83	0.95	0.79	0.70	0.19	0.43
SD	0.016	0.012	0.341	0.026	0.022	0.024	0.001	0.012	0.008	0.017	0.020	0.008	0.010	0.070	0.062	0.033
Lower	1.89	1.57	0.34	1.02	1.11	1.10	1.34	1.18	0.98	0.68	0.81	0.94	0.78	0.61	0.15	0.40
Upper	1.93	1.60	1.09	1.08	1.16	1.15	1.34	1.21	1.00	0.72	0.85	0.95	0.80	0.76	0.28	0.48
***Cyrtodactylus fluvicavus* sp. nov.** (*N* = 7)																
Mean	1.86	1.52	0.95	1.01	1.11	1.03	1.31	1.14	0.91	0.69	0.78	0.92	0.79	0.73	0.20	0.38
SD	0.027	0.009	0.013	0.017	0.018	0.012	0.007	0.011	0.011	0.007	0.016	0.008	0.011	0.006	0.04	0.02
Lower	1.82	1.51	0.94	0.98	1.10	1.01	1.30	1.13	0.90	0.68	0.76	0.91	0.78	0.72	0.14	0.35
Upper	1.89	1.54	0.98	1.04	1.15	1.05	1.32	1.16	0.93	0.70	0.81	0.94	0.81	0.74	0.24	0.40
C. interdigitalis (*N* = 4)																
Mean	1.86	1.50	0.98	1.01	1.10	1.08	1.30	1.12	0.80	0.72	0.76	0.90	0.77	0.68	0.13	0.33
SD	0.060	0.016	0.032	0.015	0.020	0.007	0.012	0.006	0.187	0.026	0.026	0.024	0.034	0.0307	0.033	0.035
Lower	1.78	1.48	0.94	0.99	1.07	1.07	1.28	1.12	0.56	0.69	0.73	0.88	0.74	0.66	0.10	0.29
Upper	1.91	1.52	1.01	1.02	1.12	1.09	1.31	1.13	0.96	0.75	0.79	0.94	0.81	0.73	0.17	0.38
***Cyrtodactylus kochangensis* sp. nov.** (*N* = 1)																
Value	1.78	1.51	1.00	0.95	1.05	1.02	1.30	1.14	0.91	0.69	0.76	0.91	0.78	0.68	0.05	0.36
C. cf. *kochangensis* sp. nov. (*N* = 1)																
Value	1.85	1.50	1.02	0.94	1.08	1.08	1.27	1.09	0.90	0.72	0.70	0.88	0.75	0.60	0.12	0.36
C. ngati (*N* = 3)																
Mean	1.83	1.47	0.91	0.99	1.06	1.05	1.31	1.08	0.85	0.57	0.76	0.86	0.81	0.74	-0.12	0.43
SD	0.009	0.002	0.004	0.007	0.000	0.006	0.001	0.003	0.010	0.035	0.016	0.015	0.004	0.009	0.019	0.008
Lower	1.82	1.47	0.91	0.98	1.06	1.04	1.31	1.08	0.84	0.55	0.74	0.85	0.80	0.73	-0.13	0.42
Upper	1.84	1.47	0.91	1.00	1.06	1.05	1.31	1.09	0.86	0.61	0.77	0.88	0.81	0.75	-0.09	0.43
***C. ngati*3** (*N* = 3)																
Mean	1.88	1.58	0.94	1.00	1.12	1.07	1.32	1.12	0.95	0.69	0.81	0.93	0.80	0.77	0.08	0.41
SD	0.039	0.001	0.002	0.02	0.001	0.017	0.007	0.002	0.014	0.003	0.004	0.007	0.006	0.022	0.016	0.01
Lower	1.85	1.58	0.93	0.98	1.12	1.05	1.31	1.12	0.94	0.69	0.80	0.92	0.79	0.74	0.07	0.40
Upper	1.92	1.58	0.94	1.02	1.12	1.09	1.33	1.12	0.96	0.69	0.81	0.94	0.80	0.78	0.10	0.42
***C. ngati*4** (*N* = 1)																
Value	1.87	1.50	0.87	1.02	1.13	1.07	1.33	1.11	0.91	0.72	0.79	0.94	0.83	0.75	0.51	0.43
***C.* cf. *ngati*1** (*N* = 1)																
Value	1.89	1.59	0.96	1.03	1.13	1.12	1.34	1.12	0.95	0.85	0.76	0.96	0.82	0.73	0.28	0.49
***C.* cf. *ngati*2** (*N* = 2)																
Mean	1.92	1.59	1.01	1.02	1.17	1.1	1.34	1.15	0.95	0.72	0.80	0.94	0.80	0.65	0.03	0.37
SD	0.035	0.000	0.000	0.000	0.000	0.000	0.000	0.000	0.000	0.000	0.000	0.000	0.000	0.000	0.000	0.000
Lower	1.89	1.59	1.01	1.02	1.17	1.10	1.34	1.15	0.95	0.72	0.80	0.94	0.80	0.65	0.03	0.37
Upper	1.94	1.59	1.01	1.02	1.17	1.10	1.34	1.15	0.95	0.72	0.80	0.94	0.80	0.65	0.03	0.37
***Cyrtodactylus rivularis* sp. nov.** (*N* = 2)																
Mean	1.85	1.53	0.89	0.98	1.04	1.03	1.30	1.16	0.91	0.76	0.80	0.91	0.77	0.75	0.05	0.34
SD	0.025	0.01	0.002	0.007	0.007	0.005	0.005	0.001	0.013	0.007	0.024	0.005	0.004	0.025	0.019	0.016
Lower	1.83	1.53	0.89	0.97	1.03	1.03	1.29	1.16	0.91	0.75	0.79	0.91	0.77	0.74	0.04	0.33
Upper	1.87	1.54	0.90	0.98	1.04	1.04	1.30	1.16	0.92	0.76	0.82	0.91	0.78	0.77	0.06	0.35
C. rukhadeva and C.* cf. *rukhadeva (*N* = 10)																
Mean	1.85	1.49	1.01	0.95	1.05	1.02	1.30	1.14	0.92	0.71	0.75	0.91	0.77	0.67	0.09	0.35
SD	0.026	0.028	0.055	0.029	0.027	0.023	0.009	0.018	0.025	0.036	0.034	0.014	0.015	0.087	0.069	0.022

Species	SVL	AG	HumL	ForL	FemL	TibL	HL	HW	HD	ED	EE	ES	EN	IO	EL	IN
Lower	1.79	1.45	0.91	0.90	0.99	0.97	1.29	1.10	0.87	0.62	0.70	0.89	0.74	0.46	0.00	0.32
Upper	1.88	1.54	1.08	1.00	1.09	1.05	1.32	1.16	0.95	0.75	0.80	0.92	0.79	0.73	0.23	0.38
***Cyrtodactylus uthaiensis* sp. nov.** (*N* = 1)																
Value	1.76	1.80	0.95	0.99	1.09	1.02	1.28	1.10	0.76	0.72	0.74	0.88	0.75	0.68	0.19	0.32
***C.* sp.9 (Thong Pha Phum)** (*N* = 8)																
Mean	1.86	1.53	0.91	0.97	1.08	1.02	1.30	1.16	0.89	0.71	0.77	0.90	0.77	0.74	0.09	0.34
SD	0.024	0.016	0.034	0.021	0.032	0.019	0.014	0.017	0.008	0.015	0.004	0.012	0.007	0.012	0.061	0.023
Lower	1.81	1.50	0.86	0.93	1.02	0.99	1.27	1.14	0.88	0.69	0.76	0.89	0.76	0.72	0.00	0.30
Upper	1.88	1.55	0.95	1.00	1.12	1.05	1.32	1.19	0.90	0.74	0.78	0.93	0.78	0.76	0.18	0.38
***C.* sp.11** (*N* = 1)																
Value	1.83	1.53	1.01	0.99	1.13	1.09	1.30	1.14	0.75	0.70	0.78	0.92	0.78	0.61	0.08	0.35
***C.* sp.13** (*N* = 2)																
Mean	1.83	1.45	0.94	0.94	1.07	1.01	1.27	1.11	0.91	0.67	0.75	0.88	0.76	0.74	0.15	0.34
SD	0.040	0.000	0.000	0.000	0.000	0.000	0.000	0.000	0.000	0.000	0.000	0.000	0.000	0.000	0.000	0.000
Lower	1.80	1.45	0.94	0.94	1.07	1.01	1.27	1.11	0.91	0.67	0.75	0.88	0.76	0.74	0.15	0.34
Upper	1.86	1.45	0.94	0.94	1.07	1.01	1.27	1.11	0.91	0.67	0.75	0.88	0.76	0.74	0.15	0.34

Cyrtodactylus rivularis sp. nov.

https://zoobank.org/B3381A9D-0049-4C5B-BEB1-DB4D60509F0E

Figs 7, 8

Suggested Common Name: Pa La-U Bent-toed Gecko

Holotype. Adult female ZMKU R 00947 from Pa La-U Waterfall, Kaeng Krachan National Park, Huai Sat Yai Subdistrict, Hua Hin District, Prachuap Khiri Khan Province, Thailand (12.53685°N, 99.45972°E, 368 m a.s.l.), collected by Attapol Rujirawan, Siriporn Yodthong, Korkhwan Termprayoon, Natee Ampai, and Piyawan Puanprapai on 15 September 2017.

Paratype. Adult female ZMKU R 00946 bearing the same data as the holotype.

Diagnosis. *Cyrtodactylus rivularis* sp. nov. can be separated from all other species of the *brevipalmatus* group by the combination of having 12 or 13 supralabials, 9–11 infralabials, 33 or 34 paravertebral tubercles, 18–20 rows of longitudinally arranged tubercles, 34–37 transverse rows of ventrals, 160–166 longitudinal rows of ventrals, nine expanded subdigital lamellae on the fourth toe, 12 or 13 unexpanded subdigital lamellae on the fourth toe, 21 or 22 total subdigital lamellae on the fourth toe; eight expanded subdigital lamellae on the fourth finger, 10–12 unexpanded subdigital lamellae on the fourth finger, 18–20 total subdigital lamellae on the fourth finger; 14–16 total enlarged femoral scales; 15 enlarged precloacals; enlarged femorals and enlarged precloacals not continuous, and lacking pores; proximal femorals less than one-half the size of the distal femorals; small tubercles on forelimbs and flanks; large dorsolateral caudal tubercles and wide ventrolateral caudal fringe; ventrolateral caudal fringe composed generally homogeneous scales; tail square in cross-section; single enlarged unpaired medial subcaudals not posteromedially furrowed; maximum SVL 73.9 mm; three or four dark transverse body bands (Tables 4, 5).

Description of holotype (Fig. 7). Adult female SVL 73.9 mm; head moderate in length (HL/SVL 0.27), width (HW/HL 0.73), depth (HD/HL 0.40), distinct from neck, triangular in dorsal profile; lores concave slightly anteriorly, weakly inflated pos-

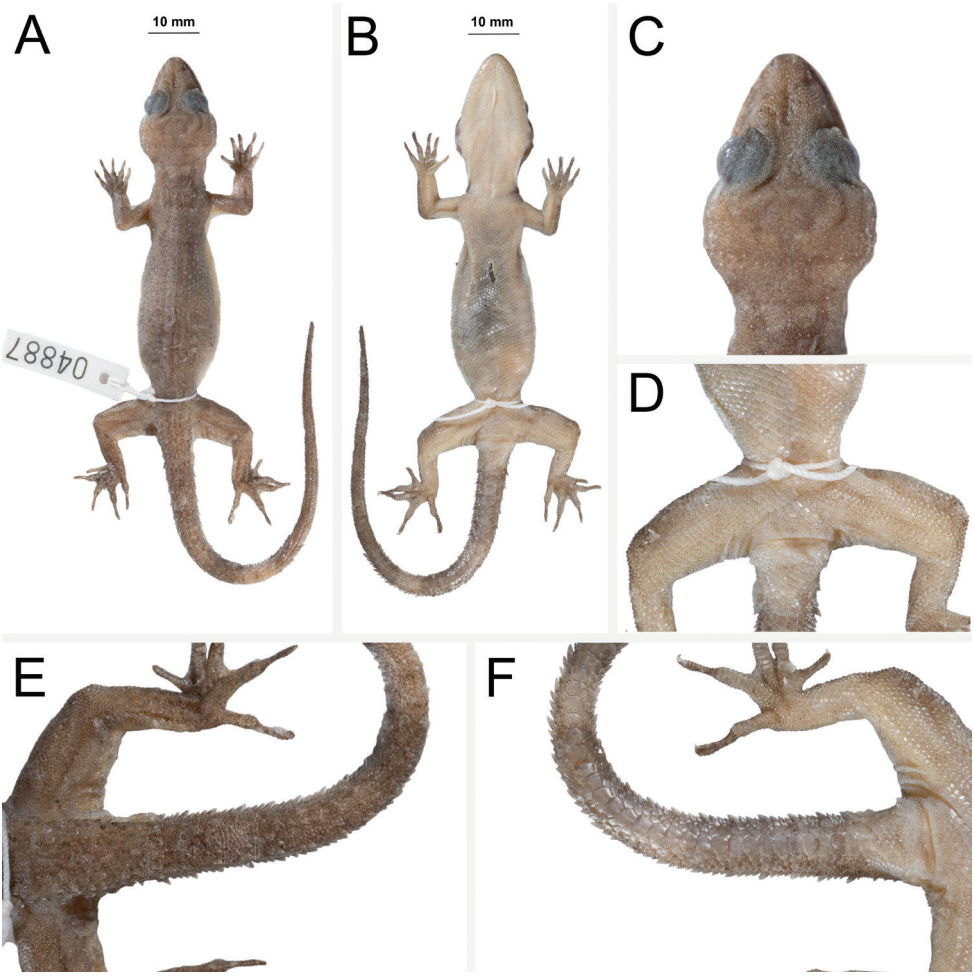

Figure 7. Holotype of *Cyrtodactylus rivularis* sp. nov. ZMKU R 00947 (field no. AA 04887) from Thailand, Prachuap Khiri Khan Province, Hua Hin District, Huai Sat Yai Subdistrict, Kaeng Krachan National Park, Pa La-U Waterfall **A** dorsal view **B** ventral view **C** dorsal view of head **D** ventral view of femoral and precloacal regions **E** dorsal view of tail **F** ventral view of tail.

teriorly; prefrontal region concave; canthus rostralis rounded; snout elongate (ES/HL 0.41), rounded in dorsal profile; eye large (ED/HL 0.29); ear opening horizontally elongate, small; eye to ear distance greater than diameter of eye; rostral rectangular, divided dorsally by a deep furrow, bordered posteriorly by large left and right supranasals and one slightly smaller azygous internasal, bordered laterally by first supralabials; external nares bordered anteriorly by rostral, dorsally by large supranasal, posteriorly by two smaller postnasals, bordered ventrally by first supralabial; 13R/12L rectangular supralabials, first two largest, then tapering abruptly below eye; 11R/10L infralabials tapering smoothly to just below eye and then more rapidly beyond posterior margin

of eye; scales of rostrum and lores flat to domed, larger than granular scales on top of head and occiput; scales of occiput intermixed with distinct, small tubercles; superciliaries subrectangular, largest anteriorly; mental triangular, bordered laterally by first infralabials, posteriorly by large left and right elongate postmentals contacting medially for approximately 40% of their length posterior to mental; one row of two (R) and four (L) slightly enlarged sublabials extending posteriorly to third(L) and second(R) infralabial, subsequent sublabials much smaller; gular and throat scales small, granular, grading posteriorly into slightly larger, flatter, smooth, imbricate, pectoral and ventral scales.

Body relatively short (AG/SVL 0.47) with well-defined ventrolateral folds; dorsal scales small, granular, interspersed with larger conical, semi-regularly arranged, weakly keeled tubercles; tubercles extend from occipital region onto base of tail and slightly beyond as paravertebral rows; tubercles of nape and occiput small; approximately 20 longitudinal rows of tubercles at midbody; approximately 34 paravertebral tubercles; tubercles on flanks nearly same size as those on dorsum; 34 longitudinal rows of flat, imbricate, ventral scales much larger than dorsal scales; 160 transverse rows of ventral scales; no pore-bearing, precloacal scales; 15 enlarged precloacal scales; no deep precloacal groove or depression; and three rows of post-precloacal scales on midline.

Forelimbs moderate in stature, relatively short (ForL/SVL 0.13); granular scales of forearm slightly larger than those on body, interspersed with tubercles; palmar scales rounded, slightly raised; digits well-developed, relatively short, inflected at basal interphalangeal joints; digits narrower distal to inflections; subdigital lamellae wide, transversely expanded proximal to joint inflections, narrower transverse lamellae distal to joint inflections; claws well-developed, claw base sheathed by a dorsal and ventral scale; 8R/8L expanded and 11R/11L unexpanded lamellae beneath the fourth finger; hind limbs larger and thicker than forelimbs, moderate in length (TibL/SVL 0.15), covered dorsally by granular scales interspersed with moderately sized, conical tubercles dorsally and posteriorly and anteriorly by flat, slightly larger, subimbricate scales; ventral scales of thigh flat, subimbricate, larger than dorsals; subtibial scales flat, imbricate; no pore-bearing femoral scales; 8R/8L enlarged femoral scales; enlarged femoral scales not contiguous with enlarged precloacal scales, terminating distally at knee; proximal femoral scales smaller than distal femoral scales, the former forming an abrupt union with much smaller, rounded, ventral scales of posteroventral margin of thigh; plantar scales flat; digits relatively long, well-developed, inflected at basal interphalangeal joints; 9R/9L wide, transversely expanded subdigital lamellae on fourth toe proximal to joint inflection that extend onto sole, and 13R/13L unexpanded lamellae beneath the fourth toe; and claws well-developed, sheathed by a dorsal and ventral scale at base.

Posterior one-half of tail regenerated, tail long 91.5 mm (TL/SVL 1.24), 4.8 mm in width at base, tapering to a point; nearly square in cross-section; dorsal scales flat, square bearing large tubercles forming a discontinuous dorsolateral longitudinal row; slightly larger, posteriorly directed, semi-spinose tubercles forming large distinct

ventrolateral caudal fringe; scales of ventrolateral fringe generally homogeneous; single medial subcaudals enlarged but not paired; subcaudal scales, larger than dorsal caudal scales; base of tail bearing hemipenial swellings; 2R/2L conical postcloacal tubercles at base of hemipenial swellings; and postcloacal scales flat, imbricate.

Coloration in life (Fig. 8). Ground color of the head, body, limbs, and tail pale brown; faint, diffuse mottling on rostrum; lores darkly colored; wide, distinct, pale-colored post-orbital stripe; nuchal band faint, bearing two posterior projections; three very faint, wide irregularly shaped body bands edged in slightly darker brown between limb insertions; band interspaces bearing irregularly shaped, faint, dark-colored markings; dark-colored speckling on limbs and digits; digits bearing pale-colored bands; four wide faint dark-colored caudal bands separated by three pale-colored bands on original portion of tail; all caudal bands encircle tail; all ventral surfaces beige, generally immaculate; iris orangish to coppery in color.

Variation (Fig. 8). The paratype (ZMKU R 00946) closely approximates the holotype in overall coloration and pattern except that it is more boldly marked. It has four dark-colored body bands as opposed to three and a complete original tail (TL

Figure 8. Type series of *Cyrtodactylus rivularis* sp. nov. from Thailand, Prachuap Khiri Khan Province, Hua Hin District, Huai Sat Yai Subdistrict, Kaeng Krachan National Park, Pa La-U Waterfall **A** holotype ZMKU R 00947 **B** paratype ZMKU R 00946.

89.0mm, TW 4.1 mm) bearing eight dark-colored and seven pale-colored bands. The pale-colored postorbital stripe is slightly thinner and less distinct. Meristic and morphometric differences are listed in Table 5.

Distribution. *Cyrtodactylus rivularis* sp. nov. is currently known from the type locality at Pa La-U Waterfall, Kaeng Krachan National Park, Huai Sat Yai Subdistrict, Hua Hin District Prachuap Khiri Khan Province, Thailand.

Etymology. The specific epithet *rivularis* is derived from the Latin *rivus*, meaning stream, brook, or creek refers to rocky brook or stream habitat of the new species.

Comparisons. *Cyrtodactylus rivularis* sp. nov. is the sister species to *C. rukhadeva* (Fig. 2) from which it differs by an uncorrected pairwise sequence divergence of 3.61% (Table 2). It differs from *C. rukhadeva* and *C.* cf. *rukhadeva* by having large versus small dorsolateral caudal tubercles and a wide versus narrow ventrolateral fringe. Although no statistical mean differences were recovered between *Cyrtodactylus rivularis* sp. nov. and *C. rukhadeva* which we attribute to the small sample sizes of both species (N = 2), they do respectively differ discretely (at this point) in their ranges of SL (12 or 13 vs. 9–11), PVT (33–34 vs. 27–30), VSM (160–166 vs. 152–154), and TL4T (21–22 vs. 18–20) and the morphometric characters of HumL, ForL, FemL, TibL, HD, ED, and IO (Table 5). Discrete differences among *Cyrtodactylus rivularis* sp. nov. and all other species and populations are presented in Tables 4, 5.

Natural history. The holotype and paratype were collected at night (1900–2055 h) on granite boulders by a rocky stream dry evergreen forest at 368 m in elevation (Fig. 9) with a temperature of 25.3 °C and relative humidity of 86.9%. The new species was found to co-occur with two other species of gekkonid lizards, *Cyrtodactylus oldhami* (Theobald, 1876) and *Gehyra mutilata* (Wiegmann, 1834).

Comments. *Cyrtodactylus rivularis* sp. nov. and *C.* cf. *rukhadeva* occur on separate branches of the phylogeny, thus neither is embedded within one another's branch indicating there is no evidence of gene flow between them. Both species are reported to occur within the boundaries of Kaeng Krachan National Park (Grismer et al. 2022). Kaeng Krachan National Park is the largest national park in Thailand, encompassing 2,914.7 km^2 across five districts through the provinces of Phetchaburi and Prachuap Khiri Khan and extending approximately 300 km in latitude. As such, it harbors a wide range of habitats from lowland forests near sea level to cloud forests at its highest peak of 1,513 m in elevation. The seven specimens of *C.* cf. *rukhadeva* (THNHM 01807, 24622, 24838, 03251–54) were obtained by various collectors between 11 March 1991 and 25 October 2015 with no specific collection data other than Phetchaburi Province. The locality reported by Grismer et al. (2021c) was an estimate obtained from Ulber (1993) from the central portion of the park in Phetchaburi Province who referred to a specimen he examined (THNHM 24838) as *C. brevipalmatus*. *Cyrtodactylus rivularis* sp. nov. however, is known only from the Park's southernmost limit in Prachuap Khiri Khan Province. Additional collecting and DNA sequencing will be required to establish the approximate distribution limits of each population.

Table 5. Sex and raw meristic, categorical, and morphometric data used in the analyses from specimens in the *Cyrtodactylus brevipalmatus* group. m = male; f = female; R/L = right/left; / = data unavailable.

Species	***C. brevipalmatus***	***C.* cf. *brevipalmatus***	***C.* cf. *brevipalmatus***	***C. brevipalmatus***	***C. brevipalmatus***	***C. elok***	***C. elok***	***C. elok***	***C. elok***	***C. interdigitalis***	***C. interdigitalis***	***C. interdigitalis***	***C. interdigitalis***	***C.* sp. 11**
Institutional catalog number	**LSUHC 1899**	**LSUHC 15076**	**LSUHC 11788**	**THNHM 10670**	**THNHM 14112**	**LSUHC 8238**	**LSUHC 12180**	**LSUHC 12181**	**ZMMU R-16144**	**THNHM 20226 paratype**	**THNHM 20228 paratype**	**THNHM 20229 paratype**	**THNHM 20227 paratype**	**ZMMU R-16492**
Sex	m	f	f	f	f	f	m	m	f	f	f	f	f	m
Meristic data														
Supralabials (SL)	11	12	10	14	12	11	8	13	9	14	12	11	12	11
Infralabials (IL)	8	10	9	11	11	11	8	11	9	9	8	8	7	9
Paravertebral tubercles (PVT)	39	37	38	37	37	0	0	0	0	32	33	33	33	30
Longitudinal rows of tubercles (LRT)	15	16	17	16	14	6	7	4	4	19	20	19	19	18
Ventral scales (VS)	38	38	38	36	39	45	45	47	36	42	40	42	43	34
Ventral scales along middle of the body (VSM)	176	170	182	154	160	190	225	234	192	187	170	187	178	160
Expanded subdigital lamellae on 4th toe (TL4E)	7	8	9	8	8	10	9	9	9	12	10	10	11	9
Unmodified subdigital lamellae on 4th toe (TL4U)	13	11	11	11	12	11	10	11	9	14	13	12	14	10
Total subdigital lamellae 4th toe (TL4T)	20	19	20	19	20	21	19	20	18	26	23	22	23	19
Expanded subdigital lamellae on 4th finger (FL4E)	8	8	8	7	8	8	9	9	9	9	8	9	9	10
Unmodified subdigital lamellae on 4th finger (FL4U)	9	11	10	10	10	12	13	9	8	12	11	12	13	9
Total subdigital lamellae 4th finger (FL4T)	17	19	18	17	18	20	22	18	17	21	21	21	22	19
Enlarged femoral scales (R/L)	0	0	0	8R/8L	7R/7L	0	0	0	0	11R/8L	10R/9L	8R/8L	9R/10L	9R/8L
Total enlarged femoral scales (FS)	16	10	11	16	14	0	0	0	0	14	19	19	19	17
Total femoral pores in males (FP)	7	0	0	0	0	0	0	0	0	0	0	0	0	17
Enlarged precloacal scales (PCS)	7	7	7	8	7	8	8	8	7	14	15	13	19	13
Precloacal pores in males (PP)	7	0	0	0	0	0	8	8	0	0	0	0	0	13
Postcloacal tubercles (PCT)	3	3	2	3	3	3	2	3	3	3	2	3	3	3
Body bands (BB)	4	6	3	5	5	5	5	3	3	5	5	5	5	3
Categorical data														

Species	*C. brevipalmatus*	*C.* cf. *brevipalmatus*	*C.* cf. *brevipalmatus*	*C. brevipalmatus*	*C. brevipalmatus*	*C. elok*	*C. elok*	*C. elok*	*C. elok*	*C. interdigitalis*	*C. interdigitalis*	*C. interdigitalis*	*C. interdigitalis*	*C.* sp.11
Institutional catalog number	**LSUHC 1899**	**LSUHC 15076**	**LSUHC 11788**	**THNHM 10670**	**THNHM 14112**	**LSUHC 8238**	**LSUHC 12180**	**LSUHC 12181**	**ZMMU R-16144**	**THNHM 20226 paratype**	**THNHM 20228 paratype**	**THNHM 20229 paratype**	**THNHM 20227 paratype**	**ZMMU R-16492**
Small tubercles on flank (FKT)	present	present	present	present	present	absent	absent	absent	absent	present	present	present	present	present
Dorsolateral caudal tubercles (DCT)	small	small	small	/	small	large	large	large	large	small	/	small	small	large
Ventrolateral caudal fringe narrow or wide (VLF1)	narrow	narrow	narrow	/	narrow	wide	wide	wide	wide	narrow	/	narrow	narrow	wide
Ventrolateral caudal fringe scales generally homogenous (VLF2)	no	no	no	/	no	no	no	no	no	yes	yes	yes	yes	yes
Tail cross-section (TLcross)	circular	circular	circular	/	circular	square	square	square	square	circular	/	circular	circular	square
Slightly enlarged medial subcaudals (SC1)	present	present	present	/	absent	absent	absent	absent	absent	absent	/	absent	absent	present
Single enlarged medial subcaudal (SC2)	absent	absent	absent	/	absent	absent	absent	absent	absent	absent	/	absent	absent	absent
Enlarged medial subcaudals intermittent, medially furrowed, posteriorly emarginate (SC3)	no	no	no	/	no	no	no	no	no	yes	/	yes	yes	no
Morphometric data														
SVL	68.8	70.8	64.1	65.95	63.79	80.2	78.2	84.8	78.6	81.19	74.80	78.56	59.70	68.1
AG	35.7	33.4	30.1	30.0	26.5	39.7	37.8	41.5	36.2	34.5	33.7	32.7	24.6	34.6
HumL	9.7	9.3	8.0	9.6	9.5	10.2	9.1	10.1	1.7	9.8	10.2	11.2	7.4	10.3
ForL	9.9	9.8	8.9	8.2	8.7	11.5	11.7	11.8	10.2	10.6	10.5	11.1	8.4	8.5
FemL	12.0	12.6	11.5	11.7	9.8	12.9	14.2	14.6	13.1	14.7	13.2	12.7	10.2	12.6
TibL	11.6	12.2	10.5	9.7	8.2	13.5	14.0	13.8	12.3	13.1	11.9	12.9	10.2	11.4
HL	19.3	19.3	19.0	17.9	18.2	21.8	21.6	21.9	21.7	20.8	19.9	21.7	16.7	18.4
HW	13.2	13.8	12.3	12.3	12.0	15.6	16.1	15.9	15.1	14.0	13.4	14.2	11.4	13.1
HD	8.0	7.6	7.6	7.3	7.0	9.6	9.8	10.4	9.8	3.4	8.6	8.7	6.6	8.3
ED	5.2	4.5	4.3	5.3	4.4	4.8	5.0	5.7	5.0	5.3	5.5	5.9	4.4	4.4
EE	5.7	5.9	4.9	5.7	5.7	6.4	7.1	7.0	6.8	5.8	6.2	6.4	4.8	6.2
ES	7.4	7.6	7.0	7.0	7.2	8.6	8.7	9.5	8.6	8.3	7.8	9.1	6.8	7.7
EN	5.7	5.4	4.9	5.3	5.4	6.0	6.2	6.5	6.2	6.0	5.5	6.8	5.1	5.5
IO	5.4	4.7	4.7	4.2	5.2	5.7	5.4	5.4	3.9	4.8	4.7	5.5	4.3	2.9
EL	1.0	1.4	1.1	1.3	1.0	1.9	1.4	1.5	1.4	1.3	1.3	1.6	1.2	0.9
IN	1.7	2.1	2.3	2.1	2.2	2.7	2.6	2.5	3.1	2.1	2.2	2.5	1.8	2.3

Table 5. Continued.

Species	*C. ngati*	*C. ngati*	*C. ngati*	*C. ngati*	*C. ngati3*	*C. ngati3*	*C. ngati3*	*C. ngati4*	*C.* cf. *ngati1*	*C.* cf. *ngati2*	*C.* cf. *ngati2*
Institutional catalog number	**HNUE-R00111 holotype**	**IEBR 4829 paratype**	**VNUF R.2020.12 paratype**	**HNUE-R00112 paratype**	**FMNH 255454**	**FMNH 270493**	**FMNH 270492**	**FMNH 265806**	**NCSM 79472**	**ZMMU R-14917**	**NCSM 80100**
Sex	m	f	f	f	f	m	m	m	f	f	f
Meristic data											
Supralabials (SL)	10	10	10	10	13	13	13	10	14	9	12
Infralabials (IL)	9	9	9	9	10	9	11	8	11	10	12
Paravertebral tubercles (PVT)	39	40	38	40	28	27	26	27	28	32	29
Longitudinal rows of tubercles (LRT)	18	18	17	22	19	18	17	19	18	24	19
Ventral scales (VS)	38	36	35	32	37	36	36	33	33	36	35
Ventral scales along middle of the body (VSM)	168	164	178	158	159	166	156	158	164	166	165
Expanded subdigital lamellae on 4th toe (TL4E)	8	10	9	9	10	10	8	10	9	8	10
Unmodified subdigital lamellae on 4th toe (TL4U)	11	10	11	10	11	11	11	11	12	10	10
Total subdigital lamellae 4th toe (TL4T)	13	16	17	16	21	21	19	21	21	18	20
Expanded subdigital lamellae on 4th finger (FL4E)	6	6	7	6	8	8	8	8	9	7	9
Unmodified subdigital lamellae on 4th finger (FL4U)	9	9	9	9	10	10	10	10	8	9	10
Total subdigital lamellae 4th finger (FL4T)	15	15	18	15	18	18	18	18	17	16	19
Enlarged femoral scales (R/L)	10R/10L	9R/8L	10R/9L	8R/9L	9R/7L	8R/9L	9R/9L	8R/8L	9R/8L	7R/8L	7R/8L
Total enlarged femoral scales (FS)	20	17	19	17	16	17	18	16	17	15	15
Total femoral pores (FP)	14	0	0	0	0	14	15	13	0	0	0
Enlarged precloacal scales (PCS)	13	13	13	13	15	13	13	13	12	13	13
Precloacal pores (PP)	0	0	0	0	13	13	13	13	0	0	0
Postcloacal tubercles (PCT)	3	2	1	2	0	0	0	0	2	3	4
Body bands (BB)	6	6	6	6	3	4	3	3	3	3	3
Categorical data											
Small tubercles on flank (FKT)	present	present	present	present	present	present	present	present	present	present	present
Dorsolateral caudal tubercles (DCT)	small	small	small	small	small	small	small	small	small	small	small
Ventrolateral caudal fringe narrow or wide (VLF1)	narrow	narrow	narrow	narrow	narrow	narrow	narrow	narrow	narrow	narrow	narrow
Ventrolateral caudal fringe scales generally homogenous (VLF2)	no	no	no	no	yes	yes	yes	yes	yes	yes	yes
Tail cross-section (TLcross)	circular	circular	circular	circular	circular	circular	circular	circular	circular	circular	circular
Slightly enlarged medial subcaudals (SC1)	present	present	present	present	/	present	present	present	present	present	present
Single enlarged medial subcaudal (SC2)	absent	absent	absent	absent	/	absent	absent	absent	absent	absent	absent
Enlarged medial subcaudals intermittent, medially furrowed, posteriorly emarginate (SC3)	no	no	no	no	/	no	no	no	no	no	no
Morphometric data											

Species	*C. ngati*	*C. ngati*	*C. ngati*	*C. ngati*	*C. ngati3*	*C. ngati3*	*C. ngati3*	*C. ngati4*	*C.* cf. *ngati1*	*C.* cf. *ngati2*	*C.* cf. *ngati2*
Institutional catalog number	**HNUE-R00111 holotype**	**IEBR 4829 paratype**	**VNUF R.2020.12 paratype**	**HNUE-R00112 paratype**	**FMNH 255454**	**FMNH 270493**	**FMNH 270492**	**FMNH 265806**	**NCSM 79472**	**ZMMU R-14917**	**NCSM 80100**
SVL	66.5	68.1	69.3	46.6	83.6	70.2	74.1	73.8	78.0	87.1	77.7
AG	28.8	29.8	30.2	19.7	41.3	35.4	37.0	31.3	38.2	41.9	36.8
HumL	7.9	8.1	8.5	5.6	8.6	8.7	8.6	6.9	8.7	11.5	9.2
ForL	9.2	10.0	10.1	6.5	10.2	9.3	10.4	10.0	10.3	10.4	10.7
FemL	11.5	11.5	11.5	7.6	13.7	12.7	13.0	13.1	13.1	15.2	14.2
TibL	10.8	11.1	11.8	7.8	12.5	11.8	11.2	11.1	12.8	12.6	12.7
HL	20.1	20.4	20.7	16.1	21.7	20.6	20.3	20.7	21.2	22.1	21.4
HW	12.6	12.0	11.8	8.8	13.8	12.5	13.0	12.3	12.7	14.8	13.5
HD	7.4	7.2	6.6	5.1	9.2	8.4	9.1	7.6	8.3	8.7	9.2
ED	3.8	4.1	3.4	2.6	4.9	4.9	4.9	4.8	6.5	4.6	6.0
EE	5.8	5.5	5.9	4.4	6.9	6.1	6.2	5.7	5.3	6.5	6.2
ES	7.5	7.6	6.9	5.0	9.0	8.3	8.3	8.2	8.7	8.8	8.4
EN	6.7	6.3	6.2	4.5	6.5	6.2	6.1	6.2	6.2	6.6	6.0
IO	5.6	5.4	5.6	4.2	6.6	5.6	5.4	5.1	4.9	3.5	5.7
EL	0.8	0.8	0.7	0.3	1.3	1.1	1.2	1.0	1.5	1.2	0.9
IN	2.8	2.6	2.6	2.0	2.8	2.5	2.5	2.3	2.7	2.2	2.5

Table 5. Continued.

Species	*C. rukhadeva*	*C. rukhadeva*	*C. rukhadeva*	*C.* cf. *rukhadeva*	*C.* cf. *rukhadeva*	*C.* cf. *rukhadeva*	*C.* cf. *rukhadeva*	*C.* cf. *rukhadeva*	*C.* cf. *rukhadeva*	*C.* cf. *rukhadeva*
Institutional catalog number	**ZMMU R-16851 holotype**	**ZMMU R-16852 paratype**	**ZMKU R 00948 topotype**	**THNHM 24622**	**THNHM 24838**	**THNHM 03251**	**THNHM 03252**	**THNHM 03253**	**THNHM 03254**	**THNHM 01807**
Sex	m	f	f	m	f	m	m	f	m	m
Meristic Data										
Supralabials (SL)	11	9	14	11	13	13	11	12	13	12
Infralabials (IL)	10	11	9	10	10	10	10	10	11	10
Paravertebral tubercles (PVT)	27	30	30	26	28	27	27	30	30	26
Longitudinal rows of tubercles (LRT)	19	20	19	18	19	18	18	19	19	19
Ventral scales (VS)	34	43	38	38	36	37	37	39	34	35
Ventral scales along middle of the body (VSM)	154	152	165	162	158	157	159	168	160	161
Expanded subdigital lamellae on 4th toe (TL4E)	9	9	9	8	9	9	10	9	10	10
Unmodified subdigital lamellae on 4th toe (TL4U)	11	11	12	11	13	12	12	15	13	13
Total subdigital lamellae 4th toe (TL4T)	20	18	21	19	22	21	22	14	23	23

Species	*C. rukhadeva*	*C. rukhadeva*	*C. rukhadeva*	*C.* cf. *rukhadeva*	*C.* cf. *rukhadeva*	*C.* cf. *rukhadeva*	*C.* cf. *rukhadeva*	*C.* cf. *rukhadeva*	*C.* cf. *rukhadeva*	*C.* cf. *rukhadeva*
Institutional catalog number	**ZMMU R-16851 holotype**	**ZMMU R-16852 paratype**	**ZMKU R 00948 topotype**	**THNHM 24622**	**THNHM 24838**	**THNHM 03251**	**THNHM 03252**	**THNHM 03253**	**THNHM 03254**	**THNHM 01807**
Expanded subdigital lamellae on 4th finger (FL4E)	9	8	8	7	8	8	8	8	8	8
Unmodified subdigital lamellae on 4th finger (FL4U)	10	9	11	10	11	10	10	12	12	12
Total subdigital lamellae 4th finger (FL4T)	19	17	19	17	17	18	18	20	20	20
Enlarged femoral scales (R/L)	9R/8L	8R/8L	9R/8L	9R/L	9R/9L	9R/7L	7R/7L	6R/7L	5R/8L	7R/7L
Total enlarged femoral scales (FS)	17	16	17	18	18	16	14	13	13	14
Total femoral pores (FP)	17	0	0	14	0	12	13	0	11	13
Enlarged precloacal scales (PCS)	17	13	15	15	15	14	13	15	15	14
Precloacal pores (PP)	17	13	0	15	0	14	13	0	15	14
Postcloacal tubercles (PCT)	3	2	2R/3L	3	2	3	2	2	3	2
Body bands (BB)	3	3	3	3	3	4	4	/	/	5
Categorical data										
Small tubercles on flank (FKT)	present	present	present	present	present	present	present	present	present	present
Dorsolateral caudal tubercles (DCT)	small	small	small	small	small	small	small	small	small	/
Ventrolateral caudal fringe narrow or wide (VLF1)	narrow	narrow	narrow	narrow	narrow	narrow	narrow	narrow	narrow	/
Ventrolateral caudal fringe scales generally homogenous (VLF2)	yes	yes	yes	yes	yes	yes	yes	yes	yes	/
Tail cross-section (TLcross)	square	square	square	square	square	square	square	square	square	/
Slightly enlarged medial subcaudals (SC1)	absent	absent	absent	absent	absent	absent	absent	absent	absent	/
Single enlarged medial subcaudal (SC2)	present	present	present	present	present	present	present	present	present	/
Enlarged medial subcaudals intermittent, medially furrowed, posteriorly emarginate (SC3)	no	no	no	no	no	no	no	no	no	no
Morphometric data										
SVL	74.9	71.7	71.6	68.3	71.8	73.6	75.3	74.7	73.2	61.5
AG	34.6	32.6	33.9	27.3	29.9	30.9	31.3	32.2	30.3	26.2
HumL	10.7	10.4	7.9	9.8	8.3	12.2	11.3	11.8	11.0	10.1
ForL	8.6	7.9	9.6	8.7	8.5	9.0	10.6	9.6	9.2	7.9
FemL	12.6	11.8	10.5	10.8	10.9	11.5	10.2	11.9	12.1	9.5
TibL	10.1	9.3	11.2	9.7	10.7	10.9	11.7	11.3	11.1	9.1
HL	20.2	19.2	19.7	19.7	19.9	20.8	21.3	20.8	21.5	17.9
HW	14.6	13.4	14.0	13.1	13.9	14.9	15.0	13.1	14.1	11.8
HD	9.2	8.5	8.3	7.3	8.9	8.2	8.2	8.1	8.9	7.5
ED	4.6	4.3	5.5	4.9	5.1	5.8	5.4	5.0	5.5	4.7
EE	6.2	6.2	5.8	5.1	6.2	5.6	5.7	5.4	6.2	4.3
ES	8.3	7.7	7.9	7.4	8.1	8.4	8.8	8.1	8.6	7.3
EN	6.3	5.7	5.8	5.4	6.0	6.2	6.4	5.8	6.2	5.3
IO	3.3	3.1	5.6	4.5	4.7	5.6	5.7	5.7	5.6	4.2
EL	1.2	1.0	1.4	1.6	1.5	1.2	1.3	1.2	1.2	0.9
IN	2.2	2.1	2.1	2.0	2.2	2.4	2.5	2.4	2.3	2.0

Table 5. Continued.

Species	*Cyrtodactylus fluvicavus* sp. nov.	*Cyrtodactylus fluvicavus* sp. nov.	*Cyrtodactylus fluvicavus* sp. nov.	*Cyrtodactylus fluvicavus* sp. nov.	*Cyrtodactylus fluvicavus* sp. nov.	*Cyrtodactylus fluvicavus* sp. nov.	*Cyrtodactylus fluvicavus* sp. nov.	*Cyrtodactylus kochangensis* sp. nov	*C.* cf. *kochangensis* sp. nov.	*Cyrtodactylus uthaiensis* sp. nov.	*Cyrtodactylus rivularis* sp. nov.	*Cyrtodactylus rivularis* sp. nov.
Institutional catalog number	**ZMKU R 00959 holotype**	**ZMKU R 00958 paratype**	**ZMKU R 00960 paratype**	**ZMKU R 00961 paratype**	**ZMKU R 00962 paratype**	**ZMKU R 00963 paratype**	**ZMKU R 00964 paratype**	**ZMKU R 00945 holotype**	**THNHM 01667**	**ZMKU R 00949 holotype**	**ZMKU R 00947 holotype**	**ZMKU R 00946 paratype**
Sex	m	m	m	f	f	f	f	f	m	m	f	f
Meristic data												
Supralabials (SL)	12R/12L	13R/12L	13R/12L	11R/12L	12R/12L	13R/12L	12R/11L	12R/13L	12	13R/15L	13R/12L	13R/12L
Infralabials (IL)	10R/10L	10R/10L	9R/10L	10R/10L	10R/10L	10R/10L	10R/10L	9R/9L	10	10R/11L	11R/10L	10R/9L
Paravertebral tubercles (PVT)	30	28	27	27	28	26	28	34	29	33	34	33
Longitudinal rows of tubercles (LRT)	17	17	14	16	17	18	16	14	19	17	20	18
Ventral scales (VS)	34	37	33	30	36	37	39	35	34	36	34	37
Ventral scales along middle of the body (VSM)	155	154	155	172	164	175	170	172	159	159	160	166
Expanded subdigital lamellae on 4th toe (TL4E)	9R/9L	10R/10L	9R/9L	9R/9L	10R/11L	9R/10L	9R/9L	9R/8L	8	8R/(broken)L	9R/9L	9R/9L
Unmodified subdigital lamellae on 4th toe (TL4U)	11R/11L	12R/11L	10R/10L	12R/12L	11R/11L	10R/10L	12R/13L	12R/11L	13	12R/(broken) L	13R/13L	12R/13L
Total subdigital lamellae 4th toe (TL4T)	20R/20L	22R/21L	19R/19L	21R/21L	21R/22L	19R/20L	22R/22L	21R/19L	21	20	22R/22L	21R/22L
Expanded subdigital lamellae on 4th finger (FL4E)	8R/8L	8R/8L	8R/8L	8R/8L	7R/7L	8R/9L	7R/7L	8R/8L	8	7R/7L	8R/8L	8R/8L
Unmodified subdigital lamellae on 4th finger (FL4U)	10R/10L	10R/10L	10R/9L	11R/11L	10R/10L	9R/9L	10R/10L	10R/10L	12	11R/11L	11R/10L	12R/12L
Total subdigital lamellae 4th finger (FL4T)	18R/18L	18R/18L	18R/17L	19R/19L	17R/17L	17R/18L	17R/17L	18R/18L	20	18R/18L	19R/18L	20R/20L
Enlarged femoral scales (R/L)	5R/6L	4R/5L	5R/6L	6R/6L	5R/6L	5R/6L	6R/6L	6R/6L	7R/7L	8R/8L	8R/8L	6R/8L
Total enlarged femoral scales (FS)	11	9	11	12	11	11	12	12	14	16	16	14
Total femoral pores (FP)	11	8	10	0	0	0	0	0	14	12	0	0
Enlarged precloacal scales (PCS)	15	14	14	15	14	15	15	12	16	14	15	15
Precloacal pores (PP)	15	14	14	0	0	0	0	0	16	14	0	0
Postcloacal tubercles (PCT)	3R/2L	3R/2L	3R/3L	1R/1L	3R/2L	3R/3L	2R/2L	1R/1L	3	3R/3L	2R/2L	3R/3L
Body bands (BB)	3	3	3	3	3	3	3	5	5	6	3	4
Categorical data												
Small tubercles on flank (FKT)	present	present	present	present	present	present	present	present	present	present	present	present

Species	***Cyrtodactylus fluvicavus* sp. nov.**	***Cyrtodactylus fluvicavus* sp. nov.**	***Cyrtodactylus fluvicavus* sp. nov.**	***Cyrtodactylus fluvicavus* sp. nov.**	***Cyrtodactylus fluvicavus* sp. nov.**	***Cyrtodactylus fluvicavus* sp. nov.**	***Cyrtodactylus fluvicavus* sp. nov.**	***Cyrtodactylus kochangensis* sp. nov**	***C.* cf. *kochangensis* sp. nov.**	***Cyrtodactylus uthaiensis* sp. nov.**	***Cyrtodactylus rivularis* sp. nov.**	***Cyrtodactylus rivularis* sp. nov.**
Institutional catalog number	**ZMKU R 00959 holotype**	**ZMKU R 00958 paratype**	**ZMKU R 00960 paratype**	**ZMKU R 00961 paratype**	**ZMKU R 00962 paratype**	**ZMKU R 00963 paratype**	**ZMKU R 00964 paratype**	**ZMKU R 00945 holotype**	**THNHM 01667**	**ZMKU R 00949 holotype**	**ZMKU R 00947 holotype**	**ZMKU R 00946 paratype**
Dorsolateral caudal tubercles (DCT)	small	small	small	small	small	small	small	large	large	large	large	large
Ventrolateral caudal fringe narrow or wide (VLF1)	narrow	narrow	narrow	narrow	narrow	narrow	narrow	wide	wide	wide	wide	wide
Ventrolateral caudal fringe scales generally homogenous (VLF2)	no	no	no	no	no	no	no	no	no	no	yes	yes
Tail cross-section (TLcross)	circular	circular	circular	circular	circular	circular	circular	square	/	circular	square	square
Slightly enlarged medial subcaudals (SC1)	present	present	present	present	present	present	present	present	present	present	absent	absent
Single enlarged medial subcaudal (SC2)	absent	absent	absent	absent	absent	absent	absent	absent	absent	absent	present	present
Enlarged medial subcaudals intermittent, medially furrowed, posteriorly emarginate (SC3)	no	no	no	no	no	no	no	no	no	yes	no	no
Morphometric data												
SVL	72.5	72.0	69.6	68.4	76.8	65.7	78.2	60.1	70.2	58.1	73.9	68.1
AG	33.4	33.6	32.0	30.4	35.6	30.6	38.1	29.0	31.5	26.6	34.8	33.2
HumL	9.1	8.8	9.0	8.0	10.0	7.5	10.1	6.5	10.2	7.0	8.1	7.6
ForL	10.5	10.3	10.5	10.1	11.1	8.8	10.8	7.6	8.6	8.3	9.7	9.1
FemL	13.1	12.5	12.5	13.5	14.1	11.5	13.9	10.4	12.1	10.0	11.4	10.4
TibL	11.3	10.6	10.2	9.9	11.2	9.4	12.3	8.4	11.8	8.4	11.2	10.3
HL	20.1	20.5	19.7	20.1	21.2	18.6	21.3	17.3	18.3	16.1	20.3	19.3
HW	14.0	13.4	12.9	13.0	14.9	13.0	15.4	11.6	12.1	10.9	14.9	13.7
HD	8.5	8.1	8.3	7.9	8.1	7.8	8.3	6.5	7.8	6.3	8.2	8.2
ED	5.0	5.0	4.9	4.7	5.1	4.5	5.3	4.2	5.2	4.6	5.8	5.6
EE	6.5	5.9	5.7	5.8	6.1	5.4	6.5	5.0	4.9	4.7	6.5	6.2
ES	8.5	8.3	8.2	8.1	9.2	7.3	9.3	6.9	7.5	6.4	8.3	7.9
EN	6.5	6.2	5.9	6.1	6.6	5.6	6.5	5.2	5.5	4.9	6.1	5.8
IO	5.5	5.4	5.3	5.1	5.6	5.0	5.6	4.2	4.0	4.3	5.8	5.5
EL	1.4	1.5	1.7	1.4	1.8	1.6	1.8	1.0	1.3	1.5	1.1	1.1
IN	2.3	2.4	2.5	2.3	2.3	2.3	2.6	1.9	2.2	1.8	2.3	2.0

Table 5. Continued.

Species	*C.* sp.9 Thong Pha Phum	*C.* sp.9 Thong Pha Phum	*C.* sp.9 Thong Pha Phum	*C.* sp.9 Thong Pha Phum	*C.* sp.9 Thong Pha Phum	*C.* sp.9 Thong Pha Phum	*C.* sp.9 Thong Pha Phum	*C.* sp.9 Thong Pha Phum	*C.* sp.13	*C.* sp.13
Institutional catalog number	**ZMKU R 00950**	**ZMKU R 00951**	**ZMKU R 00952**	**ZMKU R 00953**	**ZMKU R 00954**	**ZMKU R 00955**	**ZMKU R 00956**	**ZMKU R 00957**	**THNHM 00104**	**THNHM 27821**
Sex	f	m	f	m	m	f	m	f	f	f
Meristic Data										
Supralabials (SL)	12	13	13	14	13	13	13	13	12	15
Infralabials (IL)	8	8	10	10	9	10	10	9	10	11
Paravertebral tubercles (PVT)	32	33	34	34	36	36	30	30	33	29
Longitudinal rows of tubercles (LRT)	21	19	20	20	21	21	19	19	18	20
Ventral scales (VS)	34	33	33	34	30	33	32	33	37	36
Ventral scales along middle of the body (VSM)	173	158	156	166	159	159	150	169	159	165
Expanded subdigital lamellae on 4th toe (TL4E)	9	10	9	8	10	8	9	9	9	7
Unmodified subdigital lamellae on 4th toe (TL4U)	12	14	13	12	13	12	11	13	12	12
Total subdigital lamellae 4th toe (TL4T)	21	24	22	20	23	20	20	22	21	19
Expanded subdigital lamellae on 4th finger (FL4E)	8	7	7	8	8	8	8	8	8	8
Unmodified subdigital lamellae on 4th finger (FL4U)	10	12	12	11	12	12	11	12	11	10
Total subdigital lamellae 4th finger (FL4T)	18	19	19	19	20	20	19	20	19	18
Enlarged femoral scales (R/L)	5R/7L	8R/8L	8R/8L	7R/8L	8R/8L	7R/8L	7R/6L	8R/8L	9R/9L	7R/10L
Total enlarged femoral scales (FS)	12	16	16	15	16	15	13	16	18	17
Total femoral pores (FP)	0	16	0	14	15	14	12	0	0	0
Enlarged precloacal scales (PCS)	17	15	15	15	15	15	15	15	14	16
Precloacal pores (PP)	0	15	0	15	15	15	15	0	0	0
Postcloacal tubercles (PCT)	2	2R/3L	3	3	2R/3L	2R/3L	3	2	3	3
Body bands (BB)	3	4	3	4	3	5	4	4	3	/
Categorical data										
Small tubercles on flank (FKT)	present	present	present	present	present	present	present	present	present	present
Dorsolateral caudal tubercles (DCT)	large	large	large	large	large	large	/	large	small	small
Ventrolateral caudal fringe narrow or wide (VLF1)	wide	wide	wide	wide	wide	wide	/	wide	narrow	narrow
Ventrolateral caudal fringe scales generally homogenous (VLF2)	no	no	no	no	no	no	/	no	yes	yes
Tail cross-section (TLcross)	square	square	square	square	square	square	/	square	circular	circular
Slightly enlarged medial subcaudals (SC1)	present	present	present	present	present	present	/	present	present	present
Single enlarged medial subcaudal (SC2)	absent	absent	absent	absent	absent	absent	/	absent	absent	absent

Species	*C.* sp.9 Thong Pha Phum	*C.* sp.9 Thong Pha Phum	*C.* sp.9 Thong Pha Phum	*C.* sp.9 Thong Pha Phum	*C.* sp.9 Thong Pha Phum	*C.* sp.9 Thong Pha Phum	*C.* sp.9 Thong Pha Phum	*C.* sp.9 Thong Pha Phum	*C.* sp.13	*C.* sp.13
Institutional catalog number	**ZMKU R 00950**	**ZMKU R 00951**	**ZMKU R 00952**	**ZMKU R 00953**	**ZMKU R 00954**	**ZMKU R 00955**	**ZMKU R 00956**	**ZMKU R 00957**	**THNHM 00104**	**THNHM 27821**
Enlarged medial subcaudals intermittent, medially furrowed, posteriorly emarginate (SC3)	no	no	no	no	yes	no	/	no	no	no
Morphomeric data										
SVL	73.1	73.5	73.7	73.2	64.4	76.6	76.6	74.2	63.7	72.9
AG	34.8	33.9	35.4	33.6	28.5	37.1	33.2	35.1	25.8	30.6
HumL	8.4	7.2	9.0	9.0	7.2	8.0	8.1	8.6	7.6	10.1
ForL	9.5	9.1	9.2	9.8	9.2	10.0	8.6	9.8	8.1	9.6
FemL	12.8	11.6	12.3	12.5	10.9	13.7	10.8	12.5	10.7	12.8
TibL	10.5	10.1	10.6	10.6	9.9	11.1	10.0	11.4	10.1	10.2
HL	19.9	20.9	20.1	20.0	17.6	20.4	19.3	20.0	17.6	19.9
HW	14.5	14.3	15.7	13.9	12.8	14.7	14.4	14.1	11.9	13.8
HD	7.8	7.7	7.9	7.7	7.0	8.2	7.8	7.6	7.7	8.4
ED	5.0	5.1	5.0	5.0	4.8	5.6	5.3	4.9	4.1	5.3
EE	5.9	5.9	6.0	5.9	5.3	6.1	6.0	6.0	4.9	6.3
ES	7.9	8.5	7.9	7.9	7.3	8.2	7.9	7.9	7.2	8.0
EN	6.0	6.1	6.0	5.8	5.4	6.1	6.0	5.9	5.6	5.9
IO	5.4	5.5	5.8	5.5	4.9	5.7	5.6	5.3	4.8	6.1
EL	1.1	1.5	1.5	1.2	1.2	1.0	1.2	1.3	1.4	1.4
IN	2.3	2.4	2.2	2.0	2.0	2.3	2.2	2.2	2.1	2.3

Figure 9. Habitat of *Cyrtodactylus rivularis* sp. nov. at Thailand, Prachuap Khiri Khan Province, Hua Hin District, Huai Sat Yai Subdistrict, Kaeng Krachan National Park, Pa La-U Waterfall.

***Cyrtodactylus kochangensis* sp. nov.**
https://zoobank.org/96DF655B-BBB7-4C06-9418-744EBCD14703
Fig. 10
Suggested Common Name: Ko Chang Bent-toed Gecko

Holotype. Adult female ZMKU R 00945 from Ko Chang Island, Ko Phayam Subdistrict, Mueang Ranong District, Ranong Province, Thailand (9.82411°N, 98.43999°E, 36 m a.s.l.), collected by Siriporn Yodthong, Natee Ampai, Attapol Rujirawan, and Piyawan Puanprapai on 8 July 2017.

Additional material examined. *Cyrtodactylus* cf. *kochangensis* sp. nov. adult male THNHM 01667 from Khlong Naka Wildlife Sanctuary, Suk Samran District, Ranong Province, Thailand (~N 9.4596, E 98.5044, elevation unknown), collected by Yodchaiy Chuaynkern between 28 December 2000 and 2 January 2001.

Diagnosis (based on the holotype). *Cyrtodactylus kochangensis* sp. nov. can be separated from all other species of the *brevipalmatus* group by the combination of having 12 or 13 supralabials, nine infralabials, 34 paravertebral tubercles, 14 rows of longitudinally arranged tubercles, 35 transverse rows of ventrals, 172 longitudinal rows of ventrals, 8 or 9 expanded subdigital lamellae on the fourth toe, 11 or 12 unexpanded subdigital lamellae on the fourth toe, 19–21 total subdigital lamellae on the fourth toe; eight expanded subdigital lamellae on the fourth finger, ten unexpanded subdigital

lamellae on the fourth finger, 18 total subdigital lamellae on the fourth finger; 12 total enlarged femoral scales; 12 enlarged precloacal scales; enlarged femoral and enlarged precloacal scales not continuous; proximal femoral scales less than one-half the size of the distal femorals; small tubercles on forelimbs and flanks; large dorsolateral caudal tubercles and a wide ventrolateral caudal fringe not composed homogeneous scales; tail square in cross-section; slightly enlarged paired medial subcaudals not posteromedially furrowed; maximum SVL 60.1 mm; five dark transverse body bands (Tables 4, 5).

Description of holotype (Fig. 10). Adult female SVL 60.1 mm; head moderate in length (HL/SVL 0.29), width (HW/HL 0.67), depth (HD/HL 0.38), distinct from neck, triangular in dorsal profile; lores flat anteriorly, weakly inflated posteriorly; prefrontal region slightly concave; canthus rostralis rounded; snout elongate (ES/HL 0.40), rounded in dorsal profile; eye large (ED/HL 0.24); ear opening subcircular, small; eye to ear distance greater than diameter of eye; rostral rectangular, furrowed dorsally, bordered posteriorly by large left and right supranasals and one slightly smaller azygous internasal, bordered laterally by first supralabials; external nares bordered anteriorly by rostral, dorsally by large supranasal, posteriorly by two slightly smaller postnasals, bordered ventrally by first supralabial; 12R/13L rectangular supralabials tapering smoothly to below eye; 9R/9L infralabials tapering smoothly to below eye; scales of rostrum and lores domed, slightly larger than granular scales on top of head and occiput; scales of occiput intermixed with distinct, small tubercles; superciliaries subrectangular, largest anteriorly; mental triangular, bordered laterally by first infralabials and posteriorly by large left and right trapazoidal postmentals contacting medially for approximately 40% of their length posterior to mental; one row of six (R,L) slightly enlarged sublabials extending posteriorly fifth infralabials, subsequent sublabials much smaller; gular and throat scales small, granular, grading posteriorly into slightly larger, flatter, smooth, imbricate, pectoral and ventral scales.

Body relatively short (AG/SVL 0.48) with well-defined ventrolateral folds; dorsal scales small, granular, interspersed with larger conical, semi-regularly arranged, weakly keeled tubercles; tubercles extend from occipital region onto base of tail and slightly beyond as paravertebral rows; tubercles of nape and occiput smaller than those on body; approximately 14 longitudinal rows of tubercles at midbody; approximately 34 paravertebral tubercles; tubercles on upper flanks smaller than those on dorsum; approximately 35 longitudinal rows of flat, imbricate, ventral scales much larger than dorsal scales; approximately 172 transverse rows of ventral scales; no pore-bearing, precloacal scales; 12 enlarged precloacal scales; no deep precloacal groove or depression; and approximately three rows of post-precloacal scales on midline.

Forelimbs moderate in stature, relatively short (ForL/SVL 0.13); granular scales of forearm slightly larger than those on body, interspersed with tubercles; palmar scales rounded, slightly raised; digits well-developed, relatively short, inflected at basal interphalangeal joints; digits narrower distal to inflections; subdigital lamellae wide, transversely expanded proximal to joint inflections, narrower transverse lamellae distal to joint inflections; claws well-developed, claw base sheathed by a dorsal and ventral scale; 8R/8L expanded and 10R/10L unexpanded lamellae beneath the fourth finger; hind

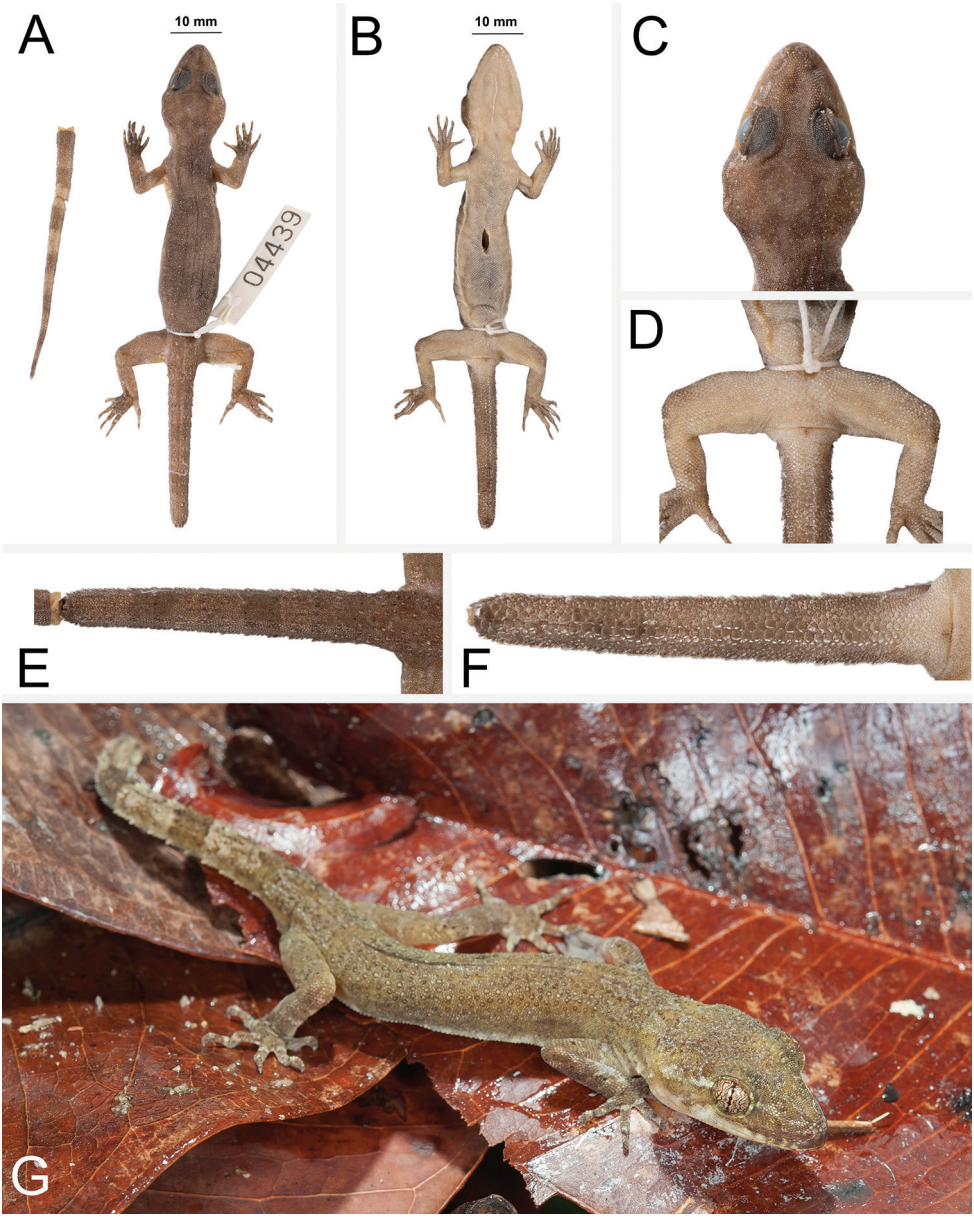

Figure 10. Holotype of *Cyrtodactylus kochangensis* sp. nov. ZMKU R 00945 (field no. AA 04439) from Thailand, Ranong Province, Mueng Ranong District, Ko Phayam Subdistrict, Ko Chang **A** dorsal view **B** ventral view **C** dorsal view of head **D** ventral view of femoral and precloacal regions **E** dorsal view of tail **F** ventral view of tail **G** holotype in life.

limbs larger and thicker than forelimbs, moderate in length (TibL/SVL 0.14), covered dorsally by granular scales interspersed with moderately sized, conical tubercles dorsally and posteriorly and anteriorly by flat, slightly larger, subimbricate scales; ventral

scales of thigh flat, subimbricate, larger than dorsals; subtibial scales flat, imbricate; no pore-bearing femoral scales; 6R/6L enlarged femoral scales; enlarged femoral scales not contiguous with enlarged precloacal scales, terminating distally at knee; proximal femoral scales smaller than distal femorals, the former forming an abrupt union with much smaller, rounded, ventral scales of posteroventral margin of thigh; plantar scales flat; digits relatively long, well-developed, inflected at basal interphalangeal joints; 9R/8L wide, transversely expanded subdigital lamellae on the fourth toe proximal to joint inflection that extend onto sole, and 12R/11L unexpanded lamellae beneath the fourth toe; and claws well-developed, sheathed by a dorsal and ventral scale at base.

Tail original (but in two pieces), long 80.3 mm (TL/SVL 1.34), 4.0 mm in width at base, tapering to a point; nearly square in cross-section; dorsal scales flat, square bearing tubercles forming paravertebral rows and large tubercles forming a dorsolateral longitudinal row; slightly larger, posteriorly directed, semi-spinose tubercles forming wide distinct ventrolateral caudal fringe; scales of ventrolateral fringe generally interspersed at regular intervals with larger spinose scales; medial subcaudal scales paired, slightly enlarged; subcaudals, larger than dorsal caudal scales; base of tail bearing hemipenial swellings; one conical postcloacal tubercle at base of hemipenial swellings; and postcloacal scales flat, imbricate.

Coloration in life (Fig. 10). Ground color of the head, body, limbs, and tail pale brown; faint, diffuse mottling on rostrum; lores darkly colored; wide, distinct, pale-colored postorbital stripe; nuchal band faint, bearing two posterior projections; three very faint, wide, irregularly shaped body bands between limb insertions edged in slightly darker brown; band interspaces bearing irregularly shaped, faint, dark-colored markings; dark-colored speckling on limbs and digits; digits bearing pale-colored bands; four wide, faint, dark-colored caudal bands separated by three pale-colored bands on original portion of tail; all caudal bands encircle tail; all ventral surfaces beige, generally immaculate; and iris orangish to coppery in color.

Variation. The additional specimen (THNHM 01667) closely approximates the holotype in overall coloration and pattern except that it is more boldly marked. It has four dark-colored body bands as opposed to three and a complete original tail bearing eight dark-colored and seven pale-colored bands. The pale-colored postorbital stripe is slightly thinner and less distinct. Meristic and morphometric differences are listed in Table 5. Given its overall morphological and color pattern similarities and close geographic proximity to the holotype (~ 40 km), we consider this individual as *C.* cf. *kochangensis* sp. nov. pending genetic data.

Distribution. *Cyrtodactylus kochangensis* sp. nov. is currently known only from the type locality at Ko Chang Island, Ko Phayam Subdistrict, Mueang Ranong District, Ranong Province, Thailand. The additional population of pending species status occurs in the Khlong Naka Wildlife Sanctuary, Suk Samran District Ranong Province.

Etymology. The specific epithet *kochangensis* is in reference to the type locality, Ko Chang, Ranong Province, Thailand

Comparisons (based on the holotype). *Cyrtodactylus kochangensis* sp. nov. forms a clade with the sister species *Cyrtodactylus rivularis* sp. nov. and *C. rukhadeva* (Fig.

Figure 11. Habitat of *Cyrtodactylus kochangensis* sp. nov. at Thailand, Ranong Province, Mueng Ranong District, Ko Phayam Subdistrict, Ko Chang.

2) from which it differs by an uncorrected pairwise sequence divergence of 12.00–12.52% and 12.52–13.68%, respectively (Table 2) and it and *C.* cf. *kochangensis* sp. nov. are separated from *C. rukhadeva* and *Cyrtodactylus rivularis* sp. nov. by geographic distance of no less than ~280–470 km (Fig. 1). The small sample size ($N = 1$) precludes it from statistical analyses, however at this point, it differs from *C. rukhadeva* and *C.* cf. *rukhadeva* in having 34 PVT versus 26–30; 14 LRT versus 18–20; 172 VSM versus 152–165; 12 FS versus 13–18; 12 PCS versus 13–17 and 1 PCT versus 2 or 3, collectively. From *C. rukhadeva* by having 12 FS versus 16 or 17; and five BB versus three. From *Cyrtodactylus rivularis* sp. nov. it differs in having 14 LRT versus 18–20; 172 VSM versus 160–166; 12 FS versus 14–16; and five BB versus three or four. Discrete differences between *Cyrtodactylus kochangensis* sp. nov. and *C.* cf. *kochangensis* sp. nov. and all other species and populations are presented in Tables 4, 5.

Natural history. The holotype (ZMKU R 00945) was collected at night (2107 h) among branches of a small tree approximately 100 cm above the ground at 36 m elevation with a temperature of 28.6 °C and relative humidity of 83.9%. The surrounding habitat was dry evergreen forest with a rocky stream nearby (Fig. 11). The new species was found to co-occur with two other species of gekkonid lizards, *Cyrtodactylus oldhami* (Theobald, 1876) and *Gekko tokehos* (Grismer, Wood, Grismer, Quah, Thy, Phimmachak, Sivongxay, Seateun, Stuart, Siler, Mulcahy, Anamza & Brown, 2019).

***Cyrtodactylus uthaiensis* sp. nov.**
https://zoobank.org/9422F241-3A46-4FAD-97C4-D6A6AF16B405
Fig. 12
Suggested Common Name: Uthai Thani Bent-toed Gecko

Holotype. Adult male ZMKU R 00949 from Thung Na Ngam Subdistrict, Lan Sak District, Uthai Thani Province, Thailand (15.37649°N, 99.63426°E, 106 m a.s.l.), collected by Attapol Rujirawan, Siriporn Yodthong, Korkhwan Termprayoon, and Natee Ampai on 18 June 2018.

Diagnosis. *Cyrtodactylus uthaiensis* sp. nov. can be separated from all other species of the *brevipalmatus* group by the combination of having 13–15 supralabials, 10–11 infralabials, 33 paravertebral tubercles, 17 rows of longitudinally arranged tubercles, 36 transverse rows of ventrals, 159 longitudinal rows of ventrals, eight expanded subdigital lamellae on the fourth toe, 12 unexpanded subdigital lamellae on the fourth toe, 20 total subdigital lamellae on the fourth toe; seven expanded subdigital lamellae on the fourth finger, 11 unexpanded subdigital lamellae on the fourth finger, 18 total subdigital lamellae on the fourth finger; 16 total enlarged femoral scales, 12 total femoral pores; 14 enlarged pore-bearing precloacals; enlarged femorals and enlarged precloacals not continuous; proximal femorals less than one-half the size of the distal femorals; small tubercles on forelimbs and flanks; large dorsolateral caudal tubercles and wide ventrolateral caudal fringe; ventrolateral caudal fringe composed scales of different size; tail circular in cross-section; slightly enlarged medial subcaudals intermittent, medially furrowed, posteriorly emarginated; maximum SVL 58.1 mm; and six dark transverse body bands (Tables 5, 6).

Description of holotype (Fig. 12). Adult male SVL 58.1 mm; head moderate in length (HL/SVL 0.28), width (HW/HL 0.68), depth (HD/HL 0.39), distinct from neck, triangular in dorsal profile; lores concave slightly anteriorly, weakly inflated posteriorly; prefrontal region slightly concave; canthus rostralis rounded; snout elongate (ES/HL 0.40), rounded in dorsal profile; eye large (ED/HL 0.29); ear opening elliptical, small; eye to ear distance greater than diameter of eye; rostral rectangular, dorsally furrowed, bordered posteriorly by large left and right supranasals, bordered laterally by first supralabials; external nares bordered anteriorly by rostral, dorsally by large supranasal, posteriorly by two smaller postnasals, ventrally by first supralabial; 13R/15L rectangular supralabials tapering smoothly to posterior margin of eye; 10R/11L infralabials tapering smoothly to posterior margin of eye; scales of rostrum and lores flat to domed, slightly larger than granular scales on top of head and occiput; scales of occiput intermixed with distinct, small tubercles; superciliaries subrectangular, largest dorsally and anteriorly; mental triangular, bordered laterally by first infralabials and posteriorly by large left and right trapezoidal postmentals contacting medially for approximately 40% of their length posterior to mental; one row of slightly enlarged, elongate sublabials extending posteriorly to fifth(L) and seventh(R) infralabial; gular and throat scales small, granular, grading posteriorly into slightly larger, flatter, smooth, imbricate, pectoral and ventral scales.

Table 6. Significant *p*-values from the results of the ANOVA analyses comparing all combinations of OTU pairs of the *Cyrtodactylus brevipalmatus* group. SVL and TL4U are not listed because no species pairs differed significantly from one another. * = Results based on a Games-Howell *post hoc* test. Character abbreviations are listed in the Materials and methods.

Morphometric characters	AG*	HumL*	ForL	FemL	TibL	HL	HW	HD*	ED*	EE*	ES	EN*	IO	EL	IN
Cyrtodactylus fluvicavus sp. nov. vs. *C. brevipalmatus*			0.00	0.01		< 0.001	0.001	0.048			< 0.001	0.004		0.002	0.004
C. interdigitalis vs. *C. brevipalmatus*			0.00		0.00	0.00					< 0.001				
C. ngati vs. *C. brevipalmatus*						0.00						0.003		0.001	< 0.001
C. ngati3 vs. *C. brevipalmatus*	0.014			0.03	0.01	< 0.001		0.008		0.038	< 0.001	0.004			0.000
C. rukhadeva vs. *C. brevipalmatus*						< 0.001	0.001	0.022			< 0.001	0.021			
C. sp.9 vs. *C. brevipalmatus*						0.01	< 0.001				< 0.001	0.03			
C. interdigitalis vs. *Cyrtodactylus fluvicavus* sp. nov.					0.01										
C. ngati vs. *Cyrtodactylus fluvicavus* sp. nov.	< 0.001	0.002		0.04			< 0.001	0.005			< 0.001			< 0.001	
C. ngati3 vs. *Cyrtodactylus fluvicavus* sp. nov.	< 0.001									0.025				0.038	
C. rukhadeva vs. *Cyrtodactylus fluvicavus* sp. nov.	0.049		< 0.001	< 0.001										0.004	
C. sp.9 vs. *Cyrtodactylus fluvicavus* sp. nov.			0.0					0.007			0.013	0.023		0.007	
C. ngati vs. *C. interdigitalis*							0.007		0.031		0.010			< 0.001	0.000
C. ngati3 vs. *C. interdigitalis*	0.011														0.003
C. rukhadeva vs. *C. interdigitalis*			0.0	0.01	0.00								0.044		
C. sp.9 vs. *C. interdigitalis*					0.00		0.007								
C. ngati3 vs. *C. ngati*	< 0.001	0.019						0.006			< 0.001			0.001	
C. rukhadeva vs. *C. ngati*		0.003					< 0.001	< 0.001	0.046		< 0.001	0.001	< 0.001	< 0.001	0.001
C. sp.9 vs. *C. ngati*	< 0.001						< 0.001	0.042			0.007	< 0.001		< 0.001	0.000
C. rukhadeva vs. *C. ngati3*	< 0.001	0.021	0.0	0.00						0.007		0.02			0.006
C. sp.9 vs. *C. ngati3*	0.001				0.01	0.03	0.003	0.043		0.001	0.019	0.019			0.003
C. sp.9 vs. *C. rukhadeva*	0.02	0.004			0.02			0.033							

Meristic characters	SL	IL*	PVT*	LRT	VS	VSM	TL4E	TL4T	FL4E	FL4U*	FL4T*	FS	PCS*	BB*
Cyrtodactylus fluvicavus sp. nov. vs. *C. brevipalmatus*							0.037						< 0.001	0.05
C. interdigitalis vs *C. brevipalmatus*				< 0.001			0.000				0.002		0.044	
C. ngati vs *C. brevipalmatus*									< 0.001			0.028	< 0.001	
C. ngati3 vs *C. brevipalmatus*				0.017									0.029	
C. rukhadeva vs *C. brevipalmatus*				< 0.001									< 0.001	
C. sp.9 vs *C. brevipalmatus*				< 0.001	0.003					0.022			< 0.001	0.05
C. interdigitalis vs *Cyrtodactylus fluvicavus* sp. nov.				0.000	0.000	0.021					< 0.001	0.000		< 0.001
C. ngati vs *Cyrtodactylus fluvicavus* sp. nov.	0.037		0.002					< 0.001	< 0.001	0.033		0.000	0.002	< 0.001
C. ngati3 vs *Cyrtodactylus fluvicavus* sp. nov.												0.005		
C. rukhadeva vs *Cyrtodactylus fluvicavus* sp. nov.				0.000								0.001		0.001
C. sp.9 vs *Cyrtodactylus fluvicavus* sp. nov.			< 0.001	< 0.001						0.001	0.004	0.020		
C. ngati vs *C. interdigitalis*			0.001		0.029			< 0.001	< 0.001	0.029				
C. ngati3 vs *C. interdigitalis*					0.029	0.025					0.005			
C. rukhadeva vs *C. interdigitalis*		0.004			0.011	0.001	0.044				0.001			0.002
C. sp.9 vs *C. interdigitalis*			0.003		< 0.001	0.005			0.043		0.01			< 0.001
C. ngati3 vs *C. ngati*	0.0267		0.001						< 0.001					
C. rukhadeva vs *C. ngati*		< 0.001	< 0.001					0.008	< 0.001	0.008			0.03	< 0.001
C. sp.9 vs *C. ngati*	0.003		0.016	0.011				0.000	< 0.001	< 0.001			< 0.001	< 0.001
C. rukhadeva vs *C. ngati3*														
C. sp.9 vs *C. ngati3*			0.001	0.042						< 0.001	0.001			
C. sp.9 vs *C. rukhadeva*	0.029		< 0.001		0.002									0.001

Body relatively short (AG/SVL 0.46) with well-defined ventrolateral folds; dorsal scales small, granular, interspersed with larger, conical, semi-regularly arranged, weakly keeled tubercles; tubercles extend from occipital region onto base of tail and slightly beyond as paravertebral rows; smaller tubercles extend anteriorly onto nape and occiput, diminishing in size anteriorly; approximately 17 longitudinal rows of tubercles at midbody; approximately 33 paravertebral tubercles; small tubercles on flanks; 36 longitudinal rows of flat, imbricate, ventral scales much larger than dorsal scales; 159 transverse rows of ventral scales; 16 total large femoral scales; 12 total femoral pores; 14 enlarged pore-bearing precloacals; no deep precloacal groove or depression; and two rows of post-precloacal scales on midline.

Forelimbs moderate in stature, relatively short (ForL/SVL 0.14); granular scales of forearm slightly larger than those on body, interspersed with large tubercles; palmar scales rounded, slightly raised; digits well-developed, relatively short, inflected at basal interphalangeal joints; digits narrower distal to inflections; subdigital lamellae wide, transversely expanded proximal to joint inflections, narrower transverse lamellae distal to joint inflections; claws well-developed, claw base sheathed by a dorsal and ventral scale; 7R/7L expanded and 11R/11L unexpanded lamellae beneath the fourth finger; hind limbs larger and thicker than forelimbs, moderate in length (TibL/SVL 0.14), covered dorsally by granular scales interspersed with moderately sized, conical tubercles dorsally and posteriorly and anteriorly by flat, slightly larger, subimbricate scales; ventral scales of thigh flat, subimbricate, larger than dorsals; subtibial scales flat, imbricate; one row of 6R/6L of enlarged pore-bearing femoral scales not continuous with enlarged pore bearing precloacal scales, terminating distally at knee; 8R/8L enlarged femoral scales; proximal femoral scales smaller than distal femorals, the former forming an abrupt union with much smaller, rounded, ventral scales of posteroventral margin of thigh; plantar scales flat; digits relatively long, well-developed, inflected at basal interphalangeal joints; 8R/(broken)L wide, transversely expanded subdigital lamellae on fourth toe proximal to joint inflection that extend onto sole, 12R/(broken)L unexpanded lamellae beneath first toe; and claws well-developed, sheathed by a dorsal and ventral scale at base.

Tail original, long 76.7 mm (TL/SVL 1.32), 4.1 mm in width at base, tapering to a point; sub-circular or nearly round in cross-section; dorsal scales flat, square bearing tubercles forming paravertebral rows and large tubercles forming a dorsolateral longitudinal row; slightly larger, posteriorly directed, semi-spinose tubercles forming small but distinct ventrolateral caudal fringe; larger scales of ventrolateral fringe occur at regular intervals; slightly enlarged medial subcaudals intermittent, medially furrowed, posteriorly; single enlarged medial subcaudals absent; subcaudal scales, larger than dorsal caudal scales; base of tail bearing hemipenial swellings; 3R/3L conical postcloacal tubercles at base of hemipenial swellings; and postcloacal scales flat, imbricate.

Coloration in life (Fig. 12). Ground color of the head, body, limbs, and tail pale-brown; dark, diffuse mottling on interorbital region and snout; dark blotch on top of head; wide, pale-colored postorbital stripe irregularly edged in dark brown extends from posterior margin of one eye across nape to posterior margin of other eye; ventral

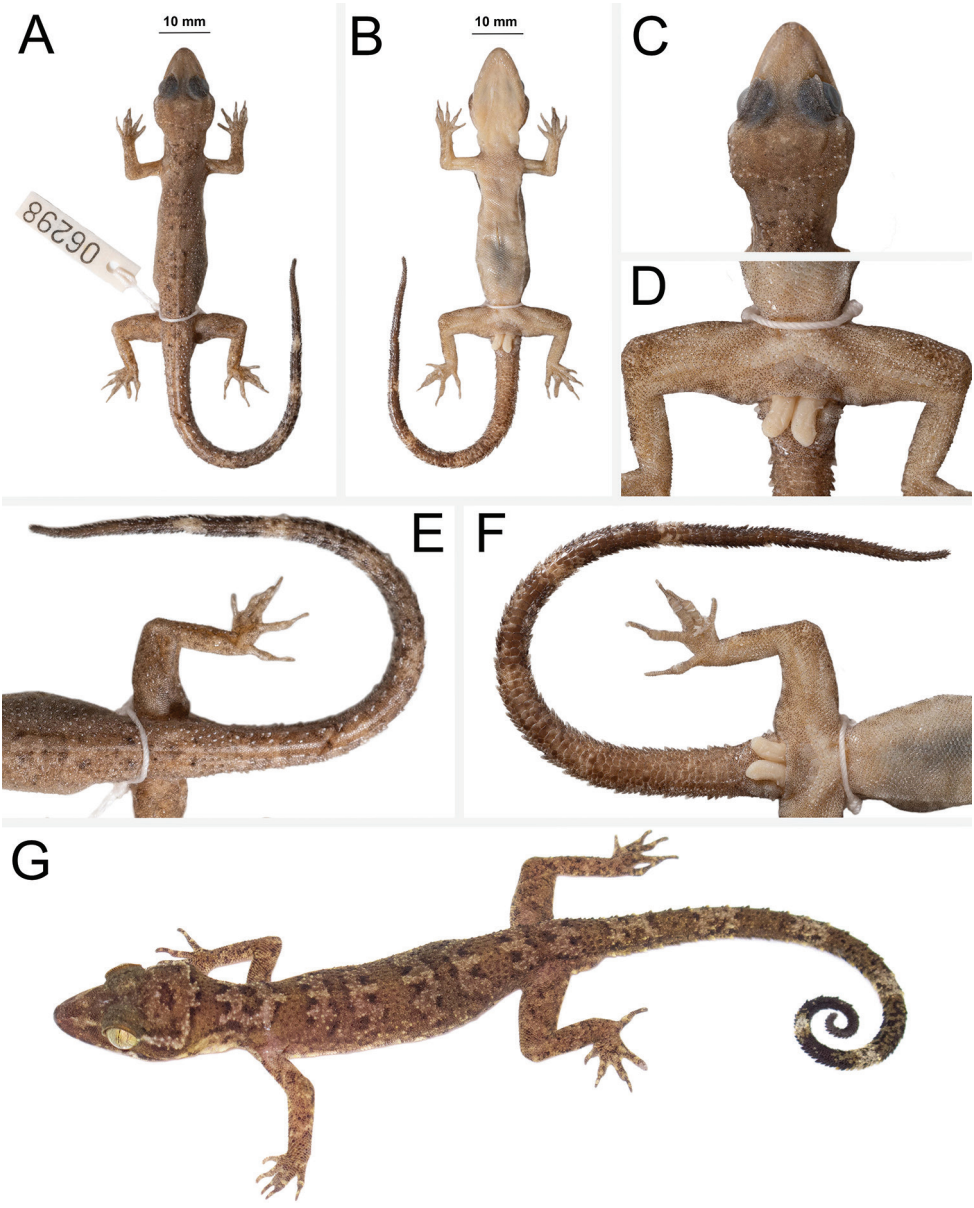

Figure 12. Holotype of *Cyrtodactylus uthaiensis* sp. nov. ZMKU R 00949 (field no. AA 06298) from Thailand, Uthai Thani Province, Lan Sak District, Thung Na Ngam Subdistrict **A** dorsal view **B** ventral view **C** dorsal view of head **D** ventral view of femoral and precloacal regions **E** dorsal view of tail **F** ventral view of tail **G** holotype in life.

portion of lores, suborbital region, and supralabials darkly mottled; wide, dark brown nuchal band, bearing two posterior projections; six irregularly shaped darkly edged body bands extending between forelimb and hind limb insertions followed by one

dark sacral band; paired dark brown paravertebral blotches on nape; band interspaces bearing irregularly shaped, dark-colored markings; dark-colored speckling on limbs and digits; digits bearing pale-colored bands; seven wide dark-colored caudal bands separated by six pale-colored bands; caudal bands encircle tail resulting in heavily mottled subcaudal region; all other ventral surfaces beige, generally immaculate; and iris gold in color.

Distribution. *Cyrtodactylus uthaiensis* sp. nov. is currently known from the type locality at Thung Na Ngam Subdistrict, Lan Sak District, Uthai Thani Province, Thailand.

Etymology. The specific epithet *uthaiensis* refers to the type locality, Uthai Thani Province, Thailand.

Comparisons. *Cyrtodactylus uthaiensis* sp. nov. is the sister species to a clade comprised the sister species *C. interdigitalis* and *C.* sp.11 (Fig. 2). Together, these taxa form the sister lineage to *C.* cf. *ngati*1, *C.* cf. *ngati*2, and all other *C. ngati. Cyrtodactylus uthaiensis* sp. nov. differs from those lineages by an uncorrected pairwise sequence divergence of 5.81–8.13% (Table 2). We are aware that any comparison based on morphometric and meristic characters are preliminary being that there is only one sample of *Cyrtodactylus uthaiensis* sp. nov. and that additional sampling may preclude some characters and being diagnostic just as it may reveal that other characters are diagnostic (see Table 5). Therefore, at this point we rely on the invariable categorical characters to separate *Cyrtodactylus uthaiensis* sp. nov. from other species in the *brevipalmatus* group. *Cyrtodactylus uthaiensis* sp. nov. differs from *C. brevipalmatus*, *Cyrtodactylus fluvicavus* sp. nov., *C. interdigitalis*, *C. ngati*, *C. ngati*3, *C.* cf. *ngati*1, *C.* cf. *ngati*2, *C. rukhadeva*, *C.* cf. *rukhadeva* and *C.* sp.13 by having large dorsolateral caudal tubercles (DCT) forming a wide ventrolateral caudal fringe (VLF1). *Cyrtodactylus uthaiensis* sp. nov. is further differentiated from *C. ngati*3, *C.* cf. *ngati*1, *C.* cf. *ngati*2, *C. interdigitalis*, *C. rukhadeva*, *C.* cf. *rukhadeva*, and sp.13 by having a ventrolateral fringe not homogenous (VLF2). It differs from *Cyrtodactylus kochangensis* sp. nov., *Cyrtodactylus rivularis* sp. nov., *C. rukhadeva*, *C.* cf. *rukhadeva*, and *C.* sp.11 by having tail that is more circular in cross-section than square (TLcross). From *Cyrtodactylus rivularis* sp. nov., *C. rukhadeva* and *C.* cf. *rukhadeva*, it differs by having enlarged, unmodified, medial subcaudal scales (SC1). From *Cyrtodactylus rivularis* sp. nov., *C. rukhadeva* and *C.* cf. *rukhadeva*, it differs by lacking single, enlarged, medial subcaudal scales (SC2). From all species in the *brevipalmatus* group except *C. interdigitalis* it differs by having posteriorly emarginated, medial subcaudals bearing a median furrow (SC3).

Natural history. *Cyrtodactylus uthaiensis* sp. nov. is the only species of the *brevipalmatus* group that occurs in an isolated hilly area within the Chao Phraya River Basin (Fig. 1). The holotype (ZMKU R 00949) was collected at night (2055 h) on a bamboo twig approximately 170 cm above ground level at 106 m elevation. The habitat was isolated karst formations within a mixed deciduous forest. This area was surrounded by agricultural fields (plantations and rice fields) and human residential areas (Fig. 13). The new species was found to co-occur with a gekkonid lizard, *Dixonius siamensis* (Boulenger, 1899).

Figure 13. Habitat of *Cyrtodactylus uthaiensis* sp. nov. at Thailand, Uthai Thani Province, Lan Sak District, Thung Na Ngam Subdistrict.

Table 7. Summary statistics from the PERMANOVA analysis of the OTUs and proposed morphogroups of the *Cyrtodactylus brevipalmatus* group.

OTU pairs	F model	R^2	*p*-value	*p*-adjusted
C. rukhadeva vs. *C.* cf. *ngati*2	6.8474	0.4064	0.015	0.544
C. rukhadeva vs. *C. ngati*3	8.8824	0.4467	0.003	0.122
C. rukhadeva vs. *C. interdigitalis*	3.3630	0.2189	0.006	0.201
C. rukhadeva vs. *C. ngati*	10.4580	0.4874	0.003	0.114
C. rukhadeva vs. *C. brevipalmatus*	6.5983	0.3367	0.000	0.012
C. rukhadeva vs. *Cyrtodactylus fluvicavus* sp. nov.	6.6357	0.3067	0.000	0.004
C. rukhadeva vs. *C.* sp.9	3.8646	0.1945	0.001	0.033
C. cf. *ngati*2 vs. *C. brevipalmatus*	15.4818	0.7559	0.048	1.000
C. cf. *ngati*2 vs. *Cyrtodactylus fluvicavus* sp. nov.	15.9186	0.6946	0.027	0.967
C. cf. *ngati*2 vs. *C.* sp.9	19.0130	0.7038	0.022	0.804
*C. ngati*3 vs. *C. interdigitalis*	4.4753	0.4723	0.029	1.000
*C. ngati*3 vs. *C. brevipalmatus*	14.9425	0.7135	0.018	0.643
*C. ngati*3 vs. *Cyrtodactylus fluvicavus* sp. nov.	8.7953	0.5237	0.009	0.317
*C. ngati*3 vs. *C.* sp.9	14.7978	0.6218	0.006	0.226
C. interdigitalis vs. *C. ngati*	9.8976	0.6644	0.029	1.000
C. interdigitalis vs. *C. brevipalmatus*	4.5646	0.3947	0.008	0.278
C. interdigitalis vs. *Cyrtodactylus fluvicavus* sp. nov.	6.7120	0.4272	0.003	0.124
C. interdigitalis vs. *C.* sp.9	5.6585	0.3614	0.002	0.067
C. ngati vs. *C. brevipalmatus*	7.4818	0.5550	0.018	0.643
C. ngati vs. *Cyrtodactylus fluvicavus* sp. nov.	22.8234	0.7405	0.008	0.283
C. ngati vs. *C.* sp.9	17.0146	0.6540	0.006	0.227
C. brevipalmatus vs. *Cyrtodactylus fluvicavus* sp. nov.	17.8585	0.6410	0.001	0.048
C. brevipalmatus vs. *C.* sp.9	9.3960	0.4607	0.001	0.025
Cyrtodactylus fluvicavus sp. nov. vs. *C.* sp.9	8.2047	0.3869	0.000	0.005

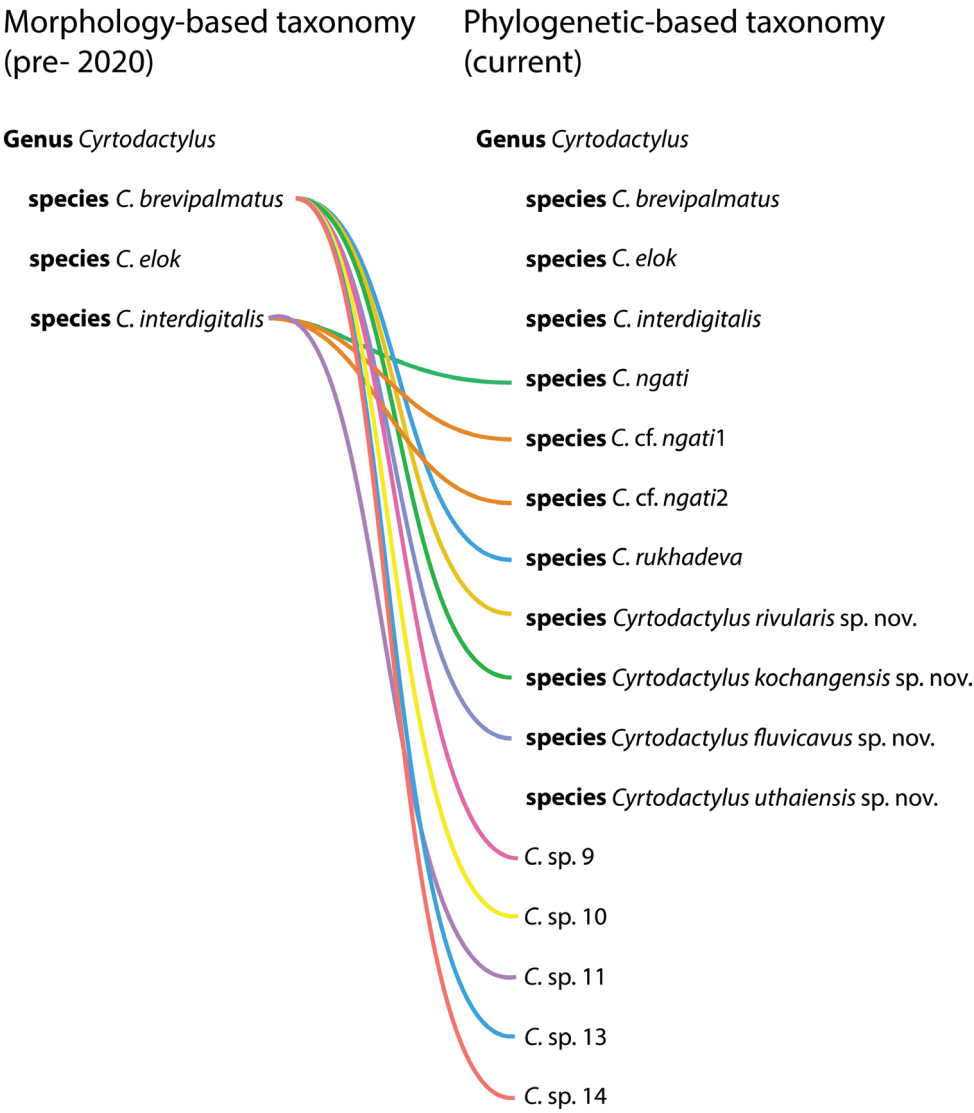

Figure 14. Comparison of a morphology-based taxonomy pre-2020 and the current phylogenetic-based taxonomy illustrating the misrepresentation of the diversity of the *Cyrtodactylus brevipalmatus* group by the former. Colored lines connecting species on the left to species on the right indicate under which name the former were masquerading as the latter.

Discussion

A taxonomy consistent with evolutionary history is paramount to any downstream comparative analyses employed to address the evolution of other features of the group be they ecology, behavior, or habitat preference. By delimiting new and existing spe-

cies using a phylogenetic analysis and then diagnosing those species using univariate and multivariate statistical analyses of their morphological data, phylogenetic history will not conflated with convergent evolution (Fig. 14). This is extremely important for conservation and natural resource management programs so that efforts can be vectored towards all recognized species without missing the species that were previously masquerading among the synonymies of an erroneous taxonomy. This is especially true for range-restricted, highly specialized species, whose general morphological similarity often does not align with their phylogenetic history as exemplified in the *brevipalmatus* group (Fig. 3). Given that upland tropical regions are currently some of the most vulnerable to climate change (Gehrig-Fasel et al. 2007; Myers-Smith et al. 2011; Scridel et al. 2018), this argument becomes especially germane for the entire *brevipalmatus* group— the majority of whose species are upland populations and potentially range-restricted.

The description of the four new species, *Cyrtodactylus fluvicavus* sp. nov., *Cyrtodactylus kochangensis* sp. nov., *Cyrtodactylus rivularis* sp. nov., and *Cyrtodactylus uthaiensis* sp. nov. adds to the rapidly growing list of new species of *Cyrtodactylus* from Thailand. Many of the poorly sampled populations reported here such as *C.* sp.9 from Thong Pha Phum National Park, Kanchanaburi Province; *C.* sp.10 from Chao Doi Waterfall, Tak Province; *C.* sp.11 from Phu Hin Rong Kla National Park, Phitsanulok Province; *C.* sp.13 from Ban Saphan Lao, Kanchanaburi Province and Thung Yai Naresuan Wildlife Sanctuary, Tak Provinces; *C.* sp.14 from Langkawi Island, Peninsular Malaysia; *C.* cf. *ngati*1 and *C.* cf. *ngati*2 from Xaignabouli and Vientiane Provinces, respectively, Laos (Figs 1, 2), will likely be described as new species when new material becomes available. Additionally, many populations listed in various non-technical websites as *C. interdigitalis* or *C. brevipalmatus* based on overall similarity or general distribution, may also be recovered as new species or delegated to some of the more recently described species. This research continues to highlight the unrealized biodiversity in climatically imperiled upland ecosystems throughout Southeast Asia.

Acknowledgements

This work was financially supported by Office of the Permanent Secretary, Ministry of Higher Education, Science, Research and Innovation (grant no. RGNS 64-038). NA was supported by Srinakharinwirot University Research Grant (no. 596/2564). This research was reviewed and approved by the Institutional Animal Care and Use Committee of Faculty of Science, Kasetsart University (ACKU64-SCI-006) and the Department of National Parks, Wildlife and Plant Conservation, Thailand provided the research permission. We would like to thank Suchai Horradee (Chaloem Rattanakosin National Park), Charoen Jaichon (Thong Pha Phum National Park) and Mana Phermpool (Kaeng Krachan National Park) for facilitating the fieldwork. Wachara Sanguansombat and Sunchai Makchai (Thailand Natural History Museum) made specimens in their care available for study. Piyawan Puanprapai assisted with fieldwork. We would like to thank Bryan L. Stuart for suggestions on this research and Truong Nguyen and an anonymous reviewer improved the manuscript.

References

Acinas SG, Klepac-Ceraj V, Hunt DE, Pharino C, Ceraj I, Distel DL, Polz MF (2004) Fine-scale phylogenetic architecture of a complex bacterial community. Nature 430(6999): 551–554. https://doi.org/10.1038/nature02649

Barraclough TG, Birky Jr CW, Burt A (2003) Diversification in sexual and asexual organisms. Evolution 57(9): 2166–2172. https://doi.org/10.1111/j.0014-3820.2003.tb00394.x

Baulechner D, Jauker F, Neubauer TA, Wolters V (2020) Convergent evolution of specialized generalists: Implications for phylogenetic and functional diversity of carabid feeding groups. Ecology and Evolution 10(20): 11100–11110. https://doi.org/10.1002/ece3.6746

Bouckaert RR, Drummond AJ (2017) bModelTest: Bayesian phylogenetic site model averaging and model comparison. BMC Evolutionary Biology 17(1): 42. https://doi.org/10.1186/s12862-017-0890-6

Chan KO, Grismer LL (2022) GroupStruct: An R package for allometric size correction. Zootaxa 5124(4): 471–482. https://doi.org/10.11646/zootaxa.5124.4.4

Coyne JA, Orr HA (1998) The evolutionary genetics of speciation. Philosophical Transactions of the Royal Society of London Series B, Biological science 353(1366): 287–305. https://doi.org/10.1098/rstb.1998.0210

de Queiroz K (2007) Species concepts and species delimitation. Systematic Biology 56(6): 879–886. https://doi.org/10.1080/10635150701701083

Dehling DM, Jordano P, Schaefer HM, Böhning-Gaese K, Schleuning M (2016) Morphology predicts species' functional roles and their degree of specialization in plant–frugivore interactions. Proceedings of the Royal Society B, Biological Sciences 283(1823): 1–7. https://doi.org/10.1098/rspb.2015.2444

Drummond AJ, Suchard MA, Xie D, Rambaut A (2012) Bayesian phylogenetics with BEAUti and BEAST 1.7. Molecular Biology and Evolution 29(8): 1969–1973. https://doi.org/10.1093/molbev/mss075

Ellis M, Pauwels OSG (2012) The bent-toed geckos (*Cyrtodactylus*) of the caves and karst of Thailand. Cave Karst Science 39(1): 16–22.

Feulner PGD, Kirschbaum F, Mamonekene V, Ketmaier V, Tiedemann R (2007) Adaptive radiation in African weakly electric fish (Teleostei: Mormyridae: *Campylomormyrus*): a combined molecular and morphological approach. Journal of Evolutionary Biology 20(1): 403–414. https://doi.org/10.1111/j.1420-9101.2006.01181.x

Fontaneto D, Herniou EA, Boschetti C, Caprioli M, Melone G, Ricci C, Barraclough TG (2007) Independently evolving species in asexual bdelloid rotifers. PLoS Biology 5(4): e87. https://doi.org/10.1371/journal.pbio.0050087

Frost DR, Hillis DM (1990) Species in concept and practice: Herpetological application. Herpetologica 46(1): 86–104.

Frost DR, Kluge AG (1994) A consideration of the epistemology in systematic biology, with special reference to species. Cladistics 10(3): 259–294. https://doi.org/10.1111/j.1096-0031.1994.tb00178.x

Gehrig-Fasel J, Guisan A, Zimmermann NE (2007) Tree line shifts in the Swiss Alps: Climate change or land abandonment? Journal of Vegetation Science 18(4): 571–582. https://doi.org/10.1111/j.1654-1103.2007.tb02571.x

Grismer LL (2008) On the distribution and identification of *Cyrtodactylus brevipalmatus* Smith, 1923 and *Cyrtodactylus elok* Dring, 1979. The Raffles Bulletin of Zoology 56(1): 177–179.

Grismer LL, Wood Jr PL, Le MD, Quah ESH, Grismer JL (2020) Evolution of habitat preference in 243 species of Bent-toed geckos (Genus *Cyrtodactylus* Gray, 1827) with a discussion of karst habitat conservation. Ecology and Evolution 10(24): 13717–13730. https://doi.org/10.1002/ece3.6961

Grismer LL, Wood Jr PL, Poyarkov NA, Le MD, Kraus F, Agarwal I, Oliver PM, Nguyen SN, Nguyen TQ, Karunarathna S, Welton LJ, Stuart BL, Luu VQ, Bauer AM, O'Connell KA, Quah ESH, Chan KO, Ziegler T, Ngo H, Nazarov RA, Aowphol A, Chomdej S, Suwannapoom C, Siler CD, Anuar S, Tri NV, Grismer JL (2021a) Phylogenetic partitioning of the third-largest vertebrate genus in the world, *Cyrtodactylus* Gray, 1827 (Reptilia; Squamata; Gekkonidae) and its relevance to taxonomy and conservation. Vertebrate Zoology 71: 101–154. https://doi.org/10.3897/vertebrate-zoology.71.e59307

Grismer LL, Wood Jr PL, Poyarkov NA, Le MD, Karunarathna S, Chomdej S, Suwannapoom C, Qi S, Liu S, Che J, Quah ESH, Kraus F, Oliver PM, Riyanto A, Pauwels OSG, Grismer JL (2021b) Karstic landscapes are foci of species diversity in the World's Third-Largest Vertebrate genus *Cyrtodactylus* Gray, 1827 (Reptilia: Squamata; Gekkonidae). Diversity 13(5): 183. https://doi.org/10.3390/d13050183

Grismer LL, Suwannapoom C, Pawangkhanant P, Nazarov RA, Yushchenko PV, Naiduangchan M, Le MD, Luu VQ, Poyarkov NA (2021c) A new cryptic arboreal species of the *Cyrtodactylus brevipalmatus* group (Squamata: Gekkonidae) from the uplands of western Thailand. Vertebrate Zoology 71: 723–746. https://doi.org/10.3897/vz.71.e76069

Grismer LL, Rujirawan A, Yodthong S, Stuart BL, Le MD, Le DT, Chuaynkern Y, Wood Jr PL, Aowphol A (2022) The taxonomy and phylogeny of the *Cyrtodactylus brevipalmatus* group (Squamata: Gekkonidae) with emphasis on *C. interdigitalis* and *C. ngati*. Vertebrate Zoology 72: 245–269. https://doi.org/10.3897/vz.72.e80615

Hillis DM (2019) Species delimitation in herpetology. Journal of Herpetology 53(1): 3–12. https://doi.org/10.1670/18-123

Huelsenbeck JP, Ronquist F, Nielsen R, Bollback JP (2001) Bayesian inference of phylogeny and its impact on evolutionary biology. Science 294(5550): 2310–2314. https://doi.org/10.1126/science.1065889

Husson F, Josse J, Le S, Mazet J (2017) FactoMine R: explortory data analysis and data mining. R package, version 1.36.

Kassambara A, Mundt F (2017) Factoextra: extract and visualize the result of multivariate data analyses. R package, version 1.0.5.999.

Knowles LL, Carstens BC (2007) Delimiting species without monophyletic gene trees. Systematic Biology 56(6): 887–895. https://doi.org/10.1080/10635150701701091

Le DT, Sitthivong S, Tran TT, Grismer LL, Nguyen TQ, Le MD, Ziegler T, Luu VQ (2021) First record of the *Cyrtodactylus brevipalmatus* group (Squamata: Gekkonidae) from Vietnam with description of a new species. Zootaxa 4969(3): 492–510. https://doi.org/10.11646/zootaxa.4969.3.3

Leach AD, Koo MS, Spencer CL, Papenfuss TJ, Fisher RN, McGuire JA (2009) Quantifying ecological, morphological, and genetic variation to delimit species in the coast horned lizard

species complex (*Phrynosoma*). Proceedings of the National Academy of Sciences of the United States of America 106(30): 12418–12423. https://doi.org/10.1073/pnas.0906380106

Lin XL, Stur E, Ekrem T (2018) Exploring species boundaries with multiple genetic loci using empirical data from non-biting midges. Zoologica Scripta 47(3): 325–341. https://doi.org/10.1111/zsc.12280

Lleonart J, Salat J, Torres GJ (2000) Removing allometric effects of body size in morphological analysis. Journal of Theoretical Biology 205(1): 85–93. https://doi.org/10.1006/jtbi.2000.2043

Manthey U, Grossmann W (1997) Amphibien and Reptilien Südostasiens. Natur und Tier Verlag, Münster, Germany, 512 pp.

McCoy MW, Bolker BM, Osenberg CW, Miner BG, Vonesh JR (2006) Size correction: Comparing morphological traits among populations and environments. Oecologia 148(4): 547–554. https://doi.org/10.1007/s00442-006-0403-6

Miller MA, Pfeiffer W, Schwartz T (2010) Creating the CIPRES Science Gateway for inference of large phylogenetic trees. In: Gateway Computing Environments Workshop (GCE), New Orleans (USA), November 2010, IEEE, 1–8. https://doi.org/10.1109/GCE.2010.5676129

Myers-Smith IH, Forbes BC, Wilmking M, Hallinger M, Lantz T, Blok D, Tape KD, Macias-Fauria M, Sass-Klaassen U, Levesque E, Boudreau S, Ropars P, Hermanutz L, Trant A, Collier LS, Weijers S, Rozema J, Rayback SA, Schmidt NM, Schaepman-Strub G, Wipf S, Rixen C, Menard CB, Venn S, Goetz S, Andreu-Hayles L, Elmendorf S, Ravolainen V, Welker J, Grogan P, Epstein HE, Hik DS (2011) Shrub expansion in tundra ecosystems: Dynamics, impacts and research priorities. Environmental Research Letters 6(4): 045509. https://doi.org/10.1088/1748-9326/6/4/045509

Nabhitabhata J, Chan-ard T (2005) Thailand Red Data: Mammals, Reptiles and Amphibians. Office of Natural Resources and Environmental Policy and Planning, Bangkok, Thailand, 234 pp.

Nabhitabhata J, Chan-ard T, Chuaynkern Y (2004) Checklist of Amphibians and Reptiles in Thailand. Office of Environmental Policy and Planning, Bangkok, Thailand, 152 pp.

Oksanen J, Blanchet FG, Friendly M, Kindt R, Legendre P, McGlinn D, Minchin PR, O'Hara RB, Simpson GL, Solymos P, Stevens MHH, Szoecs E, Wagner H (2020) Package 'vegan'. Version 2.5-7. https://cran.r-project.org/web/packages/vegan/

Pagès J (2015) Multiple Factor Analysis by Example Using R. CRC Press, New York, USA, 272 pp. https://doi.org/10.1201/b17700

Pauwels OSG, Chan-ard T (2006) Reptiles of Kaeng Krachan National Park, western Thailand. The Natural History Bulletin of the Siam Society 54(1): 89–108.

R Core Team (2018) R: A language and environment for statistical computing. R Foundation for Statistical Computing. Vienna. http://www.R-project.org [accessed 1 June 2022]

Rambaut A, Drummond AJ (2013) TreeAnnotator v1.8.0 MCMC Output Analysis. https://beast.community/treeannotator

Rambaut A, Drummond AJ, Xie D, Baele G, Suchard MA (2018) Posterior summarization in Bayesian phylogenetics using Tracer 1.7. Systematic Biology 67(5): 901–904. https://doi.org/10.1093/sysbio/syy032

Reist JD (1986) An empirical evaluation of coefficients used in residual and allometric adjustment of size covariation. Canadian Journal of Zoology 64(6): 1363–1368. https://doi.org/10.1139/z86-203

Revell LJ (2012) Phytools: An R package for phylogenetic comparative biology (and other things). Methods in Ecology and Evolution 3(2): 217–223. https://doi.org/10.1111/j.2041-210X.2011.00169.x

Ricklefs RE (2012) Species richness and morphological diversity of passerine birds. Proceedings of the National Academy of Sciences of the United States of America 109(36): 14482–14487. https://doi.org/10.1073/pnas.1212079109

Sabaj MH (2020) Codes for natural history collections in ichthyology and herpetology. Copeia 108(3): 593–669. https://doi.org/10.1643/ASIHCODONS2020

Scridel D, Brambilla M, Martin K, Lehikoinen A, Iemma A, Matteo A, Jähnig S, Caprio E, Bogliani G, Pedrini P, Rolando A, Arlettaz R, Chamberlain D (2018) A review and meta-analysis of the effects of climate change on Holarctic mountain and upland bird populations. The Ibis 160(3): 489–515. https://doi.org/10.1111/ibi.12585

Sidlauskas B (2008) Continuous and arrested morphological diversification in sister clades of characiform fishes: A phylomorphospace approach. Evolution 62(12): 3135–3156. https://doi.org/10.1111/j.1558-5646.2008.00519.x

Skalski JR, Richins SM, Townsend R (2018) A statistical test and sample size recommendations for comparing community composition following PCA. PLoS ONE 13(10): e0206003. https://doi.org/10.1371/journal.pone.0206033

Smith MA (1935) The fauna of British India, including Ceylon and Burma. Reptilia and Amphibia. Vol. II. Sauria. Taylor and Francis, London, 440 pp.

Stuart BL (1999) Amphibians and Reptiles. In: Duckworth JW, Salter RE, Khounboline K (Eds) Wildlife in Lao PDR: 1999 Status Report. IUCN-The World Conservation Union/Wildlife Conservation Society/Centre for Protected Areas and Watershed Management, Vientiane, Laos, 43–67.

Sukumaran J, Knowles LL (2017) Multispecies coalescent delimits structure, not species. Proceedings of the National Academy of Sciences of the United States of America 114(7): 1607–1612. https://doi.org/10.1073/pnas.1607921114

Tamura K, Stecher G, Kumar S (2021) MEGA11: Molecular evolutionary genetics analysis version 11. Molecular Biology and Evolution 38(7): 3022–3027. https://doi.org/10.1093/molbev/msab120

Thorpe RS (1975) Quantitative handling of characters useful in snake systematics with particular reference to intraspecific variation in the Ringed Snake *Natrix natrix* (L.). Biological Journal of the Linnean Society 7(1): 27–43. https://doi.org/10.1111/j.1095-8312.1975.tb00732.x

Thorpe RS (1983) A review of the numerical methods for recognising and analysing racial differentiation. In: Felsenstein J (Ed.) Numerical Taxonomy. NATO ASI Series, Volume 1. Springer, Berlin, Heidelberg, 404–423. https://doi.org/10.1007/978-3-642-69024-2_43

Turan C (1999) A note on the examination of morphometric differentiation among fish populations: The Truss System. Turkish Journal of Zoology 23(3): 259–263.

Ulber T (1993) Bemerkungen über cyrtodactyline Geckos aus Thailand nebst Beschreibungen von zwei neuen Arten (Reptilia: Gekkonidae). Mitteilungen aus dem Museum für Naturkunde in Berlin 69(2): 187–200. https://doi.org/10.1002/mmnz.19930690202

Vinh NX, Epps J, Bailey J (2010) Information theoretic measures for clusterings comparison: Variants, properties, normalization and correction for chance. Journal of Machine Learning Research 11: 2837–2854.

Welch KRG, Cooke PS, Wright AS (1990) Lizards of the Orient: A Checklist. Robert E. Krieger Publishing Company, Malabar, Florida, USA, 372 pp.

Wilcox TP, Zwickl DJ, Heath TA, Hillis DM (2002) Phylogenetic relationships of the Dwarf Boas and a comparison of Bayesian and bootstrap measures of phylogenetic support. Molecular Phylogenetics and Evolution 25(2): 361–371. https://doi.org/10.1016/S1055-7903(02)00244-0

Yodthong S, Rujirawan A, Stuart BL, Grismer LL, Aksornneam A, Termprayoon K, Ampai N, Aowphol A (2022) A new species in the *Cyrtodactylus oldhami* group (Squamata, Gekkonidae) from Kanchanaburi Province, western Thailand. ZooKeys 1103: 139–169. https://doi.org/10.3897/zookeys.1103.84672

Zhang JJ, Kapli P, Pavlidis P, Stamatakis A (2013) A general species delimitation method with applications to phylogenetic placements. Bioinformatics 29(22): 2869–2876. https://doi.org/10.1093/bioinformatics/btt499

Supplementary material 1

Data frame for the multiple factor analysis of the putative species of the *Cyrtodactylus brevipalmatus* group

Authors: L. Lee Grismer, Anchalee Aowphol, Siriporn Yodthong, Natee Ampai, Korkhwan Termprayoon, Akrachai Aksornneam, Attapol Rujirawan

Data type: morphological data

Explanation note: Data frame for the multiple factor analysis of the putative species of the *Cyrtodactylus brevipalmatus* group.

Link: https://doi.org/10.3897/zookeys.1129.90535.suppl1

ZooKeys 1129: 163–196 (2022)
doi: 10.3897/zookeys.1129.90287
https://zookeys.pensoft.net

RESEARCH ARTICLE

A peer-reviewed open-access journal
ZooKeys
Launched to accelerate biodiversity research

Mitogenome recovered from a 19th Century holotype by shotgun sequencing supplies a generic name for an orphaned clade of African weakly electric fishes (Osteoglossomorpha, Mormyridae)

John P. Sullivan[1,2], Carl D. Hopkins[2,3], Stacy Pirro[4], Rose Peterson[5], Albert Chakona[6,7], Tadiwa I. Mutizwa[6,7], Christian Mukweze Mulelenu[8,9,10,11], Fahad H. Alqahtani[12], Emmanuel Vreven[10,11], Casey B. Dillman[2,13]

1 *National Center for Biotechnology Information, National Library of Medicine, National Institutes of Health, Bethesda, Maryland, USA* **2** *Cornell University Museum of Vertebrates, Ithaca, New York, USA* **3** *Department of Neurobiology and Behavior, Cornell University, Ithaca, New York, USA* **4** *Iridian Genomes, Bethesda, Maryland, USA* **5** *The George Washington University, Washington, D.C., USA* **6** *NRF-South African Institute for Aquatic Biodiversity, Makhanda, South Africa* **7** *Department of Ichthyology and Fisheries Science, Rhodes University, Makhanda, South Africa* **8** *Département de Zootechnie, Faculté des Sciences Agronomiques, Université de Kolwezi, Kolwezi, Democratic Republic of the Congo* **9** *Département de Gestion des Ressources Naturelles Renouvelables, Unité de recherche en Biodiversité et Exploitation durable des Zones Humides, Université de Lubumbashi, Lubumbashi, Democratic Republic of the Congo* **10** *Laboratory of Biodiversity and Evolutionary Genomics, Katholieke Universiteit, Leuven, Belgium* **11** *Zoology Department, Ichthyology, Royal Museum for Central Africa, Tervuren, Belgium* **12** *National Centre for Bioinformatics, King Abdulaziz City for Science and Technology, Riyadh, Saudi Arabia* **13** *Department of Ecology and Evolutionary Biology, Cornell University, Ithaca, New York, USA*

Corresponding author: John P. Sullivan (sullivanjp@ncbi.nlm.nih.gov)

Academic editor: Pedro Bragança | Received 13 July 2022 | Accepted 19 September 2022 | Published 16 November 2022

https://zoobank.org/198C75C3-6E54-4C51-87C8-13E8AEFB6E49

Citation: Sullivan JP, Hopkins CD, Pirro S, Peterson R, Chakona A, Mutizwa TI, Mukweze Mulelenu C, Alqahtani FH, Vreven E, Dillman CB (2022) Mitogenome recovered from a 19th Century holotype by shotgun sequencing supplies a generic name for an orphaned clade of African weakly electric fishes (Osteoglossomorpha, Mormyridae). ZooKeys 1129: 163–196. https://doi.org/10.3897/zookeys.1129.90287

Abstract

Heteromormyrus Steindachner, 1866, a genus of Mormyridae (Teleostei: Osteoglossomorpha), has been monotypic since the description of *Heteromormyrus pauciradiatus* (Steindacher, 1866) from a single specimen. No type locality other than "Angola" was given and almost no specimens have been subse-

quently identified to this species. In order to investigate the relationship of this taxon to fresh specimens collected in Angola and elsewhere, whole genome paired-end sequencing of DNA extracted from the holotype specimen of *Heteromormyrus pauciradiatus* was performed and a nearly complete mitogenome assembled from the sequences obtained. Comparison of cytochrome oxidase I and cytochrome *b* sequences from this mitogenome to sequences from recently collected material reveal that *Heteromormyrus pauciradiatus* is closely related to specimens identified as *Hippopotamyrus ansorgii* (Boulenger, 1905), *Hippopotamyrus szaboi* Kramer, van der Bank & Wink, 2004, *Hippopotamyrus longilateralis* Kramer & Swartz, 2010, as well as to several undescribed forms from subequatorial Africa collectively referred to in the literature as the "*Hippopotamyrus ansorgii* species complex" and colloquially known as "slender stonebashers." Previous molecular phylogenetic work has shown that these species are not close relatives of *Hippopotamyrus castor* Pappenheim, 1906, the type species of genus *Hippopotamyrus* Pappenheim, 1906 from Cameroon, and are thus misclassified. *Hippopotamyrus ansorgii* species complex taxa and another species shown to have been misclassified, *Paramormyrops tavernei* (Poll, 1972), are placed in genus *Heteromormyrus* and one genetic lineage from the Kwanza and Lucala rivers of Angola are identified as conspecific *Heteromormyrus pauciradiatus*. Three additional new combinations and a synonymy in Mormyridae are introduced. The morphological characteristics and geographical distribution of the genus *Heteromormyrus* are reviewed. The electric organ discharges (EODs) of *Heteromormyrus* species are to be treated in a separate study.

Keywords
Angolan freshwater fishes, *Heteromormyrus*, *Hippopotamyrus*, historical DNA, mitogenomics, mormyrid, museomics, slender stonebasher

Introduction

Mormyrid fishes are well known for their unusual morphologies, large brains, and ability to generate and sense weak electric pulses for object location and communication (Hopkins 1986; Carlson et al. 2019; Kramer 2021). With more than 230 species placed in 21 genera, Mormyridae is by far the largest family of extant Osteoglossomorpha, among the most speciose families of freshwater fishes endemic to Africa (Froese and Pauly 2022; Sullivan and Lavoué 2022), and along with the otophysan gymnotiforms of the Neotropics one of two great continental radiations of weakly electric teleosts (Moller 1995; Lavoué et al. 2012; Crampton 2019; Ford and Albert 2022).

Despite efforts at taxonomic revision in the pre-molecular era (Géry 1968; Taverne 1971a, b, 1972) the generic classification of Mormyridae is only modestly improved since American ichthyologist George Myers termed it "chaotic" more than sixty years ago (Myers 1960). Over the last quarter century molecular phylogenetics has been instrumental in identifying both natural and artificial genera in this family (Alves-Gomes and Hopkins 1997; Lavoué et al. 2000; Sullivan et al. 2000, 2016; Levin and Golubtsov 2017; Peterson et al. 2022), but changes to mormyrid classification have not always followed hard on the heels of these discoveries. Here we describe progress clarifying generic concepts in one small segment of the Mormyridae made possible by sequencing DNA from a 19th Century holotype specimen.

The "*Hippopotamyrus ansorgii* species complex" (*Ha*SC) is an informal term used to denote *Hippopotamyrus ansorgii* (Boulenger, 1905) plus three more described and additional undescribed species of mormyrid weakly electric fishes known in anglophone southern Africa as "slender stonebashers" (Kramer et al. 2004; Chakona et al. 2018; Mutizwa et al. 2021). Previous analyses of DNA sequence data have shown that these species, while a monophyletic group, are not close relatives of *Hippopotamyrus castor* Pappenheim, 1906, the type species of *Hippopotamyrus* Pappenheim, 1906 from Cameroon, but are instead the sister group to a very large clade of mostly Congo Basin species placed in genera *Marcusenius* Gill, 1862, *Gnathonemus* Gill, 1863, *Campylomormyrus* Bleeker, 1874, *Genyomyrus* Boulenger, 1898, and *Cyphomyrus* Myers, 1960 (Sullivan et al. 2016; Peterson et al. 2022). The recent phylogenomic study of Peterson et al. (2022) additionally showed that two forms from opposite ends of the Congo Basin belong to the *Ha*SC: *Paramormyrops tavernei* (Poll, 1972) of the upper Lualaba and Lufira rivers of southeastern D.R. Congo and an undescribed species collected in the Inkisi River in southwestern D.R. Congo.

Losing their parent taxon (*Hippopotamyrus*) renders these species taxonomic orphans. Given this clade's phylogenetic position within Mormyridae it is not obvious which other genus as currently defined could accept them. Before considering introduction of a new generic name, we needed first to determine whether an available name with priority exists. We wondered if the natural home for these orphaned species might be *Heteromormyrus* Steindachner, 1866, coincidently the single valid mormyrid genus missing from published molecular datasets.

Franz Steindachner described *Mormyrus* (*Heteromormyrus*) *pauciradiatus* from a single specimen, catalogued in the Naturhistorisches Museum Vienna as NMW 22417 (Steindachner 1866, Fig. 1). The type locality was given only as "Angola." Taverne (1972) elevated the subgeneric name *Heteromormyrus* to genus, but included no additional species under it. *Heteromormyrus* has remained monotypic and the non-type holdings of *Heteromormyrus pauciradiatus* (Steindachner, 1866) in public collections consist of only a single specimen, BMNH 1910.11.28.44 from Cabiri on the Bengo River of Angola, identified by George Boulenger more than one century ago. While appearing in published faunal lists and databases as a valid species (e.g., Gosse 1984; Skelton 2019; Fricke et al. 2022), *H. pauciradiatus* is essentially a taxon inquirendum, a name known only from the original description and of doubtful application to any recently collected specimens.

Reticence of taxonomists to use either this specific or generic name during the past 150 years may be due to the holotype's unusually short caudal peduncle that places its morphometric ratios outside the range of most other specimens as well as its imprecise type locality. Nonetheless, we suspected *H. pauciradiatus* might be related to the species of the *Ha*SC both because of general phenotypic similarity and its geographic provenance: we know the freshwaters of Angola to be particularly rich in forms belonging to this mormyrid clade, many still undescribed (Mutizwa et al. 2021). If indeed *H. pauciradiatus* and the *Ha*SC constitute a monophyletic group within Mormyridae, the former could provide the generic name the latter require.

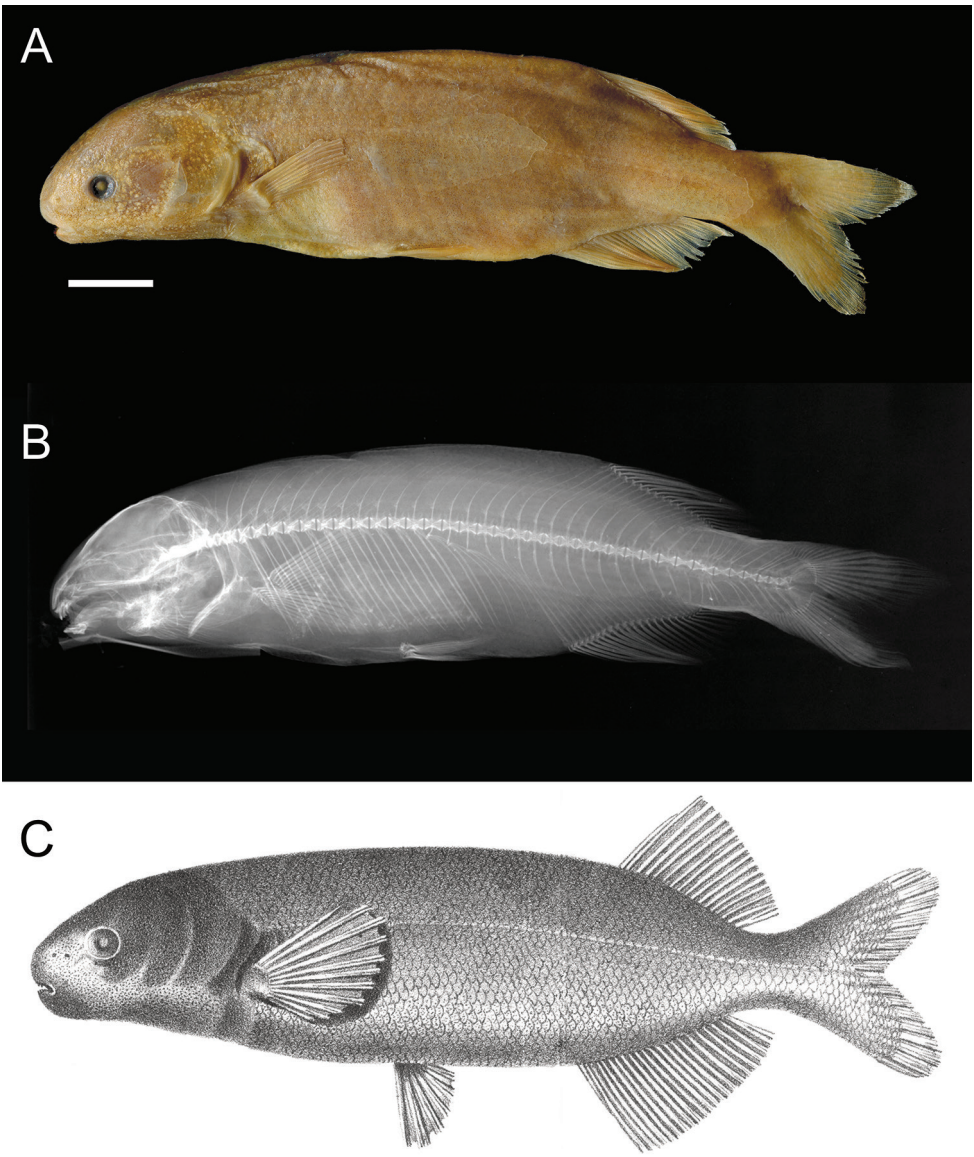

Figure 1. *Heteromormyrus pauciradiatus* (Steindacher, 1866) **A** photo **B** radiograph **C** drawing of holotype NMW 22417. Scale bar: 1 cm. Photo- and radiograph courtesy of Naturhistorisches Museum Vienna, drawing from Steindachner (1866).

Without fresh specimens identified as *H. pauciradiatus* we were prevented from exploring this question using molecular phylogenetics. However, because this type specimen appears to have been originally preserved in ethanol and never fixed in formalin, we thought it might yield DNA. We were encouraged that efforts at PCR-based

Sanger sequencing of other Steindachner types from the same era have been successful (Silva et al. 2019) but wished to explore the possibility that high throughput, whole genome short-read or "shotgun" sequencing would yield more sequence with less effort, as suggested by recent studies that have used this methodology to sequence old type specimens in other vertebrate groups (McGuire et al. 2018; Kehlmaier et al. 2019; Reyes-Velasco et al. 2021; Roos et al. 2021).

In contrast to *H. pauciradiatus*, many specimens have been identified (rightly or wrongly) to the taxon *Hippopotamyrus ansorgii* (Boulenger, 1905) during the past 117 years, although it is also a species with an uncertain type locality. However, in a recent study Mutizwa et al. (2021) examined the field notes of the collector of *H. ansorgii's* two syntypes and concluded that they must have been taken in the Kwanza River basin of Angola, a system in which the same authors identified five distinct mitochondrial lineages of the *Ha*SC, associated with different morphotypes. Mutizwa et al. (2021) informally named these K1 through K5 without determining which if any of them correspond to *H. ansorgii* sensu stricto, or if one of these might correspond to the odd-looking holotype of *H. pauciradiatus*, a fish that may or may not have come from the Kwanza.

Materials and methods

The curator of the Naturhistorisches Museum Vienna supplied us with right-side gill arch and gill filament tissue as well as a right-side pectoral fin clip from the *Heteromormyrus pauciradiatus* holotype, NMW 22417. Specimen measurements and counts performed for this study follow Kramer and Swartz (2010). Institutional abbreviations follow Sabaj (2020). Other abbreviations used: standard length = **SL**, electric organ discharge = **EOD**, base pairs = **bp**.

DNA extraction, library preparation, and sequencing

DNA extraction, Illumina platform library preparation and whole-genome short-read sequencing was performed by the GeneWiz Corporation of South Plainfield, New Jersey, USA and were conducted separately for the fin clip and the gill arch tissue samples.

Genomic DNA was extracted with a Qiagen DNeasy Kit with the following three modifications to the manufacturer-recommended procedure: (1) wide-bore pipette tips were used to minimize DNA damage by shearing; (2) the proteinase K digestion was performed for 15 minutes only; (3) elution consisted of three repeats of adding 10 µl of 0.1× TE warmed to 37 °C to the spin column, incubated for 10 min at 37 °C before collection by centrifugation.

For library preparation the Illumina TruSeq library kit was used with these modifications of the manufacturer's recommended protocol for the degraded sample: no size selection of DNA was performed and half the recommended amounts of all reagents were used.

The constructed libraries were sequenced as 150 bp paired ends on the Illumina HiSeq X Ten platform, multiplexed five samples per run. The reads were deposited into NCBI's Sequence Read Archive (**SRA**) under the accession number SRX7700131.

Mitogenome reconstruction

For a separate project on Osteoglossomorpha phylogeny Peterson et al. (2022) sequenced 40 mormyrid genomes on the Illumina platform from tissue samples originally taken from fresh specimens. Among these genomes is one from the holotype specimen of *Hippopotamyrus longilateralis* Kramer & Swartz, 2010 (SAIAB 78793), a species belonging to the *Ha*SC, a cytochrome *b* sequence from which we determined had high similarity to one we initially recovered from the *H. pauciradiatus* type specimen NMW 22417 sequence fragments (see Results below).

From the SRA of the *H. longilateralis* specimen, SRX5986274, we generated a complete mitogenome using the SMART2 (Statistical Mitogenomes Assembly with RepeaTs) pipeline (Alqahtani and Măndoiu 2020a, b). Read pairs of mitochondrial origin in this SRA are 0.2% of the total reads and the average read depth of this mitogenome is 5,450×. Subsequently we annotated the genome using MITOS (Bernt et al. 2013) and submitted it to NCBI/GenBank where it is published under accession MZ151890. This mitogenome reflects the standard complement of elements in the standard order for vertebrates: 13 protein-coding genes, 22 tRNA genes, two rRNA genes, and one control region or "d-loop," with the ND6 gene and eight tRNA genes encoded on the L-strand (Satoh et al. 2016).

The same SMART2 pipeline was unable to reconstruct the mitogenome from the SRA for the *H. pauciradiatus* holotype NMW 22417, likely due to the much lower quantity of data sequenced from the highly degraded DNA present in the extraction.

Alternatively, we used the entire *H. longilateralis* mitogenome sequence as a query sequence in a BLAST (Basic Local Alignment Search Tool) search (Standard Nucelotide BLAST) against the SRA library obtained from NMW 22417 (SRX7700131). We conducted two such searches: one using the setting for "highly similar sequences (megablast)" and the other with the setting "somewhat similar sequences (blastn)" with maximum target sequences set to 5000, max matches in a query range set to 50, and all other settings at default values. From the results page of each search, using the alignment view "query-anchored with dots for identities" and setting line length to 150, we downloaded the alignments as text files. We reconstructed the sequence of the holotype in a text editor by changing bases in the top (query) sequence where necessary to match those in the high similarity aligned sequences, using ambiguity codes and "N" for missing sites where necessary. (Assembling a long, new sequence of interest from short read sequence data in NCBI's SRA using a query sequence from a related species in NCBI's Web BLAST tool is demonstrated in an online video (Sullivan 2022) and is here termed "SRA BLASTing.") To check the quality of this mitogenome, we analyzed and annotated it with MitoFish MitoAnnotator version 3.61 (Iwasaki et al. 2013). Using the Python script MitoFish2tbl (Hahn 2020) we converted the annotation file produced by MitoAnnotator to the ".tbl" format needed for GenBank submission.

Phylogenetic methods

We used cytochrome *b* (Cyt-*b*) and cytochrome oxidase I (COI) sequences from the reconstructed mitogenome of *Heteromormyrus pauciradiatus* holotype NMW 22417 in two separate phylogenetic analyses that included previously unpublished sequences of both markers from a specimen of *Paramormyrops tavernei* (Poll, 1972), RMCA Vert 2018-032-P-0047, from the upper Lufira River in D.R. Congo and an undescribed *Ha*SC species from the Inkisi River in D.R. Congo (AMNH 247102). The latter two specimens had been included in the recent phylogenomic study of Peterson et al. (2022).

For the Cyt-*b* analysis we began with the multi-locus alignment used by Sullivan et al. (2016) of 4209 bases of mitochondrial cytochrome *b*, 12S, 16S, and nuclear *rag2* and *rps7* intron that, with the exception of *Heteromormyrus*, included representatives of all nominal genera from the Mormyrinae. Based on results of previous phylogenetic studies of Mormyroidea (Sullivan et al. 2000; Peterson et al. 2022) the tree was rooted with *Myomyrus macrops*. To this alignment we added the Cyt-*b* sequences from NMW 22417, the *P. tavernei* and Inkisi River specimens, plus previously published Cyt-*b* sequences of *Ha*SC species and populations from Kramer et al. (2004), Kramer and Swartz (2010), and Mutizwa et al. (2021) as well as new sequences from *H. szaboi*-like forms from the Kabompo River, a large left-bank affluent of the upper Zambezi in Zambia. As analyzed, this dataset included sequences from 113 individuals. Missing data was coded as "?".

The separate COI alignment included sequences from the *H. pauciradiatus* holotype NMW 22417, the *P. tavernei* and the Inkisi River specimens, plus all COI sequences from *Ha*SC species publicly available in BOLD and GenBank. The analysis included 96 individuals and was rooted with a sequence from *Marcusenius cyprinoides* from the BOLD database. This outgroup taxon was chosen as a member of the sister group to the *Heteromormyrus* clade based on the results of Peterson et al. (2022).

All ingroup specimens used in both analyses are listed in Suppl. material 1.

We inferred these two phylogenetic trees using the maximum likelihood optimality criterion in RAxML HPC v. 8.2.12 (Stamatakis 2014) on the CIPRES Science Gateway supercomputing cluster (Miller et al. 2010). In the multilocus alignment, we assigned separate partitions to each codon position of each coding gene (Cyt-*b*, *rag2*) as well as to each of the non-coding genes (12S, 16S, *rps7* intron) for a total of nine partitions. Likewise, we partitioned the COI dataset by codon position. We determined the optimal model of molecular evolution for each partition using the Bayesian information criterion in Partition Finder2 (Lanfear et al. 2012), constrained to select from models available in RAxML. The GTR+gamma or GTR+gamma+I models were selected by Partition Finder as optimal for all partitions of in both analyses. As calculation of invariant sites (I) is discouraged by the author of RAxML, we used separate GTR+gamma (GTRGAMMA) evolutionary models for all partitions and performed a non-parametric bootstrap analysis using the faster GTRCAT model to estimate support for nodes. Bootstrapping was auto-terminated using the autoMRE criterion. All other settings were left at their default values.

Results

Holotype mitogenome assembly

Sequencing the DNA extraction from the holotype fin clip yielded no data. Sequencing the DNA extraction from the gill arch tissue yielded 1.3 gigabases of paired-end sequences, available on NCBI's Sequence Read Archive under accession SRX7700131. For comparison, Illumina sequencing of 40 other mormyrid taxa from tissues sampled within the past 20 years (preserved in 95% ethanol or buffer) yielded between 21 and 32 gigabases of sequence data.

To ascertain whether mitochondrial sequences were present in the recovered data we used a 1060 bp Cyt-*b* sequence from a specimen identified as *H. ansorgii* accessioned in the GenBank Nucleotide database (AY236991) as a query sequence in a BLAST search against the SRA data in SRX7700131. BLAST hits of high similarity were matched across nearly the entire query sequence. On the BLAST search result page we set the alignment view to "query-anchored with dots for identities" with a line length of 150 characters and downloaded the results as text. We reconstructed all but 23 bases of the 1060 bp fragment from NMW 22417 in a text editor by changing bases in the top (query) sequence where necessary to match those in the high similarity aligned sequenced fragments.

We BLASTed (using megablast) this reconstructed Cyt-*b* sequence against the entire NCBI Nucleotide archive and found highest similarity (94.6% to 96.5%) to sequences identified as *Hipppopotamyrus* sp., *H. ansorgii*, *H. szaboi*, and *H. longilateralis.*

To test whether our reconstructed sequence may have been affected by the choice of query sequence we repeated the process using two different mormyrid Cyt-*b* sequences from GenBank as queries: *Marcusenius moorii* AF201595 and *Paramormyrops kingsleyae* AF477422. In both cases, the sequences we reconstructed for NMW 22417 matched the sequence reconstructed using the *H. ansorgii* query base-for-base, although many more differences were observed between the SRA sequences and these query sequences.

Using this method of "SRA BLASTing" and downloading the resulting text file (Sullivan, 2022), we reconstructed the mitogenome of the *Heteromormyrus pauciradiatus* holotype using the complete mitogenome of *H. longilateralis* (GenBank accession MZ151890) as query sequence. Short stretches of bases in the query sequence that found no matches in the BLAST search of the SRA were coded as Ns in the reconstructed sequence.

We found 100 cytosine (C) sites in the query sequence at which aligned reads from holotype NMW 22417 are both C and thymine (T), producing a Y ambiguity code in the inferred sequence. We noted a smaller but significant number (24) of ambiguous calls at sites where a guanine (G) in the query sequence is matched to holotype sequences containing both G and adenine (A) that we coded with an R ambiguity code. Sites where Ts and As in the query sequence produced ambiguity codes in the reconstructed sequence were much less common. This observation is consistent with a known consequence of sequencing template DNA that has been subject to hydrolytic deamination of cytosine

to uracil (U), a naturally occurring process as DNA degrades in an aqueous solution. In these cases the polymerase incorporates an A across from each deaminated U site in the template DNA fragments and then in turn a T across from each A on the complementary strands, producing apparent G → A and C → T substitutions (Dabney et al. 2013).

The final mitogenome consists of 16750 bp with 781 sites (4.6%) coded as N for missing, 100 coded as Y, 24 as R, 11 as M (A or C) and four as W (A or T). (In calculating the number of missing bases scored as N in the reconstructed *H. pauciradiatus* mitogenome we made the assumption that missing sequence was equal in length to the *H. longilateralis* query sequence. There are likely to be small length differences between the two mitogenomes in non-coding regions, hence the reported total length of the holotype mitogenome is inexact.) The circular genome as reconstructed by the MitoFish MitoAnnotator is shown in Fig. 2. The file from which we reconstructed the mitogenome of the holotype SRA is provided in Suppl. material 2. The annotated mitogenome was submitted to NCBI Nucleotide Database (GenBank) and is published as accession ON533765.

Using the same method, we attempted to reconstruct nuclear markers *rps7* and *rag2* from the holotype SRA using mormyrid sequences available in GenBank as query sequences, but BLAST searches found no significant matches. We suspect our greater success recovering mitochondrial sequences has to do with the far higher cellular copy number of mitochondrial versus nuclear genomes, enhancing the probability of persistence of some long DNA fragments of mitochondrial origin in highly degraded templates (Merheb et al. 2019).

Accession numbers and their GenSeq status (Chakrabarty et al. 2013) for sequences and genomes generated for this study given in Table 1.

Phylogenetic analyses

The tree produced from the phylogenetic analysis of the Cyt-*b* sequence data added to the Sullivan et al. (2016) dataset (Figs 3, 4; tree with all terminals shown in Suppl. material 3) demonstrates that the holotype of *Heteromormyrus pauciradiatus* as well as a specimen of *Paramormyrops tavernei* and an undescribed form from the Inkisi River of D.R. Congo belong to a clade within Mormyrinae containing species heretofore placed in genus *Hippopotamyrus* (*H. szaboi*, *H. longilateralis*) along with several unidentified or undescribed forms from subequatorial Africa, the group collectively referred to as the *Ha*SC in recent literature (Kramer et al. 2004; Kramer and Swartz 2010; Mutizwa et al. 2021).

In this tree the *H. pauciradiatus* holotype sequence falls within a cluster of three haplotypes from four specimens of the K4 mitochondrial lineage identified in Mutizwa et al. (2021) and with an allowance for the five bases coded "N" and two coded "Y" has an identical Cyt-*b* sequence to two of these, SAIAB 85203 (MW600881) and SAIAB 85209 (MW600880). Both of these specimens were collected in 2009 from the same site on the Lucala River in Angola with coordinates 9°25'30.0"S, 14°42'0.0"E. The remaining two K4 specimens are from downstream sites on the Lucala.

The Cyt-*b* sequence from *Paramormyrops tavernei* places it as sister lineage to a clade containing *H. szaboi* and related forms while the sequence from the Inkisi River

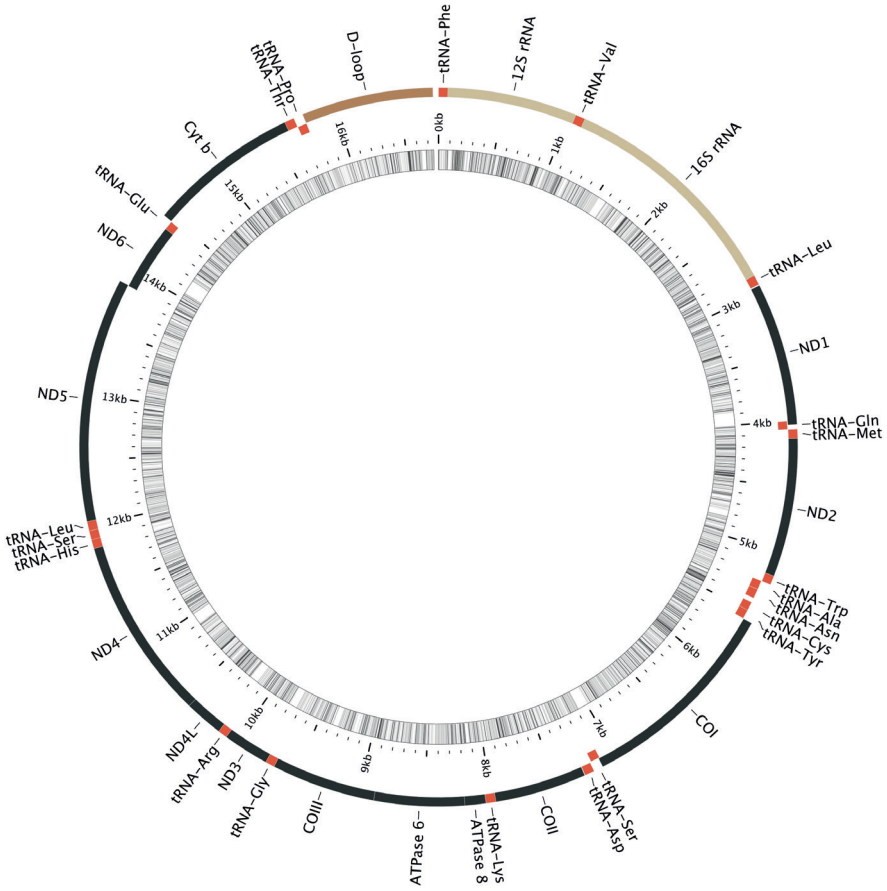

Figure 2. Visual representation of 16750 base-pair mitochondrial genome of *Heteromormyrus pauciradiatus* holotype specimen NMW 22417 as reconstructed from 150 base-pair, paired-end sequence data. Image produced from MitoFish MitoAnnotator v. 3.63. Coding genes black, non-coding regions red (tRNA genes), gold (ribosomal RNA genes) and brown (control region or D-loop). Genes transcribed on L-strand indented. Innermost circle represents percent GC per five base-pair segment, darker = higher; white areas indicate missing data. Because no sequences were recovered for the short tRNA-Ile gene, it appears absent from its normal position between genes ND1 and tRNA-Gln. Annotated mitogenome available in NCBI GenBank as accession ON533765.

specimen places it in a position subtending all other lineages within the *Ha*SC clade with the exception of the K5 lineage that is sister group to the rest.

This tree recapitulates the finding reported in Sullivan et al. (2016) and in Peterson et al. (2022) that the *Ha*SC clade is not monophyletic with *Hippopotamyrus castor* Pappenheim, 1906 from Cameroon, the type species of genus *Hippopotamyrus* and supports the conclusion that the *Ha*SC taxa are misclassified in that genus (Fig. 3).

Table 1. Accession numbers and GenSeq status for DNA sequences and genomes generated for this study, archived in NCBI GenBank and the NCBI Sequence Read Archive (SRA). WG = whole genome (unassembled Illumina paired-end reads).

Species	Voucher Catalog No.	Type Status	Locus/Loci	Sequence Read Achive	GenBank Accession(s)	GenSeq status
Heteromormyrus pauciradiatus	NMW 22417	holotype	WG, mitogenome	SRX7700131	ON533765	genseq-1 mitogenome
Heteromormyrus longilateralis	SAIAB 78793	holotype	WG, mitogenome	SRX5986274	MZ151890	genseq-1 mitogenome
Heteromormyrus tavernei	RMCA Vert 2018-032-P-0047	nontype	COI, Cyt-*b*	–	ON843622, ON858019	genseq-4 COI, genseq-4 CytB
Heteromormyrus sp. Inkisi River	AMNH 247102	nontype	COI, Cyt-*b*	–	ON843623, ON858020	–
Heteromormyrus aff. *szaboi* Kabompo EODtype1	SAIAB 210091/ KW12-AT3408/ SB8355	nontype	Cyt-*b*	–	ON088276	–
Heteromormyrus aff. *szaboi* Kabompo EODtype1	SAIAB 210127/ KW12-AT2748/ SB8356	nontype	Cyt-*b*	–	ON088277	–
Heteromormyrus aff. *szaboi* Kabompo EODtype2	SAIAB 210191/ KW12-AT3411/ SB8357	nontype	Cyt-*b*	–	ON088278	–
Heteromormyrus aff. *szaboi* Kabompo EODtype1	SAIAB 210191/ KW12-AT1012/ SB8358	nontype	Cyt-*b*	–	ON088279	–
Heteromormyrus aff. *szaboi* Kabompo EODtype1	SAIAB 210191/ KW12-AT2645/ SB8359	nontype	Cyt-*b*	–	ON088280	–
Heteromormyrus aff. *szaboi* Kabompo EODtype1	SAIAB 210191/ KW12-AT4962/ SB8360	nontype	Cyt-*b*	–	ON088281	–
Heteromormyrus aff. *szaboi* Kabompo EODtype2	SAIAB 210191/ KW12-AT2664/ SB8361	nontype	Cyt-*b*	–	ON088282	–
Heteromormyrus aff. *szaboi* Kabompo no EOD	SAIAB 210234/ KW12-AT4937/ SB8362	nontype	Cyt-*b*	–	ON088283	–
Heteromormyrus aff. *szaboi* Kabompo no EOD	SAIAB 210234/ KW12-AT2000/ SB8363	nontype	Cyt-*b*	–	ON088284	–
Heteromormyrus aff. *szaboi* Kabompo no EOD	SAIAB 210243/ KW12-AT4914/ SB8364	nontype	Cyt-*b*	–	ON088285	–
Heteromormyrus aff. *szaboi* Kabompo no EOD	SAIAB 210257/ KW12-AT4203/ SB8365	nontype	Cyt-*b*	–	ON088286	–
Heteromormyrus aff. *szaboi* Kabompo no EOD	SAIAB 210272/ KW12-AT4984/ SB8366	nontype	Cyt-*b*	–	ON088287	–
Heteromormyrus aff. *szaboi* Kabompo EODtype1	SAIAB 210149/ KW12-AT912/ SB8367	nontype	Cyt-*b*	–	ON088288	–

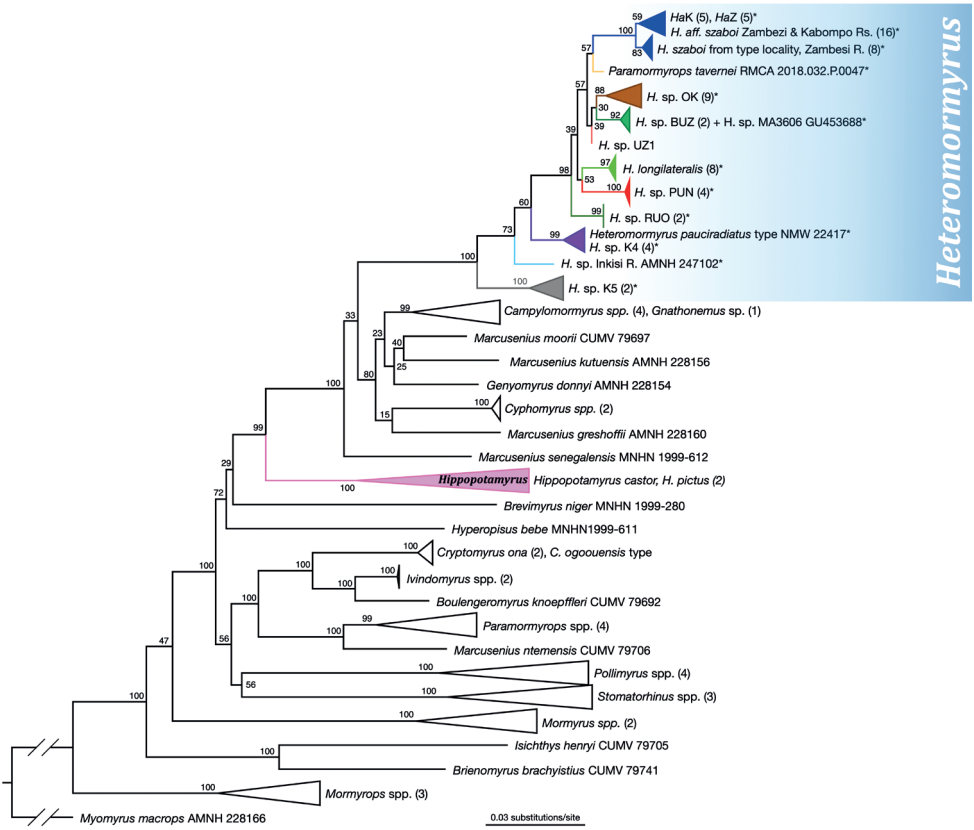

Figure 3. Phylogenetic position of *Heteromormyrus pauciradiatus* and other taxa of interest within subfamily Mormyrinae, inferred from cytochrome *b* and other markers. Maximum likelihood phylogenetic tree calculated in RAxML of 113 mormyrin OTUs, including all nominal mormyrin genera, from alignment of 4209 bases of mitochondrial cytochrome *b*, 12S, 16S and nuclear *rag2* and *rps7* intron. Rooted with *Myomyrus macrops*. Dataset is from Sullivan et al. (2016) to which was added all publicly available *Hippopotamyrus ansorgii* species complex cytochrome *b* sequences with the addition of sequences from *Heteromormyrus pauciradiatus* holotype NMW 22417, the *Hippopotamyrus longilateralis* holotype, *Paramormyrops tavernei*, an undescribed species from the Inkisi River in D.R. Congo and several sequences from *H.* aff. *szaboi* from the Zambezi and Kabompo rivers, Zambia. Asterisks indicate taxa represented by cytochrome *b* sequences only. Genus *Hippopotamyrus* is shown to be diphyletic with type species *Hippopotamyrus castor* clustering with *Hippopotamyrus pictus* separately from the *Hippopotamyrus ansorgii* species complex clade containing the holotype of *Heteromormyrus pauciradiatus*. The latter clade we reclassify as *Heteromormyrus*. Full tree with nodes uncollapsed available as Suppl. material 3. OTU names and colors match those used in Mutizwa et al. (2021).

The tree produced from the phylogenetic analysis of the COI sequence data (Fig. 5; tree with all terminals shown in Suppl. material 4) again shows the sequence from the *Heteromormyrus pauciradiatus* holotype nested within the K4 lineage clade (six unique haplotypes from 12 specimens). The holotype COI sequence is identical to one deposited in the BOLD database with sequence code SAFW518-09. This specimen, now catalogued as SAIAB 85120, was collected in 2008 at a site on the upper Lucala River

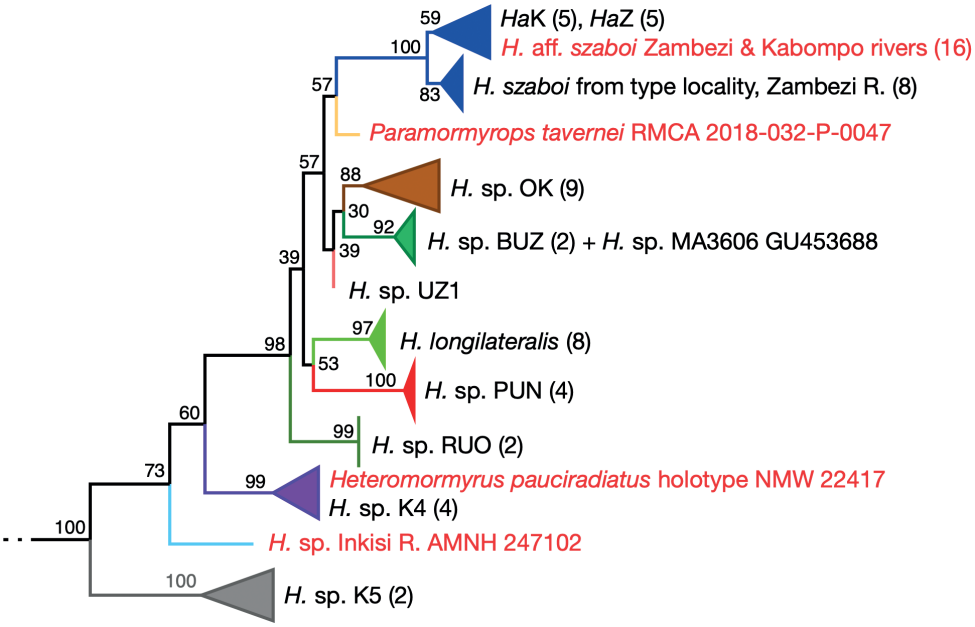

Figure 4. Enlargement of the newly recognized *Heteromormyrus* clade (including species and informally named entities formerly said to belong to the *Hippopotamyrus ansorgii* species complex) from the full tree in Fig. 3. New taxa added for this study indicated by red typeface. *Heteromormyrus pauciradiatus* holotype sequence clusters with sequences from the K4 lineage. Another misclassified taxon, *Paramormyrops tavernei*, and an undescribed taxon from the Inkisi River of the D.R. Congo appear within this clade as well, with strong bootstrap support.

just above the 105-meter-high, 400-meter-wide Kalandula Falls (09°4'26"S, 16°0'0"E). All but one of the K4 sequences are from specimens collected in the Lucala River, the northeastern tributary of the Kwanza. The remaining one, MW600858 from SAIAB 84726, is from the confluence of the Kawa and the Kwanza rivers in the lower Kwanza Basin, 09°10'17"S, 13°22'5"E. In this analysis, the undescribed species from the Inkisi River forms the sister lineage to the K4 clade and *P. tavernei* is unresolved within a large clade containing *H. szaboi*, *H. longilateralis*, K1–K3, and others.

In both analyses, bootstrap values indicate strong support for the inclusion of the *H. pauciradiatus* holotype sequences within the lineage called K4 by Mutizwa et al. (2021) and for inclusion of *P. tavernei* and the undescribed species from the Inkisi River within the larger *Ha*SC clade, itself well supported as a monophyletic group. A single topology of relationships among species and named clades within this group is not well supported by these data.

Taxonomy

Based on the phylogenetic results, we regroup six valid species into genus *Heteromormyrus* Steindachner, 1866, a name originally introduced as a subgenus of *Mormyrus* Linnaeus, 1758, but recognized by Taverne (1972) and subse-

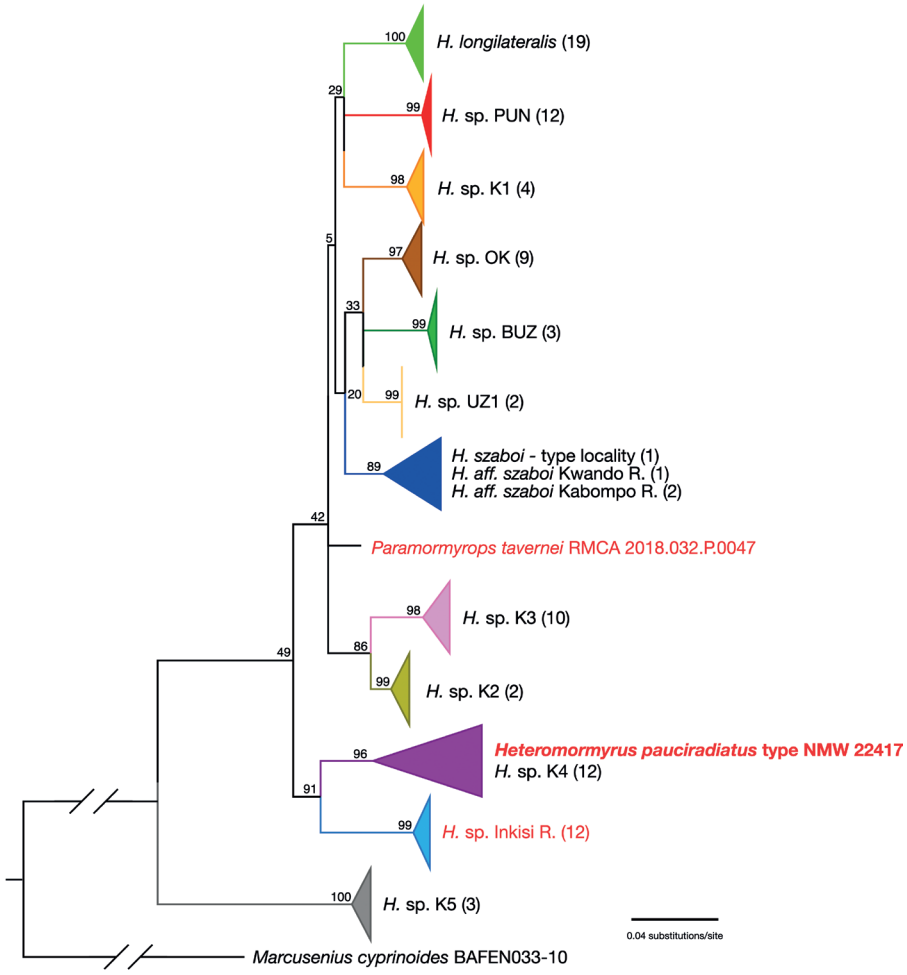

Figure 5. Maximum likelihood phylogenetic tree calculated in RAxML for 96 *Hippopotamyrus ansorgii* species complex COI sequences from the Barcode of Life Database (BOLD) with the addition of sequences from the holotype of *Heteromormyrus pauciradiatus* NMW 22417 (bold red type), *Hippopotamyrus longilateralis* holotype, *Paramormyrops tavernei* (red type) and an undescribed species from the Inkisi River in D.R. Congo (red type). Rooted with *Marcusenius cyprinoides*. Bootstrap values at selected nodes. Organismal names reproduced as they appear in BOLD. Colors of species/clades match those used in Mutizwa et al. (2021). Full tree with nodes uncollapsed in Suppl. material 4.

quent authors (Poll and Gosse 1995; Fricke et al. 2022) as a monotypic genus. *Heteromormyrus* has priority as the oldest available generic name with its type species within the clade formed by these species. The taxon indicated by the asterisk below is unsequenced and provisionally placed in *Heteromormyrus* pending study of fresh collections. For simplicity, only the original name combination and first use of subsequent combinations in the literature are shown beneath the name combination recognized here.

Family Mormyridae Bonaparte, 1831
Subfamily Mormyrinae Taverne, 1972

Genus *Heteromormyrus* Steindachner, 1866

Heteromormyrus Steindachner, 1866: 765 [as subgenus of *Mormyrus*; elevated to genus by Taverne 1972: 168; type species = *Mormyrus* (*Heteromormyrus*) *pauciradiatus* Steindachner, 1866, by original monotypy].

Species included

***Heteromormyrus pauciradiatus* (Steindacher, 1866)**

Mormyrus (*Heteromormyrus*) *pauciradiatus* Steindachner, 1866: 765, pl. 13, fig. 2.
Marcusenius pauciradiatus (Steindachner) [new combination by Boulenger 1898: 795]
Marcusenius (*Heteromormyrus*) *pauciradiatus* (Steindachner) [new subgeneric combination by Géry 1968: 76].
Pollimyrus pauciradiatus (Steindachner) [new combination by Taverne 1971a: 105].
Heteromormyrus pauciradiatus (Steindacher) [new combination by Taverne 1972: 168].

***Heteromormyrus ansorgii* (Boulenger, 1905), comb. nov.**

Marcusenius ansorgii Boulenger, 1905a: 457.
Hippopotamyrus ansorgii (Boulenger) [new combination by Taverne 1971a: 104].

Heteromormyrus pappenheimi* (Boulenger, 1910), comb. nov.

Marcusenius pappenheimi Boulenger, 1910: 540.
Hippopotamyrus pappenheimi (Boulenger) [new combination by Taverne 1971a: 104].

***Heteromormyrus tavernei* (Poll, 1972), comb. nov.**

Brienomyrus tavernei Poll, 1972: 166, fig. 2.
Paramormyrops tavernei (Poll) [new combination by Rich et al. 2017: 626].

***Heteromormyrus szaboi* (Kramer, van der Bank & Wink, 2004), comb. nov.**

Hippopotamyrus szaboi Kramer, van der Bank & Wink, 2004: 6, fig. 1A, B.

***Heteromormyrus longilateralis* (Kramer & Swartz, 2010), comb. nov.**

Hippopotamyrus longilateralis Kramer & Swartz, 2010: 2231, fig. 1A.

Images of type specimens of these species are shown in Fig. 6. Three additional new combinations and a synonymy in Mormyridae are introduced in the Discussion section below.

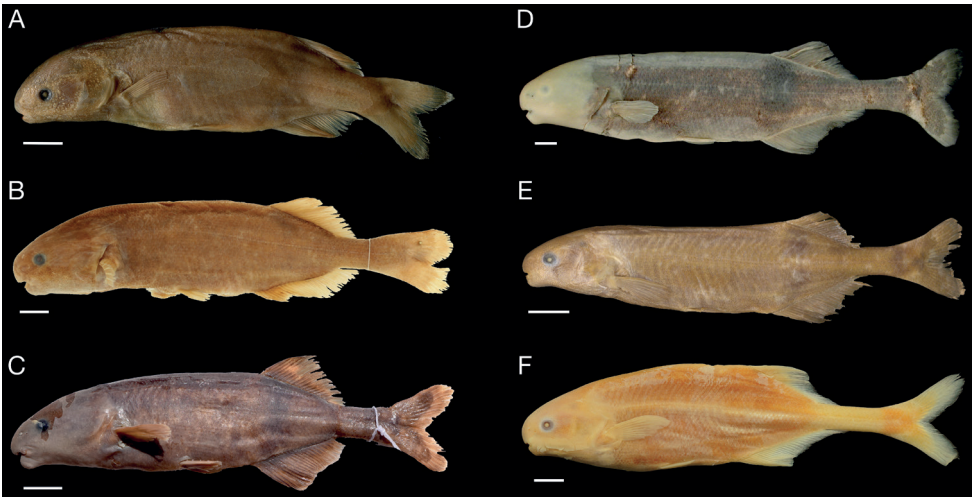

Figure 6. Images of types of *Heteromormyrus* species in left-side lateral view. **A** *Heteromormyrus pauciradiatus* (Steindacher, 1866), holotype, NMW 22417, Angola, 108 mm TL, photograph Naturhistorisches Museum Vienna **B** *Heteromormyrus tavernei* (Poll, 1972), holotype, MRAC 79-1-P-137, Masombwe, Kipepe River, tributary of Tumbwe River, Congo River basin, Democratic Republic of the Congo, 139 mm SL; photograph T. Nève, RMCA **C** *Heteromormyrus szaboi* (Kramer, van der Bank & Wink, 2004), holotype, SAIAB 67143, upper Zambezi River, Katima Mulilo, 17°29'30"S, 24°16'18"E. 94 mm SL; photograph A. Chakona **D** *Heteromormyrus longilateralis* (Kramer & Swartz, 2010), holotype, SAIAB 78793, above Epupa Falls, Kunene River, on the Namibian/Angolan border, 17°00'07"S, 013°14'57"E; 187 mm SL; photograph Kramer & Swartz **E** *Heteromormyrus ansorgii* (Boulenger, 1905a), syntype BMNH 1905.5.29.62; between Benguella and Bihé [Benguela and Bié], Angola; 96.9 mm SL; photograph J.P. Sullivan **F** *Heteromormyrus pappenheimi* (Boulenger, 1910), syntype ANSP 37971, Kwanza River at Cunga [= Cabala], Angola, 134 mm SL, right side reflected to face left; photograph K. Luckenbill, ANSP. Scale bars: 1 cm.

Discussion

A more complete history of the generic name *Heteromormyrus* is as follows. As related above, Steindachner (1866) introduced the name as a subgenus of *Mormyrus* for his new species *Mormyrus* (*Heteromormyrus*) *pauciradiatus*, based on the single specimen NMW 22417, the subject of this paper. Boulenger (1899) placed this species under *Marcusenius* Gill and subsequent authors treated this species as *Marcusenius pauciradiatus* (e.g., La-

diges 1964; Poll 1967) with Géry (1968) recognizing *Heteromormyrus* as a subgenus of *Marcusenius*, citing the specimen's unusually short caudal peduncle as a distinctive character. Without examining holotype specimen NMW 22417 and indicating that it had been lost in World War II, Taverne (1971a) initially placed the species under his new genus *Pollimyrus*. Later, recognizing that the name *Heteromormyrus* would have priority over *Pollimyrus*, Taverne (1972) gave *Heteromormyrus* separate generic status. The current collection manager of the Naturhistorisches Museum fish collection, A. Palandačić, cannot confirm that the type was ever missing.

Referring the *Ha*SC species and *P. tavernei* to genus *Heteromormyrus* is one small advance in what will have to be a much larger effort to establish natural (i.e., monophyletic) genera in the family Mormyridae. The sister clade to *Heteromormyrus* in the tree of Peterson et al. (2022) containing the polyphyletic genus *Marcusenius* as well as *Gnathonemus*, *Genyomyrus*, *Cyphomyrus*, and *Campylomormyrus* is in particular need of taxonomic attention. In this case progress was made possible by our ability to recover mitochondrial sequences from a 19th Century holotype specimen, heretofore an unconventional approach. Below we review what we know about the composition of genus *Heteromormyrus*, the morphological characteristics of these species, their geographic distribution and takeaway lessons from this first application of genomic shotgun sequencing to a problem in mormyrid taxonomy.

Was the *H. pauciradiatus* holotype collected far inland?

Franz Steindachner could not be more specific than "Angola" for the provenance of most of the species treated in his 1866 publication because he had obtained these specimens thirdhand: "all the described species with the exception of the Cyprinoidei I received during my second stay at Cadiz for a not inconsiderable amount of money from a Portuguese merchant who had just returned from Angola" (Steindachner 1866: 771). On maps from the period "Angola" referred to a much smaller area than the modern country of that name, viz. the territory extending east into the interior from Luanda on the coast, sandwiched roughly between the Congo territory north of the Rio Dande and the Benguella territory south of the Cuvo River (Baynes 1878). This region contains the central and lower reaches of the Kwanza, its main northeastern tributary, the Lucala, and the much smaller Bengo River to the north that empties separately into the Atlantic.

In his 1866 article, the first on Angolan freshwater fishes, Steindachner described eight other species (no other Mormyridae), two of which are now regarded as junior synonyms. These taxa—three cichlids, two clariid catfishes, two small barbs and one kneriid—are species characteristic of the Angolan coastal freshwater fauna (Skelton 2019). Given the limited European activity in the interior of this part of Africa at the time (Baynes 1878), we surmised the type of *Heteromormyrus pauciradiatus* had been taken near the coast. Hence our surprise to find identical sequences to that of the holotype from specimens collected more than 200 km inland from the upper Lucala River, the Kwanza River's major northeastern tributary. However, one member of the K4

mitochondrial lineage we now identify as *H. pauciradiatus* was collected in the lower Kwanza, close to the coast. Sampling remains very limited at present and future work may discover mitochondrial haplotypes in the lower Kwanza identical, or nearly so, to that of the type specimen.

Morphological characteristics of *Heteromormyrus* species

While a complete comparative morphometric and meristic treatment of *Heteromormyrus* species is beyond the scope of this study, for the purposes of preliminary comparisons we have assembled measurements taken by Harder (2000) of relevant mormyrid types (including the *H. pauciradiatus* holotype NMW 22417), measurements and counts in Kramer et al. (2004) and Kramer and Swartz (2010) of *Ha*SC species and forms, and new data taken from photos and radiographs of individuals identified as *H. pauciradiatus* in this study from their mitochondrial DNA sequences (Suppl. material 5).

The unusual appearance of the *Heteromormyrus pauciradiatus* holotype NMW 22417 is due to its short dorsal fin (17 rays) placed far back on the body and a very short (but deep) caudal peduncle. This is best captured by the morphometric ratio of the pre-dorsal length (tip of snout to origin of dorsal fin) divided by the standard length (PDL/SL). This ratio is 76% in the holotype, far higher than for any other mormyrid type or non-type specimen included in (Suppl. material 5: table S2). This ratio ranges from 66–70% in the seven measured K4 specimens. In the holotype, caudal peduncle length is only 15% of SL and caudal peduncle depth is 61% of caudal peduncle length, compared to 18–19% and 46–55% respectively in the seven measured K4 specimens now referred to *H. pauciradiatus*.

The reason for the holotype specimen's strange proportions is revealed in a radiograph showing an abnormality in the caudal skeleton (Fig. 7B). Vertebral centrum 31 in the anterior caudal peduncle is malformed and bears four neural spines and four hemal spines instead of one of each. Centrum 32 in the holotype appears to have three neural spines and two hemal spines. Centrum 33 appears normal with single neural and hemal spines, but centrum 34 bears two neural spines. The last full centrum in the holotype specimen is the 37th. Radiographs of five recently collected *H. pauciradiatus* (Fig. 7A, lineage K4 in Mutizwa et al. 2021) all show 41 total vertebrae, with caudal vertebrae bearing a single neural and hemal spine. From what appears to have been a developmental anomaly, the caudal peduncle of NMW 22417 is missing four caudal centra rendering it abnormally short for any kind of mormyrid. This short peduncle gives the specimen an odd appearance and renders all ratio measurements divided by standard length unusually high. The fact that *Heteromormyrus pauciradiatus* was defined by an individual with this deformity may help explain why this specific epithet was almost never subsequently used.

Having linked the somewhat misshapen type of *H. pauciradiatus* to recently collected specimens, we can identify some phenotypic characteristics that seem to distinguish this species from its congeners, pending more thorough study. (In the following

we remove the holotype from comparisons involving the caudal peduncle.) The body of *H. pauciradiatus* is shorter and deeper and the head is deeper than in other described *Heteromormyrus*: body depth 25–31% of SL, head depth 84–97% of head length. Predorsal distance is a greater percentage of SL than for other *Heteromormyrus*, 66–70%. The caudal peduncle is deeper than in other described *Heteromormyrus*: caudal peduncle depth 46–55% of caudal peduncle length. The eye of this species is small, 12–15% of head length.

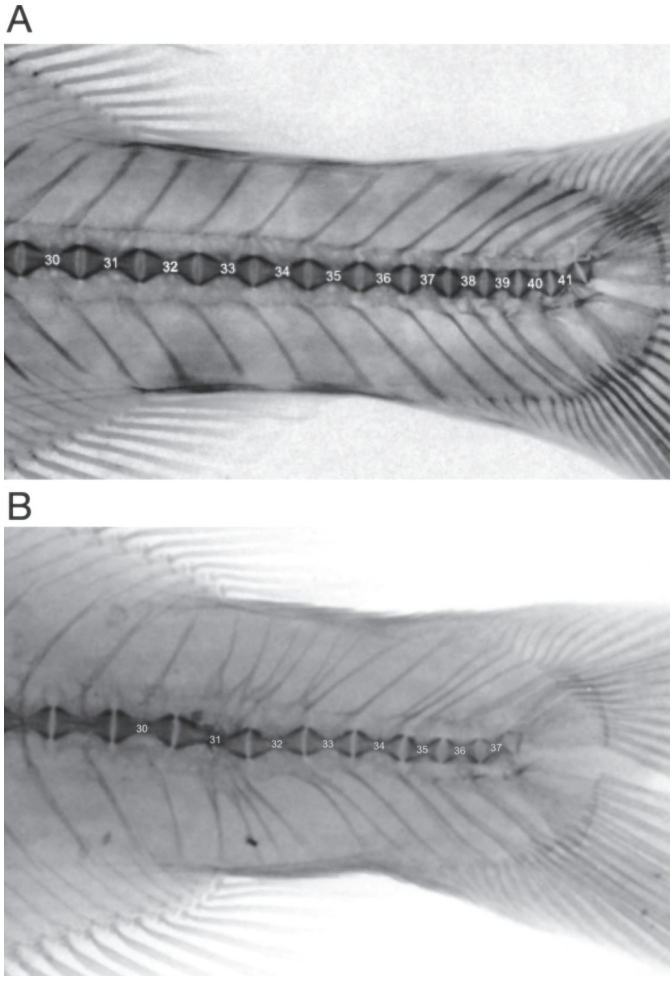

Figure 7. Radiographs showing caudal vertebrae in a recently collected *Heteromormyrus pauciradiatus* and in the *H. pauciradiatus* holotype NMW 22417. Vertebrae are numbered from first post-cranial centrum. **A** caudal peduncle of non-type *Heteromormyrus pauciradiatus* SAIAB 85120_SAF518-09(originally identified as lineage K4) from the Lucala River of Angola with 41 total vertebrae. Identical vertebral count was found in five other radiographed specimens of this species **B** caudal peduncle of *Heteromormyrus pauciradiatus* holotype NMW 22417, showing total vertebral count of 37, four fewer caudal vertebrae than a normal individual, and supernumerary neural and hemal spines at vertebrae 31, 32, and 34.

As noted above, until now only a single non-type specimen seems to have ever been referred to *H. pauciradiatus*. It is a very large individual (175 mm SL) collected by W.J. Ansorge in the Bengo River at Cabiri (8°54'52"S, 13°39'57"E), identified as *H. pauciradiatus* by George Boulenger (Boulenger 1910), BMNH 1910.11.28.44. The Bengo is a smaller coastal river emptying just to the north of the city of Luanda, Angola and the collection site near Cabiri is not far from the outskirts of the modern city. The specimen has an elongate, wide body with a blunt snout and a very deep caudal peduncle. The morphometrics are sufficiently different from those of the *H. pauciradiatus* holotype and the K4 specimens (Suppl. material 5: table S2) that we think it likely represents a distinct, undescribed species within *Heteromormyrus*, not *H. pauciradiatus*.

The peculiar holotype of *H. pauciradiatus* aside, the rather generalized appearance of all described and undescribed *Heteromormyrus* species and their lack of any obvious shared distinctive phenotypic character(s) may help explain why circumscription of this genus had to wait for molecular phylogenetic analysis. Species of the newly defined genus *Heteromormyrus*, here taken to include *H. pauciradiatus*, *H. ansorgii*, *H. pappenheimi*, *H. tavernei*, *H. szaboi*, *H. longilateralis*, as well as undescribed forms studied in Mutizwa et al. (2021) and the one included here from the Inkisi River are mormyrids of small to intermediate size (< 200 mm SL) with compressed to somewhat wide bodies for mormyrids. Heads are rounded, mouths are terminal to subterminal, chins with less developed swellings than those of species of *Marcusenius*; teeth are notched, usually 7/8 but as few as 5/7 and as many as 9/10. Median fins are situated far back on the body, with the dorsal fin (17–24 rays) origin slightly behind that of the anal (23–27 rays). Scales are 58–72 along lateral line and 12–20 around caudal peduncle. In all species there is a variously developed band of dark pigment on the body between the anterior of the median fins, several scales wide, sometimes broken along the midline. Individuals of several species and undescribed forms also show a blotch of dark pigment on the hypural plate area between the two lobes of the caudal fin.

The study of Peterson et al. (2022) showed the Nilo-Sudanic *Hippoptamyrus pictus* (Marcusen, 1864) and *Hippopotamyrus paugyi* Lévêque & Bigorne, 1985 from Upper Guinea to be close relatives of *H. castor*, the type species of genus *Hippopotamyrus*. All three have larger eyes and longer median fins (30 or more rays in both fins) that are equal in length to each other and symmetrically apposed (versus anal origin ahead of dorsal) compared to species and forms of *Heteromormyrus* and so the two genera are in fact not so morphologically similar.

Species of *Heteromormyrus* more closely resemble species of *Brienomyrus* Taverne, 1971, *Paramormyrops* Taverne, Thys van den Audenaerde & Heymer, 1977 and *Ivindomyrus* Taverne & Géry, 1975 in body proportions and counts, hence the mistaken placement of *H. tavernei* originally in *Brienomyrus* and its subsequent transfer to *Paramormyrops* (Rich et al. 2017). These genera are yet more distantly related to *Heteromormyrus* than is *Hippopotamyrus* (Fig. 3; Peterson et al. 2022). Species of *Paramormyrops*, *Ivindomyrus* and *Brienomyrus* lack the strong pigment between dorsal and anal (although some *Paramormyrops* do have very light, diffuse pigment in this

location) and the pigment blotch on the hypural region seen in many *Heteromormyrus* species and forms is absent.

It is our hope that targeted study of these similar-appearing clades of mormyrids using computed tomography (CT) will reveal heretofore missed osteological differences and diagnostic characters for some of these genera.

Newly recognized *Heteromormyrus* species and forms

***Heteromormyrus ansorgii* (Boulenger, 1905), Fig. 6E**

Boulenger (1905a) described *Marcusenius ansorgii* from two specimens collected by W.J. Ansorge from an indefinite location or locations "between Benguella and Bihé," an area extending more than 400 km from the coast to the interior of what is the modern country of Angola, including the headwaters of several important watersheds (Kramer et al. 2004). However, upon review of Ansorge's field notes Mutizwa et al. (2021) made the case that these type specimens must have been taken in the Kwanza River basin and so may correspond to one of the five Kwanza lineages (K1–K5) they identified. In his description of *Marcusenius ansorgii* Boulenger noted the similarity of his new species with *H. pauciradiatus* saying "this species is intermediate between *M. lhuysii*, Stdr., and *M. pauciradiatus*, Stdr." (*Mormyrus lhuysii* is today a subjective synonym of *Brevimyrus niger*). Given that the type of *H. pauciradiatus* was a malformed individual, might *H. ansorgii* in fact be a junior synonym of *H. pauciradiatus*? We think not. While Mutizwa et al. (2021) did not explicitly identify *H. ansorgii* with one of the mitochondrial lineages documented in the Kwanza Basin, their morphometric and meristic principal component analyses seem to point to their K3 lineage as the best match and rule out K4 that we herein identify as *H. pauciradiatus*. The *H. ansorgii* syntypes are much more elongate than both the *H. pauciradiatus* type and newly collected specimens, even excluding the post-anal body (Suppl. material 5: table S2), and both the holotype and recently collected examples of *H. pauciradiatus* exhibit a more rounded snout and fusiform body profile than the *H. ansorgii* types and indeed the other described species of *Heteromormyrus.* (The common name "slender stonebasher," while fitting for *H. ansorgii*, *H. szaboi*, and *H. longilateralis*, would not likely have been applied to *H. pauciradiatus*.)

***Heteromormyrus szaboi* (Kramer, van der Bank & Wink, 2004), Fig. 6C** ***Heteromormyrus longilateralis* (Kramer & Swartz, 2010), Fig. 6D**

Quite opposite the example of the unused taxon *Heteromormyrus pauciradiatus*, the name *Marcusenius ansorgii* / *Hippopotamyrus ansorgii* was initially overapplied to allopatric populations now recognized as multiple species of slender stonebasher (Mutizwa et al. 2021). Work combining morphometrics and meristics, DNA and EOD characters by Bernd Kramer and colleagues showed *H. szaboi* from the upper Zambezi along the Caprivi Strip of Namibia (Kramer et al. 2004) and *H. longilateralis* from the

Kunene River at the Namibia/Angola border (Kramer and Swartz 2010) to be distinct species from each other and from the syntypes of *H. ansorgii*.

In the description of *H. szaboi*, additional forms "HaZ" (for Zambezi River) and "HaK" (for Kwando River) were recognized based on EOD and sequence differences from *H. szaboi* but not described as species. The HaZ form was reported to occur in sympatry with *H. szaboi* at its type locality in the Zambezi. More recently, one of us (A.C.) has collected two EOD morphs of a *szaboi*-like fish in the Kabompo River, a major left-bank tributary of the upper Zambezi in northwestern Zambia. These were included in our phylogenetic analysis of Cyt-*b* sequences which establishes that *H. szaboi* and these *szaboi*-like forms (HaK, HaZ, unrecorded Zambezi fish, and Kabompo EOD morphs 1 and 2) constitute a monophyletic group. This group is divided into two subclades: one consisting of *H. szaboi* sensu stricto and the other containing all the other *szaboi*-like forms. Within the latter subclade there is little structure, despite evident morphological and EOD differences among the specimens (pers. obs.). The species status of these *szaboi*-like forms, referred to as *H. szaboi* in Mutizwa et al. (2021) and here as *H.* aff. *szaboi*, remains for future studies to determine.

Research teams from the South African Institute for Aquatic Biodiversity (NRF-SAIAB) have collected other slender stonebashers in southeastern Africa that merit further study and consideration of species status in the Ruo, Buzi, and Pungwe rivers. DNA sequences from these were included in the study of Mutizwa et al. (2021) and in this one.

Heteromormyrus pappenheimi **(Boulenger, 1910), Fig. 6F**

Boulenger (1910) described this species from W.J. Ansorge's Angolan collection based on numerous specimens taken at Cunga (Fazenda Cunga / Vila da Cabala on modern maps near the Kwanza River bridge ca. 09°16'54"S, 013°44'48"E). This is the only described species currently placed in *Hippopotamyrus* we are transferring to *Heteromormyrus* without the benefit of sequence data. We know of no other collections of this species since those of Ansorge despite the easy accessibility of the type locality on the lower Kwanza River. This species is something of an outlier morphologically from the others, with a more compressed body, a long, narrow caudal peduncle and higher median fin ray counts than the other species now placed in *Heteromormyrus.* The syntypes today have a bleached appearance but Boulenger's description indicates the transverse band of pigment between dorsal and anal typical for *Heteromormyrus* species was originally visible. The long peduncle and other differences could be related to its particular habitat in the main channel of lower Kwanza as opposed to the fast flowing, clear-water rocky streams typical of the others. Boulenger comments in his description that this species is "allied to [*Ivindomyrus*] *marchei* and [*Paramormyrops*] *kingsleyae*," two species from the Ogooué system far to the north. It does bear some similarity to the former of these in particular, another species found in large river channels with a long caudal peduncle. However, no member of the Lower Guinea Clade sensu Sullivan et al. (2016) to which those taxa belong has been recorded south of the Congo Basin. We can be confident it does not belong to genus

Hippopotamyrus and sequence data from freshly collected specimens will one day test our hypothesis that this species belongs with its Kwanza Basin rivermates in the genus *Heteromormyrus*.

Heteromormyrus tavernei **(Poll, 1972), Figs 6B, 8C**

From the upper Lualaba and Lufira basins upstream of Lake Upemba in northern Katanga of D.R. Congo, this is the only described species of *Heteromormyrus* from a part of the Congo Basin. Originally placed in genus *Brienomyrus* by Poll (1972), it was recently transferred to genus *Paramormyrops* by Rich et al. (2017), a genus to which many species formerly classified in *Brienomyrus* had been earlier transferred (Hopkins et al. 2007). This species has a distinctively wide head and body with a thick caudal peduncle. The transverse band of pigment between dorsal and anal typical of *Heteromormyrus* species is present although less prominent than in others. Its true affinities were unknown until its inclusion in Peterson et al. (2022) and in this study. The EOD characteristics of *H. tavernei* will be considered in a separate study. This species is currently the subject of doctoral research by C.M.M.

Heteromormyrus **sp. Inkisi River (undescribed), Fig. 8D**

Wamuini Lunkayilakio et al. (2010) recorded a fish they called *Hippopotamyrus* aff. *ansorgii* from the Inkisi River in D.R. Congo. The Inkisi is a faunistically interesting river that flows due north from Angola, emptying into the Lower Congo River downstream of Pool Malebo. Individuals of this undescribed species were COI barcoded in Sonet et al. (2019). The specimen sequenced for Peterson et al. (2022) and used here comes from a collection by Melanie Stiassny at the American Museum of Natural History in New York. The COI sequenced from this specimen (accession ON84362) is a perfect match to those deposited in GenBank by Sonet et al. (2019). This specimen is a deeper bodied fish, similar to *H. pauciradiatus* in body proportions. Indeed, the COI sequence from it places it as sister lineage to *H. pauciradiatus* (Fig. 5) while Cyt-*b* places it as sister to all *Heteromormyrus* but *H*. sp. K5 (Figs 3, 4). Whichever topology is accurate, we believe it most likely represents an undescribed species distinct from *H. pauciradiatus*.

Remaining problematic taxa in *Hippopotamyrus*

Even after removing the misclassified *Ha*SC species, genus *Hippopotamyrus* requires more attention as it contains several species that have never been well studied. Below we perform some housekeeping with four species currently classified in this genus, three of which belong neither in *Hippopotamyrus* nor in *Heteromormyrus*. Three of these four determinations lack DNA sequence data and are based on the sum total of available information, including original descriptions and photographs of types available on the Mormyridae Scratchpad website (Sullivan & Lavoué, 2022) and reports from field workers.

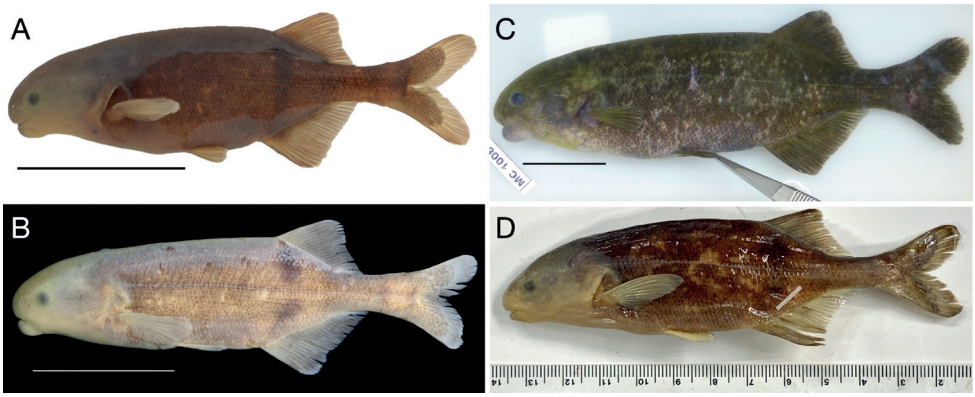

Figure 8. Images of recently collected *Heteromormyrus* specimens from which DNA sequences are used in this study **A** *Heteromormyrus pauciradiatus* SAIAB 85120_RM, Lucala River above Kalendula Falls, Kwanza Basin, Angola. Partial COI sequence from this specimen is identical to that recovered from *H. pauciradiatus* holotype **B** *Heteromormyrus pauciradiatus* SAIAB 84683_RM, Lucala River at N'dalatando Farm, Kwanza Basin, Angola **C** *Heteromormyrus tavernei* RMCA Vert 2018-032-P-0047 tag no. MC-1008, upper Lufira River before the confluence with Panda River, Democratic Republic of the Congo. Specimen sequenced for Peterson et al. (2022) and for this study **D** *Heteromormyrus* sp. Inkisi River AMNH 247102, Democratic Republic of the Congo. Specimen sequenced in Peterson et al. (2022) and for this study. Scale bars: 3 cm (**A–C**); millimeter scale (**D**). Photograph credits: SAIAB (**A, B**), J.P.S. (**C**), C.D.H. (**D**).

Hippopotamyrus harringtoni (Boulenger, 1905) = junior synonym of *Hippopotamyrus pictus* (Marcusen, 1864)

Boulenger's description of this species (in *Marcusenius*, later placed by some authors in *Gnathonemus* before Taverne (1971a) transferred it to *Hippopotamyrus*) from a single specimen from the Baro River (White Nile) of Ethiopia (Boulenger 1905b) is of dubious status. Lévêque and Bigorne (1985) suggested that the *H. harringtoni* type may simply have been a large specimen of *H. pictus* in which the somewhat more pronounced snout and absence of a lateral band of dark pigment between the dorsal and anal fins are concomitant features of this specimen's large size (305 mm TL). These authors document the phenomenon of this mark fading in other large specimens of *H. pictus* from West Africa that had been identified as *H. harringtoni.* Their examination of the holotype revealed a faint band between the median fins, similar to the dark one usually seen in *H. pictus*. They reidentified all West African *H. harringtoni* as *H. pictus* but did not formally synonymize the species themselves. Typical *H. pictus* are present in the Baro River of Ethiopia, type locality of *H. harringtoni* (J.P.S.; B. Levin, pers. comm.). We know of no recent specimens from the Baro as large as the *H. harringtoni* type or conforming closely to its phenotype. As more than a century has passed without new specimens corresponding to the description of the *H. harringtoni* type, we think it appropriate to formally place *H. harringtoni* as a junior synonym of *H. pictus*.

***Hippopotamyrus macroterops* (Boulenger, 1920) = *Pollimyrus macroterops* (Boulenger, 1920), comb. nov.**

Boulenger remarks that this species from Poko, Bas Uélé Province in D.R. Congo, described as *Marcusenius macroterops*, is "*très voisine*" to *M. tumifrons* Boulenger, 1902 which today is placed in genus *Pollimyrus* Taverne, 1971. With its large eye and dorsal fin terminus farther posterior than the anal fin terminus, it bears even more resemblance in our opinion to *Pollimyrus plagiostoma* (Boulenger, 1898), also from the Congo Basin. There can be little doubt this species belongs in *Pollimyrus*, a genus shown to be monophyletic in Peterson et al. (2022), although this species was not sequenced in that study.

***Hippopotamyrus weeksii* (Boulenger, 1902) = *Cyphomyrus weeksii* (Boulenger, 1902), comb. nov.**

Another Boulenger species from the Congo Basin described as a *Marcusenius*, later transferred to *Hippopotamyrus* by Taverne (1971a), *H. weeksi* resembles the type species of *Cyphomyrus*, *C. psittacus* (Boulenger, 1897) in having a deep body and a short, blunt snout. However dorsal and anal fins are nearly equal (instead of longer dorsal) and scales are larger than those of other *Cyphomyrus* species. The tree published in Peterson et al. (2022) places a sequenced specimen of this species as the sister to the included *Cyphomyrus* species, rendering *Cyphomyrus* the only sensible placement for it.

***Hippopotamyrus grahami* (Norman, 1928) = *Cyphomyrus grahami* (Norman, 1928), comb. nov.**

This unsequenced species originally described under *Marcusenius* is from the Kagera River and Lake Victoria in eastern Africa. It should be placed in genus *Cyphomyrus* Myers, 1960 by virtue of its arched dorsum and longer dorsal than anal fin. Photographs of specimens from recent collections of this species (D. Twedle, pers. comm.) show it to bear close resemblance to *Cyphomyrus discorhynchus* (Peters, 1852).

Distribution of *Heteromormyrus* species

The known distribution of *Heteromormyrus* species and populations extends from Atlantic to Indian Ocean watersheds between the latitudes of approximately 5°–20°S, making it the only mormyrid genus restricted to subequatorial Africa (Fig. 9).

The center of diversity for the clade appears to be the Kwanza Basin of Angola in which at least five genetic lineages (K1–K5) occur, some in sympatry (Mutizwa et al. 2021); one of these (K4) we identify here as *H. pauciradiatus*. The type locality of *H. pappenheimi* is on the lower Kwanza and the unspecified type locality of *H. ansorgii* is likely to be somewhere in the upper Kwanza (Mutizwa et al. 2021). While seemingly absent from the central Congo, representatives of this clade occur in opposite southern corners of this basin: the upper Lualaba and Lufira rivers in the east (*H. tavernei*) and

the Inkisi River, a left-bank affluent of the lower Congo that flows north from Angola, in the west (undescribed species). The pattern is the opposite that observed for all other mormyrid genera occurring in southern Africa (*Cyphomyrus*, *Marcusenius*, *Mormyrops*, *Mormyrus*, *Petrocephalus*, *Pollimyrus*) that are more diverse in the Congo Basin than in river systems to the south. *Heteromormyrus* species are present in the upper Zambezi Basin (*H. szaboi* and different forms here called *H.* aff. *szaboi*) as well as the lower Zambezi (*H.* sp. "Ruo") but so far absent in collections from the middle Zambezi (Mutizwa et al. 2021).

Lessons from whole genome shotgun sequencing of a fish holotype specimen

Since the early 1900s the standard practice for preserving fish specimens destined for collections has been fixation in a 10% formalin (= 4% formaldehyde) solution for days or weeks before transfer to 70–75% ethanol or 50% isopropanol. Earlier, fish specimens were simply preserved directly in "spirits," i.e., an ethanol solution of uncertain concentration. Formalin fixation greatly impairs DNA extraction procedures by cross-linking proteins to the DNA molecules and shearing DNA strands (Zimmermann et al. 2008). Hence 19th Century fish specimens are often the better candidates for DNA extraction and sequencing than those more recently collected, but formalin-fixed.

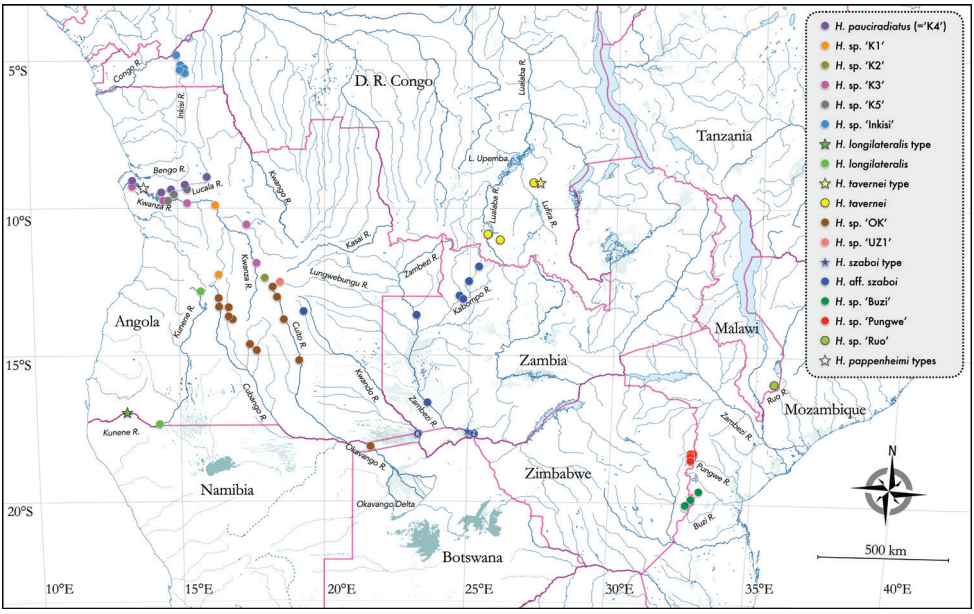

Figure 9. Map of continental Africa between 3° South latitude and Tropic of Capricorn showing distribution of *Heteromormyrus* species and lineages (sequenced specimens and other identified specimens). Type localities shown as star symbols. The localities of two EOD types of *H.* aff. *szaboi*, termed HaK and HaZ in Kramer et al. (2004), are indicated by the letters K and Z respectively inside two of the marker dots for *H.* aff. *szaboi*. Some points represent multiple adjacent collection sites. Basemap from FaunAfri (Paugy et al. 2008).

Sometimes referred to as "museomics," the application of high throughput sequencing (HTS) to historical DNA (hDNA) from museum specimens (those not originally intended to preserve genetic material and usually less than two centuries old) is emerging as a field distinct from the one concerned with recovery of ancient DNA (aDNA) from much older, naturally preserved samples (Raxworthy and Smith 2021). For hDNA samples, HTS may offer an alternative to the much more time- and labor-intensive Sanger method in which primers must be designed to amplify short stretches of the marker(s) of interest and these fragments separately amplified, sequenced and aligned.

Old fish type specimens have been sequenced before to solve taxonomic puzzles (e.g., Silva et al. 2017) but this may be the first application of whole genome HTS to such a case. Here, employing minimally altered protocols for DNA extraction and Illumina paired-end library preparation we recovered sufficient sequence to use the relatively simple method of "SRA BLASTing" to reconstruct a near-complete mitogenome from a fish holotype preserved more than 150 years ago. We used two markers from the holotype mitogenome to place this taxon in phylogenetic trees produced from sequences of recently collected specimens, resolving the longstanding question of its identity and putting its formerly unshared generic name to good use organizing mormyrid diversity. This approach could be a promising one for countless similar problems across taxonomic ichthyology.

Acknowledgements

The authors are indebted to A. Palandačić, Naturhistorisches Museum, Vienna, Austria for providing the tissue samples and radiograph of *Heteromormyrus pauciradiatus* holotype NMW 22417, K. Luckenbill, Academy of Natural Sciences of Philadelphia, USA for providing the photograph of the *H. pappenheimi* paratype, T. Nève, Royal Museum for Central Africa, Tervuren, Belgium (RMCA) for the photo of the *H. tavernei* type, I. Măndoiu, University of Connecticut, Storrs, Connecticut, USA for assistance with *H. longilateralis* mitogenome assembly, M. Stiassny, American Museum of Natural History, New York, USA for access to and tissue from the *H.* sp. Inkisi River specimen, B. Levin, Russian Academy of Sciences, Moscow, Russia for thoughts on *H. harringtoni*, D. Leipe, National Center for Biotechnology Information (NLM/NIH), Bethesda, Maryland, USA for translation of the Steindachner text from the German. From the South African Institute of Aquatic Biology (SAIAB), Makhanda, South Africa, we thank N. Mazungula for radiographs of Angolan *Heteromormyrus* specimens, P. Bragança for photographs of the same specimens and D. Tweddle for thoughts on *H. grahami.* We are grateful to P. Skelton, formerly of SAIAB, for stimulating early discussions on the identity of *Heteromormyrus pauciradiatus.* We thank B. Kramer and two anonymous reviewers for their useful comments on an early draft of this article and P. Bragança (again) for his contributions as editor. The authors' collaboration on *Heteromormyrus* grew out of a September 2018 workshop on mormyrid fishes held at the University of Lubumbashi (UNILU) in Lubumbashi, D.R. Congo, funded by the Mbisa Congo II Project, a framework agreement between the RMCA and the Belgian Development Cooperation. Sequencing was funded by a grant from Iridian Genomes, RG_2018_042

"Genomic Studies of Mormyrid Fishes" to R. Peterson. This research was supported in part by the National Center for Biotechnology Information of the National Library of Medicine (NLM), National Institutes of Health, Bethesda, Maryland, USA and by Computercraft Corporation, Washington, D.C., USA.

Finally, the authors pay tribute here to Franz Steindachner (1838–1919) for his devotion to the Naturhistorisches Museum Vienna and for his enormous contributions to ichthyology and herpetology (see: Jordan 1921, Wiley 1921, Kähsbauer 1959, Irmscher 2021).

References

Alqahtani F, Măndoiu I (2020a) Statistical Mitogenome Assembly with RepeaTs. Journal of Computational Biology 27(9): 1407–1421. https://doi.org/10.1089/cmb.2019.0505

Alqahtani F, Măndoiu I (2020b) SMART2: Multi-library Statistical Mitogenome Assembly with Repeats. Computational Advances in Bio and Medical Sciences, 184–198. https://doi.org/10.1007/978-3-030-46165-2_15

Alves-Gomes J, Hopkins C (1997) Molecular insights into the phylogeny of mormyriform fishes and the evolution of their electric organs. Brain, Behavior and Evolution 49(6): 324–329. https://doi.org/10.1159/000113001

Baynes TS (1878) Angola. Encyclopaedia Britannica 9th Edn. (v.2): 45. https://en.wikisource.org/wiki/Encyclop%C3%A6dia_Britannica,_Ninth_Edition/Angola

Bernt M, Donath A, Jühling F, Externbrink F, Florentz C, Fritzsch G, Pütz J, Middendorf M, Stadler P (2013) MITOS: Improved de novo metazoan mitochondrial genome annotation. Molecular Phylogenetics and Evolution 69(2): 313–319. https://doi.org/10.1016/j.ympev.2012.08.023

Boulenger GA (1898) A revision of the genera and species of fishes of the family Mormyridœ. Proceedings of the Zoological Society of London 66(4): 775–821. https://doi.org/10.1111/j.1096-3642.1898.tb03181.x

Boulenger GA (1905a) Descriptions of four new freshwater fishes discovered by Dr. W. J. Ansorge in Angola. Annals and Magazine of Natural History [Series 7] 15(89): 457–459. https://www.biodiversitylibrary.org/page/19244007

Boulenger GA (1905b) LVIII.—Description of a new mormyrid fish from the White Nile. Annals and Magazine of Natural History (Series 7) 15(89): 457–457. https://doi.org/10.1080/03745480509442833

Boulenger GA (1910) On a large collection of fishes made by Dr. W. J. Ansorge in the Quanza and Bengo rivers, Angola. Annals and Magazine of Natural History [Series 8] 6(36): 537–561. https://doi.org/10.1080/00222931008692887

Carlson BA, Sisneros JA, Popper AN, Fay RR (2019) Electroreception: Fundamental Insights from Comparative Approaches. ASA Press & Springer International Publishing, Cham, Switzertland, 367 pp. https://doi.org/10.1007/978-3-030-29105-1

Chakona A, Kadye W, Bere T, Mazungula D, Vreven E (2018) Evidence of hidden diversity and taxonomic conflicts in five stream fishes from the Eastern Zimbabwe Highlands freshwater ecoregion. ZooKeys 768: 69–95. https://doi.org/10.3897/zookeys.768.21944

Chakrabarty P, Warren M, Page L, Baldwin C (2013) GenSeq: An updated nomenclature and ranking for genetic sequences from type and non-type sources. ZooKeys 346: 29–41. https://doi.org/10.3897/zookeys.346.5753

Crampton WR (2019) Electroreception, electrogenesis and electric signal evolution. Journal of Fish Biology 95(1): 92–134. https://doi.org/10.1111/jfb.13922

Dabney J, Meyer M, Paabo S (2013) Ancient DNA Damage. Cold Spring Harbor Perspectives in Biology 5(7): a012567. https://doi.org/10.1101/cshperspect.a012567

Ford KL, Albert JS (2022) Is the medium the message? Functional diversity across abiotic gradients in freshwater electric fishes. Integrative & Comparative Biology 62: icac010. https://doi.org/10.1093/icb/icac010

Fricke R, Eschmeyer WN, Van der Laan R (2022) Eschmeyer's Catalog of Fishes: Genera, Species, References. http://researcharchive.calacademy.org/research/ichthyology/catalog/fishcatmain.asp [Accessed on: 2022-3-20]

Froese R, Pauly D (2022) Fishbase. http://www.fishbase.org [Accessed on: 2022-5-12]

Géry J (1968) Poissons du bassin de l'Ivindo IV. Note sur la nomenclature des Mormyridae. Biologia Gabonica 4(1): 73–81. http://mormyrids.myspecies.info/node/102

Gosse JP (1984) Mormyridae. In: Daget J, Gosse JP, Thys van den Audenaerde DF (Eds) CLOFFA 1: Check-List of the Freshwater Fishes of Africa. 1. ORSTOM, MRAC, Paris, Tervuren, 410 pp. https://horizon.documentation.ird.fr/exl-doc/pleins_textes/divers13-06/15357.pdf

Hahn C (2020) MitoFish2tble. C. Hahn (Github repository). https://github.com/chrishah/MitoFish2tbl

Harder W (2000) Mormyridae and other Osteoglossomorpha. Springer Verlag, New York. ETI-UNESCO (World Biodiversity Database CD-ROM Series).

Hopkins CD (1986) Behavior of Mormyridae. In: Bullock TH, Heiligenberg WF (Eds) Electroreception. John Wiley & Sons, New York, 722 pp. http://pages.nbb.cornell.edu/neurobio/hopkins/Reprints/Behavior_Mormyridae.pdf

Hopkins CD, Lavoué S, Sullivan JP (2007) Mormyridae. In: Stiassny ML, Teugels GG, Hopkins CD (Eds) The Fresh and Brackish Water Fishes of Lower Guinea, West-Central Africa. Vol.1. IRD-MNHN-MRAC, Paris & Tervuren, 115 pp.

Irmscher C (2021) In Gedanken in Amerika: The Evolution of Franz Steindachner In: Zacharasiewicz W, Nagl-Docekal H (Eds) Transatlantic elective affinities: traveling ideas and their mediators. Austrian Academy of Sciences Press, Vienna, 79–106. https://doi.org/10.2307/j.ctv1zqdvdj.7

Iwasaki W, Fukunaga T, Isagozawa R, Yamada K, Maeda Y, Satoh TP, Sado T, Mabuchi K, Takeshima H, Miya M, Nishida M (2013) MitoFish and MitoAnnotator: A Mitochondrial Genome Database of Fish with an Accurate and Automatic Annotation Pipeline. Molecular Biology and Evolution 30(11): 2531–2540. https://doi.org/10.1093/molbev/mst141

Jordan DS (1921) Franz Steindachner. Science 53(1360): 68. https://doi.org/10.1126/science.53.1360.68.a

Kähsbauer P (1959) Intendant Dr. Franz Steindachner, sein Leben und Werle. Annalen des Naturhistorischen Museums in Wien 63: 3–30. https://www.zobodat.at/pdf/ANNA_63_0001-0030.pdf

Kehlmaier C, Zhang X, Georges A, Campbell PD, Thomson S, Fritz U (2019) Mitogenomics of historical type specimens of Australasian turtles: Clarification of taxonomic confusion and

old mitochondrial introgression. Scientific Reports 9(1): 5841. https://doi.org/10.1038/s41598-019-42310-x

Kramer B (2021) Communication and waveform analysis in weakly electric fishes with special emphasis on mormyrids. In: Fritzsch B, Bleckmann H (Eds) The Senses: A Comprehensive Reference Second Edition, Vol. 7. Elsevier, Academic Press, Amsterdam, 258–280. [ISBN 9780128054086]

Kramer B, Swartz E (2010) A new species of Slender Stonebasher within the *Hippopotamyrus ansorgii* complex from the Cunene River in southern Africa (Teleostei: Mormyriformes). Journal of Natural History 44(35): 2213–2242. https://doi.org/10.1080/00222931003764089

Kramer B, Van Der Bank H, Wink M (2004) *Hippopotamyrus ansorgii* species complex in the Upper Zambezi River System with a description of a new species, *H. szaboi* (Mormyridae). Zoologica Scripta 33(1): 1–18. https://doi.org/10.1111/j.1463-6409.2004.00132.x

Ladiges W (1964) Beiträge zur zoogeographie und Oekologie der süßwasserfische Angolas. Mitteilungen aus dem Hamburgischen Zoologischen Museum und Institut 61: 221–272.

Lanfear R, Calcott B, Ho SYW, Guindon S (2012) PartitionFinder: Combined Selection of Partitioning Schemes and Substitution Models for Phylogenetic Analyses. Molecular Biology and Evolution 29(6): 1695–1701. https://doi.org/10.1093/molbev/mss020

Lavoué S, Bigorne R, Lecointre G, Agnèse J (2000) Phylogenetic relationships of mormyrid electric fishes (Mormyridae; Teleostei) inferred from cytochrome b sequences. Molecular Phylogenetics and Evolution 14(1): 1–10. https://doi.org/10.1006/mpev.1999.0687

Lavoué S, Miya M, Arnegard ME, Sullivan JP, Hopkins CD, Nishida M (2012) Comparable ages for the independent origins of electrogenesis in African and South American weakly electric fishes. PLoS ONE 7(5): e36287. https://doi.org/10.1371/journal.pone.0036287

Lévêque C, Bigorne R (1985) Le genre *Hippopotamyrus* (Pisces, Mormyridae) en Afrique de l'Ouest, avec la description d'*Hippopotamyrus paugyi* n. sp. Cybium 9(2): 175–192. https://sfi-cybium.fr/fr/le-genre-hippopotamyrus-pisces-mormyridae-en-afrique-de-louest-avec-la-description-dhippopotamyrus

Levin B, Golubtsov A (2017) New insights into the molecular phylogeny and taxonomy of mormyrids (Osteoglossiformes, Actinopterygii) in northern East Africa. Journal of Zoological Systematics and Evolutionary Research 56(1): 61–76. https://doi.org/10.1111/jzs.12186

McGuire JA, Cotoras DD, O'Connell B, Lawalata SZS, Wang-Claypool CY, Stubbs A, Huang X, Wogan GOU, Hykin SM, Reilly SB, Bi K, Riyanto A, Arida E, Smith LL, Milne H, Streicher JW, Iskandar DT (2018) Squeezing water from a stone: High-throughput sequencing from a 145-year old holotype resolves (barely) a cryptic species problem in flying lizards. PeerJ 6: e4470. https://doi.org/10.7717/peerj.4470

Merheb M, Matar R, Hodeify R, Siddiqui SS, Vazhappilly CG, Marton J, Azharuddin S, Al Zouabi H (2019) Mitochondrial DNA, a Powerful Tool to Decipher Ancient Human Civilization from Domestication to Music, and to Uncover Historical Murder Cases. Cells 8(5): 433. https://doi.org/10.3390/cells8050433

Miller MA, Pfeiffer W, Schwartz T (2010) Creating the CIPRES Science Gateway for inference of large phylogenetic trees. 2010 Gateway Computing Environments Workshop (GCE). IEEE, New Orleans, 8 pp. https://doi.org/10.1109/GCE.2010.5676129

Moller P (1995) Electric Fishes: History and Behavior. Chapman & Hall, London/New York, 584 pp. https://www.springer.com/gp/book/9780412373800 [ISBN 0412373807]

Mutizwa T, Kadye W, Chakona A (2021) Deep genetic and morphological divergence in the *Hippopotamyrus ansorgii* species complex (Teleostei: Mormyridae) in southern Africa. Journal of Fish Biology 99(2): 543–556. https://doi.org/10.1111/jfb.14743

Myers GS (1960) The mormyrid genera *Hippopotamyrus* and *Cyphomyrus.* Stanford Ichthyological Bulletin 7(4): 123–125. https://mormyrids.myspecies.info/en/node/111

Paugy D, Zaiss R, Troubat JJ (2008) FaunAfri. http://www.poissons-afrique.ird.fr/faunafri/ [Accessed on: 2021-8-20]

Peterson RD, Sullivan JP, Hopkins CD, Santaquiteria A, Dillman CB, Pirro S, Betancur-R R, Arcila D, Hughes LC, Ortí G (2022) Phylogenomics of bony-tongue fishes (Osteoglossomorpha) shed light on the craniofacial evolution and biogeography of the weakly electric clade Mormyridae. Systematic Biology 71(5): 1032–1044. https://doi.org/10.1093/sysbio/syac001

Poll M (1967) Contribution à la Faune Ichthyologique de l'Angola. Publicações Culturais 75. Companhia dos Diamentes de Angola (DIAMANG), Lisbon, 381 pp.

Poll M (1972) Description de deux espèces nouvelles de Mormyridae du Bassin du Congo appartenant aux genres *Brienomyrus* Tav. et *Pollimyrus* Tav. Revue de Zoologie et de Botanique Africaines 85(1–2): 163–168. https://mormyrids.myspecies.info/en/node/99

Poll M, Gosse J-P (1995) Genera des poissons d'eau douce de l'Afrique. Mémoire de la Classe des Sciences. 9. Académie royale de Belgique, Brussels, 324 pp. http://zoobank.org/04ac5500-17ca-442f-820f-10d93bbbe388

Raxworthy CJ, Smith BT (2021) Mining museums for historical DNA: Advances and challenges in museomics. Trends in Ecology & Evolution 36(11): 1049–1060. https://doi.org/10.1016/j.tree.2021.07.009

Reyes-Velasco J, Goutte S, Freilich X, Boissinot S (2021) Mitogenomics of historical type specimens clarifies the taxonomy of Ethiopian *Ptychadena* Boulenger, 1917 (Anura, Ptychadenidae. ZooKeys 1070: 135–149. https://doi.org/10.3897/zookeys.1070.66598

Rich M, Sullivan J, Hopkins C (2017) Rediscovery and description of *Paramormyrops sphekodes* (Sauvage, 1879) and a new cryptic *Paramormyrops* (Mormyridae: Osteoglossiformes) from the Ogooué River of Gabon using morphometrics, DNA sequencing and electrophysiology. Zoological Journal of the Linnean Society 180(3): 618–646. https://doi.org/10.1093/zoolinnean/zlw004

Roos C, Miguez RP, Sabin R, Louis Jr EE, Hofreiter M, Zinner D (2021) Mitogenomes of historical type specimens unravel the taxonomy of sportive lemurs (*Lepilemur* spp.) in Northwest Madagascar. Zoological Research 42(4): 428–432. https://doi.org/10.24272/j.issn.2095-8137.2021.157

Sabaj MH (2020) Codes for Natural History Collections in Ichthyology and Herpetology. Copeia 108(3): 593–669. https://doi.org/10.1643/ASIHCODONS2020

Satoh TP, Miya M, Mabuchi K, Nishida M (2016) Structure and variation of the mitochondrial genome of fishes. BMC Genomics 17(1): 719. https://doi.org/10.1186/s12864-016-3054-y

Silva P, Malabarba M, Malabarba L (2017) Using ancient DNA to unravel taxonomic puzzles: the identity of *Deuterodon pedri* (Ostariophysi: Characidae). Neotropical Ichthyology 15(01): e160141. https://doi.org/10.1590/1982-0224-20160141

Silva P, Malabarba MC, Vari R, Malabarba L (2019) Comparison and optimization for DNA extraction of archived fish specimens. MethodsX 6: 1433–1442. https://doi.org/10.1016/j.mex.2019.06.001

Skelton P (2019) The Freshwater Fishes of Angola. In: Huntley BJ, Russo V, Lages F, Ferrand N (Eds) Biodiversity of Angola. Springer Open, Cham, Switzerland, 207–242. https://doi.org/10.1007/978-3-030-03083-4_11

Sonet G, Snoeks J, Nagy Z, Vreven E, Boden G, Breman F, Decru E, Hanssens M, Ibala Zamba A, Jordaens K, Mamonekene V, Musschoot T, Van Houdt J, Van Steenberge M, Lunkayilakio Wamuini S, Verheyen E (2019) DNA barcoding fishes from the Congo and the Lower Guinean provinces: Assembling a reference library for poorly inventoried fauna. Molecular Ecology Resources 19(3): 728–743. https://doi.org/10.1111/1755-0998.12983

Stamatakis A (2014) RAxML version 8: A tool for phylogenetic analysis and post-analysis of large phylogenies. Bioinformatics 30(9): 1312–1313. https://doi.org/10.1093/bioinformatics/btu033

Steindachner F (1866) Ichthyologische Mittheilungen (IX.) Über einige neue Süsswasserfische aus Angola. Verhandlungen der K.-K. zoologisch-botanischen Gesellschaft in Wien 16. https://www.biodiversitylibrary.org/page/26723992

Sullivan JP (2022) SRA BLASTing [Video]. YouTube. https://youtu.be/L7yhxtXcyDM

Sullivan JP, Lavoué S (2022) Mormyridae - African Weakly Electric Fishes Scratchpad. http://mormyrids.myspecies.info [Accessed on: 2022-5-03]

Sullivan JP, Lavoué S, Hopkins CD (2000) Molecular systematics of the African electric fishes (Mormyroidea: Teleostei) and a model for the evolution of their electric organs. The Journal of Experimental Biology 203(4): 665–683. https://doi.org/10.1242/jeb.203.4.665

Sullivan JP, Lavoué S, Hopkins CD (2016) *Cryptomyrus*: A new genus of Mormyridae (Teleostei, Osteoglossomorpha) with two new species from Gabon, West-Central Africa. ZooKeys 561: 117–150. https://doi.org/10.3897/zookeys.561.7137

Taverne L (1971a) Note sur la systématique des poissons Mormyriformes. Le problème des genres *Gnathonemus* Gill, *Marcusenius* Gill, *Hippopotamyrus* Pappenheim, *Cyphomyrus* Myers et les nouveaux genres *Pollimyrus* et *Brienomyrus*. Revue de Zoologie et de Botanique Africaines 84(1–2): 99–110. https://mormyrids.myspecies.info/en/node/446

Taverne L (1971b) Ostéologie des Genres *Marcusenius* Gill, *Hippopotamyrus* Pappenheim, *Cyphomyrus* Myers, *Pollimyrus* Taverne et *Brienomyrus* Taverne (Pisces Mormyriformes). Annales du Musée Royal de l'Afrique Centrale Sér. IN-8°. Sciences Zoologiques 188: 1–144.

Taverne L (1972) Ostéologie des genres *Mormyrus* Linné, *Mormyrops* Müller, *Hyperopisus* Gill, *Myomyrus* Boulenger, *Stomatorhinus* Boulenger et *Gymnarchus* Cuvier. Considérations générales sur la systématique des poissons de l'ordre des Mormyriformes. Annales du Musée Royal de l'Afrique Centrale Sér. IN-8°. Sciences Zoologiques 200: 1–194.

Wamuini Lunkayilakio S, Vreven E, Vandewalle P, Mutambue S, Snoeks J (2010) Contribution à la connaissance de l'ichtyofaune de l'Inkisi au Bas-Congo (RD du Congo). Cybium 34(1): 83–91. https://doi.org/10.26028/cybium/2010-341-009

Wiley HW (1921) Franz Steindachner. Science 53(1377): 486. https://doi.org/10.1126/science.53.1377.486.a

Zimmermann J, Hajibabaei M, Blackburn DC, Hanken J, Cantin E, Posfai J, Evans Jr TC (2008) DNA damage in preserved specimens and tissue samples: A molecular assessment. Frontiers in Zoology 5(1): 18. https://doi.org/10.1186/1742-9994-5-18

Supplementary material 1

List of *Heteromormyrus* specimens examined and/or included in molecular analyses
Author: John P. Sullivan
Data type: Excel table.

Link: https://doi.org/10.3897/zookeys.1129.90287.suppl1

Supplementary material 2

***Heteromormyrus pauciradiatus* holotype NMW 22417 mitogenome reconstruction**
Author: John P. Sullivan
Data type: Text.
Explanation note: Results of BLASTn search of complete mitogenome of *Hippopotamyrus longilateralis* SAIAB 79793 against SRA archive SRX7700131 of *Heteromormyrus pauciradiatus* holotype NMW 22417 and inference of its mitochondrial sequence.

Link: https://doi.org/10.3897/zookeys.1129.90287.suppl2

Supplementary material 3

Cyt *b* plus nuclear markers phylogenetic analysis
Author: John P. Sullivan
Data type: Image (pdf file).
Explanation note: Full tree from RAxML analysis with uncollapsed nodes.

Link: https://doi.org/10.3897/zookeys.1129.90287.suppl3

Supplementary material 4

COI phylogenetic analysis
Author: John P. Sullivan
Data type: Image (pdf file).
Explanation note: Full tree from RAxML analysis with uncollapsed nodes.

Link: https://doi.org/10.3897/zookeys.1129.90287.suppl4

Supplementary material 5

Measurements and counts of *Heteromormyrus* specimens and relevant mormyrid types from existing literature and taken from photographs & radiographs of newly sequenced individuals
Author: John P. Sullivan
Data type: Excel table.

Link: https://doi.org/10.3897/zookeys.1129.90287.suppl5

ZooKeys 1129: 197–200 (2022)
doi: 10.3897/zookeys.1129.95715
https://zookeys.pensoft.net

CORRIGENDA

A peer-reviewed open-access journal
ZooKeys
Launched to accelerate biodiversity research

Corrigendum: Filander ZN, Kitahara MV, Cairns SD, Sink KJ, Lombard AT (2021) Azooxanthellate Scleractinia (Cnidaria, Anthozoa) from South Africa. ZooKeys 1066: 1–198. https://doi.org/10.3897/zookeys.1066.69697

Zoleka N. Filander[1,2], Marcelo V. Kitahara[3,4], Stephen D. Cairns[5], Kerry J. Sink[6,7], Amanda T. Lombard[7]

1 *Biodiversity and Coastal Research, Oceans and Coasts, Department of Forestry, Fisheries, and Environment, Cape Town, South Africa* **2** *Zoology Department, Nelson Mandela University, Port Elizabeth, South Africa* **3** *Universidade Federal de São Paulo, Departamento de Ciências do Mar, Santos, Brazil* **4** *Centro de Biologia Marinha, Universidade de São Paulo, São Sebastião, Brazil* **5** *Department of Invertebrate Zoology, Smithsonian Institution, Washington DC, USA* **6** *South African National Biodiversity Institute, Cape Town, South Africa* **7** *Institute for Coastal and Marine Research, Nelson Mandela University, Port Elizabeth, South Africa*

Corresponding author: Zoleka N. Filander (zfilander@gmail.com)

Academic editor: James Reimer | Received 27 September 2022 | Accepted 28 September 2022 | Published 16 November 2022

https://zoobank.org/E2488A6A-B88B-4B4C-957E-E4977D38C1ED

Citation: Filander ZN, Kitahara MV, Cairns SD, Sink KJ, Lombard AT (2022) Corrigendum: Filander ZN, Kitahara MV, Cairns SD, Sink KJ, Lombard AT (2021) Azooxanthellate Scleractinia (Cnidaria, Anthozoa) from South Africa. ZooKeys 1066: 1–198. https://doi.org/10.3897/zookeys.1066.69697. ZooKeys 1129: 197–200. https://doi.org/10.3897/zookeys.1129.95715

This is a short communication to revise the plates presented in the Filander et al. (2021) monograph on the South African azooxanthellate coral fauna. The authors moreover take this opportunity to retract the addition of *Paracontrochus capensis* (Gardiner, 1904) as a synonym of *Monohedotrochus capensis* (Gardiner, 1905). Cairns and Parker (1992) based their new combination of *P. capensis* on *Duncania capensis* Gardiner, 1904. In other words, Gardiner's (1904) species is *P. capensis* and should be considered to occur in South Africa. Below we present the updated species synonymy and the revised figures.

Revised figures

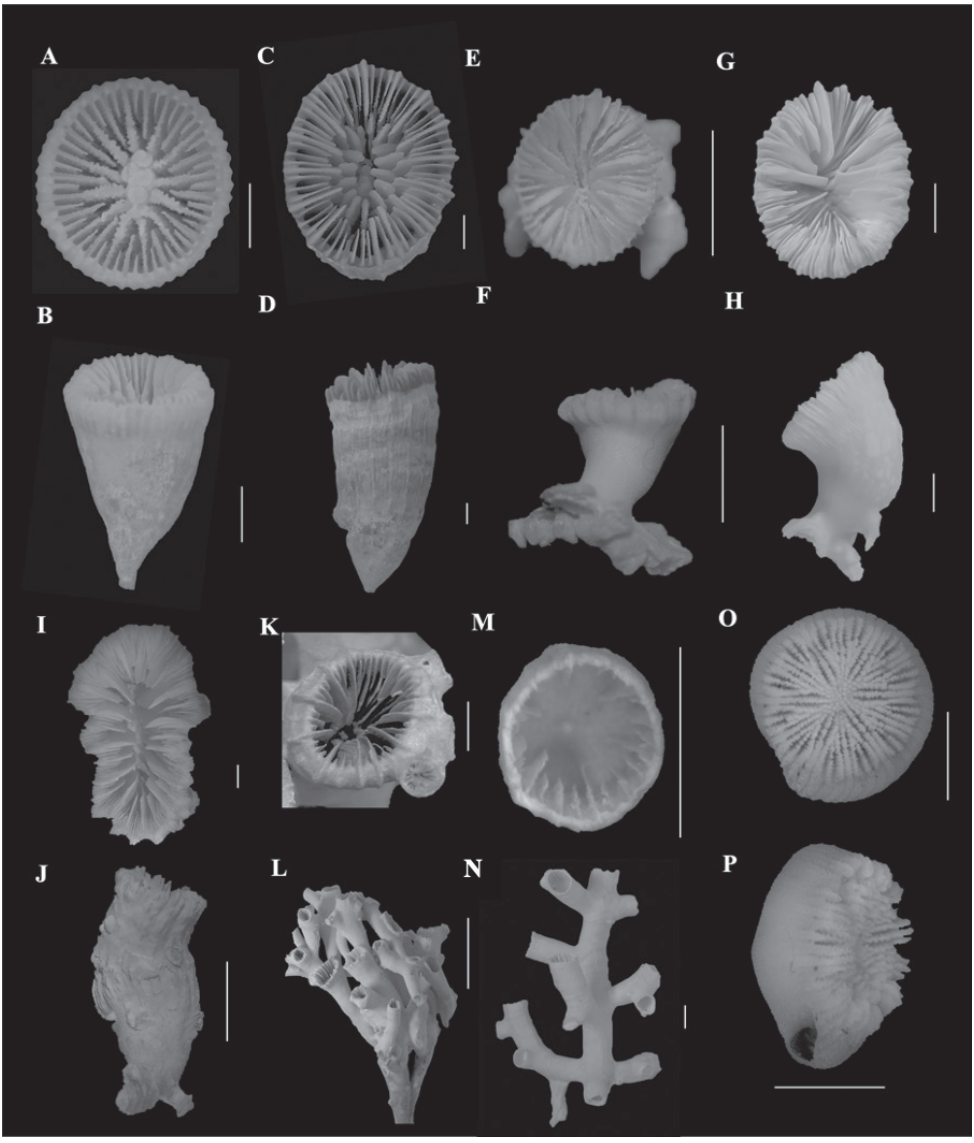

Figure 3. A, B *Caryophyllia* (*Caryophyllia*) *stellula* (SAM_H1485, off Agulhas, 200 m) **A** calicular view **B** lateral view **C, D** *Caryophyllia* (*Caryophyllia*) *valdiviae* (SAM_H3108, off Durban, depth unknown) **C** calicular view **D** lateral view **E, F** *Crispatotrochus cornu* (UCT_NAD 17 F, off Isipingo, 49 m) **E** calicular view **F** lateral view **G, H, I, J** *Desmophyllum dianthus* **G, H** (SAMC_A077974, off Paternoster, 440 m) **G** calicular view **H** lateral view **I, J** (BMNH.1939.7.20.218, locality data unknown) **I** calicular view **J** lateral view **K, L** *Desmophyllum pertusum* (SAM_H1605, off Melkbosstrand, depth unknown) **K** calicular view **L** lateral view **M, N** *Goniocorella dumosa* (SAM_H3190, off Kidds Beach, 760 m) **M** calicular view **N** lateral view **O, P** *Heterocyathus aequicostatus* (SAMC_A073186, off Durban, 150 m) **O** calicular view **P** lateral view. Scale bars: 10 mm (**A–I, K–P**); 100 mm (**J**).

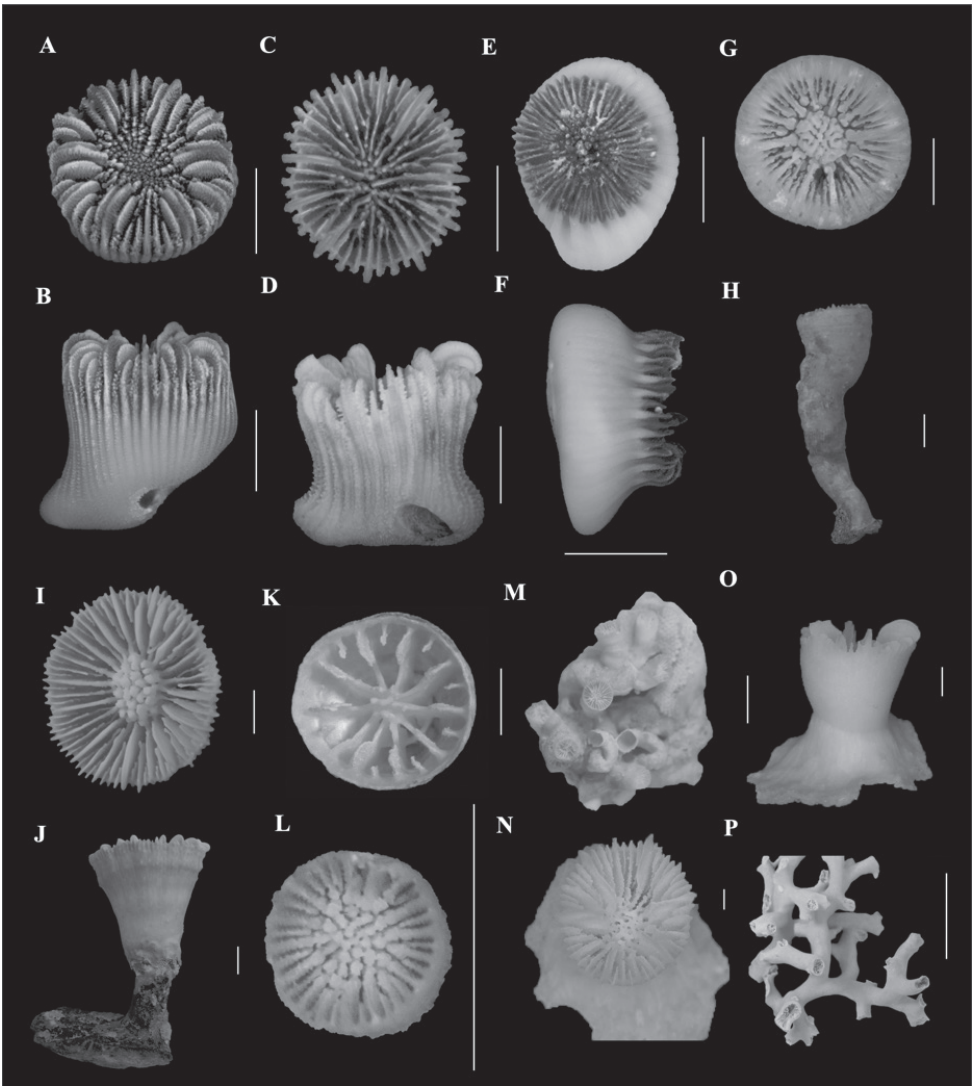

Figure 4. A, B *Heterocyathus alternatus* (ORI_DIIIe1_1, locality data unknown) **A** calicular view **B** lateral view **C, D** *Heterocyathus monileseptatum* sp. nov. (SAM_H1431, off Durban Harbour, 99 m) **C** calicular view **D** lateral view **E, F** *Heterocyathus sulcatus* (SAMC_A073123, off Shaka's Rock, 100–105 m) **E** calicular view **F** lateral view **G, H** *Labyrinthocyathus delicatus* (SAM_H2836, off East London, 146–238 m) **G** calicular view **H** lateral view **I, J, K** *Monohedotrochus capensis* comb. nov. **I, J** (SAMC_A088924, off Kidds Beach, 247–147 m) **I** calicular view **J** lateral view **K** (SAM_H3210, off Scottburgh, 690 m) calicular view **L, M** *Polycyathus* sp. (USNM 91677, off Port Dunford, 69 m) **L** calicular view **M** full view **N, O** *Rhizosmilia robusta* (USNM 91689, off Kosi Bay Estuary, 74 m) **N** calicular view **O** lateral view **P** *Solenosmilia variabilis* (SAM_H3158, off Cintsa, 630 m) full view. Scale bars: 10 mm (**A–G, I–O**); 100 mm (**H, P**).

Text revision

***Monohedotrochus* Kitahara & Cairns, 2005**

Diagnosis. Corallum solitary, attached, straight, and elongate-conical to trochoid. Base monocyclic. Septotheca costate. Pedicel and base thick. Pali may be present, indistinguishable from columella. Columella papillose.

Type species. *Monohedotrochus capitolii* Kitahara & Cairns, 2005, by original designation.

***Monohedotrochus capensis* (Gardiner, 1904), comb. nov.**
Fig. 4I–K

Caryophyllia capensis Gardiner 1904: 113–114, pl. 1, fig. 4A–D. – Boshoff 1981: 36. – Zibrowius and Gill 1990: 44.
Desmophyllum cristagalli. – Boshoff 1981: 37.
Balanophyllia capensis. – Boshoff 1981: 40 (in part).

References

Boshoff P (1981) An annotated checklist of southern African Scleractinia. South African Association for Marine Biological Research, Oceanographic Research Institute, Durban. Investigational Report 49: 1–45.

Cairns S, Parker S (1992) Review of the Recent Scleractinia of South Australia, Victoria, and Tasmania. Records of the South Australian Museum. Monograph Series 3: 1–82. https://repository.si.edu/handle/10088/7228

Filander ZN, Kitahara MV, Cairns SD, Sink KJ, Lombard AT (2021) Azooxanthellate Scleractinia (Cnidaria, Anthozoa) from South Africa. ZooKeys 1066: 1–198. https://doi.org/10.3897/zookeys.1066.69697

Gardiner J (1904) The turbinolid corals of South Africa, with notes on their anatomy and variation. Marine Investigations of South Africa 3(4): 97–129.

Kitahara M, Cairns S (2005) *Monohedotrochus capitolii*, a new genus and species of solitary azooxanthellate coral (Scleractinia, Caryophylliidae) from southern Brazil. Zoölogische Mededeelingen 79(3): 117–123. https://repository.si.edu/handle/10088/166

Zibrowius H, Gili J (1990) Deep–Water Scleractinia (Cnidaria: Anthozoa) from Namibia, South Africa, and Walvis Ridge, Southeastern Atlantic. Scientia Marina 54(1): 19–46.